Finite-Temperature Quantum Field Theory and the Structure Functions of the Nucleon

Jean Joubert

A thesis submitted in partial fulfilment of the
requirements for the degree of
Doctor of Philosophy
in the Department of Physics
University of Cape Town

January 1992

DST 530 JOUB

92/9100

Abstract

We consider deep inelastic scattering of leptons off a proton in the statistical model first proposed by J. Cleymans and R.L. Thews. The interior of the nucleon is viewed as a thermalized assembly of up and down quarks and gluons. This enables one to incorporate features which are absent in the parton model. They include the presence of identical quarks and gluons in initial and final states and of quantum statistical correlations which also have a role to play in the propagation of particles when considering Feynman diagrams containing internal lines in next-to-leading-order calculations. These features are incorporated through the use of Fermi-Dirac and Bose-Einstein distributions for quarks and gluons, respectively. Stimulated emission factors for final-state gluons and Pauli-blocking factors for final-state quarks are incorporated. The propagation of particles through a many-body medium is taken into account by using thermal Feynman rules for propagators and vertices. The statistical model could also be seen as an attempt to describe the interior of the nucleon at a more fundamental level than that attained through the use of arbitrary parton distributions containing many parameters in the parton model.

Our zeroth order in the strong coupling constant α_S calculation of the structure function F_2 versus x at $Q^2 = 4$ GeV^2 produced a good fit to the recent 1990 data of J. Kwiecinski et al. for $x \geq 0.4$. The analytical calculations by J. Cleymans and I. Dadić of the $\mathcal{O}(\alpha_S)$ corrections are discussed in this work. The inclusion of the $\mathcal{O}(\alpha_S)$ corrections in our numerical calculations allowed the extension of the reproduction of the data of Kwiecinski et al. to values of x smaller than 0.4. A fit could be obtained for values of $x \geq 0.25$. This is compatible with our estimate for the limited range of validity of our theory ($x \geq 0.21$) due to a finite-size effect arising from the finite volume of the nucleon. The latter fit is possible for values of temperature and chemical potential in the immediate vicinity of $T = 0.067$ GeV and $\mu_{\mathrm{up}} = 0.133$ GeV only (with $\mu_{\mathrm{down}} = \mu_{\mathrm{up}}/2^{\frac{1}{3}}$ and $\alpha_S = 0.2$).

The latter values of parameters, however, give rise to a large misfit of the structure function $R = \sigma_L/\sigma_T$ to the experimental data of L.W. Whitlow. Even when taking into account the fact that all measurements of R suffer from large experimental errors due to the weak dependence of the deep inelastic cross section for charged leptons on R, the size of the misfit remains unacceptable. It indicates a shortcoming of the statistical model in its present form to reproduce the spin structure of the proton.

Acknowledgements

I would like to express my gratitude to:

My supervisor, Prof. Jean Cleymans, for the opportunity to study under him and for introducing me to the interesting field of finite-temperature quantum field theory and its applications.

Our collaborator, Dr. Ivan Dadić from the Ruđer Bošković Institute in Zagreb, Croatia, for fruitful discussions and the generous hospitality extended to me by him, his wife, Višnja, and sons during my visit to lovely Croatia in 1991.

Dr. Gary Tupper for providing clarity on various aspects of physics during many detailed discussions.

Prof. Jim Reid from the University of Tulsa, USA, for dazzling conversations about physics and life in general during his visits to UCT.

Prof. Raoul Viollier for constantly keeping seminars lively by his active participation.

Prof. Fritz Hahne, Dr. Frikkie Scholtz, Prof. Hendrik Geyer and the late Prof. Chris Engelbrecht, all from the University of Stellenbosch, who contributed greatly to my joy in physics during my earlier graduate career.

Joletta Payne for providing much needed moral support.

The Foundation for Research Development and the University of Cape Town for financial support.

Last but not least, staff members, fellow students, family and friends for their friendship and understanding during this task.

Preface

To assist the reader in obtaining a perspective on the composition of this work, a brief guide is provided in this preface.

The summary, appearing in Chapter 5, serves as a quick means of orientation to the reader.

A lengthier overview of this work could be obtained by reading the relatively short Chapters 2 and 4 and Appendix D.

In our so-called statistical model, the nucleon is viewed as a thermalized assembly (heat bath) of quarks and gluons. Our main attention is directed to the application of this model to the process of deep inelastic scattering of leptons off a proton. We take into account the propagation of particles through a many-body medium by using thermal Feynman rules which stem from the real-time formalism of finite-temperature quantum field theory. Our review of the latter formalism, comprising the entire Chapter 1, is to a great extent independent of the rest of the thesis and should only be regarded as a broad and general background to our special application in the rest of the thesis. The main connection of this review with the rest of the thesis (which is exclusively devoted to the consideration of deep inelastic scattering of leptons off a proton in the statistical model and, as such, carries the most weight) are the discussions, in Section 1.3.1, on the nature and manner of application of the thermal Feynman rules in the real-time formalism. However, it is to be noted that the discussions in Chapter 1 occur in the context of a scalar field theory. Nonetheless, the manner of application of the thermal Feynman rules for quarks and gluons is the same as that discussed in Section 1.3.1 for scalar particles, but with the Feynman rules themselves replaced by those given in Table 3.1.

It is hoped that the many cross references provided throughout will clarify the connections between the different parts of this work.

Contents

List of Figures

List of Tables

Chapter 1

Real-Time Green Functions in Finite-Temperature Quantum Field Theory (FTQFT)

1.1 Introduction

Whenever thermal effects are expected to be important in physical systems, quantum field theory must be generalized to include such effects. In order to facilitate later discussions, we shall assume that the physical system under consideration is in thermal equilibrium and described, as a heuristic example, by a theory of scalar fields:

$$\mathcal{L} = \frac{1}{2}[(\partial^\mu \phi)\partial_\mu \phi - m^2\phi^2] - \frac{\lambda}{3!}\phi^3.$$

The results for the cases of fermions and gauge bosons are given in refs. [1, 39, 40] (see also Section 3.2).

At finite temperature the system will be statistically distributed over all of its excited levels. In calculating Green functions, the ground (or vacuum) state expectation value, which is used at zero temperature,

$$G_{T=0}(x_1, \ldots, x_n) \;=\; < 0|T[\hat{\phi}(x_1)\ldots\hat{\phi}(x_n)]|0 >$$

must now be replaced by a statistical ensemble average,

$$G_{T\neq 0}(x_1, \ldots, x_n) \;=\; \frac{\mathrm{Tr}\left[\mathrm{e}^{-\beta\hat{H}}T[\hat{\phi}(x_1)\ldots\hat{\phi}(x_n)]\right]}{\mathrm{Tr}[\mathrm{e}^{-\beta\hat{H}}]},$$

where

$$x_i \;=\; (x_i^0, \vec{x}_i).$$

In these expressions, as in the rest of this chapter, it is assumed that the chemical potential is zero ($\mu = 0$). Non-zero values for the chemical potential could be introduced, if required (see, for example, Section 3.2).

In this chapter we shall mainly discuss ways of evaluating such thermal Green functions and emphasize the advantages of the most recently developed methods. For further reading the review article in ref. [2], which contains a very good reference list, is strongly recommended.

Finite-temperature quantum field theory is used in the study of, for example:

(a) Thermal effects in condensed-matter physics [3] – [6]:

- Thermodynamics of superconductors;
- Interaction of condensed matter with X-rays and neutrons;
- Transport properties, heat capacity, etc. of condensed matter.

(b) Early-universe calculations:

- Restoration of spontaneously broken gauge symmetries at sufficiently high temperature [7], e.g., $T_c \sim 10^2$ GeV for the Weinberg–Salam phase transition and $T_c \sim 10^{14}$ GeV for the grand unification transition;
- Primordial nucleosynthesis [8] – [10], where decay and scattering reactions take place in the presence of high matter and radiation densities.

(c) Possible existence of a quark–gluon plasma [11]:

- In the early universe ($T_c \sim 200$ MeV for the deconfinement transition);
- In the centre of neutron stars (high baryon number densities at relatively low temperatures, $T \sim 10$ MeV);
- It is expected that a short-lived quark–gluon plasma may be created in the laboratory by means of ultra-relativistic heavy-ion collisions.

The evaluation of radiative corrections to the thermal production of $\mu^+\mu^-$ pairs in a quark–gluon plasma in thermal equilibrium (see Figure 1.1) serves as a good example of the considerations involved in finite-temperature calculations. The strong-interaction parts of the physical processes, depicted in Figure 1.1, do not take place in the ordinary vacuum, but in a heat bath consisting of the background of quarks, antiquarks and gluons present at the temperature under consideration. In consequence, the phase space integrals, associated with the external quark, antiquark and gluon lines, become generalized from the zero-temperature case to the finite-temperature case as follows [12, p.349], [13, p.547–549]:

For $\mathbf{T = 0}$ we have

$$\int \frac{d^3k}{(2\pi)^3 2\omega_k} = \int \frac{d^4k}{(2\pi)^4} 2\pi\theta(k_0)\delta(k^2 - m^2)$$

where $\omega_k = \sqrt{\vec{k}^2 + m^2}$ and $k = (k_0, \vec{k})$, and for $\mathbf{T \neq 0}$ we have for bosons for an incoming particle

$$\int \frac{d^3k}{(2\pi)^3 2\omega_k} n_{\mathrm{B}}(\omega_k)$$

and an outgoing particle

$$\int \frac{d^3k}{(2\pi)^3 2\omega_k} [1 + n_{\mathrm{B}}(\omega_k)],$$

where $n_{\mathrm{B}}(k) = \dfrac{1}{e^{\beta\omega_k} - 1}$.

For fermions we have for an incoming particle

$$\sum_{\text{spins}} \int \frac{d^3k}{(2\pi)^3 2\omega_k} n_{\mathrm{F}}(\omega_k)$$

and for an outgoing particle

$$\sum_{\text{spins}} \int \frac{d^3k}{(2\pi)^3 2\omega_k} [1 - n_{\mathrm{F}}(\omega_k)]$$

where $n_{\mathrm{F}}(k) = \dfrac{1}{e^{\beta\omega_k} + 1}$.

One notices that the incoming particles are in their thermal distributions, $n_{\mathrm{B}}(k)$ and $n_{\mathrm{F}}(k)$ for bosons and fermions, respectively. For outgoing bosons, the factor, $[1 + n_{\mathrm{B}}(k)]$, denotes the effect of stimulated emission similar to the same effect in a laser system. Due to the Pauli exclusion principle applying to fermions in a many-body medium, we have the Pauli-blocking factor, $[1 - n_{\mathrm{F}}(k)]$, for outgoing fermions.

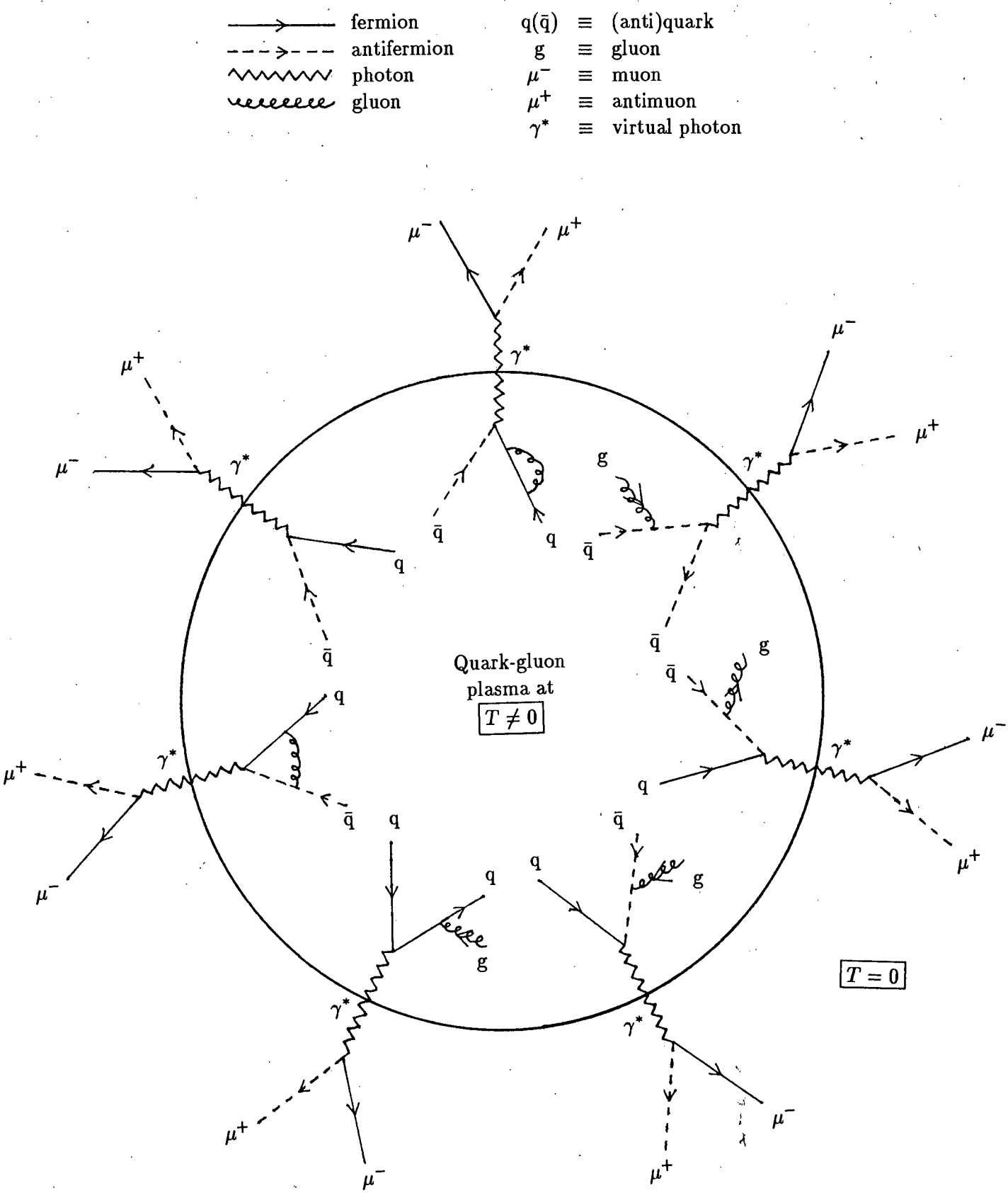

Figure 1.1: Schematic illustration of some contributions to the thermal production of $\mu^+\mu^-$ pairs in a quark-gluon plasma in thermal equilibrium. In this case, the quark-gluon plasma is assumed to be created in an ultrarelativistic heavy-ion collision.

One also requires expressions for vertices and internal lines of graphs, and it would therefore be very convenient to obtain Feynman rules adapted for the finite-temperature case. In the rest of this chapter we shall not discuss the specific process of $\mu^+\mu^-$ pair production, but rather concentrate on the methods which are used in the description of a general system at finite temperature.

The various approaches to the evaluation of thermal Green functions, discussed in this chapter, can be summed up by noting the form of the free scalar propagator in each approach: for $T = 0$ the free propagator is given by

$$\underset{k}{\longrightarrow} = iD(k) = \frac{i}{k^2 - m^2 + i\epsilon}$$

where $k^2 = {k_0}^2 - \vec{k}^2$, and for $T \neq 0$ the **imaginary-time** free propagator is given by

$$\underset{\omega_n, \vec{k}}{\longrightarrow} = iD_\beta(\omega_n, \vec{k}) = \frac{i}{{\omega_n}^2 - \vec{k}^2 - m^2}$$

where $\omega_n = \dfrac{2\pi n}{-i\beta}$, $n = 0, \pm 1, \pm 2, \ldots$; $\beta = \dfrac{1}{kT}$.

Analytic continuation from the *discrete* imaginary energies, ω_n [corresponding via a Fourier transformation to a *finite* imaginary-time *interval*, see eq. (1.11) further on and the sentence before it], to real continuous energies, k_0 (corresponding to real time in configuration space), produces the **indirectly derived real-time** free propagator given by

$$\underset{k}{\longrightarrow} = iD_\beta(k) = \frac{i}{k^2 - m^2 + i\epsilon} + \frac{2\pi}{e^{\beta|k_0|} - 1}\delta(k^2 - m^2) \quad , \quad k^2 = {k_0}^2 - \vec{k}^2.$$

Direct derivation of real-time Green functions, without analytic continuation, produces a 2×2 matrix structure for the **directly derived real-time** free propagator given by

$$\underset{k}{\longrightarrow} = iD_\beta(k)$$

$$= \begin{pmatrix} \dfrac{i}{k^2 - m^2 + i\epsilon} + \dfrac{2\pi}{e^{\beta|k_0|} - 1}\delta(k^2 - m^2) & \dfrac{-2\pi e^{-\beta|k_0|/2}}{1 - e^{-\beta|k_0|}}\delta(k^2 - m^2) \\ \dfrac{-2\pi e^{-\beta|k_0|/2}}{1 - e^{-\beta|k_0|}}\delta(k^2 - m^2) & \dfrac{-i}{k^2 - m^2 - i\epsilon} + \dfrac{2\pi}{e^{\beta|k_0|} - 1}\delta(k^2 - m^2) \end{pmatrix}.$$

The shortcomings of the earlier approaches and improvements brought about by the later approaches will be pointed out.

Some of the recent examples of where the results from the direct derivation of real-time thermal Green functions have been applied in diagrammatic perturbation expansions appear

in refs. [14] – [22], [8, 1]. Proceedings of two workshops on thermal-field theories and their applications appeared in refs. [23] and [24](a). In ref. [25] recent developments in relativistic thermal field theories are reviewed. In refs. [26] and [27], Landsman criticizes the standard perturbation theory of thermal-field theories. His criticism includes the possibility that the whole idea of diagrammatic perturbation theory might have to be abandoned. Gabellini et al. [17, p.11] have referred to Landsman's criticism in their work on electron–positron annihilation in thermal quantum chromodynamics.

1.2 Imaginary-time formalism

The imaginary-time formalism provides the oldest and most commonly employed way of evaluating thermal Green functions. Its development started at about the time of the work by Matsubara [28] in 1955. In the following example of the derivation of the imaginary-time 2-point function [see eq. (1.5)] for non-interacting scalar fields, we notice a formal analogy between inverse temperature, β, and imaginary time,viz.

$$\text{Inverse temperature, } \beta \quad \longleftrightarrow \quad \text{Imaginary time.}$$

We make use of a generalization to imaginary time of the well-known time evolution equations for operators,

$$e^{i\hat{H}x_0}\hat{\phi}(0,\vec{x})e^{-i\hat{H}x_0} = \hat{\phi}(x_0,\vec{x}). \tag{1.1}$$

In the derivation of the thermal propagator we come across the quantity in (1.2). By rewriting this quantity in the form appearing in (1.3) and comparing it with eq. (1.1), we can identify the expression in (1.3) as the time evolution of the field operator to the imaginary time, $-i\beta$, as denoted in (1.4).

$$e^{\beta\hat{H}}\hat{\phi}(0,\vec{x})e^{-\beta\hat{H}} \tag{1.2}$$

$$= e^{i\hat{H}(-i\beta)}\hat{\phi}(0,\vec{x})e^{-i\hat{H}(-i\beta)} \tag{1.3}$$

$$= \hat{\phi}(-i\beta,\vec{x}). \tag{1.4}$$

1.2.1 Derivation of the imaginary-time free propagator

Boundary conditions which arise from the structure of the statistical average in

$$iD_\beta(x-y) = \frac{\mathrm{Tr}(e^{-\beta\hat{H}}T[\hat{\phi}(x)\hat{\phi}(y)])}{\mathrm{Tr}(e^{-\beta\hat{H}})} \equiv < T[\hat{\phi}(x)\hat{\phi}(y)] > \tag{1.5}$$

are used to obtain a solution to the Klein–Gordon equation for the free propagator in,

$$(\Box_x + m^2)D_\beta(x-y) = -\delta^4(x-y) \tag{1.6}$$

where $x = (x_0, \vec{x})$ and $\Box_x = \dfrac{\partial^2}{\partial {x_0}^2} - \vec{\nabla}_x^2$.

Since imaginary times are involved, one treats the time arguments, x_0 and y_0, of $D_\beta(x-y)$ as imaginary and lying on a contour in the complex-time plane as shown in Figure 1.2. Time-

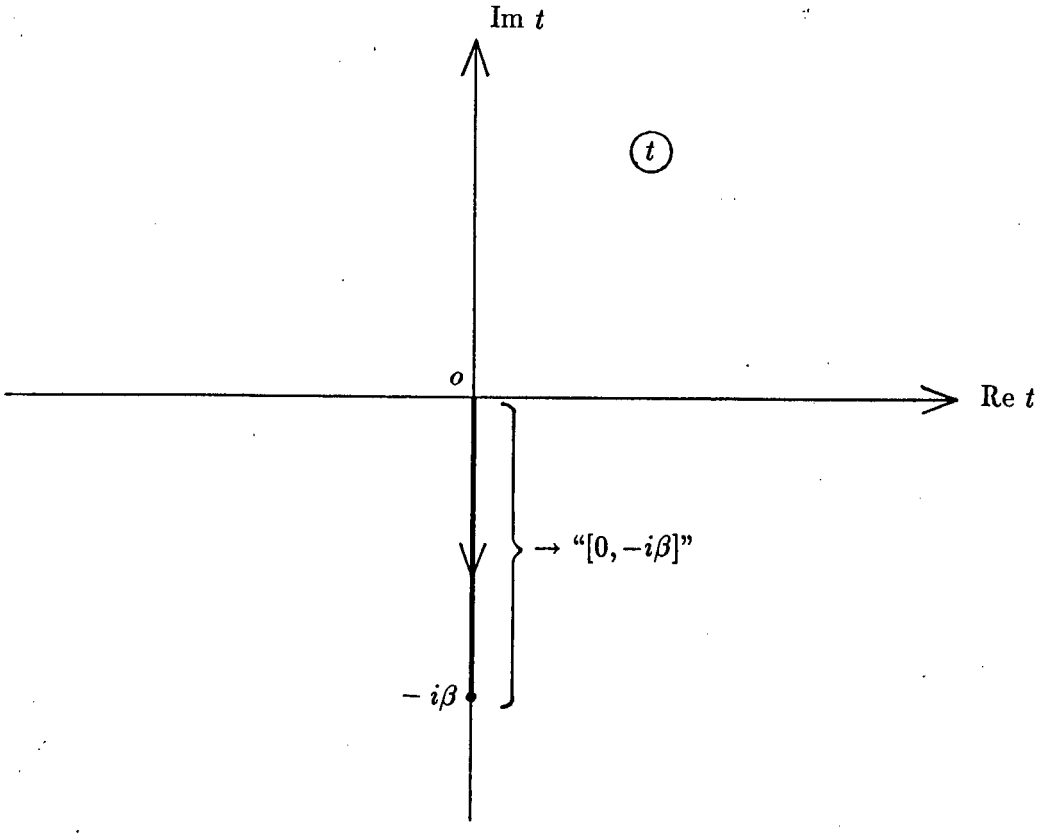

Figure 1.2: The finite imaginary-time interval of the imaginary-time formalism as a contour in the complex-time plane.

ordering for imaginary times on this contour is defined in analogy to the zero-temperature definition, i.e., the imaginary time nearest to the end point, $-i\beta$, of the contour is regarded as the 'latest' time,

$$x_0, y_0 \in [0, -i\beta] \quad \Rightarrow \quad ix_0, iy_0 \in [0, \beta]$$

$$iD_\beta(x-y) = < T[\hat{\phi}(x)\hat{\phi}(y)] >$$

$$= \begin{cases} < \hat{\phi}(x)\hat{\phi}(y) > & \text{for } ix_0 > iy_0, \quad \text{i.e. when } x_0 \text{ is nearer to } -i\beta \text{ than } y_0 \\ < \hat{\phi}(y)\hat{\phi}(x) > & \text{for } iy_0 > ix_0, \quad \text{i.e. when } y_0 \text{ is nearer to } -i\beta \text{ than } x_0 \end{cases}$$

In the following steps, the periodicity condition [also called the KMS (Kubo–Martin–Schwinger) condition; see second-last paragraph of Section 1.3.6],

$$iD_\beta(x-y)|_{x_0=0} = iD_\beta(x-y)|_{x_0=-i\beta} \tag{1.7}$$

is obtained by making use of the cyclic property of the trace in eq. (1.8), inserting an identity operator in eq. (1.9) and making use of the imaginary-time evolution equation, expressions (1.2), (1.3) and (1.4), in eq. (1.10):

$$\begin{aligned}
[\mathrm{Tr}e^{-\beta\hat{H}}]iD_\beta(x-y)\Big|_{x_0=0} &= \mathrm{Tr}\left(e^{-\beta\hat{H}}T[\hat{\phi}(x_0,\vec{x})\hat{\phi}(y_0,\vec{y})]\right)\Big|_{x_0=0} \\
&= \mathrm{Tr}\left(e^{-\beta\hat{H}}\hat{\phi}(y_0,\vec{y})\hat{\phi}(0,\vec{x})\right) \\
&= \mathrm{Tr}\left(\hat{\phi}(0,\vec{x})e^{-\beta\hat{H}}\hat{\phi}(y_0,\vec{y})\right) \qquad (1.8) \\
&= \mathrm{Tr}\left(\underbrace{e^{-\beta\hat{H}}e^{\beta\hat{H}}}_{1}\hat{\phi}(0,\vec{x})e^{-\beta\hat{H}}\hat{\phi}(y_0,\vec{y})\right) \qquad (1.9) \\
&= \mathrm{Tr}\left(e^{-\beta\hat{H}}\hat{\phi}(-i\beta,\vec{x})\hat{\phi}(y_0,\vec{y})\right) \qquad (1.10) \\
&= \mathrm{Tr}\left(e^{-\beta\hat{H}}T[\hat{\phi}(x_0,\vec{x})\hat{\phi}(y_0,\vec{y})]\right)\Big|_{x_0=-i\beta} \\
&= [\mathrm{Tr}\,e^{-\beta\hat{H}}]iD_\beta(x-y)\Big|_{x_0=-i\beta}.
\end{aligned}$$

Due to this periodicity condition over the *finite interval* along the imaginary-time axis ("$[0,-i\beta]$" as in Figure 1.2), the Fourier representation of $iD_\beta(x-y)$ contains a sum over *discrete* imaginary energies:

$$iD_\beta(x-y) = \frac{1}{-i\beta}\sum_{n=0,\pm1,\pm2,\ldots} e^{-i\omega_n(x_0-y_0)}\int\frac{d^3k}{(2\pi)^3}e^{i\vec{k}.(\vec{x}-\vec{y})}iD_\beta(\omega_n,\vec{k}) \tag{1.11}$$

where $\omega_n = \dfrac{2\pi n}{-i\beta}$.

The Fourier-transformed free propagator, $iD_\beta(\omega_n,\vec{k})$ in eq. (1.11), is expressed in terms of the discrete imaginary energy, ω_n, and is obtained from the Klein–Gordon equation in eq. (1.6):

$$iD_\beta(\omega_n,\vec{k}) = \frac{i}{{\omega_n}^2 - \vec{k}^2 - m^2}. \tag{1.12}$$

1.2.2 Analytic continuation from imaginary time to real time

The absence of real time in the imaginary-time formalism has to do with the fact that time dependence is absent in a system in thermal equilibrium in the sense that thermodynamic quantities, such as, for example, energy density, pressure, entropy and number densities are static in a system in thermal equilibrium. The imaginary-time Green functions or temperature Green functions, as they are also called [4, 5], are thus well suited for the evaluation of static thermodynamic quantities. [The terminology, 'thermal Green function', as opposed to 'temperature Green function' may be used to denote the general (i.e. imaginary-time or real-time) Green function at finite temperature.] In practice one can, for example, set up a diagrammatic expansion of the thermodynamic potential in terms of imaginary-time Green functions, from which many thermodynamic quantities can be derived [4, 5], [29] – [32].

But there are dynamical questions which intrinsically involve real time. For example, in the description of a scattering process in a heat bath, the propagators express the presence of a particle at one position and time in terms of its presence at another position and another time. Since these times assume values on the continuous real axis, we need, after a Fourier transformation to momentum space, Feynman diagrams with continuous real energies on external lines. The imaginary-time Green functions can be extended from the discrete imaginary energies to real continuous energies through a process of analytic continuation. But, for n-point functions with $n > 2$ or for graphs beyond the one-loop level, the analytic continuation becomes impracticable [12, p.329], [2, p.144].

The analytic continuation of the free propagator from imaginary time to real time is performed in an article by Dolan and Jackiw [33, p.3336]. This corresponds, in momentum space, to the analytic continuation from discrete imaginary energies, ω_n in eq. (1.13), to continuous real energies, k_0 in eq. (1.14):

$$iD_\beta(\omega_n, \vec{k}) = \frac{i}{{\omega_n}^2 - \vec{k}^2 - m^2} \tag{1.13}$$

where $\omega_n = \dfrac{2\pi n}{-i\beta}$, i.e., ω_n discrete and imaginary,

$$iD_\beta(k) = \frac{i}{k^2 - m^2 + i\epsilon} + \frac{2\pi}{e^{\beta|k_0|} - 1}\delta(k^2 - m^2), \tag{1.14}$$

where $k^2 = {k_0}^2 - \vec{k}^2$, k_0 real and continuous.

The first term in eq. (1.14) is the usual zero-temperature free propagator. The second term is interpreted in ref. [34] as the contribution from particles in the heat bath. This interpretation is motivated by considering, in addition to a zero-temperature process, processes in which on mass shell particles emerging from or going into the heat bath participate, and by noting that, since in a heat bath the initial and final states in the two cases are completely identical, one cannot distinguish such processes from the usual zero-temperature process by any observations.

When one writes down the real-time Feynman rules for, for example, the graph in Figure 1.3, one notices [as shown in eq. (1.15)] that one picks up a factor, $[\delta(k^2 - m^2)]^2$, due to the same momentum, k, on two of the internal lines of the graph. But, such a product of two Dirac delta functions with the same arguments is not a well-defined quantity:

$$\begin{aligned} \left(\underset{k}{\longrightarrow}\right)^2 &= [iD_\beta(k)]^2 = \left[\frac{i}{k^2 - m^2 + i\epsilon} + \frac{2\pi}{e^{\beta|k_0|} - 1}\delta(k^2 - m^2)\right]^2 \\ &= \cdots + \left(\frac{2\pi}{e^{\beta|k_0|} - 1}\right)^2 [\delta(k^2 - m^2)]^2. \end{aligned} \tag{1.15}$$

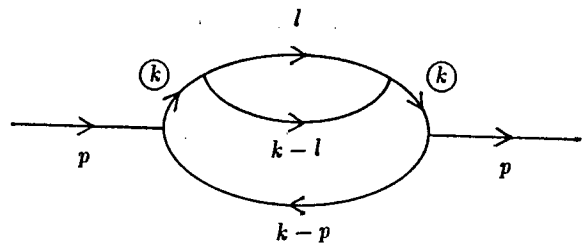

Figure 1.3: An example of a graph where the use of the indirectly derived real-time free propagator leads to an ill-defined expression.

1.3 Real-time formalism

In order to get around all the problems mentioned in the previous section, two methods that derive real-time Green functions directly (i.e., without analytic continuation) have been developed relatively recently:

(a) An operator formulation of finite-temperature quantum field theory, called thermo-field dynamics (TFD), was introduced in refs. [35, p.224] and [36]. Reference [36] contains the more general and readable introduction.

(b) The path integral approach (also called the time-path method) to the derivation of real-time Green functions was followed in ref. [37].

Both methods lead to similar Feynman rules. To give an idea of what we are aiming at, the Feynman rules will be shown first and, after that, aspects of their derivation will be discussed. In Section 1.3.7 it will be explained in what sense the work of Mills [38] and others may be considered forerunners to the above-mentioned methods.

1.3.1 Feynman rules for real-time thermal Green functions [37, 39, 40]

The free propagator acquires a 2×2 matrix structure corresponding to the presence of two kinds of fields, the physical field, ϕ_1, which is called type-1, and a thermal ghost field, ϕ_2, called type-2:

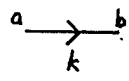

$$= iD_\beta^{ab}(k)$$

$$= \begin{pmatrix} \dfrac{i}{k^2 - m^2 + i\epsilon} + \dfrac{2\pi}{e^{\beta|k_0|} - 1}\delta(k^2 - m^2) & \dfrac{-2\pi e^{-\beta|k_0|/2}}{1 - e^{-\beta|k_0|}}\delta(k^2 - m^2) \\ \dfrac{-2\pi e^{-\beta|k_0|/2}}{1 - e^{-\beta|k_0|}}\delta(k^2 - m^2) & \dfrac{-i}{k^2 - m^2 - i\epsilon} + \dfrac{2\pi}{e^{\beta|k_0|} - 1}\delta(k^2 - m^2) \end{pmatrix} \tag{1.16}$$

We shall see how this so-called doubling of degrees of freedom arises in the derivation of the Feynman rules and further reasons for its appearance will be given in Section 1.3.5.

For the vertex one obtains the rule:

$$\begin{pmatrix} -i\lambda & 0 \\ 0 & i\lambda \end{pmatrix} \tag{1.17}$$

which may be interpreted as the presence of two types of vertices, namely,

type-1 vertex: $-i\lambda$,

type-2 vertex: $i\lambda$,

As will be seen in Section 1.3.3, only the physical type-1 fields appear on the external lines:

$$\text{external line:} \qquad \begin{pmatrix} \phi_1 \\ \phi_2 \end{pmatrix} = \begin{pmatrix} \phi_1 \\ 0 \end{pmatrix} . \tag{1.18}$$

The topological and combinatorical structures of Feynman diagrams do not change in going from zero to non-zero temperature. Corresponding to each diagram at zero temperature, one will have the same diagram at non-zero temperature, but the 2×2 matrix structure of the free propagator and vertex in eqs. (1.16) and (1.17), respectively, and the rule for the external line in eq. (1.18) amount to the following situation (see the example in Figure 1.4): Each diagram effectively becomes a sum of terms with type-1 vertices for the vertices connected to external lines and all possible combinations of type-1 and type-2 vertices for the other internal vertices. This leads to a serious increase in the number of diagrams. However, the number of diagrams to be evaluated may be greatly reduced by making use of the recently developed Cutkosky rules at finite temperature [12]. In the latter reference, Kobes and Semenoff found a correspondence in the real-time formalism between decay amplitudes and the graphs involved in finding the imaginary part of an associated self-energy diagram at finite temperature. These techniques were applied in, amongst others, refs. [14] and [20], in which the rate of $\mu^+\mu^-$ pairs, produced in a thermalized quark–gluon plasma, is related to the imaginary part of the associated electromagnetic thermal vacuum-polarization tensor, which is then evaluated up to the two-loop level by means of the elegant finite-temperature Cutkosky rules. Further discussions about finite-temperature Cutkosky rules appear in ref. [43].

One notices that the 1–1 component of the propagator in eq. (1.16) is identical to the real-time propagator in eq. (1.14), which was obtained by analytic continuation of the imaginary-time propagator. One would thus expect the same problem with products of Dirac delta functions with coinciding arguments as in Figure 1.3. The other components of the propagator in eq. (1.16) can also contribute to singularities. However, the two-component structure of the formalism causes to each order the cancellation of singularities among themselves [42], [2, p.205], [44]. Additional advantages of this formalism are discussed in Section 1.4.

T = 0 :

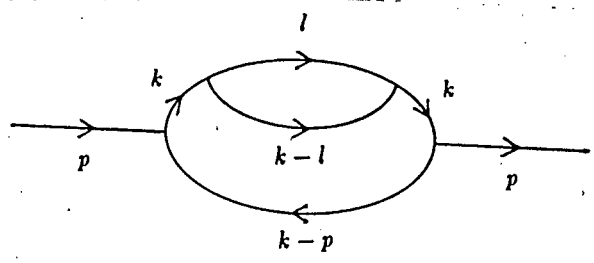

T ≠ 0 :

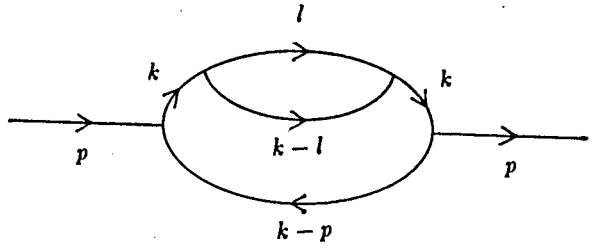

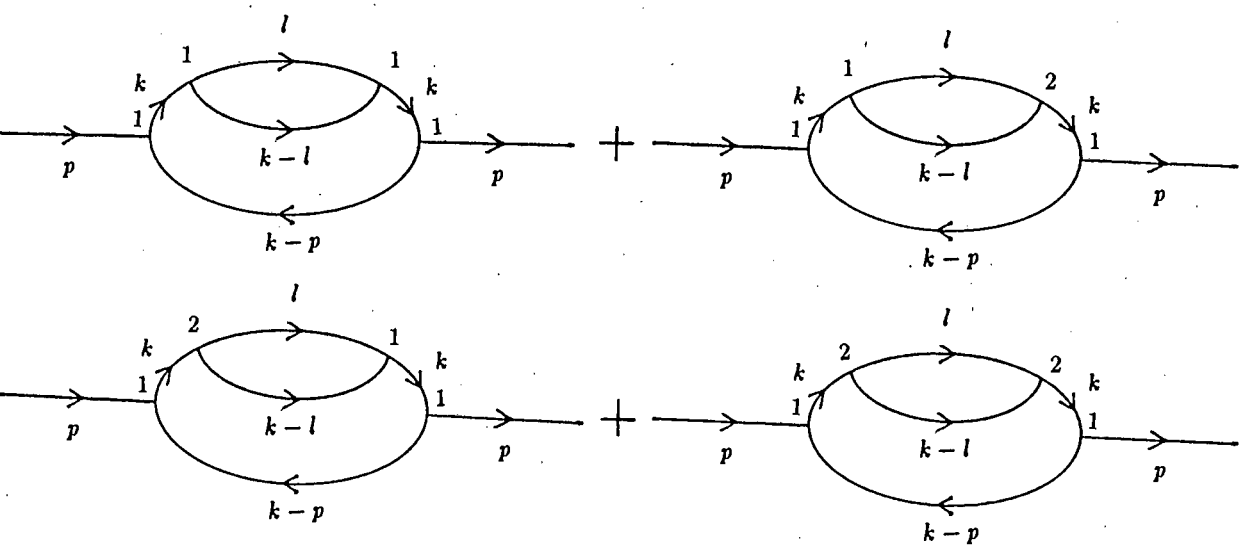

where, e.g.:

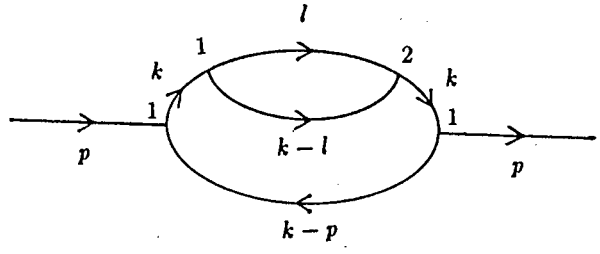

$$= \int \frac{d^4k}{(2\pi)^4}\frac{d^4l}{(2\pi)^4}\phi_1^*(p)(-i\lambda)iD_\beta^{11}(k-p)(-i\lambda)iD_\beta^{11}(k)(-i\lambda)iD_\beta^{12}(l)$$
$$\times iD_\beta^{12}(k-l)(i\lambda)iD_\beta^{21}(k)\phi_1(p)$$

where $\phi_1(p) = 1$ for the scalar theory under consideration [41, p.149].

Figure 1.4: An example of the application of the real-time thermal Feynman rules

1.3.2 Derivation of the Feynman rules for real-time thermal Green functions

In this section we follow the derivation of the 2×2 matrix structure of the real-time thermal Green functions in the path-integral approach [37]. We are interested in a perturbative evaluation of

$$G_\beta(x_1, x_2, \ldots, x_n) = \frac{\mathrm{Tr}\left[\mathrm{e}^{-\beta\hat{H}} T[\hat{\phi}(x_1)\ldots\hat{\phi}(x_n)]\right]}{\mathrm{Tr}[\mathrm{e}^{-\beta\hat{H}}]}$$

where, for real-time Green functions, the time component, t_i, of each argument, $x_i = (t_i, \vec{x}_i)$, of G_β, must be real. We shall derive a path-integral representation of a generating functional, $Z[j]$, such that, if one takes functional derivatives with respect to the source, j, with real time arguments, one obtains real-time Green functions,

$$G_\beta(x_1, \ldots, x_n) = \frac{1}{Z[0]} \frac{\delta}{i\delta j(x_n)} \cdots \frac{\delta}{i\delta j(x_2)} \frac{\delta}{i\delta j(x_1)} Z[j]\Big|_{j=0} \tag{1.19}$$

where the definition of a functional derivative is

$$\frac{\delta Z[j(x')]}{\delta j(x)} = \lim_{\epsilon \to 0} \frac{Z[j(x') + \epsilon\delta^4(x' - x)] - Z[j(x')]}{\epsilon} .$$

An example of the operation of functional differentiation is

$$\frac{\delta}{\delta j(x)} \int d^4x' j(x')\phi(x') = \phi(x) .$$

We introduce a generating functional defined as follows:

$$Z[j] = \mathrm{Tr}\left\{\mathrm{e}^{-\beta\hat{H}} T_C \left[\exp\left(i\int_C d\tau \int d^3x j(\tau, \vec{x})\hat{\phi}(\tau, \vec{x})\right)\right]\right\}, \tag{1.20}$$

where C is in general a contour in the complex-time plane (see Figure 1.5 for an example) and T_C is a time ordering operator for times on the contour. This contour time ordering operator is defined in a similar way to that which we had in Section 1.2.1 for the contour in Figure 1.2, namely, times nearest to the end point of the contour, C, are treated as the 'latest' times. The alternative name, 'time-path method', for the path-integral approach, stems from the consideration of contours in the complex-time plane.

If the contour of time integration in eq. (1.20) includes the complete real-time axis, then $Z[j]$ will be a candidate for a generating functional of the required real-time Green functions. If not, the functional differentiation with respect to a source, j, with a specific real time argument will fail to produce a Green function with that real time argument, if that real time argument does not lie on the contour.

In order to evaluate the Green functions perturbatively, we shall *have to* treat the inverse temperature, β, appearing in eq. (1.20), as an imaginary time (see equations (1.27) and (1.28)). In the derivation it will then be *necessary* that the contour, C, also covers times with non-zero imaginary parts. In consequence, the Heisenberg fields appearing in eq. (1.20) will once again be generalized to include complex time arguments. For the moment we assume the contour to be the one in Figure 1.5. More will be said about this specific choice of contour later on. Some entities which will appear in the following derivations are as follows (τ is in general a complex time):

$\hat{\phi}(\tau,\vec{x})$ — field operator in the Heisenberg picture

$|\phi(\vec{x});\tau>$ — Heisenberg picture state vector describing a state which at time, τ, is an eigenstate of the field operator, $\hat{\phi}(\tau,\vec{x})$, with eigenvalue, $\phi(\vec{x})$:

$$\hat{\phi}(\tau,\vec{x})|\phi(\vec{x});\tau> \;=\; \phi(\vec{x})|\phi(\vec{x});\tau>\,. \tag{1.21}$$

At any given time, τ, the state vectors form a complete set of states [45, p.373]:

$$\int \mathcal{D}\phi|\phi;\tau><\phi;\tau| = 1\,.$$

Time evolution is given by

$$\hat{\phi}(\tau+\tau',\vec{x}) \;=\; e^{i\hat{H}\tau'}\hat{\phi}(\tau,\vec{x})e^{-i\hat{H}\tau'}, \tag{1.22}$$

$$|\phi(\vec{x});\tau+\tau'> \;=\; e^{i\hat{H}\tau'}|\phi(\vec{x});\tau>\,. \tag{1.23}$$

For the trace in eq. (1.20) we use a complete set of eigenstates of the field operator at the time $\tau = 0$:

$$Z[j] = \int \mathcal{D}\phi <\phi;0|\exp(-\beta\hat{H})T_C\exp\left[i\int_C j\hat{\phi}\right]|\phi;0> \tag{1.24}$$

where, from now on,

$$i\int_C j\hat{\phi} \equiv i\int_C d\tau\int d^3x j(\tau,\vec{x})\hat{\phi}(\tau,\vec{x}) \equiv i\int_C d^4x j(x)\hat{\phi}(x).$$

In eq. (1.25) we insert an identity operator, in eq. (1.26) we make use of the cyclic property of the trace and in eqs. (1.27) and (1.28) we make use of eq. (1.23) to translate states in time to obtain

$$Z[j] \;=\; \int \mathcal{D}\phi <\phi;0|\underbrace{e^{-i\hat{H}R}e^{i\hat{H}R}}_{1}\exp(-\beta\hat{H})T_C\exp\left[i\int_C j\hat{\phi}\right]|\phi;0> \tag{1.25}$$

$$= \int \mathcal{D}\phi < \phi; 0|e^{i\hat{H}R} \exp(-\beta\hat{H}) T_C \exp\left[i\int_C j\hat{\phi}\right] e^{-i\hat{H}R}|\phi; 0> \quad (1.26)$$

$$= \int \mathcal{D}\phi < \phi; -R| \exp(-\beta\hat{H}) T_C \exp\left[i\int_C j\hat{\phi}\right] |\phi; -R> \quad (1.27)$$

$$= \int \mathcal{D}\phi < \phi; -R - i\beta|T_C \exp\left[i\int_C j\hat{\phi}\right] |\phi; -R> . \quad (1.28)$$

We next insert in eq. (1.28) a complete set of states at the times R, $R - i\beta/2$ and $-R - i\beta/2$

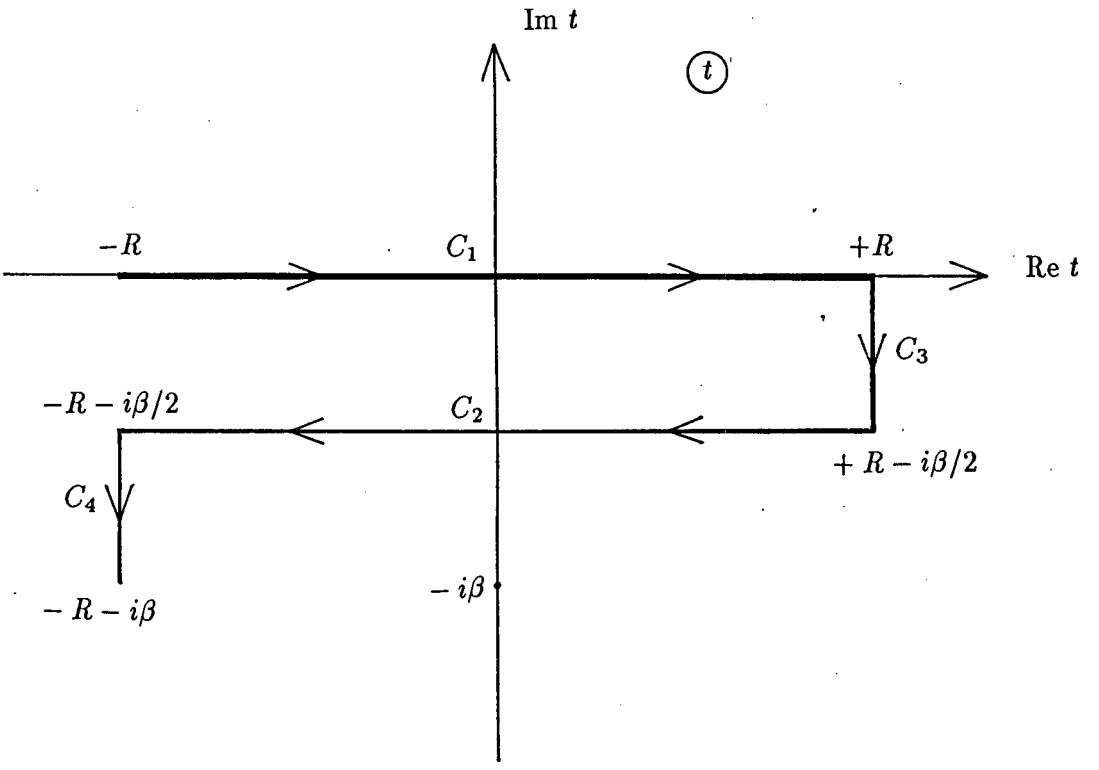

Figure 1.5: The contour, C, of e.g. eq.(1.24) consisting of segments C_1, C_3, C_2 and C_4 in the complex time plane. In order to have that C includes the complete real time axis, the limit, $R \to \infty$, is implied.

(on the contour, C, in Figure 1.5) and obtain

$$\begin{aligned} Z[j] = & \int \mathcal{D}\phi\mathcal{D}\phi'\mathcal{D}\phi''\mathcal{D}\phi''' < \phi; -R - i\beta|T_C \exp\left[i\int_{C_4} j\hat{\phi}\right] |\phi'''; -R - i\beta/2> \\ & \times < \phi'''; -R - i\beta/2|T_C \exp\left[i\int_{C_2} j\hat{\phi}\right] |\phi''; +R - i\beta/2> \\ & \times < \phi''; +R - i\beta/2|T_C \exp\left[i\int_{C_3} j\hat{\phi}\right] |\phi'; R> \\ & \times < \phi'; R|T_C \exp\left[i\int_{C_1} j\hat{\phi}\right] |\phi; -R> . \end{aligned} \quad (1.29)$$

Each matrix element in eq. (1.29) has a path-integral representation. Standard manipulations

[46, 47], [2, p.156] result in the representation

$$Z[j] = N \int [d\phi][d\pi] \exp\left\{ i \int_C d\tau \int d^3x [\pi(\tau,\vec{x})\dot{\phi}(\tau,\vec{x}) - \mathcal{H}[\phi,\pi] + j(\tau,\vec{x})\phi(\tau,\vec{x})] \right\} \quad (1.30)$$

where $\dot{\phi}$ is a time derivative of ϕ with direction tangential to the contour, C. In going from eq. (1.29) to eq. (1.30), the field operators, $\hat{\phi}(\tau,\vec{x})$, have been replaced by c-numbers, $\phi(\tau,\vec{x})$. The time argument, τ, of such a number indicates at which time it is considered to be an eigenvalue in eq. (1.21):

$$\hat{\phi}(\tau,\vec{x})|\phi(\vec{x});\tau> = \phi(\tau,\vec{x})|\phi(\vec{x});\tau> . \quad (1.31)$$

Take note that $\phi(\tau,\vec{x})$ is actually independent of time,

$$\phi(\tau,\vec{x}) = \phi(\vec{x}), \quad (1.32)$$

in the following sense. In the Schrödinger picture one has

$$\hat{\phi}_S(\vec{x})|\phi(\vec{x})> = \phi(\vec{x})|\phi(\vec{x})>_S . \quad (1.33)$$

The Heisenberg-picture quantities in eq. (1.31) in terms of Schrödinger-picture quantities are as follows:

$$\begin{aligned} \hat{\phi}(\tau,\vec{x}) &= e^{i\hat{H}\tau}\hat{\phi}_S(\vec{x})e^{-i\hat{H}\tau}, \\ |\phi(\vec{x});\tau> &= e^{i\hat{H}\tau}|\phi(\vec{x})>_S . \end{aligned}$$

Thus, from eq. (1.31), we have

$$\begin{aligned} \hat{\phi}(\tau,\vec{x})|\phi(\vec{x});\tau> &= e^{i\hat{H}\tau}\hat{\phi}_S(\vec{x})e^{-i\hat{H}\tau}e^{i\hat{H}\tau}|\phi(\vec{x})>_S \\ &= e^{i\hat{H}\tau}\hat{\phi}_S(\vec{x})|\phi(\vec{x})>_S \\ &= e^{i\hat{H}\tau}\phi(\vec{x})|\phi(\vec{x})>_S \qquad \text{[by using eq. (1.33)]} \\ &= \phi(\vec{x})|\phi(\vec{x});\tau)> . \end{aligned} \quad (1.34)$$

Comparison of eqs. (1.31) and (1.34) produces eq. (1.32). The trace operation in eq. (1.20) leads, via equations eqs. (1.24) to (1.29), to the presence of a leftmost bra, $<\phi;-R-i\beta|$, and a rightmost ket, $|\phi;-R>$, in eq. (1.29). In the latter two kets the presence of the same symbol, ϕ [as opposed to e.g. ϕ', ϕ'' and ϕ''' in the other kets appearing in eq. (1.29)], points

to the fact that these two kets have the same eigenvalue, $\phi(\vec{x})$. In consequence, the path integration in eq. (1.30) is over all fields satisfying the periodicity condition:

$$\phi(-R,\vec{x}) = \phi(-R - i\beta,\vec{x}). \tag{1.35}$$

With a Hamiltonian density of the form

$$\mathcal{H}[\phi,\pi] = \frac{1}{2}\pi^2 + \frac{1}{2}\phi(-\vec{\nabla}^2 + m^2)\phi + V[\phi]$$

where, for example,

$$V[\phi] = \frac{\lambda}{3!}\phi^3,$$

eq. (1.30) becomes, after the integration over the canonical momentum variables, $\pi(x)$, and up to a normalization constant,

$$Z[j] = \int [d\phi] \exp i \int_C (\mathcal{L}[\phi] + j\phi) \tag{1.36}$$

where

$$\mathcal{L}[\phi] = \frac{1}{2}\phi(-\Box_C - m^2)\phi - V[\phi], \qquad \Box_C = \frac{\partial^2}{\partial\tau^2} - \vec{\nabla}^2 \tag{1.37}$$

and where the time derivative is the directional derivative along the contour. In eq. (1.36), the change of variables

$$\phi(x) \to \phi(x) + \int_C d^4y D_\beta(x-y)j(y), \tag{1.38}$$

where

$$(-\Box_C - m^2)D_\beta(x-y) = \delta_C(x-y), \tag{1.39}$$

leads to

$$Z[j] = \exp\left\{-i\int_C d^4x' V\left[\frac{1}{i}\frac{\delta}{\delta j(x')}\right]\right\} \exp\left\{-\frac{i}{2}\int_C d^4x \int_C d^4y j(x) D_\beta(x-y) j(y)\right\} \tag{1.40}$$

By introducing a contour step function

$$\theta_C(\tau_x - \tau_y) = \int_C^{\tau_x} d\tau'' \delta_C(\tau'' - \tau_y)$$

one may write

$$D_\beta(x-y) = D_\beta^>(x-y)\theta_C(\tau_x - \tau_y) + D_\beta^<(x-y)\theta_C(\tau_y - \tau_x) \tag{1.41}$$

The change of variable in eq. (1.38) and the periodicity condition, eq. (1.35), lead, via the representation of $D_\beta(x-y)$ in eq. (1.41), to the boundary condition (also called the KMS condition; see second-last paragraph before Section 1.3.7) for eq. (1.39):

$$D_\beta^>(\tau_x-\tau_y-i\beta,\vec{x}-\vec{y}) = D_\beta^<(\tau_x-\tau_y,\vec{x}-\vec{y}). \tag{1.42}$$

After Fourier transforming with respect to the spatial coordinates, the solution (an explicit derivation is given in reference [48, p.279]) is [37, p.112]

$$\begin{aligned} D_\beta(\tau-\tau';\omega_k) &= \frac{-i}{2\omega_k}\frac{1}{1-\mathrm{e}^{-\beta\omega_k}}\Big\{[\mathrm{e}^{-i\omega_k(\tau-\tau')}+\mathrm{e}^{-\beta\omega_k+i\omega_k(\tau-\tau')}]\theta_C(\tau-\tau') \\ &\quad +[\mathrm{e}^{i\omega_k(\tau-\tau')}+\mathrm{e}^{-\beta\omega_k-i\omega_k(\tau-\tau')}]\theta_C(\tau'-\tau)\Big\}, \end{aligned}$$

where

$$\omega_k = \sqrt{\vec{k}^2+m^2}\,.$$

We next focus on the crucial steps leading to the 2×2 matrix structure. When one takes the limit, $R\to\infty$, in order for the contour, C, in Figure 1.5 to include the complete real-time axis, one obtains

$$D_\beta(\tau_1-\tau_2;\omega_k)\to 0 \qquad \text{as} \qquad R\to\infty \tag{1.43}$$

if τ_1 lies on C_1 or C_2 and τ_2 lies on C_3 or C_4. This result follows from the Riemann–Lebesgue lemma, the application of which in this case is explained in detail in ref. [2, p.171–173]. (See also ref. [49, p.1202] for some further considerations involving this lemma.) The result in eq. (1.43) has the immediate consequence that $Z[j]$ in eq. (1.40) factorizes:

$$Z[j] = Z[j;C_1C_2]Z[j;C_3C_4] \tag{1.44}$$

where

$$\begin{aligned} Z[j;C_1C_2] &= \exp\left\{-i\int_{C_1C_2}d^4x'V\left[\frac{1}{i}\frac{\delta}{\delta j(x')}\right]\right\} \\ &\quad \times\exp\left\{-\frac{i}{2}\int_{C_1C_2}d^4x\int_{C_1C_2}d^4y j(x)D_\beta(x-y)j(y)\right\} \end{aligned} \tag{1.45}$$

and where $\int_{C_1C_2}d^4x$ means that the integration variable, x_0, is restricted to C_1 and C_2 and $Z[j;C_3C_4]$ is similarly defined.

Real-time Green functions are generated by functional differentiation of $Z[j]$ with respect to sources, j, with real time arguments. Since only the factor, $Z[j;C_1C_2]$ in (1.44), contains

sources, j, with time arguments on the real-time axis, C_1, the factor, $Z[j;C_3C_4]$, is irrelevant in obtaining real-time Green functions and may be absorbed into the normalization of $Z[j]$:

$$Z[j] = Z[j;C_1C_2].$$

The time integrals over C_2 in eq. (1.45) cover times with non-zero imaginary part. All the time integrals in eq. (1.45) may be rewritten in terms of real-time integrals by some appropriate redefinitions. Let

$$j_1(x) = j(x), \qquad j_2(x) = j\left(x_0 - \frac{i\beta}{2}, \vec{x}\right), \tag{1.46}$$

$$D_\beta^{11}(x-y) = D_\beta(x-y), \qquad D_\beta^{22}(x-y) = D_\beta(y-x), \tag{1.47}$$

$$D_\beta^{12}(x-y) = -D_\beta^{<}\left(x_0 - \left[y_0 - \frac{i\beta}{2}\right], \vec{x}-\vec{y}\right), \tag{1.48}$$

$$D_\beta^{21}(x-y) = -D_\beta^{>}\left(\left[x_0 - \frac{i\beta}{2}\right] - y_0, \vec{x}-\vec{y}\right), \tag{1.49}$$

where all the time components, x_0 and y_0, appearing in arguments of quantities on the left-hand sides of each of the above six definitions are strictly real.

These definitions enable one to rewrite eq. (1.45) as:

$$\begin{aligned} Z[j;C_1C_2] &= \exp\left\{-i\int_{C_1C_2} d^4x' V\left[\frac{1}{i}\frac{\delta}{\delta j(x')}\right]\right\} \\ &\quad \times \exp\left\{-\frac{i}{2}\int_{C_1C_2} d^4x \int_{C_1C_2} d^4y j(x) D_\beta(x-y) j(y)\right\} \qquad (1.50) \\ &= \exp\left\{-i\int_{-\infty}^{\infty} dx_0' \int d^3x' \left(V\left[\frac{1}{i}\frac{\delta}{\delta j_1(x')}\right] - V\left[\frac{1}{i}\frac{\delta}{\delta j_2(x')}\right]\right)\right\} \\ &\quad \times \exp\left\{-\frac{i}{2}\int_{-\infty}^{\infty} dx_0 \int d^3x \int_{-\infty}^{\infty} dy_0 \int d^3y\, j_a(x) D_\beta^{ab}(x-y) j_b(y)\right\} \qquad (1.51) \\ &\equiv Z[j_1, j_2] \qquad (1.52) \end{aligned}$$

where a, $b = 1, 2$ and a sum over a and b is implied.

The indices, a and b, in D_β^{ab} label the matrix elements of the 2×2 matrix propagator for which the momentum space expression is given in eq. (1.16). Note that a, $b = 1$ in eqs. (1.46)–(1.49) and (1.51) are associated with times on C_1 in eq. (1.50), while a, $b = 2$ are associated with times on C_2 in eq. (1.50).

Since all time integrations in eq. (1.51) run from $-\infty$ to ∞ along the real-time axis, but C_2 in eq. (1.50) runs anti-parallel to the real-time axis, one obtains a relative minus sign between the two V's in eq. (1.51) and a factor of -1 in eqs. (1.48) and (1.49). When times

are on different contour segments, as in eqs. (1.48) and (1.49), the propagator is necessarily retarded or advanced.

1.3.3 The physical and thermal ghost fields

In order to see the emergence of the physical and thermal ghost fields one may rewrite $Z[j_1, j_2]$ in eq. (1.52), after comparison with $Z[j]$ in eq. (1.36), as [37, p.113]

$$\begin{aligned} Z[j_1,j_2] &= \int [d\phi_1][d\phi_2] \exp\left\{\frac{i}{2}\int_{-\infty}^{\infty} dx_0 \int d^3x \int_{-\infty}^{\infty} dy_0 \int d^3y \phi_a(x) D_\beta^{-1^{ab}}(x-y)\phi_b(y)\right. \\ &\left. +i\int_{-\infty}^{\infty} dx_0 \int d^3x(-V[\phi_1]+V[\phi_2]+j_a(x)\phi_a(x))\right\} \end{aligned} \tag{1.53}$$

where, similar to eq. (1.46),

$$\phi_1(x) = \phi(x), \qquad \phi_2(x) = \phi(x_0 - \frac{i\beta}{2}, \vec{x}). \tag{1.54}$$

Since, for real-time Green functions, the x_i in eq. (1.19) must have real time components, the functional derivatives with respect to j's in eq. (1.19) correspondingly become functional derivatives with respect to the j_1's and not the j_2's of eq. (1.46):

$$G_\beta(x_1,\ldots,x_n) = \frac{1}{Z[0,0]}\frac{\delta}{i\delta j_1(x_n)}\cdots\frac{\delta}{i\delta j_1(x_1)} Z[j_1,j_2]\Big|_{j_1=j_2=0}. \tag{1.55}$$

From the factor,

$$\exp\left\{i\int_{-\infty}^{\infty} dx_0 \int d^3x j_a(x)\phi_a(x)\right\},$$

in eq. (1.53), it may be seen that functional derivatives with respect to j_1's will yield ϕ_1's, i.e., fields $\phi(x_0, \vec{x})$ with x_0 on the real-time axis, C_1. Thus, the real-time Green functions, $G_\beta(x_1,\ldots,x_n)$ in eq. (1.55), in terms of diagrams, will only have the physical ϕ_1 fields on the external lines [corresponding to eq. (1.18)] while the ϕ_2 fields will only appear on internal lines and are therefore called thermal ghost fields.

From eqs. (1.53) and (1.54) one sees that the physical field, ϕ_1, 'lives' on the contour, C_1, while the ghost field, ϕ_2, 'lives' on the contour, C_2. Each of the two types of fields self-interacts but they are not directly coupled to each other as may be seen from the interaction terms ($V[\ldots]$) in eqs. (1.51) and (1.53). They are, however, indirectly coupled through the off-diagonal components of the propagator in eq. (1.16) (see also Figure 1.4.). The interaction vertices for each of the two types of fields differ in sign [see eq. (1.17)] due to the relative minus sign between the two V's in eq. (1.51).

An alternative way of understanding the emergence of thermal ghost fields is in the context of thermo field dynamics as may be seen in Section 1.3.6.

1.3.4 The choice of contour, C

At this stage we discuss the specific choice of contour, C, in Figure 1.5. The step, (1.28), tells us that the contour, C, must start at $-R$ and end at $-R-i\beta$. It seems that one could choose an arbitrary contour which starts at $-R$ and ends at $-R-i\beta$. Any specific choice would depend on one's choice of times at which complete sets of states are inserted, in the same manner as was done in eq. (1.29). We already mentioned that a restriction on a choice of contour would be that it includes the complete real-time axis in order to enable one to generate real-time Green functions.

A further restriction is that a time point, which moves along C from $-R$ to $-R-i\beta$, must have a non-increasing imaginary part, i.e., the contour, C, must never 'rise' in the complex-time plane. This restriction comes from considering the domain of analyticity in the time arguments of the Green functions [2, pp. 149, 150],[38, pp. 72–75], [37, p.111]. Consider, for example, the two-point Green function

$$G_\beta(x_1,x_2)=\theta_C(t_1-t_2)G^>_\beta(x_1,x_2)+\theta_C(t_2-t_1)G^<_\beta(x_1,x_2). \tag{1.56}$$

Suppressing reference to spatial coordinates and expanding in eigenstates, $|n>$, of $\hat{H}$, one obtains for $G^>_\beta(x_1,x_2)$:

$$\begin{aligned}
[\mathrm{Tr}\ \mathrm{e}^{-\beta\hat{H}}]G^>_\beta(t_1,t_2) &= \mathrm{Tr}[\mathrm{e}^{-\beta\hat{H}}\mathrm{e}^{i\hat{H}t_1}\hat{\phi}(0)\mathrm{e}^{-i\hat{H}t_1}\mathrm{e}^{i\hat{H}t_2}\hat{\phi}(0)\mathrm{e}^{-i\hat{H}t_2}] \\
&= \sum_n <n|\mathrm{e}^{i\hat{H}(t_1-t_2+i\beta)}\hat{\phi}(0)\underbrace{\sum_m |m><m|}_{1}\mathrm{e}^{-i\hat{H}(t_1-t_2)}\hat{\phi}(0)|n> \\
&= \sum_{m,n}\left|<n|\hat{\phi}(0)|m>\right|^2\mathrm{e}^{iE_n(t_1-t_2+i\beta)}e^{-iE_m(t_1-t_2)}.
\end{aligned} \tag{1.57}$$

On the assumption that the exponentials dominate the convergence of the sum in eq. (1.57), one sees that they converge whenever

$$-\beta<\mathrm{Im}(t_1-t_2)<0.$$

The limit of an analytic function on the boundary of its domain of analyticity is a generalized function (distribution) so that $G^>_\beta(t_1,t_2)$ may be regarded as well-defined for

$$-\beta\leq\mathrm{Im}(t_1-t_2)\leq 0. \tag{1.58}$$

In a similar way, it can be shown that $G^{<}_{\beta}(t_1, t_2)$ is well-defined for

$$0 \leq \mathrm{Im}(t_1 - t_2) \leq \beta. \tag{1.59}$$

Thus one may conclude that the domain of definition of $G_{\beta}(t_1, t_2)$ is given by eq. (1.58) if t_2 precedes t_1 as one moves along C, while the domain is given by eq. (1.59) if t_1 precedes t_2. {In ref. [2, p. 150], the statement,

'the two-point Green function is well defined on the strip

$$-\beta \leq \mathrm{Im}(t_1 - t_2) \leq \beta$$

if we have $\theta_C(t_1 - t_2) = 0$ for $\mathrm{Im}(t_1 - t_2) \geq 0$.'

is not completely correct since, when $\mathrm{Im}(t_1 - t_2) = 0$, one wants $\theta_C(t_1 - t_2) \neq 0$ when t_2 precedes t_1 on a horizontal segment of C.} These conditions on the domain of analyticity of $G_{\beta}(t_1, t_2)$ impose the already mentioned restriction on C that a time point which moves along C must have a non-increasing imaginary part. This restriction on C also guarantees the analyticity of all higher order thermal Green functions with time arguments on C [2, p. 150].

The freedom that is left in the choice of contour, after the above restrictions on C, leads, as discussed for the cases in Section 1.3.7, to the same statistical averages of time-ordered products of fields. Take note that the contour in Figure 1.5 satisfies the above restrictions.

1.3.5 The doubling of degrees of freedom in the real-time formalism

The presence of physical and thermal ghost fields, as discussed in Section 1.3.3, is also referred to as the doubling of degrees of freedom. There are three ways of understanding this doubling of degrees of freedom:

(a) As was shown in Section 1.3.2, only the two infinite contour segments, C_1 and C_2 in Figure 1.5, are relevant in the path-integral approach to the evaluation of real-time thermal Green functions. Each of these two contour segments has its own field associated with it (see Section 1.3.3 where the existence of a physical and thermal ghost field was pointed out). The necessity of having at least both these contour segments in the real-time formalism comes from setting out with the trace in eq. (1.24), requiring the inclusion of the complete real-time axis and treating the factor, $\mathrm{e}^{-\beta\hat{H}}$ in eq. (1.20), perturbatively. The latter treatment requires, via eqs. (1.27) and (1.28) and bearing

in mind the intermediate path-integral expressions, eqs. (1.30) and (1.35), that the contour, after having included the real-time axis, has to return to the point $-R - i\beta$. This requirement gives rise to at least a second infinitely long contour segment which, for the case in Figure 1.5, is C_2.

(b) The path-integral (time-path) method discussed so far is by its nature a method on the level of Green functions. It is limited in the sense that one does not have available all the tools of quantum field theory, since it is not on the level of operators. As was mentioned at the beginning of Section 1.3, an operator formulation of finite-temperature quantum field theory, called thermo field dynamics, has recently been developed. In this theory one has at one's disposal all the techniques of quantum field theory including not only the Green function method and the Feynman diagram method, but also the method of canonical transformations of operators as well as the concept of the finite-temperature vacuum [50].

In Section 1.3.6 it is demonstrated how, in thermo field dynamics, a doubling of degrees of freedom naturally arises when one attempts to represent the statistical ensemble average of an arbitrary operator, $\hat{A}$, which involves a trace over an infinite number of states, by the expectation value of $\hat{A}$ in a single finite-temperature vacuum, $|0(\beta)>$:

$$< \hat{A} >= [\mathrm{Tr}\ \mathrm{e}^{-\beta\hat{H}}]^{-1}\mathrm{Tr}(\mathrm{e}^{-\beta\hat{H}}\hat{A}) =< 0(\beta)|\hat{A}|0(\beta) > . \qquad (1.60)$$

(c) The requirement of a doubling of degrees of freedom has also been shown in the formal and abstract field of axiomatic statistical physics through the use of the C^*-algebra [2, pp. 181–193]. The relation between this operator-algebra approach and thermo field dynamics [referred to under the previous point (b)] has been clarified by Ojima [51].

1.3.6 Thermo field dynamics [36, 3]

The need for an operator formulation of finite-temperature quantum field theory was explained under point 1.3.5(b). In this section we follow some of the main ideas presented in the paper by Takahashi and Umezawa [36] on such a formulation, called thermo field dynamics. The ideas are easy to follow and are illustrated by simple examples.

The idea is to replace the trace operation in the evaluation of a statistical average by an expectation value in a finite-temperature vacuum, $|0(\beta)>$, as indicated in eq. (1.60). Such

a vacuum, however, cannot be constructed in the original Hilbert space as may be seen as follows: Expand $|0(\beta)>$ in terms of energy eigenstates, $|n>$,

$$|0(\beta)>=\sum_n |n> f_n(\beta), \tag{1.61}$$

where

$$\hat{H}|n> = E_n|n>, \tag{1.62}$$

$$<n|m> = \delta_{mn}. \tag{1.63}$$

Require that $|0(\beta)>$ in eq. (1.61) satisfies eq. (1.60), i.e.:

$$<0(\beta)|\hat{A}|0(\beta)>=Z^{-1}(\beta)\sum_n <n|\hat{A}|n> \mathrm{e}^{-\beta E_n}, \tag{1.64}$$

where

$$Z(\beta) = \mathrm{Tr}(\mathrm{e}^{-\beta\hat{H}}).$$

Substituting eq. (1.61) into eq. (1.64), one obtains

$$<0(\beta)|\hat{A}|0(\beta)>=\sum_{nm} f_n^*(\beta) f_m(\beta) <n|\hat{A}|m>$$

which implies that

$$f_n^*(\beta) f_m(\beta) = Z^{-1}(\beta)\mathrm{e}^{-\beta E_n}\delta_{nm} \tag{1.65}$$

in order to satisfy eq. (1.64). It is, however, impossible for c-numbers to satisfy eq. (1.65), as may be seen by considering the case $n = m$ in eq. (1.65):

$$|f_n(\beta)|^2 = Z^{-1}(\beta)\mathrm{e}^{-\beta E_n}. \tag{1.66}$$

By writing $f_n(\beta)$ in eq. (1.66) in the form

$$f_n(\beta) = \left(|Z^{-1}(\beta)|\mathrm{e}^{-\beta E_n}\right)^{\frac{1}{2}} \mathrm{e}^{i\theta} \tag{1.67}$$

for some θ and substituting eq. (1.67) into the left-hand side of eq. (1.65), one sees that one can have

$$f_n^*(\beta) f_m(\beta) \neq 0 \qquad \text{for } n \neq m,$$

which contradicts eq. (1.65).

Takahashi and Umezawa [36] get around this problem by introducing a second fictitious dynamical system, identical to the original one, and denoting quantities associated with the second system by the tilde,

$$\tilde{\hat{H}}|\tilde{n}> = E_n|\tilde{n}> \tag{1.68}$$

$$<\tilde{n}|\tilde{m}> = \delta_{nm} \tag{1.69}$$

with E_n the same as in eq. (1.62). They then work in the space spanned by the direct product of $|n>$ and $|\tilde{m}>$, which is denoted by $|n,\tilde{m}>$. Corresponding to

$$\hat{A} \equiv \hat{A} \otimes \hat{1}$$

one has

$$\tilde{\hat{A}} \equiv \hat{1} \otimes \tilde{\hat{A}}$$

so that

$$<\tilde{m},n|\hat{A}|n',\tilde{m}'> = <n|\hat{A}|n'>\delta_{mm'}, \tag{1.70}$$

$$<\tilde{m},n|\tilde{\hat{A}}|n',\tilde{m}'> = <m|\tilde{\hat{A}}|m'>\delta_{nn'}. \tag{1.71}$$

The finite-temperature vacuum is constructed in the direct-product space as follows:

$$|0(\beta)>= Z^{-\frac{1}{2}}(\beta)\sum_n \mathrm{e}^{-\beta E_n/2}|n,\tilde{n}> . \tag{1.72}$$

This construction leads, via eq. (1.70), to the required property in eq. (1.64).

By considering the simple example of an ensemble of free fermions with frequency, ω, it may be seen how a complete set of orthonormal vectors containing $|0(\beta)>$ is constructed [36]. The Hamiltonian is

$$\hat{H} = \omega a^\dagger a \tag{1.73}$$

with

$$\{a,a^\dagger\} = 1, \qquad \{a,a\} = 0. \tag{1.74}$$

The orthonormal state vectors are $|0>$ and $a^\dagger|0>$ where

$$a|0>= 0 \qquad \text{and} \qquad <0|0>= 1.$$

To construct $|0(\beta)>$, a second, fictitious system is introduced:

$$\tilde{\hat{H}} = \omega\tilde{a}^\dagger\tilde{a}$$

with

$$\{\tilde{a}, \tilde{a}^\dagger\} = 1 \qquad \{\tilde{a}, \tilde{a}\} = 0 \tag{1.75}$$

and where it is required that [51, p.5]

$$\{a, \tilde{a}\} = \{a, \tilde{a}^\dagger\} = \{a^\dagger, \tilde{a}\} = \{a^\dagger, \tilde{a}^\dagger\} = 0. \tag{1.76}$$

The state vector space of the total system is spanned by

$$|0>, \quad a^\dagger|0>, \quad \tilde{a}^\dagger|0>, \quad a^\dagger\tilde{a}^\dagger|0> \tag{1.77}$$

where $|0, \tilde{0}>$ is denoted by $|0>$. The state, $|0(\beta)>$, is then constructed by using the recipe in eq. (1.72):

$$|0(\beta)>= \frac{1}{\sqrt{1+\mathrm{e}^{-\beta\omega}}}\{|0> + \mathrm{e}^{-\beta\omega/2}a^\dagger\tilde{a}^\dagger|0>\}. \tag{1.78}$$

It is then straightforward to check that the statistical average of the number operator is

$$\begin{aligned} < 0(\beta)|a^\dagger a|0(\beta) > &= \frac{1}{\mathrm{e}^{\beta\omega}+1} \\ &\equiv n_{\mathrm{F}}(\omega) \end{aligned}$$

as required for a system of fermions in thermal equilibrium.

It may also be seen that the state, $|0(\beta)>$, is obtained from $|0> \equiv |0, \tilde{0}>$ by a Bogoliubov transformation. Let

$$u(\beta) = \sqrt{1 - n_{\mathrm{F}}(\omega)}, \qquad v(\beta) = \sqrt{n_{\mathrm{F}}(\omega)}. \tag{1.79}$$

Then

$$\begin{aligned} u(\beta)^2 + v(\beta)^2 &= 1, \\ |0(\beta)> &= \{u(\beta) + v(\beta)a^\dagger\tilde{a}^\dagger\}|0> \\ &= \mathrm{e}^{-iG_{\mathrm{F}}}|0>, \end{aligned}$$

where

$$G_{\mathrm{F}} = G_{\mathrm{F}}^\dagger = -i\theta(\beta)(\tilde{a}a - a^\dagger\tilde{a}^\dagger),$$

with

$$\cos\theta(\beta) = u(\beta).$$

The operators, a,$\tilde{a}$, are Bogoliubov-transformed as follows:

$$a(\beta) = \mathrm{e}^{-iG_{\mathrm{F}}} a \mathrm{e}^{iG_{\mathrm{F}}} = u(\beta)a - v(\beta)\tilde{a}^{\dagger} \tag{1.80}$$

$$\tilde{a}(\beta) = \mathrm{e}^{-iG_{\mathrm{F}}} \tilde{a} \mathrm{e}^{iG_{\mathrm{F}}} = u(\beta)\tilde{a} + v(\beta)a^{\dagger}. \tag{1.81}$$

These newly defined temperature-dependent operators on the left-hand sides of eqs. (1.80) and (1.81) and their hermitian conjugates satisfy the same anti-commutation relations as in eqs. (1.74), (1.75) and (1.76). Since

$$a(\beta)|0(\beta)>= \tilde{a}(\beta)|0(\beta)>= 0, \tag{1.82}$$

the state, $|0(\beta)>$, is called the finite-temperature or thermal vacuum. The physical picture behind the Bogoliubov transformation is that $a^{\dagger}$ creates thermally unstable quanta, whereas the quasiparticles created by $a^{\dagger}(\beta)$ are stable in view of eq. (1.82). The Fock space obtained from eq. (1.77) by the Bogoliubov transformation is

$$|0(\beta)>, \quad a^{\dagger}(\beta)|0(\beta)>, \quad \tilde{a}^{\dagger}(\beta)|0(\beta)>, \quad a^{\dagger}(\beta)\tilde{a}^{\dagger}(\beta)|0(\beta)> .$$

The latter states are not eigenstates of $\hat{H}$ in eq. (1.73). They are eigenstates of the combination

$$\hat{\tilde{H}} \equiv \hat{H} - \hat{\tilde{H}} = \omega(a^{\dagger}a - \tilde{a}^{\dagger}\tilde{a}) = \omega\left[a^{\dagger}(\beta)a(\beta) - \tilde{a}^{\dagger}(\beta)\tilde{a}(\beta)\right],$$

$$\hat{\tilde{H}}|0(\beta)>= 0, \qquad \hat{\tilde{H}}a^{\dagger}(\beta)\tilde{a}^{\dagger}(\beta)|0(\beta)>= 0,$$
$$\hat{\tilde{H}}a^{\dagger}(\beta)|0(\beta)>= \omega a^{\dagger}(\beta)|0(\beta)>, \qquad \hat{\tilde{H}}\tilde{a}^{\dagger}(\beta)|0(\beta)>= -\omega\tilde{a}^{\dagger}(\beta)|0(\beta)> .$$

Thus, $\hat{\tilde{H}}$ can be viewed as the 'total' Hamiltonian of the system consisting of non-tilde and tilde quanta. When one is interested in the statistical average of the energy of a system at finite temperature, one evaluates $< 0(\beta)|\hat{H}|0(\beta) >$ and not $< 0(\beta)|\hat{\tilde{H}}|0(\beta) >$. In the discussion following eq. (1.88) more will be said about the meaning of $\hat{\tilde{H}}$.

In ref. [36], the cases of bosons, free fields and interacting fields are also treated along similar lines as above. In the case of an ensemble of free *bosons* with frequency, ω, one obtains, for example for $|0(\beta) >$, instead of eq. (1.78),

$$|0(\beta)>= \sqrt{1 - \mathrm{e}^{-\beta\omega}} \exp(\mathrm{e}^{-\beta\omega/2} a^{\dagger}\tilde{a}^{\dagger})|0,\tilde{0}> . \tag{1.83}$$

The general rule which relates operators with tilde to those without tilde is formulated in refs. [3, pp. 125–127] and [2, p. 188]. For any Heisenberg operator, $\hat{A}$, which may, for

example, be a function of fields, $\hat{\phi}(x)$, a dual operator, $\hat{\tilde{A}}$, is obtained by the following rules:

$$\widetilde{\hat{A}_1\hat{A}_2} = \hat{\tilde{A}}_1\hat{\tilde{A}}_2 , \tag{1.84}$$

$$\widetilde{\lambda_1\hat{A}_1 + \lambda_2\hat{A}_2} = \lambda_1^*\hat{\tilde{A}}_1 + \lambda_2^*\hat{\tilde{A}}_2 , \tag{1.85}$$

where λ_1 and λ_2 are complex numbers. In ref. [52, p.537] an indication is given as to why the tilde conjugate of a c-number is its complex conjugate. The tilde form of the Heisenberg equation [where the Hamiltonian in eq. (1.86) may contain interaction terms too],

$$[i\hat{H}, \hat{\phi}] = \dot{\hat{\phi}} \tag{1.86}$$

is obtained by means of the rules in eqs. (1.84) and (1.85) as

$$[-i\hat{\tilde{H}}, \hat{\tilde{\phi}}] = \dot{\hat{\tilde{\phi}}}. \tag{1.87}$$

By taking into account the (anti-) commutativity between the tilde and non-tilde objects [see, e.g., eq. (1.76)], eqs. (1.86) and (1.87) can be unified into

$$[i(\hat{H} - \hat{\tilde{H}}), \hat{\phi}] = \dot{\hat{\phi}} \qquad \text{and} \qquad [i(\hat{H} - \hat{\tilde{H}}), \hat{\tilde{\phi}}] = \dot{\hat{\tilde{\phi}}}. \tag{1.88}$$

The operator,

$$\hat{\bar{H}} = \hat{H} - \hat{\tilde{H}}, \tag{1.89}$$

is thus the generator of time translations in the doubled space. In accordance with eq. (1.89) the 'total' Lagrangian is

$$\hat{\bar{\mathcal{L}}} = \hat{\mathcal{L}} - \hat{\tilde{\mathcal{L}}}. \tag{1.90}$$

The minus sign in eq. (1.90) is reminiscent of the minus sign between the two V's in eq. (1.51) and will also lead to a difference of sign between the type-1 vertices for the ordinary fields and the type-2 vertices for the tilde fields in the thermo field dynamics method. By defining a 'thermal doublet' [53],

$$\begin{pmatrix} \hat{\phi}_1 \\ \hat{\phi}_2 \end{pmatrix} = \begin{pmatrix} \hat{\phi} \\ \hat{\tilde{\phi}}^\dagger \end{pmatrix}$$

one can derive an expression for the free propagator by evaluating

$$< 0(\beta)|T\left[\begin{pmatrix} \hat{\phi}(x) \\ \hat{\tilde{\phi}}^\dagger(x) \end{pmatrix}\left(\hat{\phi}^\dagger(y)\ ,\ \hat{\tilde{\phi}}(y)\right)\right]|0(\beta)> .$$

The result is similar to the 2×2 matrix propagator obtained in the path-integral approach. Real-time thermal Green functions can therefore also be obtained in the formalism of thermo field dynamics where perturbative expansions involve similar Feynman rules as in the path-integral approach.

We conclude this section by drawing attention to a remarkable feature of thermo field dynamics which follows from the tilde substitution law (also called the thermal state condition). The tilde substitution law is as follows [36, p.66]:

$$e^{\beta\hat{\tilde{H}}/2}\hat{A}|0(\beta)>=\sigma_A e^{\beta\hat{H}/2}\hat{\tilde{A}}^{\dagger}|0(\beta)> \tag{1.91}$$

where $\hat{A}$ is an arbitrary monomial of bose and fermi operators, b, $b^{\dagger}$, a and $a^{\dagger}$, of non-tilde type, $\hat{\tilde{A}}$ is obtained from $\hat{A}$ by the rules in eqs. (1.84) and (1.85) and σ_A is a certain phase factor such that $|\sigma_A| = 1$. The tilde substitution rule may be rewritten in terms of Heisenberg operators,

$$\hat{A}(t) \equiv e^{i\hat{H}t}\hat{A}e^{-i\hat{H}t}, \qquad \hat{\tilde{A}}(t) \equiv e^{-i\hat{\tilde{H}}t}\hat{\tilde{A}}e^{i\hat{\tilde{H}}t}$$

as follows:

$$\hat{A}(t)|0(\beta)>=\sigma_A\hat{\tilde{A}}^{\dagger}(t-i\beta/2)|0(\beta)>. \tag{1.92}$$

It is derived in refs. [36, pp. 62,66] and [3, pp. 142–144] by generalizing eq. (1.96). The tilde substitution rule is the origin of the KMS (Kubo–Martin–Schwinger) condition [54, 55] in thermo field dynamics [36, p.66],[3, p.145]. [In the C^*-algebra formalism for statistical mechanics, mentioned under point 1.3.5(c), the KMS condition is a basic axiom whereas, in the path-integral approach to real-time Green functions and in the imaginary-time formalism, the KMS condition is embodied in eqs. (1.42) and (1.7), respectively.]

From eq. (1.92), there follows the remarkable feature of thermo field dynamics that, for an arbitrary $\hat{A}(t)$, there always exists a certain combination of $\hat{A}(t)$ and $\hat{\tilde{A}}^{\dagger}(t)$, i.e.,

$$\hat{A}(t) - \sigma_A\hat{\tilde{A}}^{\dagger}(t-i\beta/2),$$

which annihilates the finite-temperature vacuum, $|0(\beta)>$. The fact that any operator is associated with a generalized annihilation operator, provides one with a very wide class of reduction formulae which frequently helps practical computations [56]. It also helps one express retarded Green functions in terms of causal ones, which is useful in response theory [56].

1.3.7 The relation between thermo field dynamics and the time-path method

The time-path method discussed so far can be traced back [2, pp. 144, 152] to the early work of Schwinger [57], Craig [58], Keldysh [59] and others on non-equilibrium quantum statistics where a closed contour in the complex-time plane, running along the entire real-time axis and back, was considered (the 'closed time-path method'). As noted by Marinaro [60], one may regard the imaginary-time formalism of Matsubara, the time-path and thermo field dynamics methods in the real-time formalism and the closed time-path method for non-equilibrium systems from a unified point of view by considering the work of Mills [38].

In 1969, Mills introduced a finite-temperature formalism by generalizing (in order to consider statistical averages) the evolution operator at zero temperature [4],

$$\hat{U}(t,t_0) = \sum_{n=0}^{\infty} \frac{(-i)^n}{n!} \int_{t_0}^{t} dt_1 \ldots \int_{t_0}^{t} dt_n T[\hat{H}_{\rm I}(t_1)\ldots\hat{H}_{\rm I}(t_n)]$$

where the time integrals are along the real axis (from t_0 to t) and $\hat{H}_{\rm I}(t)$ is the interaction Hamiltonian in the interaction picture, to

$$\hat{U}(\tau,\tau_0) = \sum_{n=0}^{\infty} \frac{(-i)^n}{n!} \int_{C} d\tau_1 \ldots \int_{C} d\tau_n T_C[\hat{H}_{\rm I}(\tau_1)\ldots\hat{H}_{\rm I}(\tau_n)],$$

where T_C is defined just after eq. (1.20) and C is an arbitrary path in the complex-time plane with the only restriction that it must nowhere 'rise' in the complex-time plane [38, pp. 73–75]. This restriction is the same as the one derived in Section 1.3.4. The formalism of Mills is the canonical quantization version of the time-path method already discussed in the path-integral quantization approach (wherein different time paths may be considered) and, as such, may also be referred to as a time-path method. Mills showed that the Matsubara method (corresponding to the time path in Figure 1.2) and the closed time-path method of non-equilibrium quantum statistics are particular cases of his general perturbative expansion.

Matsumoto et al. [61] took this point further by showing that the perturbative expansions obtained from the thermo field dynamics method and the Mills method coincide, provided that the time path in the Mills method is suitably chosen. They considered a class of contours in the Mills time-path method by varying σ in Figure 1.6. They obtained a 2×2 matrix for the two-point function with σ-dependent off-diagonal elements, which reduces to the two-point function in thermo field dynamics for the choice $\sigma = \beta/2$ (corresponding to the contour in Figure 1.5).

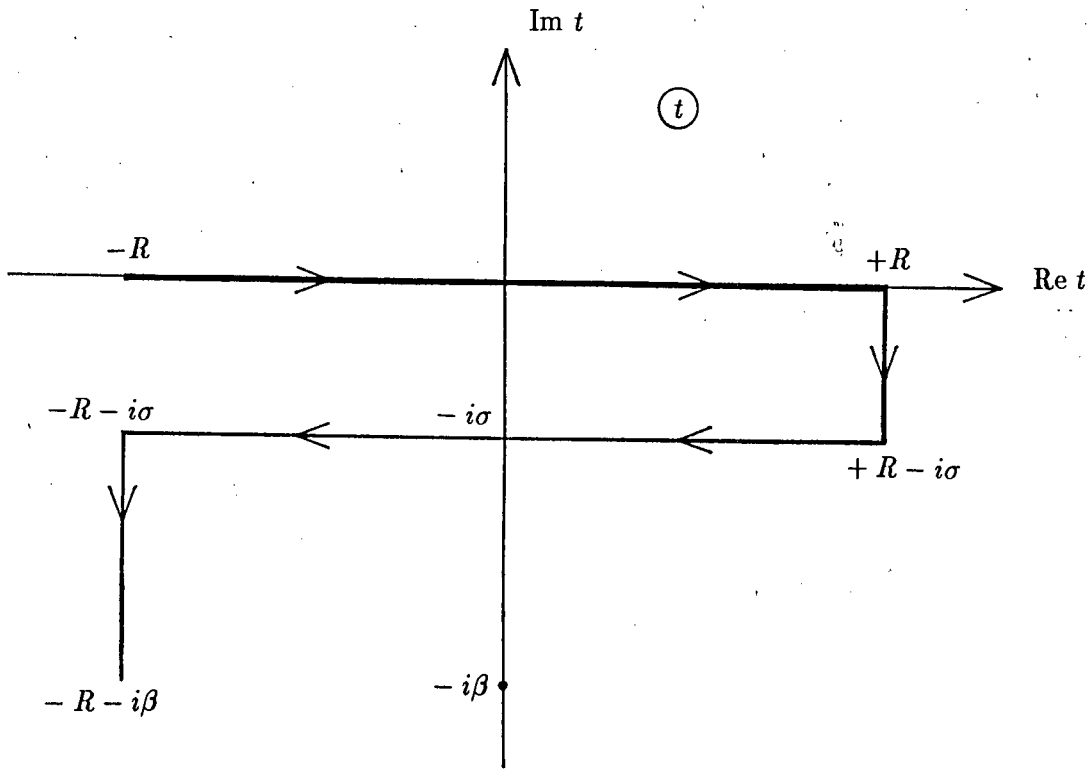

Figure 1.6: The time-path considered by Matsumoto et al. in refs. [60, 61].

Furthermore, they were able to construct a perturbative expansion in a quantum field theoretical formulation (which is a generalization, to some extent, of the thermo field dynamics discussed in Section 1.3.6) corresponding to each perturbative expansion obtained in the Mills time-path method for a specific choice of σ. They did this by making the correspondences,

$$\hat{\phi}(t) \to \hat{\phi}(t,\gamma), \qquad \hat{\phi}^\dagger(t) \to \hat{\phi}^\dagger(t,\gamma), \tag{1.93}$$

$$\hat{\phi}(t-i\sigma) \to \hat{\tilde{\phi}}^\dagger(t,\gamma), \qquad \hat{\phi}^\dagger(t-i\sigma) \to \hat{\tilde{\phi}}(t,\gamma), \tag{1.94}$$

where $\gamma = \sigma - \beta/2$, t is real and spatial coordinates are suppressed. The fields on the left-hand sides of the arrows in eqs. (1.93) and (1.94) are those in the time-path method having support on the horizontal contour segments in Figure 1.6, while those on the right-hand sides are the newly introduced fields in the generalized thermo field dynamics. The latter fields are regarded as satisfying the following relation (amongst others stated in ref. [61]):

$$[\hat{\phi}(t,\gamma), \hat{\tilde{\phi}}(t,\gamma)] = 0 \tag{1.95}$$

even though the corresponding [via eqs. (1.93) and (1.94)] original fields $\hat{\phi}(t)$ and $\hat{\phi}^\dagger(t-i\sigma)$

in the time-path method do not commute. Thus, even thoughcontour, C, of e.g. eq.(1.24) consisting of segments C_1, C_3, C_2 and C_4 in, corresponding to a specific value of σ, the perturbative expansions derived from the generalized thermo field dynamics and the Mills method coincide, it is not correct to directly equate the tilde field, $\tilde{\hat{\phi}}^{\dagger}(t,\gamma)$ of thermo field dynamics, with the corresponding type-2 field, $\hat{\phi}(t - i\sigma)$ (associated with the lower horizontal contour segment), in the time-path method. The reason for this, according to Landsman [2, p. 192], is that different representations of the algebra of operator fields [referred to under point 1.3.5(c)] are involved.

Matsumoto et al. [61] furthermore prove that observable quantities are independent of the value of σ, which corresponds to the discovery by Mills [38] that physical results are independent of the particular choice of contour in the complex-time plane. The proof of Matsumoto et al. is based on energy conservation which holds separately for the tilde and non-tilde fields.

In an ensuing article by Matsumoto et al. [62], they considered the class of contours depicted in Figure 1.7. Again they generalized thermo field dynamics by associating an independent field with each of the $2N$ horizontal contour segments, obtaining one physical field and $2N - 1$ thermal ghost fields. For each choice of the ρ_i and σ_i, where

$$i = 1, 2, \ldots, N; \qquad 0 = \rho_1 < \sigma_1 < \rho_2 < \sigma_2 < \ldots < \rho_N < \sigma_N \leq \beta,$$

the perturbative expansions derived from the generalized thermo field dynamics and the corresponding time-path method coincided.

Since the two-point function involves a $2N \times 2N$ matrix, this formalism is not convenient. The hermiticity of operators in the generalized thermo field dynamics can also not be preserved for $N > 1$ while it can be preserved for $N = 1$ (corresponding to a two-component formalism) *and* $\sigma = \beta/2$. In addition, the 2×2 matrix propagator becomes symmetric when $\sigma = \beta/2$. Thus the value $\sigma = \beta/2$ for the case $N = 1$, corresponding to the contour in Figure 1.5, seems to be a privileged value in the two-component real-time formalism.

A four-component formalism (corresponding to $N = 2$) has found application in the treatment of a quantum field theory coupled to a classical gravitational field [63].

1.3.8 Attempts to interpret the tilde objects in thermo field dynamics

According to Ojima [51, p. 2],

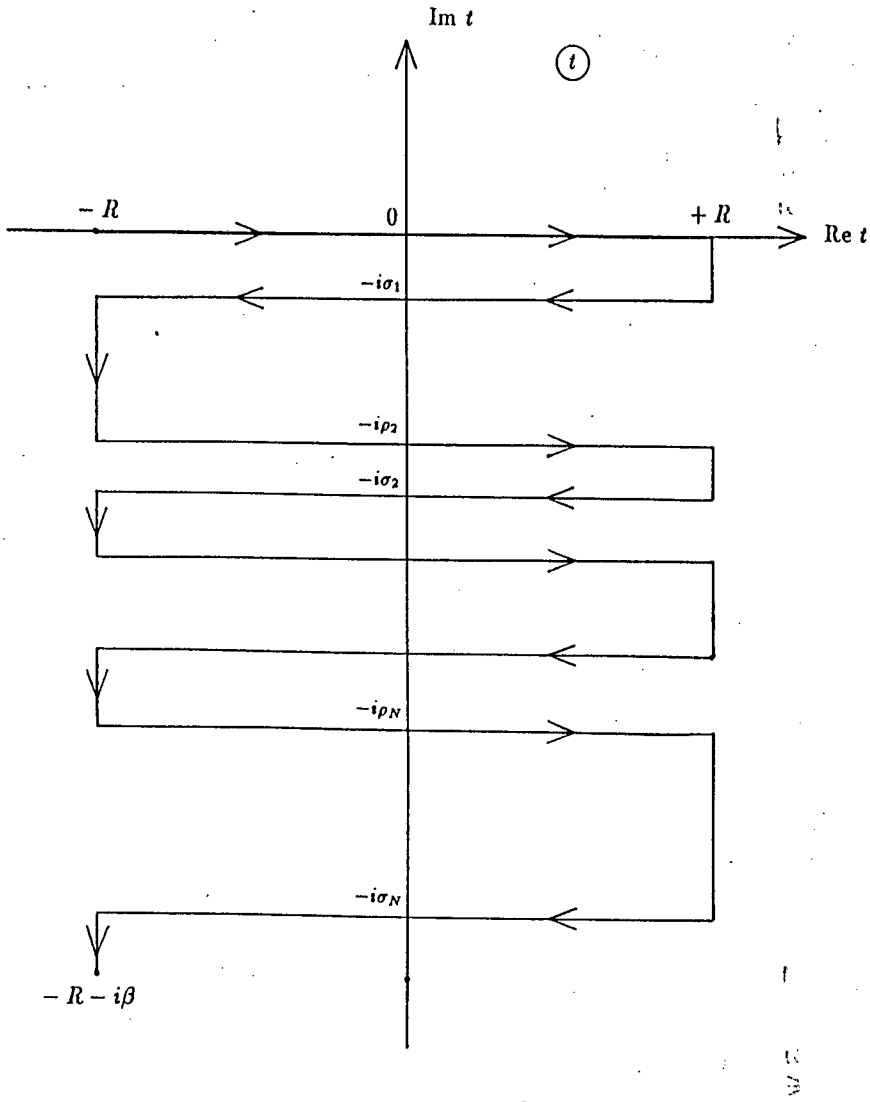

Figure 1.7: The time-path considered by Matsumoto et al. in ref. [61].

'the physical meaning of the tilde objects $\tilde{A}$ is rather unclear'.

Umezawa, who introduced thermo field dynamics in 1974 [35], has the following to say in 1989 [64, p.313]:

> 'Where does the tilde freedom come from? I simply do not have any answer to this question.'

Nevertheless, attempts to interpret the tilde objects appear in the literature. We refer to some of them.

Takahashi and Umezawa [36, p. 59] consider the 'one particle state',

$$a^\dagger(\beta)|0(\beta)>$$

where, in this discussion, we use quantities defined in Section 1.3.6. From eqs. (1.81) and (1.82), it follows that,

$$\tilde{a}(\beta)|0(\beta)>=\left(u(\beta)\tilde{a}+v(\beta)a^{\dagger}\right)|0(\beta)>=0$$

and therefore,

$$\frac{1}{v(\beta)}\tilde{a}|0(\beta)>=-\frac{1}{u(\beta)}a^{\dagger}|0(\beta)>. \tag{1.96}$$

The relations in eqs. (1.80) and (1.81) may be inverted:

$$a = u(\beta)a(\beta)+v(\beta)\tilde{a}^{\dagger}(\beta), \tag{1.97}$$

$$\tilde{a} = u(\beta)\tilde{a}(\beta)-v(\beta)a^{\dagger}(\beta). \tag{1.98}$$

From eqs. (1.96), (1.98), (1.82) and (1.79) it then follows that

$$\begin{aligned} a^{\dagger}(\beta)|0(\beta)> &= -\frac{1}{\sqrt{n_{\mathrm{F}}(\omega)}}\tilde{a}|0(\beta)> \\ &= \frac{1}{\sqrt{1-n_{\mathrm{F}}(\omega)}}a^{\dagger}|0(\beta)>. \end{aligned} \tag{1.99}$$

Takahashi and Umezawa loosely interpret eq. (1.99) as follows:

> "the 'one particle state' is built from the thermal equilibrium state $|0(\beta)>$ by adding one particle or by eliminating one particle with tilde. We may interpret therefore that the particle with tilde is a hole of the physical particle."

They interpret the normalization factor, $\sqrt{1-n_{\mathrm{F}}(\omega)}$, as characteristic of the quantum process in which one quantum is added to a system containing $n_{\mathrm{F}}(\omega)$ quanta. (Recall our discussion on the Pauli-blocking factor in Section 1.1.)

Considering expressions for $|0(\beta)>$ such as those in eqs. (1.78) or (1.83), one may state that there are an equal number of particles and holes in the thermal vacuum. Umezawa et al. elaborate on these interpretations in ref. [3, p. 120]: For a system immersed in a heat bath, there is a two-way exchange of energy between the system and the heat bath. The presence of the heat bath maintains excited quanta in the system. Therefore the system absorbs energy either by exciting additional quanta or by annihilating 'holes' of particles maintained by the heat bath. When the latter process takes place, they say that an $\tilde{a}$-quantum (hole) with negative energy, $(-\omega)$, is annihilated. The excitation of an additional quantum is described by the creation operator, $a^{\dagger}(\beta)$, while the annihilation of an $\tilde{a}$-quantum is described by $\tilde{a}(\beta)$.

Since $a^\dagger$ performs two independent operations, it is a linear combination of $a^\dagger(\beta)$ and $\tilde{a}(\beta)$ as in the hermitian conjugate of eq. (1.97). These dual roles, according to Rivers [48, p. 275], suggest the doubling of degrees of freedom discussed in Section 1.3.5.

Leplae et al. [35, p. 229] state that, since one needs only the non-tilde quanta in the zero-temperature formalism, the tilde quanta are superfluous at zero temperature. However, the states which contain tilde quanta become important at non-zero temperature. The existence of the tilde quanta is a manifestation of the freedom of thermal excitation and they call the tilde quantum the thermon.

In refs. [52, pp. 538, 554] and [64, p. 312], the tilde quanta are regarded as hidden variables but it is explained how, by modifying the thermal situation, they can have an observable physical effect. It is also argued that the effect of randomization in statistical mechanics is produced by the effects of the hidden tilde quanta.

Kreuzer and Kuper [65, 66] describe the approach of a system to thermal equilibrium by allowing a weak interaction between the physical and tilde systems. This represents a generalization of the thermo field dynamics formalism for systems at thermal equilibrium for which no interaction between physical and tilde particles exist. In their analysis the system of tilde particles is regarded as a representative member of a Gibbsian statistical ensemble.

The tilde-type freedom naturally appears in another area of physics. In an article by Israel [67], who gives further references, attention is directed to the thermal character of the 'vacuum' perceived by stationary observers outside a black hole and also by uniformly accelerated observers in Minkowski space-time. This is a consequence of the information loss associated with the presence of event horizons. Israel elucidates the close parallel of these results with thermo field dynamics: Whereas in thermo field dynamics the system of tilde particles has a merely formal significance, in the context of Israel's work, it can be interpreted in terms of particle states on the hidden side of the horizon. Umezawa himself too discusses this point in ref. [64, p. 313].

1.4 Conclusion: Advantages of the real-time formalism

Real-time thermal Green functions are needed in calculations involving time-dependent processes in a heat bath, such as decay and scattering reactions, and even in ref. [42] for the evaluation of thermodynamic quantities. One of the main advantages of the real-time

formalism is the direct way in which real-time thermal Green functions can be derived without having to perform potentially very complicated analytic continuations of imaginary-time Green functions. The elegance of the formalism naturally leads to further advantages.

The Feynman diagram method involving thermal real-time causal Green functions is formulated very much like in the conventional zero-temperature formalism. The topological and combinatorical structures of Feynman diagrams do not change in going from zero to non-zero temperature, but are generalized to a two-component formalism so that, e.g., the free propagator acquires a 2×2 matrix structure. This so-called doubling of degrees of freedom provides a mechanism for the cancellation of singularities, which arise (see the end of Sections 1.2.2 and 1.3.1) from products of Dirac delta functions with coinciding arguments, among themselves. As discussed in Section 1.3.1, the two-component formalism leads to an increase in the number of diagrams, but, the number of diagrams to be evaluated may be reduced by making use of finite-temperature Cutkosky rules.

In Section 1.2.2 it was mentioned that the thermodynamic potential, from which static thermodynamic quantities can be derived, could be evaluated in the imaginary-time formalism. However, the discrete energy summations [see eq. (1.11)] associated with loops can be very tedious to evaluate, especially in the presence of overlapping loops. These summations are usually transformed into contour integrals. On the other hand, in the real-time formalism the continuous energy integrals associated with loops simplify calculations. Niemi and Semenoff [42] applied real-time methods to calculations of thermodynamic quantities and found them much simpler than the imaginary-time methods. They were able to perform systematic low-temperature and high-temperature expansions, whereas low-temperature expansions are less accessible in the imaginary-time formalism. The reason for this is that, in the real-time formalism, the zero-temperature and finite-temperature contributions to the free thermal propagator [eq. (1.16)] are well separated. This is not the case in the imaginary-time formalism [see eq. (1.13)]. One notices that, in the zero-temperature limit ($\beta \to \infty$), the off-diagonal matrix elements of the real-time free thermal propagator vanish and therefore also the indirect coupling between the type-1 and type-2 fields. Since the second terms in each of the diagonal matrix elements of the real-time free thermal propagator vanish too, the zero-temperature theory for the decoupled type-1 fields is recovered.

The influence of finite-temperature effects on the established results for zero-temperature

quantum field theory has been extensively investigated. Usually, the real-time methods have been found to be better suited for these investigations than imaginary-time methods. For example, Matsumoto et al. [68] found the proof of renormalizability more transparent and systematic using real-time methods. They found that all ultraviolet divergences in perturbation expansions of real-time causal Green functions at finite temperature can be eliminated to all orders by the counterterms prepared at zero temperature, provided the theory is renormalizable at zero temperature. The same result has been found in the imaginary-time formalism, but with increased difficulty [69]. The fact that, at finite temperature, ultraviolet divergences are treated in the same way as at zero temperature, stems from the fact that ultraviolet divergences arise from the singular short-distance behaviour of quantum field theory, which is unaffected by the presence of a heat bath. The presence of the heat bath, however, does worsen the infrared divergences owing to an additional divergence in the Bose–Einstein statistical weights. This may be seen, for example, from the expression of the free thermal propagator in eq. (1.16) where a factor, such as

$$\frac{1}{e^{\beta|k_0|}-1},$$

diverges in the limit, $k_0 \to 0$. Using real-time methods, the cancellation of all infrared divergences at finite temperature has been proven for some physical processes although, so far, only up to one-loop order [14] – [17], [20] – [22], [8]. In these references, a requirement for the infrared singularities to cancel is that there exists a relation between the distributions of fermions and bosons. This relation is provided by the principle of detailed balance existing for thermal equilibrium.

Finite-temperature field theory is not manifestly Lorentz invariant, since the heat bath defines a preferred frame of reference. It is, however, possible to maintain manifest Lorentz covariance in the real-time formalism by introducing a four-velocity for the heat bath [70]:

$$u^\mu = \gamma(1, \vec{v}),$$

$$\gamma = (1-\vec{v}^2)^{-\frac{1}{2}}, \qquad u^2 = 1, \qquad c = 1.$$

The boson thermal distribution function, *for example*, is then written as

$$n_{\rm B}(k) = \frac{1}{e^{\beta|k.u|}-1},$$

where β is considered to be a Lorentz invariant parameter and interpreted as the inverse temperature of the heat bath for $\vec{v} = 0$. Thus, the expressions used in this thesis, e.g.,

$$\frac{1}{e^{\beta|k_0|} - 1}$$

are those for the heat bath at rest ($\vec{v} = 0$). The importance of a Lorentz covariant treatment of a system at finite temperature has been stressed by Ruiz Ruiz and Alvarez–Estrada [70].

In the thermo field dynamics approach to a real-time formalism, one has at one's disposal all the techniques of quantum field theory, including not only the Green function method and the Feynman diagram method, but also the method of canonical transformations of operators as well as the concept of the finite-temperature vacuum [50]. This leads to further advantages of real-time methods in the thermo field dynamics approach (see, e.g., the last paragraph before Section 1.3.7). In refs. [50, 64], Umezawa lists the achievements of thermo field dynamics, which range from applications in condensed-matter physics to applications in high-energy physics.

We conclude with an observation by Umezawa [64], the father of thermo field dynamics:

> 'It impresses me very much that so many areas in physics seem to be gradually developing a unified picture of laws in nature. The thermal field theories seem to be very important elements in this new development.'

Chapter 2

A Statistical Model for the Structure Functions of the Nucleon

2.1 Introduction

In this work we consider deep inelastic scattering of leptons off a heat bath of quarks and gluons to first order in the strong coupling constant α_S. This process is of interest for a discussion of models of the nucleon, the nucleus, the EMC-effect or any other situation where the effect of leptons on a system of thermalized quarks and gluons is needed. In this work we restrict our attention to a model for the structure functions of the nucleon.

In ref. [71] Cleymans and Thews proposed a statistical model for the structure functions of the nucleon based on the MIT-bag model [72] where hadrons are composed of almost free quarks and gluons confined by the vacuum pressure. They calculated the scattering of high energy leptons from a thermalized gas of quarks and gluons confined to a region of space equal to the volume of the nucleon by considering lowest-order diagrams in perturbative QCD. In ref. [15] Cleymans and Dadić extended these considerations to the first order in the strong coupling constant α_S since the effect of gluons is absent in zeroth order.

The statistical model incorporates features which are absent in the parton model [73]. The parton model has been successful in describing deep inelastic lepton-nucleon scattering processes $\mu N \to \mu X$ and $\nu N \to \mu X$, prompt photon production $pp \to \gamma X$ and the Drell-Yan process $pN \to \mu^+\mu^- X$. However, all predictions depend on the parton distribution functions which are arbitrary functions containing many parameters [see e.g. eqs. (4.1), (4.2) and (4.3) which contain values for a total of 13 parameters].

The phenomenological success of the parton model indicates that the number of constituents (partons) of the nucleon is very large due to the $1/x$ behaviour of the structure functions at small x, where x is the fraction of the nucleon's momentum carried by the parton. To the extent that one takes this fact literally it diminishes, on the one hand, the acceptability of the parton model due to the implied infinite number of soft spin-$\frac{1}{2}$ particles inside the nucleon which contradicts the Pauli exclusion principle. On the other hand this same fact supports the idea of viewing the interior of the nucleon as a heat bath of quarks and gluons.

Another shortcoming in the parton model is the neglect of the presence of identical quarks and gluons in the initial and final states and of quantum statistical correlations which also have a role to play in the propagation of particles when considering Feynman diagrams containing internal lines in next-to-leading-order calculations. In the statistical model these shortcomings are removed through the use of Fermi-Dirac and Bose-Einstein distributions for quarks and gluons, respectively. Stimulated emission factors for final-state gluons and Pauli-blocking factors for final-state quarks are incorporated. The propagation of particles through a many-body medium is taken into account by using thermal Feynman rules for propagators and vertices given in Table 3.1.

The assumption of a thermalized assembly of quarks and gluons could also be seen as an attempt to describe the "chaotic motion" of quarks and gluons inside the nucleon at a more fundamental level than that attained through the use of arbitrary parton distributions containing many parameters in the parton model.

In their study of deep inelastic scattering of leptons off a heat bath of quarks and gluons, Cleymans and Dadić [15] took all processes contributing to order α_S (see Figure 2.2) exactly into account. They were able to cancel all infrared, collinear and ultraviolet divergences in the framework provided by the real-time formalism of finite-temperature quantum field theory (reviewed in Chapter 1). These analytical calculations are discussed in Chapter 3 and their final expressions given in Appendix D. In Chapter 4 we present results from numerical calculations of these expressions. There it is shown to what extent recent deep inelastic scattering data can be reproduced by the statistical model.

Research projects which are the most closely related to ours have been reported on by groups working in Nice [17] and Annecy [20] in France and Bielefeld [14] in West Germany.

The main difference between our project and the latter projects, besides being on different but related physical processes, is the kinematics involved. The fact that the Lorentz invariance property, which is used in the usual zero temperature calculations, is lost due to the preferred frame of reference defined by the heat bath, has the immediate consequence that the number of calculations required is increased dramatically. For this reason all the above-mentioned groups reduce the complexity of their calculations significantly by using special kinematics [e.g. in lepton pair production from a thermalized quark gluon plasma they would use a virtual photon with zero spatial momentum: $q = (q_0, \vec{q} = 0)$]. In our case we perform calculations for the case of general kinematics [i.e. $q = (q_0, \vec{q} \neq 0)$].

In ref. [24](b) Cleymans and Dadić presented results from analytical calculations of dilepton production from a quark-gluon plasma to order α_S ($q^2 > 0$ for the photon giving rise to the lepton pair) which is closely related to the process of deep inelastic scattering of leptons off a heat bath of quarks and gluons ($q^2 < 0$ for the photon stemming from the lepton beam).

2.2 Deep Inelastic Electron-Proton Scattering $e^- p \to e^- X$

Deep inelastic electron-proton scattering allows us to determine the quark and gluon structure of the proton. A first order picture of the quark structure of the proton already presents itself at $\mathcal{O}(\alpha_S^0)$, but one needs to consider at least $\mathcal{O}(\alpha_S)$ contributions in order to take the effects of gluons into account. The substructure of the proton can be revealed by increasing the $-q^2$ of the photon to give better spatial resolution. For very large $-q^2$, the large transfer of energy breaks up the proton into multiparticle states as shown in Fig. 2.1.

In our treatment of the case of deep inelastic scattering of electrons off a heat bath of quarks and gluons, we simplify the calculations by considering only the part of the diagram below the dashed line in Figure 2.1. This means that we consider the scattering of a *virtual* photon with 4-momentum q off the proton (considered as a heat bath of quarks and gluons) with 4-momentum p_B. To order α_S the processes depicted in Figure 2.2 contribute. According to Figure 2.2 there can be more than two particles in the initial state of a reaction so that the rate of reactions (as opposed to a cross section) is the natural quantity to consider when relating the measured structure functions on the hadronic level with the results from our calculations of thermal averages of the fundamental (virtual) photon-quark interaction

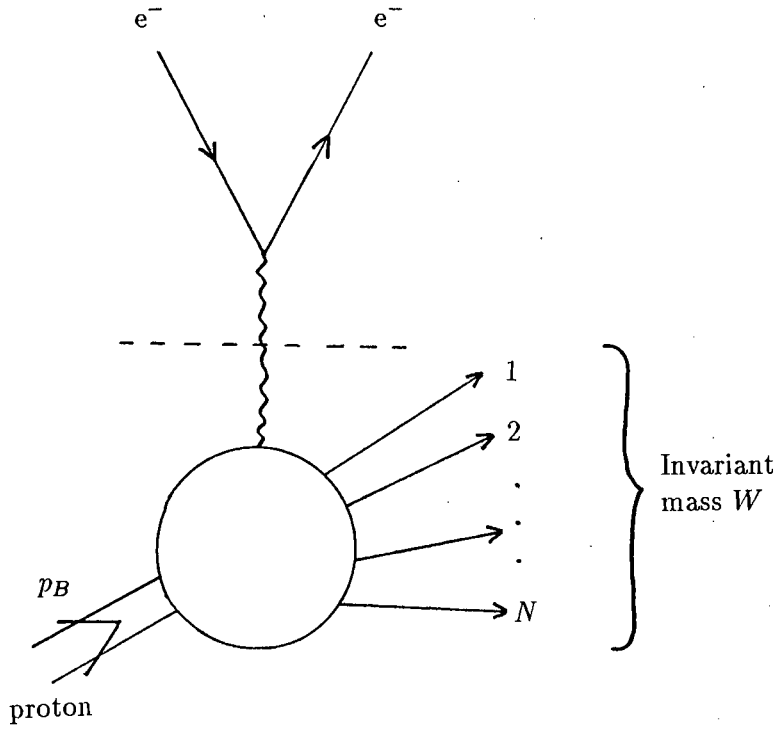

Figure 2.1: Picture of $e^-p \rightarrow e^-X$. In our calculation we work in the laboratory frame: $p_B = (M,0,0,0)$.

processes. The interaction rate on the hadronic level is proportional to the hadronic tensor [41]

$$W^{\mu\nu}(p_B,q) = W_1(\nu,q^2)\left(-g^{\mu\nu}+\frac{q^\mu q^\nu}{q^2}\right)+W_2(\nu,q^2)\frac{1}{M^2}\left(p_B^\mu-\frac{p_B\cdot q}{q^2}q^\mu\right)\left(p_B^\nu-\frac{p_B\cdot q}{q^2}q^\nu\right). \tag{2.1}$$

The functions W_1 and W_2 are functions of the Lorentz scalar variables that can be constructed from the four-momenta at the hadronic vertex and M is the proton mass. The invariant mass W of the final hadronic system is defined by

$$W^2 = (p_B+q)^2.$$

Since

$$W^2 = (p_B+q)^2 = M^2+2p_B\cdot q+q^2,$$

and, for inelastic scattering, the invariant mass, W, may assume many different values for the same fixed q^2, one sees that there are two independent Lorentz scalar variables which we

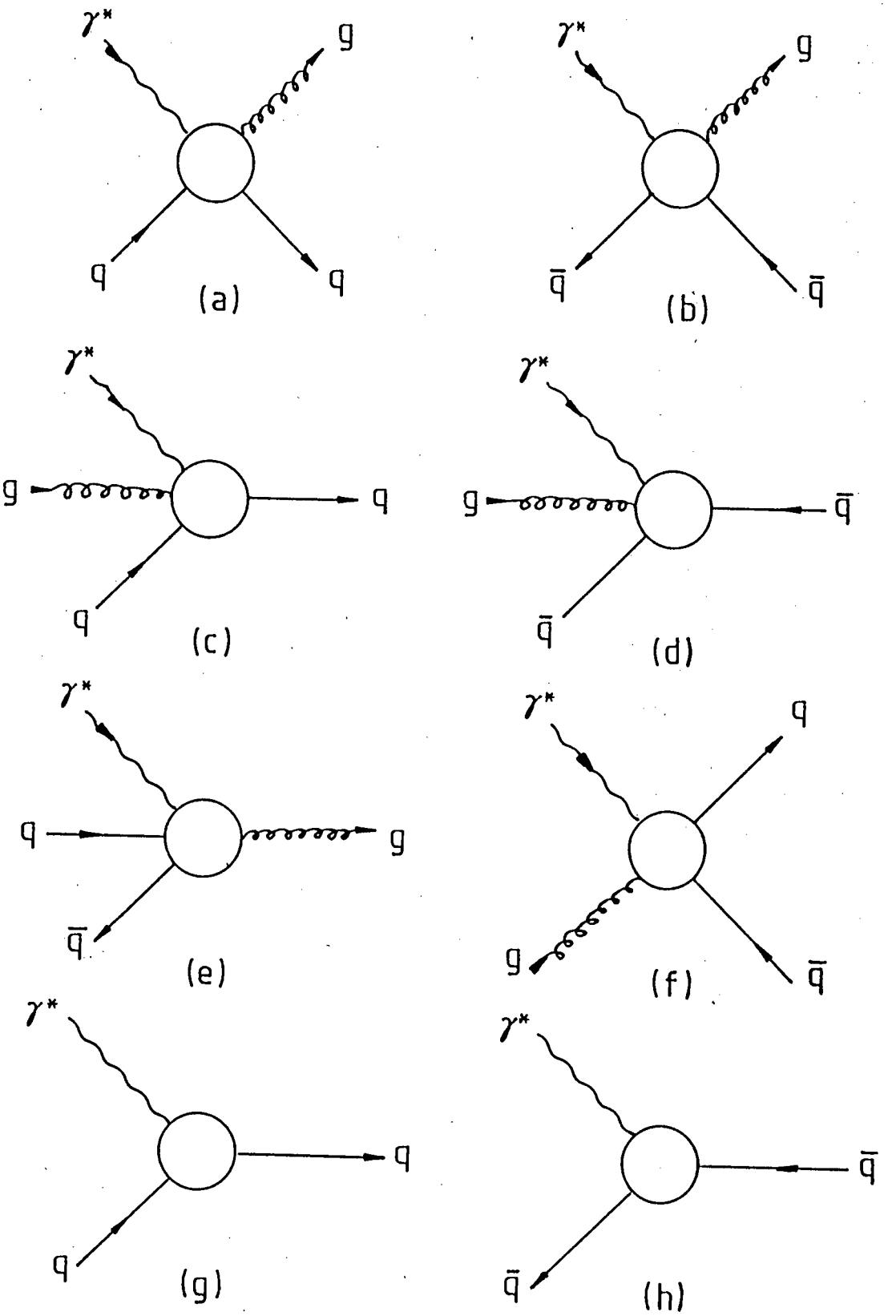

Figure 2.2: Processes contributing to deep inelastic scattering to first order in α_S.

choose to be

$$q^2 \qquad \text{and} \qquad \nu \equiv \frac{p_B \cdot q}{M}. \tag{2.2}$$

The definition of the total cross section for scattering a space-like ($q^2 < 0$) photon with polarization, ϵ_λ, inelastically off a proton is [41, p.185]

$$\sigma_\lambda(\gamma^* p \to X) \equiv \frac{e^2}{2K2M}[\epsilon_\lambda^\mu]^* \epsilon_\lambda^\nu 4\pi M W_{\mu\nu} = \frac{4\pi^2\alpha}{K}[\epsilon_\lambda^\mu]^* \epsilon_\lambda^\nu W_{\mu\nu}.$$

where $K = \nu + q^2/(2M)$ is the "energy" of the virtual photon according to the Hand convention, α is the fine structure constant and the factor $4\pi M$ originates from the standard convention for the normalization of $W_{\mu\nu}$.

With $\vec{q}$ chosen along the z axis [$q = (\nu, 0, 0, q_z)$], the polarization vectors of the virtual photons (helicity λ) are [41, p.185]

$$\lambda = \pm 1: \qquad \epsilon_\pm = \mp\sqrt{\frac{1}{2}}(0, 1, \pm i, 0) \tag{2.3}$$

$$\lambda = 0: \qquad \epsilon_0 = \frac{1}{\sqrt{-q^2}}(q_z, 0, 0, \nu). \tag{2.4}$$

By using the facts that $W_{\mu\nu}$ has the form given in eq. (2.1), that

$$q.\epsilon_\lambda = 0 \tag{2.5}$$

for each λ [41, p.185] and that

$$\sum_{\lambda=\pm1,0} (-1)^{\lambda+1}[\epsilon_\lambda^\mu]^* \epsilon_\lambda^\nu = -g^{\mu\nu} + \frac{q^\mu q^\nu}{q^2} \tag{2.6}$$

for a virtual space-like photon [41, p.185], the transverse and longitudinal cross sections, respectively, may be written as

$$\sigma_T \equiv \frac{1}{2}(\sigma_+ + \sigma_-) = \frac{4\pi^2\alpha}{K} W_1(\nu, q^2) \tag{2.7}$$

$$\sigma_L \equiv \sigma_0 = \frac{4\pi^2\alpha}{K}\left[\left(1 - \frac{\nu^2}{q^2}\right) W_2(\nu, q^2) - W_1(\nu, q^2)\right]. \tag{2.8}$$

Structure functions are defined as usual [41]:

$$F_1(\nu, q^2) = M W_1(\nu, q^2) \tag{2.9}$$

$$F_2(\nu, q^2) = \nu W_2(\nu, q^2) \tag{2.10}$$

$$R(\nu, q^2) = \frac{\sigma_L}{\sigma_T} \tag{2.11}$$

In the one-photon exchange approximation, the deep inelastic cross section for charged leptons can be written in such a form that it depends linearly on F_2 and non-linearly and very weakly on R [74]. Experimentally, F_2 and R can be disentangled by measuring deep inelastic cross sections at the same (x, Q^2) point but at different values of the incident beam energy. In practice, as these cross sections depend only weakly on R, all measurements of R suffer from large experimental errors. The structure function F_2 is much more precisely measured than R.

According to our definitions we have

$$F_1 = \frac{4\pi^2\alpha}{K} M\sigma_{\mathrm{T}} \tag{2.12}$$

$$F_2 = \frac{4\pi^2\alpha}{K}(\sigma_{\mathrm{T}} + \sigma_{\mathrm{L}})\frac{-q^2\nu}{q_z^2} \tag{2.13}$$

$$R = \frac{Mq_z^2}{-q^2\nu}\frac{F_2}{F_1} - 1 \tag{2.14}$$

With the index i serving as an index to distinguish between each contributing process one can write

$$\sigma_\lambda = \sum_i \sigma_\lambda^i$$

The relation between the measured structure functions on the hadronic level and the results from our calculations of thermal averages of the fundamental (virtual) photon-quark interaction processes is discussed in refs. [71] and [15]. Applied to the above definitions, one obtains on the hadronic level, as an example, for the $\mathcal{O}(\alpha_{\mathrm{S}})$ process of gluon emission from a quark in Figure 2.2(a):

$$\sigma_\lambda^{(\mathrm{a})} = \frac{V}{2K}\sum_q \int \frac{d^3k}{(2\pi)^3 2k_0} n_{\mathrm{F}}(x_k) \int \frac{d^3k'}{(2\pi)^3 2k_0'}[1 - n_{\mathrm{F}}(x_{k'})] \int \frac{d^3p}{(2\pi)^3 2p_0}[1 + n_{\mathrm{B}}(|p_0|)]$$
$$\times (2\pi)^4\delta^4(q + k - k' - p)\frac{N_{\mathrm{C}}^2 - 1}{2} 4\pi\alpha_{\mathrm{S}} 4\pi\alpha e_q^2 \sum_{\substack{\pm s, \pm s' \\ \text{g polarizations}}} |M_{\epsilon_\lambda}|^2 \tag{2.15}$$

according to the momentum assignments in Figure 3.2 and where V is the volume of the nucleon. By ignoring the factors e and g in eqs. (3.4), (3.5) and (3.6), the latter three equations provide explicit expressions for the matrix element as it stands in eq. (2.15) (with coupling constants, colour factors and fractional charges factored out into explicit normalization constants). We take $N_{\mathrm{C}} = 3$ and include up and down quarks only in our model:

$$e_q = +\frac{2}{3} \qquad \text{for } q \text{ an up quark}$$

$$e_q = -\frac{1}{3} \qquad \text{for } q \text{ a down quark.}$$

The fermion and boson distribution functions appearing in eq. (2.15) are defined in eqs. (3.1), (3.2) and (3.3).

Values for variables appearing in our model are given in Chapter 4 where numerical calculations are discussed. These variables are the four-momentum squared of the virtual photon (q^2), the chemical potential for each flavour of quark (μ_q), the temperature (T) and the strong coupling constant (α_S). Standard values for the proton mass appearing in eq. (2.12) and the radius of the nucleon are used and are given in Table 4.1.

Chapter 3

Deep Inelastic Scattering (DIS) of Electrons off a Heat Bath of Quarks and Gluons

3.1 Introduction

According to the statistical model, discussed in the previous chapter, we consider deep inelastic scattering of electrons off a heat bath of quarks and gluons. In this chapter we discuss the phase space integrations of the matrix element squared from contributing processes. Their final expressions are summarized in Appendix D and their numerical evaluation discussed in Chapter 4.

3.2 Feynman Rules for Quarks and Gluons at $T \neq 0$ and $\mu \neq 0$

In order to take into account the propagation of particles through a many-body medium, we use the thermal Feynman rules as shown in Table 3.1. The rules for the fermion and gauge boson propagators that are used in this work are from ref. [40]. In the latter reference minus sign ambiguities in earlier literature on thermal Feynman rules are pointed out and corrected. Further information about the expressions appearing in Table 3.1 is as follows:

Fermion and boson distribution functions can be defined in such a manner that they are valid for both positive and negative energies. In Table 3.1 they are for a fermion

$$n_{\rm F}(x_k) = \frac{1}{{\rm e}^{\beta x_k} + 1} \tag{3.1}$$

Table 3.1: Feynman rules for quarks and gluons at $T \neq 0$ and $\mu \neq 0$. Further information about these rules and the symbols appearing in them is given in Section 3.2.

Fermion (quark) propagator, $iS^{ab}(k)$	$iS^{11}(k) = \dfrac{i}{\not{k} - m + i\epsilon} - 2\pi(\not{k} + m)\delta(k^2 - m^2)n_{\rm F}(x_k)$ $iS^{12}(k) = 2\pi(\not{k} + m)\delta(k^2 - m^2)n_{\rm F}(x_k)\mathrm{e}^{\beta(x_k+\mu)/2}$ $iS^{21}(k) = -2\pi(\not{k} + m)\delta(k^2 - m^2)n_{\rm F}(x_k)\mathrm{e}^{\beta(x_k-\mu)/2}$ $iS^{22}(k) = \dfrac{-i}{\not{k} - m - i\epsilon} - 2\pi(\not{k} + m)\delta(k^2 - m^2)n_{\rm F}(x_k)$
Gauge boson (gluon) propagator, $-g^{\mu\nu}iD^{ab}(k)$ (Feynman gauge)	$iD^{11}(k) = \dfrac{i}{k^2 - m^2 + i\epsilon} + 2\pi\delta(k^2 - m^2)n_{\rm B}(\lvert k_0\rvert)$ $iD^{12}(k) = -2\pi\delta(k^2 - m^2)n_{\rm B}(\lvert k_0\rvert)\mathrm{e}^{\beta\lvert k_0\rvert/2}$ $iD^{21}(k) = -2\pi\delta(k^2 - m^2)n_{\rm B}(\lvert k_0\rvert)\mathrm{e}^{\beta\lvert k_0\rvert/2}$ $iD^{22}(k) = \dfrac{-i}{k^2 - m^2 - i\epsilon} + 2\pi\delta(k^2 - m^2)n_{\rm B}(\lvert k_0\rvert)$
Quark–qluon vertex (type 1)	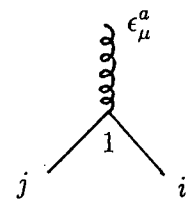 $= -ig\gamma^\mu(T_a)_{ij}$
Quark–qluon vertex (type 2)	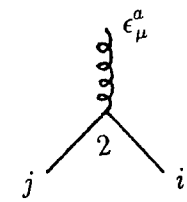 $= ig\gamma^\mu(T_a)_{ij}$
Quark–photon vertex (type 1)	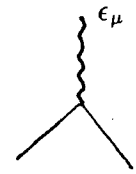 $= ie\gamma^\mu$

where

$$x_k = |k_0| - \mu\epsilon(k_0) \tag{3.2}$$

where $\epsilon(k_0)$ gives the sign of k_0 and for a boson

$$n_B(|k_0|) = \frac{1}{e^{\beta|k_0|} - 1}. \tag{3.3}$$

The typical QCD Lagrangian [41, p. 319]

$$\mathcal{L}_{QCD} = \bar{q}(i\gamma^\mu\partial_\mu - m)q - g(\bar{q}\gamma^\mu T_a q)G^a_\mu - \frac{1}{4}G^a_{\mu\nu}G^{\mu\nu}_a,$$

where $G^a_{\mu\nu} = \partial_\mu G^a_\nu - \partial_\nu G^a_\mu - g f_{abc} G^b_\mu G^c_\nu$, gives rise to the rule for the type 1 quark–gluon vertex shown in Table 3.1, which is the same as the usual zero-temperature quark–gluon vertex. The reason for the relative minus sign for the type 2 quark–gluon vertex in Table 3.1 is the same as that given in the context of a scalar field theory in the second-last paragraph of Section 1.3.3. Since our calculations are only up to $\mathcal{O}(\alpha_S)$, the type 2 quark–gluon vertex will only appear in self-energy graphs since the vertices in all other graphs will be connected to external lines and will therefore be of type 1 (see Section 1.3.1).

The photon stemming from the electron beam in deep inelastic scattering is not considered to be thermalized so that only the usual zero-temperature (type 1) quark–photon vertex need to be considered. The plus sign for the quark–photon vertex stems from the use of the typical QED Lagrangian [41, p. 317]

$$\mathcal{L}_{QED} = \bar{\psi}(i\gamma^\mu\partial_\mu - m)\psi + e\bar{\psi}\gamma^\mu A_\mu\psi - \frac{1}{4}F_{\mu\nu}F^{\mu\nu}$$

where $F_{\mu\nu} = \partial_\mu A_\nu - \partial_\nu A_\mu$ and where $e > 0$.

3.3 The Processes Contributing to DIS

The processes contributing to $\mathcal{O}(\alpha_S)$ to deep inelastic scattering are shown in Figure 2.2. We consider the four-particle process of gluon emission from quarks [Figure 2.2(a)] as an example in the next section. Corresponding to the process in Figure 2.2(a) one has the Feynman diagrams depicted in Figure 3.2. The results for this and the other four-particle processes [Figures 2.2(b) —(f)] are summarized in Appendix D.

The three-particle processes (g) and (h) in Figure 2.2 also contribute to $\mathcal{O}(\alpha_S)$. For example, corresponding to process (g), one has the Feynman diagrams depicted in Figure 3.1.

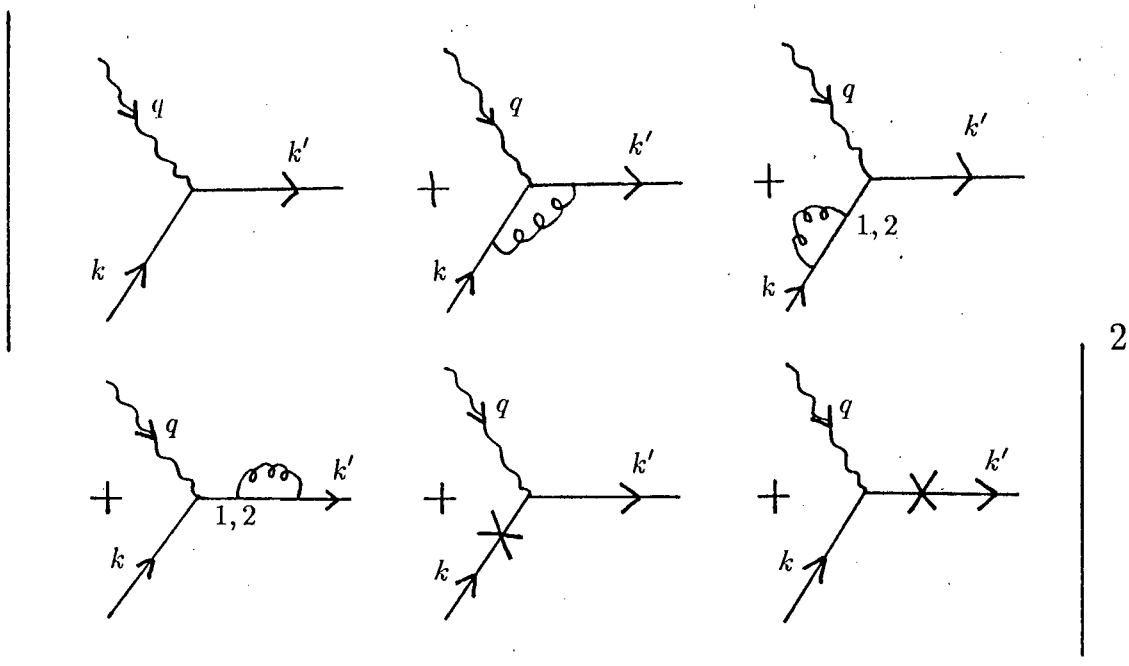

$$\equiv |M_{3a} + M_{3b} + M_{3c} + M_{3d} + M_{3e} + M_{3f}|^2$$

Figure 3.1: Diagrams for three-particle processes involving quarks.

In Section 3.5 we discuss the vertex correction to a quark arising from the interference of diagrams M_{3a} and M_{3b} in Figure 3.1. In Section 3.6 we discuss self-energy corrections to a quark. The results for three-particle processes are also summarized in Appendix D.

3.4 Gluon Emission from Quarks

3.4.1 The Matrix Element Squared

The diagrams to be calculated for gluon emission from quarks are shown in Figure 3.2. Kinematical relations which we use for this process appear in Appendix A. The corresponding matrix element for a given polarization, ϵ_{γ^*}, of the space-like ($q^2 < 0$) virtual photon (γ^*) stemming from the electron beam is given by

$$M_{\epsilon_{\gamma^*}} = M_1 + M_2 \tag{3.4}$$

where

$$M_1 = \bar{u}(k', s')(-ig\gamma_\mu)[\epsilon_g^\mu(p)]^* iS^{11}(k+q)(ie\gamma_\nu)\epsilon_{\gamma^*}^\nu(q)u(k, s) \tag{3.5}$$

$$M_2 = \bar{u}(k', s')(ie\gamma_\mu)\epsilon_{\gamma^*}^\mu(q)iS^{11}(k-p)(-ig\gamma_\nu)[\epsilon_g^\nu(p)]^* u(k, s) \tag{3.6}$$

and where we suppress reference to colour factors and fractional charges. For convenience we write $iS^{11}(k)$ in the form

$$iS^{11}(k) = i(\not{k} + m)\bar{S}^{11}(k) \tag{3.7}$$

where, due to the expression given for $iS^{11}(k)$ in Table 3.1, one has

$$\bar{S}^{11}(k) = \frac{1}{k^2 - m^2 + i\epsilon} + 2\pi i\delta(k^2 - m^2)\frac{1}{e^{\beta x_k} + 1} \tag{3.8}$$

where x_k is given in eq. (3.2).

In our calculations we have the following for the masses:

$$\begin{aligned} &\text{quark mass} = 0 \\ &\text{gluon mass} \equiv m \neq 0 \end{aligned}$$

The gluon mass regularizes infrared and collinear singularities.

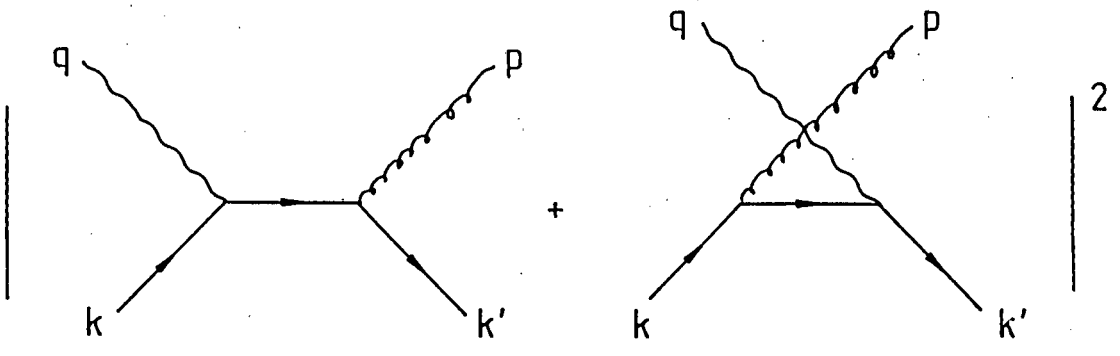

Figure 3.2: Diagrams for gluon emission from quarks.

By squaring the matrix element, summing over all the spins for a massless quark according to

$$\sum_{s=1,2} u^{(s)}(p)\bar{u}^{(s)}(p) = \not{p}$$

and summing over the gluon polarizations according to

$$\sum_{\substack{\text{gluon} \\ \text{polarizations}}} [\epsilon_g^{\mu}(p)]^* \epsilon_g^{\nu}(p) = -g^{\mu\nu} + \frac{p^{\mu}p^{\nu}}{m^2} \tag{3.9}$$

we obtain

$$\sum_{\substack{\pm s,\pm s' \\ \text{g polarizations}}} |M_{\epsilon_{\gamma^*}}|^2$$
$$= -e^2 g^2 \{ \mathrm{Tr}\,[\not{k}'\gamma_\mu(\not{k}+\not{q})\,\not{\epsilon}_{\gamma^*}(q)\,\not{k}[\not{\epsilon}_{\gamma^*}(q)]^*(\not{k}+\not{q})\gamma^\mu]\,|\bar{S}^{11}(k+q)|^2$$
$$+ \mathrm{Tr}\,[\not{k}'\gamma_\mu(\not{k}+\not{q})\,\not{\epsilon}_{\gamma^*}(q)\,\not{k}\gamma^\mu(\not{k}-\not{p})[\not{\epsilon}_{\gamma^*}(q)]^*]\,\bar{S}^{11}(k+q)[\bar{S}^{11}(k-p)]^*$$
$$+ \mathrm{Tr}\,[\not{k}'\,\not{\epsilon}_{\gamma^*}(q)(\not{k}-\not{p})\gamma_\mu\,\not{k}\gamma^\mu(\not{k}-\not{p})[\not{\epsilon}_{\gamma^*}(q)]^*]\,|\bar{S}^{11}(k-p)|^2$$
$$+ \mathrm{Tr}\,[\not{k}'\,\not{\epsilon}_{\gamma^*}(q)(\not{k}-\not{p})\gamma_\mu\,\not{k}[\not{\epsilon}_{\gamma^*}(q)]^*(\not{k}+\not{q})\gamma^\mu]\,\bar{S}^{11}(k-p)[\bar{S}^{11}(k+q)]^*\} \quad (3.10)$$

where the second term on the right-hand side of eq. (3.9) does not contribute in eq. (3.10) due to the requirement of gauge invariance.

The first trace in eq. (3.10) is evaluated by using the trace theorems in ref. [75, p. 104, 105]. The resultant expression is simplified further by making use of the assumption of massless quarks embodied by $k^2 = 0$ and $k'.k' = 0$ and the fact that $q.\epsilon = 0$ for each polarization state of the virtual photon [see eq. (2.5)]. By dropping the subscript (γ^*) of ϵ the first term in eq. (3.10) then becomes

$$\mathrm{Tr}\,[\not{k}'\gamma_\mu(\not{k}+\not{q})\,\not{\epsilon}_{\gamma^*}(q)\,\not{k}[\not{\epsilon}_{\gamma^*}(q)]^*(\not{k}+\not{q})\gamma^\mu]$$
$$= 8[2(k.q)(k.\epsilon)(k'.\epsilon^*) + 2(k.q)(k.\epsilon^*)(k'.\epsilon) + 2(k.q)(q.k')(\epsilon.\epsilon^*) - 4(k.k')(k.\epsilon)(k.\epsilon^*) \quad (3.11)$$
$$-(k.k')q^2(\epsilon.\epsilon^*) - 4(k.\epsilon)(k.\epsilon^*)(q.k') + (k.\epsilon)q^2(k'.\epsilon^*) + (k.\epsilon^*)q^2(k'.\epsilon).$$

We write the latter expression in terms of the invariant variables

$$s = (k+q)^2 = (k'+p)^2 \quad (3.12)$$

and

$$t = (k'-q)^2 = (k-p)^2 \quad (3.13)$$

by making use of the exact relations

$$\begin{aligned} q.k &= \frac{1}{2}(s-q^2), \\ q.k' &= \frac{1}{2}(q^2-t), \\ k.k' &= \frac{1}{2}(s+t-q^2-m^2). \end{aligned}$$

and obtain

$$\begin{aligned}&\mathrm{Tr}\,[\not k'\gamma_\mu(\not k+\not q)\not\epsilon_{\gamma^*}(q)\not k[\not\epsilon_{\gamma^*}(q)]^*(\not k+\not q)\gamma^\mu]\\&=4\,[-4(k.\epsilon)(k.\epsilon^*)s+4(k.\epsilon)(k.\epsilon^*)m^2+2(k.\epsilon)(k'.\epsilon^*)s\\&\quad+2(k.\epsilon^*)(k'.\epsilon)s+q^2(\epsilon.\epsilon^*)m^2-(\epsilon.\epsilon^*)st]\,.\end{aligned}\tag{3.14}$$

The last three traces in eq. (3.10) are evaluated by following the same steps as described for evaluating the first trace and, in addition, by making use of energy–momentum conservation:

$$p=k+q-k'.$$

The result is

$$\begin{aligned}&\sum_{\substack{\pm s,\pm s'\\ \text{g polarizations}}}|M_{\epsilon_{\gamma^*}}|^2\\&=-e^2g^2 4\,\{[-4(k.\epsilon)(k.\epsilon^*)s+4(k.\epsilon)(k.\epsilon^*)m^2+2(k.\epsilon)(k'.\epsilon^*)s+2(k.\epsilon^*)(k'.\epsilon)s\\&\quad+q^2(\epsilon.\epsilon^*)m^2-(\epsilon.\epsilon^*)st]\,|\bar S^{11}(k+q)|^2\\&\quad+\left[-2(k.\epsilon)(k.\epsilon^*)q^2+2(k.\epsilon)(k.\epsilon^*)t-(q^2)^2(\epsilon.\epsilon^*)-2q^2(k'.\epsilon)(k'.\epsilon^*)+q^2(\epsilon.\epsilon^*)s\right.\\&\quad\left.+q^2(\epsilon.\epsilon^*)t-q^2(\epsilon.\epsilon^*)m^2+2(k'.\epsilon)(k'.\epsilon^*)s\right]2\mathrm{Re}\left\{\bar S^{11}(k+q)[\bar S^{11}(k'-q)]^*\right\}\\&\quad+\left[2(k.\epsilon)(k'.\epsilon^*)q^2-2(k.\epsilon)(k'.\epsilon^*)s-2(k.\epsilon)(k'.\epsilon^*)t\right.\\&\quad\left.+4(k.\epsilon)(k'.\epsilon^*)m^2-2(k.\epsilon^*)(k'.\epsilon)q^2\right]\bar S^{11}(k+q)[\bar S^{11}(k'-q)]^*\\&\quad+\left[-2(k.\epsilon)(k'.\epsilon^*)q^2+2(k.\epsilon^*)(k'.\epsilon)q^2-2(k.\epsilon^*)(k'.\epsilon^*)s\right.\\&\quad\left.-2(k.\epsilon^*)(k'.\epsilon)t+4(k.\epsilon^*)(k'.\epsilon)m^2\right]\bar S^{11}(k'-q)[\bar S^{11}(k+q)]^*\\&\quad+\left[2(k.\epsilon)(k'.\epsilon^*)t+2(k.\epsilon^*)(k'.\epsilon)t+q^2(\epsilon.\epsilon^*)m^2-4(k'.\epsilon)(k'.\epsilon^*)t\right.\\&\quad\left.+4(k'.\epsilon)(k'.\epsilon^*)m^2-(\epsilon.\epsilon^*)st\right]|\bar S^{11}(k'-q)|^2\Big\}\,.\end{aligned}\tag{3.15}$$

In eq. (3.15) one has, for example,

$$\bar S^{11}(k+q)=\mathcal{P}\frac{1}{s}-i\pi\delta(s)+2\pi i\delta(s)\frac{1}{e^{\beta x_{k+q}}+1}\tag{3.16}$$

where use has been made of eqs. (3.8) and (3.12) and the relation

$$\frac{1}{s\pm i\epsilon}=\mathcal{P}\frac{1}{s}\mp i\pi\delta(s).\tag{3.17}$$

In Appendix A it is shown that $s > 0$ and $t < 0$ for $m^2 > 0$. These inequalities imply that terms containing the factors $\delta(s)$ and $\delta(t)$ in the expressions for $\bar{S}^{11}(k+q)$ [see eq. (3.16)] and $\bar{S}^{11}(k'-q)$ do not contribute to the matrix element squared. Thus from now on we take

$$\begin{aligned} |\bar{S}^{11}(k+q)|^2 &= \frac{1}{s^2} \\ |\bar{S}^{11}(k'-q)|^2 &= \frac{1}{t^2} \\ \bar{S}^{11}(k+q)[\bar{S}^{11}(k'-q)]^* &= \frac{1}{st} \end{aligned}$$

in what follows. The expression in eq. (3.15) may then be written in the simplified form

$$\begin{aligned} &\sum_{\substack{\pm s,\pm s' \\ \text{g polarizations}}} |M_{\epsilon_{\gamma^*}}|^2 \\ &= e^2 g^2 \left\{ 4\epsilon.\epsilon^* \left(\frac{t}{s} + \frac{s}{t} - \frac{2q^2}{s} - \frac{2q^2}{t} \right) \right. \\ &\quad + \frac{1}{s^2} \left[-4\epsilon.\epsilon^* m^2 q^2 - 16(k.\epsilon)(k.\epsilon^*) m^2 \right] \\ &\quad + \frac{1}{t^2} \left[-4\epsilon.\epsilon^* m^2 q^2 - 16(k'.\epsilon)(k'.\epsilon^*) m^2 \right] \\ &\quad + \frac{1}{st} \left[8\epsilon.\epsilon^* q^4 + 8\epsilon.\epsilon^* m^2 q^2 + 16q^2(k.\epsilon)(k.\epsilon^*) + 16q^2(k'.\epsilon)(k'.\epsilon^*) \right. \\ &\quad \left. \left. - 16m^2(k.\epsilon)(k'.\epsilon^*) - 16m^2(k'.\epsilon)(k.\epsilon^*) \right] \right\}. \end{aligned} \tag{3.18}$$

The matrix element squared for the longitudinal polarization, ϵ_0, of the virtual photon is calculated from eq. (3.18) by using the expression for ϵ_0 given in eq. (2.4):

$$\epsilon_0.\epsilon_0^* = 1 \tag{3.19}$$

$$(k.\epsilon_0)(k.\epsilon_0^*) = -\frac{1}{q^2}(q_z k_0 - \nu k_z)^2 \tag{3.20}$$

$$(k'.\epsilon_0)(k'.\epsilon_0^*) = -\frac{1}{q^2}(q_z k'_0 - \nu k'_z)^2 \tag{3.21}$$

$$\begin{aligned} (k.\epsilon_0)(k'.\epsilon_0^*) &= (k'.\epsilon_0)(k.\epsilon_0^*) \\ &= -\frac{1}{q^2}(q_z k_0 - \nu k_z)(q_z k'_0 - \nu k'_z)^2. \end{aligned} \tag{3.22}$$

Since, in the rest frame of the heat bath, we choose the z axis to be along the direction of the virtual photon, we have $q = (\nu, 0, 0, q_z)$ and threrefore that

$$s = (q+k)^2 = q^2 + 2\nu k_0 - 2q_z k_z$$

$$\Rightarrow \qquad k_z = \frac{q^2 + 2\nu k_0 - s}{2q_z}$$

and

$$t = (k' - q)^2 = q^2 - 2\nu k'_0 + 2q_z k'_z$$
$$\Rightarrow \qquad k'_z = \frac{t + 2\nu k'_0 - q^2}{2q_z}.$$

With these expressions for k_z and k'_z inserted into eqs. (3.20–3.22) we obtain from eq. (3.18):

$$\begin{aligned} M_0 \equiv & \sum_{\substack{\pm s, \pm s' \\ \text{g polarizations}}} |M_{\epsilon_0}|^2 \\ = e^2 g^2 \Bigg\{ & -\frac{4q^2}{q_z^2}\left(\frac{t}{s} + \frac{s}{t}\right) + \frac{8q^2}{q_z^2 t}(2k_0\nu + q^2) + \frac{8q^2}{q_z^2 s}(-2k'_0\nu + q^2) \\ & -\frac{4q^2}{q_z^2}\frac{1}{st}\left[(2k_0 + \nu + q_z)(2k_0 + \nu - q_z) + (2k'_0 - \nu + q_z)(2k'_0 - \nu - q_z)\right] \\ & + \frac{4m^2q^2}{q_z^2}(2k_0 + \nu + q_z)(2k_0 + \nu - q_z)\frac{1}{s^2} + \frac{4m^2q^2}{q_z^2}(2k'_0 - \nu + q_z)(2k'_0 - \nu - q_z)\frac{1}{t^2} \\ & + \frac{4m^2q^2}{q_z^2}\left[q_z^2 + (2k_0 + \nu)(2k'_0 - \nu)\right]\frac{1}{st}\Bigg\}. \end{aligned} \tag{3.23}$$

The matrix element squared for the transverse polarizations, ϵ_+ and ϵ_-, of the virtual photon can be obtained from that for longitudinal polarization in eq. (3.23) and the sum over all polarizations:

$$\begin{aligned} M_\Sigma \equiv & \sum_{\lambda=\pm 1,0} (-1)^{\lambda+1} \sum_{\substack{\pm s, \pm s' \\ \text{g polarizations}}} |M_{\epsilon_{\gamma^*}}|^2 \\ = & \sum_{\substack{\pm s, \pm s' \\ \text{g polarizations}}} \left\{|M_{\epsilon_+}|^2 + |M_{\epsilon_-}|^2 - |M_{\epsilon_0}|^2\right\}. \end{aligned} \tag{3.24}$$

By using eq. (2.6) we obtain from eqs. (3.24) and (3.18)

$$\begin{aligned} M_\Sigma = & e^2 g^2 \Bigg\{ -16\left(\frac{t}{s} + \frac{s}{t} - \frac{2q^2}{s} - \frac{2q^2}{t}\right) + 16m^2q^2\left(\frac{1}{s^2} + \frac{1}{t^2}\right) \\ & + \frac{32}{st}(-q^4 - m^2q^2 + m^2 k.k') + 4\left(\frac{t}{s} + \frac{s}{t} - \frac{2q^2}{s} - \frac{2q^2}{t}\right) \\ & + \frac{1}{s^2}\left(-4m^2q^2 - 16\frac{(k.q)^2}{q^2}m^2\right) + \frac{1}{t^2}\left(-4m^2q^2 - 16\frac{(k'.q)^2}{q^2}m^2\right) \\ & + \frac{8}{st}\left(q^4 + m^2q^2 + 2(q.k)^2 + 2(q.k')^2 - 4m^2\frac{(k.q)(k'.q)}{q^2}\right)\Bigg\} \end{aligned} \tag{3.25}$$

where the first three terms and the remaining terms on the right hand side of eq. (3.25) are associated with the $-g^{\mu\nu}$ term and the $q^\mu q^\nu/q^2$ term of eq. (2.6), respectively. By using the relations

$$\begin{aligned} k.q &= \frac{1}{2}(s-q^2) \\ k'.q &= \frac{1}{2}(q^2-t) \\ k.k' &= \frac{1}{2}(s+t-m^2-q^2) \end{aligned}$$

in eq. (3.25) we obtain

$$\begin{aligned} M_\Sigma &= -8e^2g^2\left\{\frac{t}{s}+\frac{s}{t}+2(q^2+m^2)^2\frac{1}{st}\right. \\ &\quad \left.-2(q^2+m^2)\left(\frac{1}{s}+\frac{1}{t}\right)-m^2q^2\left(\frac{1}{s^2}+\frac{1}{t^2}\right)\right\}. \end{aligned} \tag{3.26}$$

The matrix element squared for the transverse polarizations can thus be obtained from the expressions we derived for M_Σ and $|M_0|^2$:

$$\begin{aligned} M_T &\equiv \frac{1}{2}\sum_{\substack{\pm s,\pm s' \\ \text{g polarizations}}}\left\{|M_{\epsilon_+}|^2+|M_{\epsilon_-}|^2\right\} \\ &= \frac{1}{2}(M_\Sigma+M_0). \end{aligned} \tag{3.27}$$

3.4.2 The Phase Space Integral for Gluon Emission from a Quark

For the phase space integral for gluon emission from a quark we have in accordance with our discussion in Section 1.1

$$\int d\mu n_{\rm F}(x_k)[1-n_{\rm F}(x_{k'})][1+n_{\rm B}(|p_0|)] \tag{3.28}$$

where the fermion and boson distribution functions are given in eqs. (3.1) and (3.3) and where

$$d\mu = \frac{d^3k}{(2\pi)^3 2k_0}\frac{d^3k'}{(2\pi)^3 2k_0'}\frac{d^3p}{(2\pi)^3 2p_0}(2\pi)^4\delta^4(q+k-k'-p). \tag{3.29}$$

Thus we start off with nine integration variables which may be reduced to the four variables k_0, k_0', z and z' as explained below. In Section 3.4.5 we show how the angular integrations over z and z' are analytically performed, leaving us with only the two integration variables k_0 and k_0'. This last double integral will be calculated numerically.

The integrand is a function of s and t appearing in the matrix element and the energies appearing in the thermal distribution functions, phase space factors and the matrix element.

In eq. (3.29) the integral over d^3p is trivially performed using $\delta^3(\vec{k}+\vec{q}-\vec{k'}-\vec{p})$. Wherever it appears, $\vec{p}$ is therefore substituted by $\vec{p}=\vec{k}+\vec{q}-\vec{k'}$ and therefore

$$p_0 = (|\vec{k}+\vec{q}-\vec{k'}|^2+m^2)^{\frac{1}{2}}. \tag{3.30}$$

We are left with six degrees of freedom in $\int d^3k d^3k'$ and they are

$$k_0,\ k_0',\ \theta,\ \theta',\ \phi,\ \phi'$$

as shown in Figure 3.3 ($k_0 = |\vec{k}|$ and $k_0' = |\vec{k'}|$ for massless quarks).

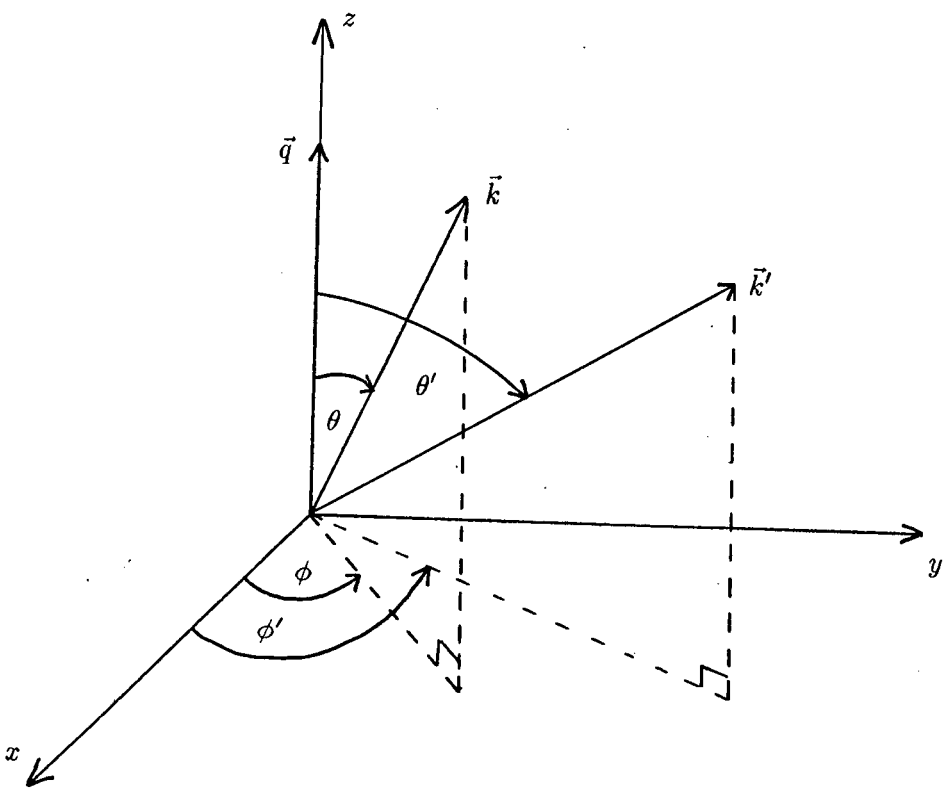

Figure 3.3: A pictorial representation of variables in the phase space integral

We concentrate next on the azimuthal integrals,

$$\int_0^{2\pi} d\phi \int_0^{2\pi} d\phi'$$

in $\int d^3k d^3k'$. It is to be understood in the following discussion that k_0, k'_0, θ and θ' are kept fixed in the outer integrals while the inner azimuthal integrations over ϕ and ϕ' are performed. The only place where one finds azimuthal angles in the integrand is in

$$\vec{k}.\vec{k}' = k_0 k'_0[\cos\theta\cos\theta' + \sin\theta\sin\theta'\cos(\phi - \phi')] \tag{3.31}$$

which appears via eq. (3.30) in

$$\frac{1}{2p_0}[1 + n_B(|p_0|)]\delta(\nu + k_0 - p_0 - k'_0). \tag{3.32}$$

As far as the dependence of the integrand on the azimuthal angles is concerned, it may be seen from eq. (3.31) that the integrand depends on only the relative azimuthal angle $\phi^- = \phi - \phi'$. We therefore introduce the change of variables:

$$\phi^- = \phi - \phi' \tag{3.33}$$

$$\phi^+ = \frac{1}{2}(\phi + \phi'). \tag{3.34}$$

For any integrand f which, as far as its dependence on ϕ and ϕ' is concerned, is a function of only $\cos(\phi - \phi')$, one can use the identity

$$\int_0^{2\pi} d\phi \int_0^{2\pi} d\phi' f(\cos(\phi - \phi')) = 4\pi \int_0^{\pi} f(\cos\phi^-) d\phi^-. \tag{3.35}$$

As already referred to at eq. (3.32), we have for the case at hand

$$f(\cos\phi^-) = \frac{1}{2p_0}[1 + n_B(|p_0|)]\delta(\nu + k_0 - p_0 - k'_0) \tag{3.36}$$

$$\Rightarrow \quad 4\pi \int_0^{\pi} f(\cos\phi^-) d\phi^- = 4\pi \left(\left| \frac{\partial p_0}{\partial \phi^-} \right|_{p_0 = \nu + k_0 - k'_0} \right)^{-1} \left[\frac{1}{2p_0}[1 + n_B(|p_0|)] \right]_{p_0 = \nu + k_0 - k'_0} \tag{3.37}$$

where, according to eq. (3.30), p_0 is given by

$$\begin{aligned} p_0 &= (|\vec{k} + \vec{q} - \vec{k}'|^2 + m^2)^{\frac{1}{2}} \\ &= (|\vec{k} + \vec{q}|^2 + {k'_0}^2 - 2|\vec{k} + \vec{q}|k'_0\cos\rho + m^2)^{\frac{1}{2}} \end{aligned} \tag{3.38}$$

where

$$\cos\rho \equiv \frac{\vec{k}'.(\vec{k} + \vec{q})}{k'_0|\vec{k} + \vec{q}|}.$$

In order to calculate the derivative of p_0 with respect to ϕ^- appearing in eq. (3.37), we shall refer in the following to Figure 3.4 which shows, amongst others, the newly introduced angles

ρ and β. For this purpose we make a convenient choice of axes in Figure 3.4: As is done in Appendix A, the z axis is chosen along the direction of $\vec{q}$. Since at this stage of the discussion the integration over the angle ϕ^+ has been done and, according to eq. (3.35), the remaining relative azimuthal angle, $\phi^- = \phi - \phi'$, ranges from 0 to π, we may now choose, for each case of fixed values for k'_0, θ', k_0 and θ in the outer integrations, a new reference frame such that $\vec{k}'$ lies in the x–z plane. In the reference frame shown in Figure 3.4 we then have:

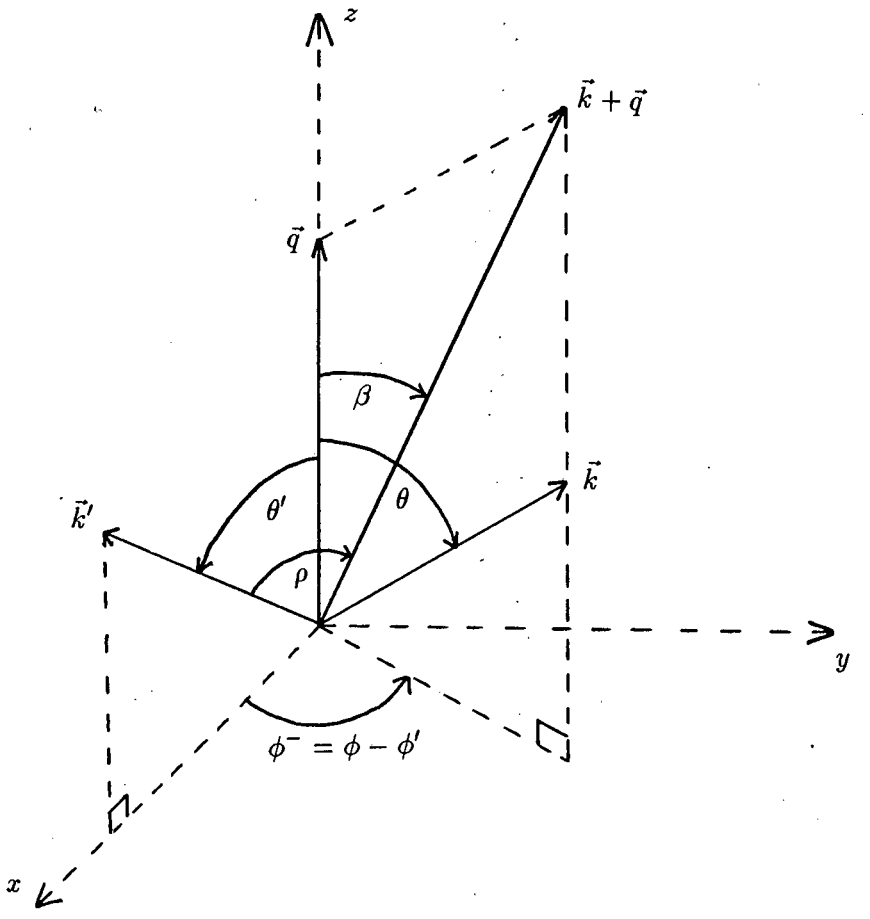

Figure 3.4: The angle ϕ^- in terms of the angles ρ, β and θ' for calculating the derivative of p_0 with respect to ϕ^-. We have $\phi' = 0$ for this choice of frame.

$$\begin{aligned} \vec{k}' &= k'_0(\sin\theta', 0, \cos\theta') \\ \vec{k}+\vec{q} &= |\vec{k}+\vec{q}|(\sin\beta\cos\phi^-, \sin\beta\sin\phi^-, \cos\beta) \\ \Rightarrow \quad \cos\rho &= \frac{\vec{k}'.(\vec{k}+\vec{q})}{k'_0|\vec{k}+\vec{q}|} = \sin\theta'\sin\beta\cos\phi^- + \cos\beta\cos\theta' \end{aligned} \tag{3.39}$$

$$\Rightarrow \quad \cos\phi^- = \frac{\cos\rho - \cos\beta\cos\theta'}{\sin\theta'\sin\beta}. \tag{3.40}$$

The restriction that the derivative,

$$\frac{\partial p_0}{\partial \phi^-},$$

in eq. (3.37) has to be calculated for fixed values of k_0', θ', k_0 and θ in the outer integrations means, as may be seen from Figure 3.4, that, when we vary ϕ^-, ρ will also vary while θ' and β will remain constant. The latter insight enables us to proceed with the differentiation of p_0 with respect to ϕ^-. According to eq. (3.38), p_0 depends on ϕ^- via ρ only [see eq. (3.39)]. Thus

$$\begin{aligned} \frac{\partial p_0}{\partial \phi^-} &= \frac{\partial p_0}{\partial \cos\rho}\frac{\partial \cos\rho}{\partial \phi^-} \\ &= \frac{1}{2p_0}(-2|\vec{q}+\vec{k}|k_0')(-\sin\theta'\sin\beta\sin\phi^-) \end{aligned} \tag{3.41}$$

but

$$\begin{aligned} \sin^2\phi^- &= 1-\cos^2\phi^- \\ &= \frac{-\gamma(\cos\beta,\cos\theta',\cos\rho)}{\sin^2\beta\sin^2\theta'} \end{aligned} \tag{3.42}$$

where eq. (3.40) has been used and where

$$\gamma(x,y,z) = x^2+y^2+z^2-2xyz-1. \tag{3.43}$$

Since $\phi^- \in [0,\pi]$ we must have that $\sin\phi^- \in [0,1]$. This implies that we must take the positive square root of the expression in eq. (3.42):

$$\sin\phi^- = \frac{\sqrt{-\gamma(\cos\beta,\cos\theta',\cos\rho)}}{\sin\beta\sin\theta'}. \tag{3.44}$$

The sign of the latter expression is correct since $\sin\beta\sin\theta'$ is positive as may be seen from the following considerations:

$$\theta' \in [0,\pi] \quad \Rightarrow \quad \sin\theta' \in [0,1]$$

and from Figure 3.4 it can be seen that, since $\theta \in [0,\pi]$ and $\beta \leq \theta$, $\beta \in [0,\pi]$ so that $\sin\beta \in [0,1]$.

Substitution of $\sin\phi^-$ according to eq. (3.44) into eq. (3.41) leads to

$$\frac{\partial p_0}{\partial \phi^-} = \frac{|\vec{q}+\vec{k}|k_0'}{p_0}\sqrt{-\gamma(\cos\beta,\cos\theta',\cos\rho)}.$$

Thus eq. (3.37) becomes

$$4\pi\int_0^{\pi} f(\cos\phi^-)d\phi^- = 4\pi\frac{p_0}{|\vec{q}+\vec{k}|k_0'\sqrt{-\gamma(\cos\beta,\cos\theta',\cos\rho)}}\left[\frac{1}{2p_0}[1+n_B(|p_0|)]\right]_{p_0=\nu+k_0-k_0'}$$

where, for the purpose of later performing the integration over $z=\cos\theta$, we obtain from eq. (3.38)

$$\cos\rho = \frac{|\vec{k}+\vec{q}|^2+k_0'^2+m^2-p_0^2}{2k_0'|\vec{k}+\vec{q}|} = \frac{k_0^2+2k_0q_zz+q_z^2+k_0'^2+m^2-p_0^2}{2k_0'\sqrt{k_0^2+2k_0q_zz+q_z^2}} \tag{3.45}$$

and from Figure 3.4

$$\cos\beta = \frac{\vec{q}.(\vec{k}+\vec{q})}{q_z|\vec{k}+\vec{q}|} = \frac{q_zk_0z+q_z^2}{q_z\sqrt{k_0^2+2k_0q_zz+q_z^2}}. \tag{3.46}$$

The foregoing discussions enable us now to write eq. (3.29) as

$$\begin{aligned} d\mu &= \frac{k_0^2dk_0\sin\theta d\theta}{(2\pi)^32k_0}\frac{k_0'^2dk_0'\sin\theta'd\theta'}{(2\pi)^22k_0'}\frac{1}{2p_0}\left.\frac{4\pi p_0}{|\vec{q}+\vec{k}|k_0'\sqrt{-\gamma(\cos\theta',\cos\beta,\cos\rho)}}\right|_{p_0=\nu+k_0-k_0'} \\ &= \frac{1}{8(2\pi)^4}dk_0dk_0'd\Omega \end{aligned} \tag{3.47}$$

where

$$d\Omega = \left.\frac{2k_0dzdz'}{|\vec{q}+\vec{k}|\sqrt{-\gamma(\cos\theta',\cos\beta,\cos\rho)}}\right|_{p_0=\nu+k_0-k_0'} \tag{3.48}$$

and where use has been made of

$$\int_0^{\pi}\sin\theta d\theta = \int_{-1}^{1}dz.$$

For the integration over z in eq. (3.47) one must be aware of the fact that $\cos\beta$ and $\cos\rho$ appearing in eq. (3.48) are dependent on z as may be seen from eqs. (3.45) and (3.46).

3.4.3 The Origin of Four Subregions in the k_0, k_0' plane for Gluon Emission from a Quark

In this section we shall see that the upper and lower limits which are to be used for the integrals over z and z' in eqs. (3.47) and (3.48) depend on the values of k_0 and k_0' in the outer integrals. For some regions of the k_0, k_0' plane the restrictions imposed by the energy–momentum conserving Dirac delta function in eq. (3.29) cause one to replace the usual upper limit of 1 and/or the usual lower limit of -1 for z or z' by expressions in terms of k_0 and k_0'. In the following we show step by step how this reasoning leads to distinguishing four subregions in the k_0, k_0' plane according to the combination of upper and lower limits for

z and z' which are obtained for each subregion. These regions are shown in Figure 3.6. In consequence, the integrations over z and z' will lead to different analytical results for each subregion.

We start by determining the upper and lower limits of z and z'. We have for gluon emission from a quark that

$$\begin{aligned} |\vec{q}+\vec{k}| &= |\vec{k}'+\vec{p}| \\ \Rightarrow \quad z=\cos\theta &= \frac{k_0'^2+2k_0|\vec{p}|\cos\theta_{\vec{k}'\vec{p}}+|\vec{p}|^2-k_0^2-q_z^2}{2k_0q_z}. \end{aligned}$$

The quantities, k_0, k_0', $|\vec{p}|$ and q_z are all fixed as far as the angular integrations are concerned so that z ranges between $z_{\rm U}$ and $z_{\rm L}$ where

$$z_{\rm U,L} = \frac{(k_0' \pm |\vec{p}|)^2 - k_0^2 - q_z^2}{2k_0q_z}. \tag{3.49}$$

Since one must have that $-1 \le z \le 1$ but the expression for $|z_{\rm U,L}|$ obtainable from eq. (3.49) could become larger than one as one moves around in the k_0, k_0' plane, we conclude that

$$\begin{aligned} z_{\text{upper limit}} &\equiv z_{\rm M} = \min(1, z_{\rm U}) \\ z_{\text{lower limit}} &\equiv z_{\rm m} = \max(-1, z_{\rm L}). \end{aligned}$$

Limits on $z' = \cos\theta'$ are obtained analogously:

$$\begin{aligned} |\vec{q}-\vec{k}'| &= |\vec{p}-\vec{k}| \\ \Rightarrow \quad z'=\cos\theta' &= \frac{|\vec{p}|^2-2|\vec{p}|k_0\cos\theta_{\vec{p}\vec{k}}+k_0^2-q_z^2-k_0'^2}{-2q_zk_0'} \\ \Rightarrow \quad z'_{\rm U,L} &= -\frac{(k_0 \mp |\vec{p}|)^2 - k_0'^2 - q_z^2}{2k_0'q_z} \\ \Rightarrow \quad z'_{\rm M} &= \min(1, z'_{\rm U}) \\ z'_{\rm m} &= \max(-1, z'_{\rm L}). \end{aligned} \tag{3.50}$$

Thus far we know that for gluon emission from a quark we have at least

$$\int_0^\infty dk_0 \int_0^\infty dk_0' \int_{z_{\rm m}}^{z_{\rm M}} dz \int_{z'_{\rm m}}^{z'_{\rm M}} dz'. \tag{3.51}$$

In the following discussions it may be seen how the region of support in the k_0, k_0' plane embodied in expression (3.51) is reduced to that shown in Figure 3.6 and how the subregions arise. From $k_0 + \nu = k_0' + p_0$ we may deduce that $k_0' \le k_0 + \nu - m$ always. In the limit of

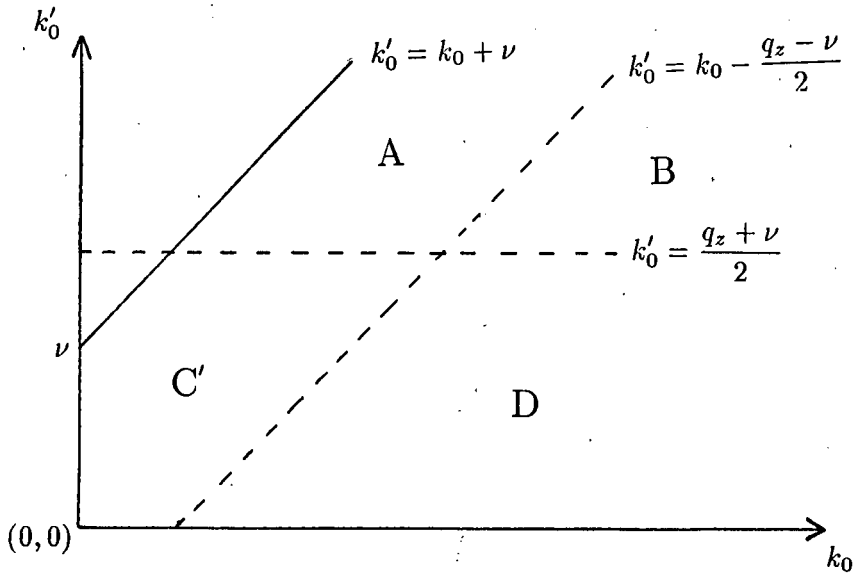

Figure 3.5: Subregions in the k_0, k'_0 plane for the process of gluon emission from a quark. Subregion C' can be further reduced to subregion C shown in Figure 3.6.

massless gluons this immediately provides us with the line, $k'_0 = k_0 + \nu$ in Figure 3.5. As was already mentioned and as we shall see shortly, for certain values of k_0 and k'_0, some of the quantities $z_{\mathrm{U,L}}$ and $z'_{\mathrm{U,L}}$ could acquire magnitudes in excess of one. For such values of k_0 and k'_0 we force the integrations over dz and/or dz' to range over a meaningful interval by choosing a 1 or -1 instead of z_{U}, z'_{U} or z_{L}, z'_{L}, respectively, for z_{M}, z'_{M} or z_{m}, z'_{m}, respectively. However, when , e.g., $-1 \leq z_{\mathrm{L}} \leq 1$ is always satisfied for a certain region of the k_0, k'_0 plane, we may safely choose $z_{\mathrm{m}} = z_{\mathrm{L}}$ for that region. If, for another region of the k_0, k'_0 plane, $z_{\mathrm{L}} \leq -1$ we choose $z_{\mathrm{m}} = -1$ for that region. Similar reasoning applies for z_{U}, z'_{L} and z'_{U}. Thus the k_0, k'_0 plane consists of regions according to what we must take for z_{m}, z_{M}, z'_{m} and z'_{M}.

We start by investigating the condition $z_{\mathrm{L}} \geq -1$. By replacing $|\vec{p}|$ by p_0 (in the limit of massless gluons) and subsequently incorporating energy conservation through $p_0 = \nu + k_0 - k'_0$ the condition,

$$z_{\mathrm{L}} = \frac{(k'_0 - |\vec{p}|)^2 - k_0^2 - q_z^2}{2k_0 q_z} \geq -1,$$

leads to

$$k'_0 \leq k_0 - \frac{q_z - \nu}{2} \quad \text{if} \quad k'_0 \leq \frac{q_z + \nu}{2} \tag{3.52}$$

and

$$k_0' \geq k_0 - \frac{q_z - \nu}{2} \quad \text{if} \quad k_0' \geq \frac{q_z + \nu}{2}. \tag{3.53}$$

The relations in (3.52) and (3.53) provide us with the lines $k_0' = k_0 - (q_z - \nu)/2$ and $k_0' = (q_z + \nu)/2$ in Figure 3.5 with (3.52) describing subregion D and (3.53) describing subregion A.

The fastidious reader would be interested to know the consequences of the simultaneous condition $z_{\rm L} \leq 1$. By using arguments similar to those used in the case of the condition $z_{\rm L} \geq -1$ we find that the condition $z_{\rm L} \leq 1$ leads to

$$k_0' \geq k_0 + \frac{q_z + \nu}{2} \quad \text{if} \quad k_0' \leq -\frac{q_z - \nu}{2} \tag{3.54}$$

and

$$k_0' \leq k_0 + \frac{q_z + \nu}{2} \quad \text{if} \quad k_0' \geq -\frac{q_z - \nu}{2}. \tag{3.55}$$

The relations in (3.54) and (3.55) do not lead to any further subdivisions of the regions A, B, C′ and D shown in Figure 3.5, but they do provide the assurance that, by using $z_{\rm m} = z_{\rm L}$ in regions A and D, $z_{\rm L}$ as given in eq. (3.49) will never become greater than one.

We may thus conclude that $z_{\rm m} = z_{\rm L}$ in regions A and D since in these regions we always have $-1 \leq z_{\rm L} \leq 1$. In the remaining regions B and C′ shown in Figure 3.5 we must take $z_{\rm m} = -1$. The region C′ in Figure 3.5 can be reduced to the region C shown in Figure 3.6 by introducing the line $k_0 = (q_z - \nu)/2$ in Figure 3.6 which can be obtained from the following argument: From eq. (A.7) we have for $m^2 > 0$

$$\begin{aligned} s = (q+k)^2 &> 0 \\ \Rightarrow \quad q^2 + 2k_0(\nu - q_z\cos\theta) &> 0. \end{aligned} \tag{3.56}$$

But we have proven above that $z_{\rm m} = -1$ in the region C′ shown in Figure 3.5. This means that the $\cos\theta$ in eq. (3.56) can become equal to -1. Thus the condition, $s > 0$, leads in region C′ to the condition

$$2k_0(\nu + q_z) > -q^2 = -(\nu - q_z)(\nu + q_z) \tag{3.57}$$

$$\Rightarrow \quad k_0 > \frac{q_z - \nu}{2}. \tag{3.58}$$

This provides us with the line $k_0 = (q_z - \nu)/2$ in Figure 3.6.

It is to be noted that, for the process of gluon emission from a quark in the context of deep inelastic scattering under consideration, the four-momentum conservation not only puts

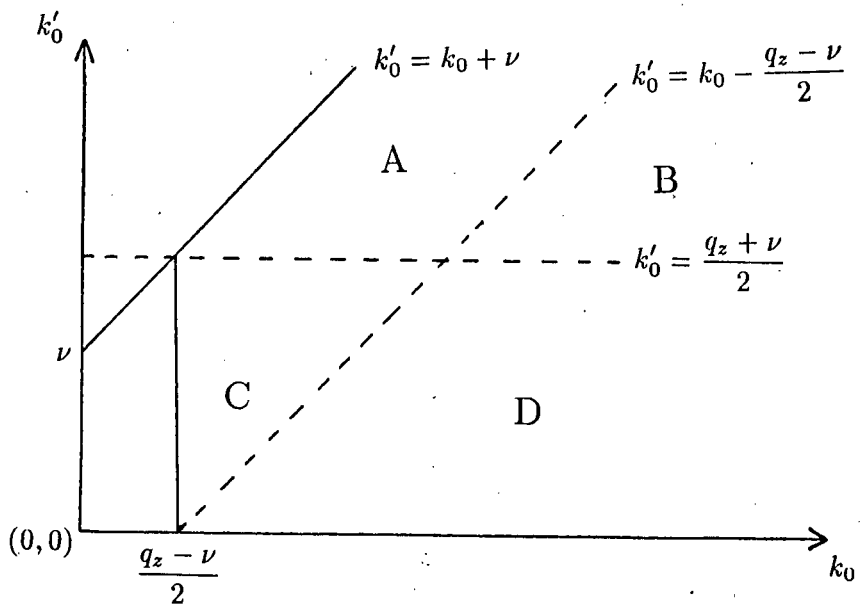

Figure 3.6: Subregions in the k_0, k'_0 plane for the process of gluon emission from a quark. Subregion C is obtained from subregion C′ in Figure 3.5 by making use of the kinematical constraint in (3.58).

the restriction $k_0 > (q_z - \nu)/2$ on the energy of the incoming quark but also on the angle, θ, which it makes with the space-like photon as can be seen by writing the inequality (3.56) in the form

$$\cos\theta < \frac{\nu + q^2/(2k_0)}{q_z} \quad (< \frac{\nu}{q_z} < 1),$$

i.e., the maximum value that $\cos\theta$ can take is ν/q_z (< 1).

Next we investigate the condition $-1 \leq z_U \leq 1$. By replacing $|\vec{p}|$ by p_0 (in the limit of massless gluons) and subsequently incorporating energy conservation through $p_0 = \nu + k_0 - k'_0$ in eq. (3.59) we obtain

$$\begin{aligned} z_U &= \frac{(k'_0 + |\vec{p}|)^2 - k_0^2 - q_z^2}{2k_0 q_z} \\ &= \frac{\nu}{q_z} + \frac{q^2}{2k_0 q_z} \\ &< 1 \end{aligned} \tag{3.59}$$

since k_0, ν and q_z are each greater than or equal to 0 and $q^2 < 0$ for deep inelastic scattering which also implies that $\nu < q_z$.

We may thus conclude that the upper limit of z can always be taken as z_U (and not necessarily 1) in all the regions A, B, C and D in Figure 3.6.

The condition, $z_U \geq -1$, leads to $k_0 \geq (q_z - \nu)/2$ which is satisfied in all the regions A, B, C and D so that the choice $z_M = z_U$ for all these regions will be safe also in this respect.

We may thus conclude that $z_M = z_U$ in all the regions A, B, C and D since in these regions we always have $-1 \leq z_U \leq 1$.

Next we investigate the condition $-1 \leq z'_L \leq 1$. Similar to the way conditions (3.52) and (3.53) were derived, the condition $z'_L \geq -1$ leads to

$$k'_0 \geq k_0 - \frac{q_z - \nu}{2} \quad \text{if} \quad k_0 \geq -\frac{q_z + \nu}{2} \tag{3.60}$$

and

$$k'_0 \leq k_0 - \frac{q_z - \nu}{2} \quad \text{if} \quad k_0 \leq -\frac{q_z + \nu}{2}. \tag{3.61}$$

The relations in (3.60) describe regions A and C while the relations in (3.61) are irrelevant for the process of gluon emission from a quark because they do not apply to regions A, B, C and D for which $k_0 > 0$.

The condition $z'_L \leq 1$ leads to

$$k'_0 \leq k_0 + \frac{q_z + \nu}{2} \quad \text{if} \quad k_0 \geq \frac{q_z - \nu}{2}$$

and

$$k'_0 \geq k_0 + \frac{q_z + \nu}{2} \quad \text{if} \quad k_0 \leq \frac{q_z - \nu}{2}.$$

These results show that $z'_L \leq 1$ is satisfied in all the regions A, B, C and D and, thus, specifically in regions A and C where $z'_m = z'_L$ can be taken.

We may thus conclude that $z'_m = z'_L$ in regions A and C since in these regions we always have $-1 \leq z'_L \leq 1$. In the remaining regions B and D we must take $z'_m = -1$.

Next we investigate the condition $-1 \leq z'_U \leq 1$. The condition $z'_U \leq 1$ leads to (since $q_z > \nu$)

$$k'_0 \geq \frac{\nu + q_z}{2}$$

which describes regions A and B. The condition $z'_U \geq -1$ leads to

$$k'_0 \geq -\frac{q_z - \nu}{2}$$

which means that $z'_U \geq -1$ is satisfied in all the regions A, B, C and D and, thus, specifically in regions A and B where $z'_M = z'_U$ can be taken.

We may thus conclude that $z'_M = z'_U$ in regions A and B since in these regions we always have $-1 \leq z'_U \leq 1$. In the remaining regions C and D we must take $z'_M = 1$.

The values of (z_m, z_M) and (z'_m, z'_M) obtained in this section may be summarized as follows:

region A: (z_L, z_U), (z'_L, z'_U)

region B: $(-1, z_U)$, $(-1, z'_U)$

region C: $(-1, z_U)$, $(z'_L, 1)$

region D: (z_L, z_U), $(-1, 1)$.

3.4.4 The Origin of Collinear Divergences for Gluon Emission from a Quark

From the expressions for s and t given in eqs. (A.9)-(A.12) there follows that

$$\begin{aligned} s(z_U) &= -\left[(k'_0 + p_0)^2 - k_0^2 - q_z^2 - q^2 - 2k_0\nu\right] \\ &= m^2 \frac{k'_0 + p_0}{p_0} + \mathcal{O}(m^4) \end{aligned}$$

where the latter step follows from eq. (B.24). Similarly one can prove that

$$t(z'_U) = m^2 \frac{p_0 - k_0}{p_0} + \mathcal{O}(m^4).$$

As mentioned at line (3.64), s and/or t appear in denominators of terms in the matrix elements and therefore give rise to divergences in the limit of massless gluons whenever $z_M = z_U$ and/or $z'_M = z'_U$, respectively, in angular integrations. These divergences are called collinear divergences as may be seen as follows from the definitions of z_U and z'_U in eqs. (3.49) and (3.50), respectively: Eqs. (3.49) and (3.50) were derived by putting $\theta_{\vec{k}'\vec{p}} = 0$ and $\theta_{\vec{k}\vec{p}} = 0$, respectively, which means having a gluon collinear with the final quark and initial quark, respectively.

3.4.5 The Integration over the Polar Angles

In this section we focus on the $\int dz \int dz'$ part of the phase space integrations referred to in expressions (3.28), (3.47) and (3.48). For these integrations, knowledge of the z and z' dependence of the integrand is required.

From the expressions for the matrix elements squared in eqs. (3.23) and (3.26) we see that they contribute to the z and z' dependence of the integrand through the quantities s

and t only where, from eqs. (A.9) and (A.10),

$$s = -2k_0 q_z (z - d) \equiv s(z) \tag{3.62}$$

and

$$t = 2k_0' q_z (z' - l) \equiv t(z'). \tag{3.63}$$

The terms appearing in eqs. (3.23) and (3.26) depend on s and t through factors of the following types:

$$\frac{1}{s}\ ;\ \frac{1}{t}\ ;\ \frac{s}{t}\ ;\ \frac{t}{s}\ ;\ \frac{1}{s^2}\ ;\ \frac{1}{t^2}\ \text{ and }\ \frac{1}{st}. \tag{3.64}$$

In addition, the quantity,

$$|\vec{q} + \vec{k}| \sqrt{-\gamma(z', \cos\beta, \cos\rho)}$$

appearing in the expression for $d\Omega$ in eq. (3.48), contributes to the z and z' dependence of the integrand since, apart from the explicit z' dependence, the quantities $|\vec{q} + \vec{k}|$, $\cos\beta$ and $\cos\rho$ are dependent on z as may be seen from the expressions for $\cos\rho$ and $\cos\beta$ in eqs. (3.45) and (3.46), respectively and

$$|\vec{q} + \vec{k}| = \sqrt{q_z^2 + 2q_z k_0 z + k_0^2}.$$

The Integration over z'

We perform the integration over z' first. As far as this integration is concerned we need to evaluate

$$A_m \equiv \int dz' \frac{t^m}{\sqrt{-\gamma(z', \cos\beta, \cos\rho)}} \tag{3.65}$$

where, as may be seen from line (3.64), the cases $m = 0,\ \pm 1,\ -2$ need to be considered and, as may be seen from eqs. (3.45) and (3.46), $\cos\rho$ and $\cos\beta$ are independent of z'.

We start with the easiest case $m = 0$ in eq. (3.65):

$$A_0 = \int_a^b dz' \frac{t^0}{\sqrt{-\gamma(z', \cos\beta, \cos\rho)}} \tag{3.66}$$

$$= \int_a^b dz' \frac{1}{\sqrt{(z' - \cos\theta_+)(\cos\theta_- - z')}} \tag{3.67}$$

where the integration limits a and b will be specified shortly and where

$$\cos\theta_\pm = \cos\rho\cos\beta \pm \sin\rho\sin\beta = \cos(\rho \mp \beta) \tag{3.68}$$

are the roots of the equation

$$\gamma(z', \cos\beta, \cos\rho) = z'^2 + \cos^2\beta + \cos^2\rho - 2z'\cos\beta\cos\rho - 1 = 0.$$

From eq. (B.6) in Appendix B we obtain

$$A_0 = \arcsin\left[\frac{z' - \cos\rho\cos\beta}{\sin\rho\sin\beta}\right]\Bigg|_{z'=a}^{z'=b}. \tag{3.69}$$

The limits a and b are obtained from the condition that the argument of the square root in eq. (3.66) must be positive:

$$-\gamma(z', \cos\beta, \cos\rho) > 0. \tag{3.70}$$

This condition may be seen to also follow from eq. (3.42) where the trivial requirement, $\sin^2\phi^- > 0$, leads to the condition in (3.70). From Figure 3.7 we see that the condition in (3.70) requires that z' lies between the roots of the equation, $\gamma(z', \cos\beta, \cos\rho) = 0$. These

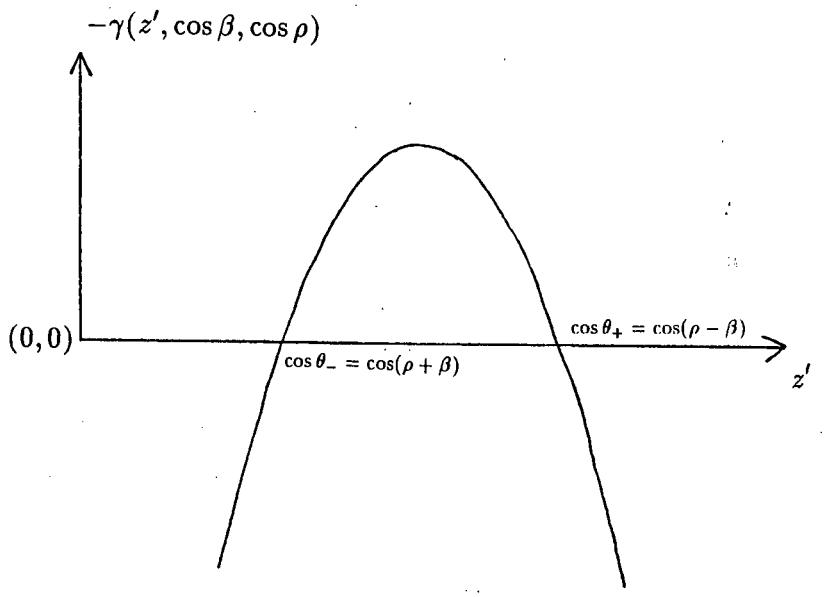

Figure 3.7: The graph of $-\gamma(z', \cos\beta, \cos\rho)$ versus z' which needs to be considered in the integration over z'.

roots are given in eq. (3.68).

Next we show, by referring to Figure 3.4, that the root $\cos\theta_-$ is smaller than the root $\cos\theta_+$. We have $\theta \in [0, \pi]$ but, as may be seen from Figure 3.4, $\beta < \theta$ and therefore $\beta \in [0, \pi]$ so that

$$\sin\beta \geq 0. \tag{3.71}$$

Furthermore, as may be seen from eq. (3.35), $\phi^- \in [0,\pi]$ which implies, by referring to Figure 3.4, that $\rho \in [0,\pi]$ so that

$$\sin\rho \geq 0 \tag{3.72}$$

and we can conclude that

$$\cos\theta_- = \cos\rho\cos\beta - \sin\rho\sin\beta \leq \cos\rho\cos\beta + \sin\rho\sin\beta = \cos\theta_+.$$

For the integration over z' we take

$$a = \cos(\rho+\beta) \qquad b = \cos(\rho-\beta) \tag{3.73}$$

for all the regions A, B, C and D as opposed to the possibly expected

$$a = z'_{\rm m} \qquad b = z'_{\rm M} \tag{3.74}$$

with $z'_{\rm m}$ and $z'_{\rm M}$ given, for each of the regions A, B, C and D, in the last paragraph before Section 3.4.4.

The choice of limits for z' given in (3.73) could be elucidated as follows: The fact that we deviate from the choice of limits in (3.74) has to do with our choice to do the z' integration before the z integration. In consequence, $z_{\rm m}$ and $z_{\rm M}$ as given in the last paragraph before Section 3.4.4 will remain as the limits for the outer z integration. However, for limits given in (3.73) not to exceed the strict limits given in (3.74), we must have

$$\cos(\rho+\beta) \geq z'_{\rm m} \qquad \text{and} \qquad \cos(\rho-\beta) \leq z'_{\rm M}. \tag{3.75}$$

That this is indeed the case may be seen from Figure 9 in ref. [15]. There it is shown that, if we take $z_{\rm m}$ and $z_{\rm M}$ as the limits for the outer z integration, the limits for the inner z' integration, given in (3.73) and obtained from the condition in (3.70), will not range beyond their strict limits $z'_{\rm m}$ and $z'_{\rm M}$. Furthermore, as one integrates over z from $z_{\rm m}$ to $z_{\rm M}$, Figure 9 in ref. [15] shows that the equal signs in (3.75) are valid for certain values of z in this range. The latter fact guarantees that collinear singularities, originating from powers of t in denominators (see Section 1.48), are indeed encountered in regions of the k_0, k'_0 plane where $z'_{\rm M} = z'_{\rm U}$. This is to be expected since encounters with collinear singularities should not depend on the order of integrations over z and z'.

The qualitative behaviour depicted in Figure 9 of ref. [15] was determined by investigation of asymptotic limits of the relevant expressions. As an alternative and somewhat more

physical suggestion to the origin of the inequalities in (3.75) we show in the following that if one of the latter two inequalities would be violated, it would mean that ϕ^- ranges over only a subset of the interval $[0,\pi]$ which seems implausible when reminded of eq. (3.35) and Figure 3.4. From Figure 3.4 we see that

$$z' \equiv \cos\theta' = \cos(\rho+\beta) \quad \text{when} \quad \phi^- = 0$$

and that

$$z' \equiv \cos\theta' = \cos(\rho-\beta) \quad \text{when} \quad \phi^- = \pi.$$

For values of ϕ^- between 0 and π, $z' \equiv \cos\theta'$ assumes values between $\cos(\rho+\beta)$ and $\cos(\rho-\beta)$. (This dependence of z' on ϕ^- could, of course, be traced back to eqs. (3.35) and (3.36) where the imposition of the Dirac delta function $\delta(\nu+k_0-p_0-k_0')$ introduced, via eqs. (3.30) and (3.31), the dependence of z' on ϕ^-.) If one of the inequalities in (3.75) would be violated, e.g. if $\cos(\rho-\beta) > z'_{\rm M}$, it would mean that we are forced to take $z'_{\rm M}$ as the upper limit for z' since we have already determined that $z'_{\rm M}$ is a strict upper limit. But since, in this hypothetical case, z' would then not be allowed to become equal to $\cos(\rho-\beta)$ it would mean, according to the above discussions, that ϕ^- is not allowed to become equal to π and, therefore, ranges over only a subset of the interval $[0,\pi]$.

From eqs. (3.69), (3.73) and (3.68) there follows that

$$\begin{aligned} A_0 &= \arcsin(1) - \arcsin(-1) = \frac{\pi}{2} - \left(-\frac{\pi}{2}\right) \\ &= \pi. \end{aligned} \tag{3.76}$$

Next we consider the case $m=-1$ in eq. (3.65):

$$\begin{aligned} A_{-1} &= \int_a^b dz' \frac{t^{-1}}{\sqrt{-\gamma(z',\cos\beta,\cos\rho)}} \\ &= \int_a^b dz' \frac{1}{2k_0' q_z (z'-l)\sqrt{-\gamma(z',\cos\beta,\cos\rho)}} \end{aligned} \tag{3.77}$$

where a and b are given in (3.73).

Before commencing with the evaluation of eq. (3.77) we show that only the case

$$l > \cos(\rho-\beta) \tag{3.78}$$

out of the possible cases $l < \cos(\rho+\beta)$, $\cos(\rho+\beta) \le l \le \cos(\rho-\beta)$ and $l > \cos(\rho-\beta)$ needs to be considered in the evaluation. The case $l < \cos(\rho+\beta)$ is irrelevant since the relations,

$$\cos(\rho+\beta) \le z' \le \cos(\rho-\beta) \tag{3.79}$$

obtained from (3.73) and

$$t < 0 \quad \Rightarrow \quad z' < l, \tag{3.80}$$

obtained from eq. (A.10), must hold simultaneously. The case $\cos(\rho+\beta) \leq l \leq \cos(\rho-\beta)$ is considered irrelevant too since, according to (3.80), l is a strict upper limit for z' so that, for the same reason we required that $\cos(\rho-\beta) < z'_{\rm M}$ in (3.75) [The suggested reason is put forward in the paragraph following on (3.75).]; we require that

$$l > \cos(\rho-\beta).$$

This requirement guarantees, as explained at line (B.8), that

$$\gamma(l, \cos\beta, \cos\rho) > 0.$$

This condition in turn ensures that the argument of the square root is positive in the result for A_{-1} derived in Appendix B and given in eq. (B):

$$A_{-1} = \frac{-\pi}{2k'_0 q_z \sqrt{\gamma(l, \cos\beta, \cos\rho)}} \tag{3.81}$$

Next we consider the case $m = -2$ in eq. (3.65):

$$\begin{aligned} A_{-2} &= \int_a^b dz' \frac{t^{-2}}{\sqrt{-\gamma(z', \cos\beta, \cos\rho)}} \\ &= \frac{1}{(2k'_0 q_z)^2} \int_a^b dz' \frac{1}{(z'-l)^2 \sqrt{-\gamma(z', \cos\beta, \cos\rho)}} \end{aligned}$$

where a and b are given in (3.73). The final expression for A_{-2} is obtainable from that of A_{-1} given in eq. (3.81):

$$\begin{aligned} A_{-2} &= \frac{1}{(2k'_0 q_z)^2} \frac{d}{dl} \int_a^b dz' \frac{1}{(z'-l)\sqrt{-\gamma(z', \cos\beta, \cos\rho)}} \\ &= \frac{1}{(2k'_0 q_z)} \frac{d}{dl} A_{-1} \\ &= \frac{1}{(2k'_0 q_z)^2} \frac{d}{dl} \frac{-\pi}{\sqrt{\gamma(l, \cos\beta, \cos\rho)}} \\ &= \frac{\pi}{(2k'_0 q_z)^2} \frac{l - \cos\beta\cos\rho}{[\gamma(l, \cos\beta, \cos\rho)]^{3/2}}. \end{aligned}$$

Next we consider the case $m = 1$ in eq. (3.65):

$$\begin{aligned} A_1 &= \int_a^b dz' \frac{t}{\sqrt{-\gamma(z', \cos\beta, \cos\rho)}} \\ &= 2k'_0 q_z \int_a^b dz' \frac{z'-l}{\sqrt{-\gamma(z', \cos\beta, \cos\rho)}}. \end{aligned} \tag{3.82}$$

The final expression for A_1 derived in Section (c) of Appendix B is

$$A_1 = 2k_0' q_z \pi(\cos\beta\cos\rho - l). \tag{3.83}$$

The Integration over z

At the start of this Section 3.4.5 we described how the integrand for the $\int dz \int dz'$ part of the phase space integrations depends on z and z'. Subsequently we obtained the results for the integrations over z' by evaluating the expression in eq. (3.65) for each of the cases $m = 0,\ \pm 1,\ -2$ which represent all the relevant z' dependent terms.

In the rest of this section we consider the subsequent integration over z. As an illustrative example we explicitly evaluate:

$$I\left(\frac{1}{st}\right) \equiv \int \frac{1}{st} d\Omega.$$

With s, t and $d\Omega$ given in eqs. (3.62), (3.63) and (3.48), respectively, we can write:

$$\begin{aligned} I\left(\frac{1}{st}\right) &= \frac{2k_0}{(-2k_0 q_z)(2k_0' q_z)} \int\int dz dz' \frac{1}{(z-d)(z'-l)\sqrt{-\gamma(z',\cos\beta,\cos\rho)}|\vec{q}+\vec{k}|} \\ &= \frac{\pi}{2k_0' q_z^2} \int_{z_m}^{z_M} dz \frac{1}{(z-d)|\vec{q}+\vec{k}|\sqrt{\gamma(l,\cos\beta,\cos\rho)}} \end{aligned} \tag{3.84}$$

where, in the latter step, use has been made of eqs. (3.77) and (3.81), and, z_m and z_M are given in the last paragraph before Section 3.4.4. As discussed just after (3.64), the quantities $\cos\beta$, $\cos\rho$ and $|\vec{q}+\vec{k}|$ are z dependent. In order to make the integration over z in eq. (3.84) tractable, we make use of the identity (the proof is sketched in Section (d) of Appendix B):

$$|\vec{q}+\vec{k}|^2 \gamma(l,\cos\beta,\cos\rho) = \frac{k_0^2}{k_0'^2}(k_0' - \nu)^2 \gamma(z,H,J) \tag{3.85}$$

where

$$H = 1 + \frac{m^2}{2k_0(k_0' - \nu)} \tag{3.86}$$

$$J = \frac{q^2}{2q_z(k_0' - \nu)} + \frac{\nu}{q_z}. \tag{3.87}$$

Thereby the z dependence is explicit in the right hand side of eq. (3.85) since H and J are z independent. According to (B.8), $\gamma(l,\cos\beta,\cos\rho) > 0$ in the left hand side of eq. (3.85). Therefore, it follows from eq. (3.85) that

$$\gamma(z,H,J) > 0 \tag{3.88}$$

so that we obtain from eq. (3.85):

$$\begin{aligned} |\vec{q}+\vec{k}|\sqrt{\gamma(l,\cos\beta,\cos\rho)} &= \frac{k_0}{k_0'}|k_0'-\nu|\sqrt{\gamma(z,H,J)} \\ \Rightarrow \quad I\left(\frac{1}{st}\right) &= \frac{\pi}{2k_0|k_0'-\nu|q_z^2}\int_{z_{\rm m}}^{z_{\rm M}}\frac{dz}{(z-d)\sqrt{\gamma(z,H,J)}}. \end{aligned} \tag{3.89}$$

In Section (e) of Appendix B we show that the change of variables,

$$\tau \equiv \frac{1}{z-d} - \frac{HJ-d}{\tilde{c}}, \tag{3.90}$$

leads to

$$I\left(\frac{1}{st}\right) = -\frac{\pi}{2k_0q_z^2|k_0'-\nu|}\int_{\tau(z_{\rm M})}^{\tau(z_{\rm m})} d\tau\left[\tilde{c}\left(\tau^2+\frac{\Delta}{4\tilde{c}^2}\right)\right]^{-1/2} \tag{3.91}$$

where

$$\tilde{c} \equiv \gamma(d,H,J) \tag{3.92}$$

$$\Delta \equiv -4(H^2-1)(J^2-1). \tag{3.93}$$

Since the quantities, $\tilde{c}$ and Δ, appear in the argument of a square root in eq. (3.91), their signs will be important in further calculations. According to eq. (B.25), $\tilde{c}$ is positive in all the regions A, B, C and D (see Figure 3.6) under consideration:

$$\tilde{c} > 0 \quad \text{in regions A,B,C,D.} \tag{3.94}$$

The sign of Δ is determined as follows:

$$\Delta = -4(H^2-1)(J^2-1) \tag{3.95}$$

but, from eq. (3.86), there follows that

$$(H^2-1) = (H-1)(H+1) = \frac{m^2}{2k_0(k_0'-\nu)}\left(2+\frac{m^2}{2k_0(k_0'-\nu)}\right). \tag{3.96}$$

From Figure 3.6 it may be seen that $k_0' > \nu$ in regions A and B whereas both the cases $k_0' > \nu$ and $k_0' < \nu$ are possible in regions C and D. Therefore it may be seen from eq. (3.96) that

$$H^2-1 \begin{cases} > 0 & \text{in regions A,B} \\ > 0 & \text{in regions C,D if } k_0' > \nu \\ < 0 & \text{in regions C,D if } k_0' < \nu. \end{cases} \tag{3.97}$$

From eq. (3.87) there follows that:

$$\begin{aligned} J \pm 1 &= \frac{\nu^2 - q_z^2 + 2k_0'\nu - 2\nu^2 \pm 2q_z(k_0'-\nu)}{2q_z(k_0'-\nu)} = \frac{(\nu \pm q_z)(2k_0' - \nu \mp q_z)}{2q_z(k_0'-\nu)} \\ \Rightarrow \quad J^2-1 &= (J+1)(J-1) = \frac{q^2(2k_0'-\nu-q_z)(2k_0'-\nu+q_z)}{4q_z^2(k_0'-\nu)^2}. \end{aligned} \tag{3.98}$$

From Figure 3.6 it may be seen that $2k_0' - \nu - q_z$ is positive in regions A and B and negative in regions C and D whereas, since $q_z > \nu$, $2k_0' - \nu + q_z$ is positive in each of regions A, B, C and D. Therefore

$$J^2 - 1 \quad \begin{cases} < 0 & \text{in regions A,B} \\ > 0 & \text{in regions C,D.} \end{cases} \tag{3.99}$$

The relations in (3.95), (3.97) and (3.99) enable us to conclude that

$$\Delta \quad \begin{cases} > 0 & \text{in regions A,B} \\ < 0 & \text{in regions C,D if } k_0' > \nu \\ > 0 & \text{in regions C,D if } k_0' < \nu. \end{cases} \tag{3.100}$$

In the following, we continue with the calculation of the integral appearing in eq. (3.91) for the two cases, $\Delta > 0$ and $\Delta < 0$, shown in (3.100):

For $\Delta > 0$:

$$\begin{aligned} -E_{\Delta>0} &\equiv \int_{\tau(z_M)}^{\tau(z_m)} d\tau \left[\tilde{c}\left(\tau^2 + \frac{\Delta}{4\tilde{c}^2}\right)\right]^{-1/2} \\ &= \frac{1}{\sqrt{\tilde{c}}} \int_{\tau(z_M)}^{\tau(z_m)} d\tau \left(\frac{\sqrt{\Delta}}{2\tilde{c}} \sqrt{\frac{4\tau^2\tilde{c}^2}{\Delta} + 1}\right)^{-1} \\ &= \frac{1}{\sqrt{\tilde{c}}} \int_{x_1}^{x_2} \frac{dx}{\sqrt{x^2+1}} \end{aligned} \tag{3.101}$$

where we changed variable:

$$x = \frac{2\tilde{c}}{\sqrt{\Delta}}\tau \tag{3.102}$$

$$x_1 = \frac{2\tilde{c}}{\sqrt{\Delta}}\tau(z_M) \qquad x_2 = \frac{2\tilde{c}}{\sqrt{\Delta}}\tau(z_m). \tag{3.103}$$

The further change of variable, $x = \sinh y$, leads to

$$\begin{aligned} -E_{\Delta>0} &= \frac{1}{\sqrt{\tilde{c}}} \int_{\operatorname{arcsinh} x_1}^{\operatorname{arcsinh} x_2} dy \\ &= \frac{1}{\sqrt{\tilde{c}}} \left[\operatorname{arcsinh}\left(\frac{2\tilde{c}}{\sqrt{\Delta}}\tau(z_m)\right) - \operatorname{arcsinh}\left(\frac{2\tilde{c}}{\sqrt{\Delta}}\tau(z_M)\right)\right]. \end{aligned} \tag{3.104}$$

In the calculation of $E_{\Delta<0}$ below we shall see that the result will involve arccosh as opposed to the case of $E_{\Delta>0}$ above which involved arcsinh. Since, as may be seen from Figure 3.8, the argument of arccosh must be positive we shall see in the following that, as opposed to the case in eq. (3.102), a minus sign must be included in the change of variable in eq. (3.109) in order to ensure that this requirement is met. Since the argument will, as in the case of eq.

(3.104), be proportional to $\tau(z_{\rm m})$ and $\tau(z_{\rm M})$ we first investigate the signs of these quantities. In Section (f) of Appendix B it is shown that

$$\tau(z_{\rm m}) > 0 \quad \text{and} \quad \tau(z_{\rm M}) < 0 \quad \text{in regions A,B} \tag{3.105}$$

$$\tau(z_{\rm m}) < 0 \quad \text{and} \quad \tau(z_{\rm M}) < 0 \quad \text{in regions C,D.} \tag{3.106}$$

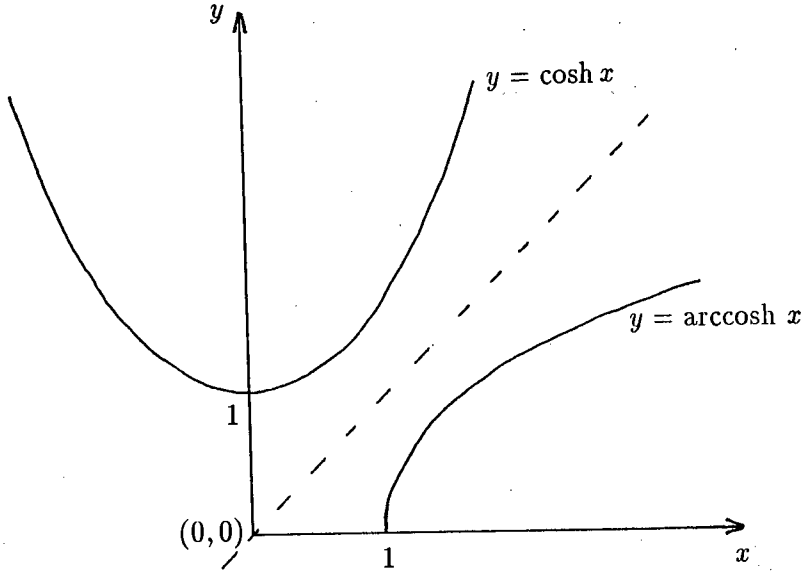

Figure 3.8: The graph of arccosh$x$ versus x which needs to be considered in the derivation of eq. (3.111).

For $\Delta < 0$ one has $\Delta = -|\Delta|$ so that

$$-E_{\Delta<0} \equiv \int_{\tau(z_{\rm M})}^{\tau(z_{\rm m})} d\tau \left[\tilde{c}\left(\tau^2 + \frac{\Delta}{4\tilde{c}^2}\right)\right]^{-1/2} \tag{3.107}$$

$$= \frac{1}{\sqrt{\tilde{c}}} \int_{\tau(z_{\rm M})}^{\tau(z_{\rm m})} d\tau \left(\sqrt{\tau^2 - \frac{|\Delta|}{4\tilde{c}^2}}\right)^{-1}$$

$$= \frac{1}{\sqrt{\tilde{c}}} \int_{\tau(z_{\rm M})}^{\tau(z_{\rm m})} d\tau \left(\frac{\sqrt{|\Delta|}}{2\tilde{c}} \sqrt{\frac{4\tau^2\tilde{c}^2}{|\Delta|} - 1}\right)^{-1}$$

$$= -\frac{1}{\sqrt{\tilde{c}}} \int_{x_1'}^{x_2'} \frac{dx'}{\sqrt{x'^2 - 1}} \tag{3.108}$$

where we changed variable:

$$x' = -\frac{2\tilde{c}}{\sqrt{|\Delta|}}\tau \tag{3.109}$$

$$x_1' = -\frac{2\tilde{c}}{\sqrt{|\Delta|}}\tau(z_{\rm M}) = \left|\frac{2\tilde{c}}{\sqrt{|\Delta|}}\tau(z_{\rm M})\right| \qquad x_2' = -\frac{2\tilde{c}}{\sqrt{|\Delta|}}\tau(z_{\rm m}) = \left|\frac{2\tilde{c}}{\sqrt{|\Delta|}}\tau(z_{\rm m})\right| . \tag{3.110}$$

The relations in line (3.110) only hold, as far as the expressions containing absolute value signs are concerned, in regions C,D [see (3.94) and (3.106)] which are the relevant regions to consider for the case of $\Delta < 0$ under consideration [see (3.100)].

The further change of variable, $x' = \cosh y'$, leads to

$$\begin{aligned} -E_{\Delta<0} &= -\frac{1}{\sqrt{\tilde{c}}}\int_{\operatorname{arccosh} x_1'}^{\operatorname{arccosh} x_2'} dy' \\ &= \frac{1}{\sqrt{\tilde{c}}}\left[\operatorname{arccosh}\left(\left|\frac{2\tilde{c}}{\sqrt{|\Delta|}}\tau(z_{\mathrm{M}})\right|\right) - \operatorname{arccosh}\left(\left|\frac{2\tilde{c}}{\sqrt{|\Delta|}}\tau(z_{\mathrm{m}})\right|\right)\right]. \end{aligned} \tag{3.111}$$

The results obtained thus far may be summarized as follows:

In regions A,B and in regions C,D for $k_0' < \nu$ we obtain, from eqs. (3.91), (3.104) and the relations in (3.100),:

$$I\left(\frac{1}{st}\right) = -\frac{\pi}{2k_0 q_z^2 |k_0' - \nu|\sqrt{\tilde{c}}}\left[\operatorname{arcsinh}\left(\frac{2\tilde{c}}{\sqrt{|\Delta|}}\tau(z_{\mathrm{m}})\right) - \operatorname{arcsinh}\left(\frac{2\tilde{c}}{\sqrt{|\Delta|}}\tau(z_{\mathrm{M}})\right)\right]. \tag{3.112}$$

In regions C,D for $k_0' > \nu$ we obtain, from eqs. (3.91) and (3.111),:

$$I\left(\frac{1}{st}\right) = -\frac{\pi}{2k_0 q_z^2 |k_0' - \nu|\sqrt{\tilde{c}}}\left[-\operatorname{arccosh}\left(\left|\frac{2\tilde{c}\tau(z_{\mathrm{m}})}{\sqrt{|\Delta|}}\right|\right) + \operatorname{arccosh}\left(\left|\frac{2\tilde{c}\tau(z_{\mathrm{M}})}{\sqrt{|\Delta|}}\right|\right)\right]. \tag{3.113}$$

The form which the latter results take in the limit, $m \to 0$, can be obtained from the following relations which are proven in Section (f) of Appendix B:

In regions A,B,C,D:

$$\begin{aligned} \frac{2\tilde{c}|\tau(z_{\mathrm{M}})|}{\sqrt{|\Delta|}} &= \frac{2\tilde{c}|\tau(z_{\mathrm{U}})|}{\sqrt{|\Delta|}} \\ &= \frac{-q^2 p_0^3}{(k_0+\nu)m^3}\sqrt{\frac{-q^2}{k_0(2k_0'+q_z-\nu)|k_0'-\nu||q_z+\nu-2k_0'|}} + \mathcal{O}(m^{-1}) \qquad (3.114) \\ \tilde{c} &= \left(\frac{-q^2 p_0}{2q_z k_0(k_0'-\nu)}\right)^2 + \mathcal{O}(m^2) \qquad (3.115) \end{aligned}$$

In regions A,D:

$$\frac{2\tilde{c}|\tau(z_{\mathrm{m}})|}{\sqrt{|\Delta|}} = \frac{2\tilde{c}|\tau(z_{\mathrm{L}})|}{\sqrt{|\Delta|}} = \frac{p_0}{4mk_0'}\sqrt{\frac{-q^2(2k_0'+q_z-\nu)|q_z+\nu-2k_0'|}{k_0|k_0'-\nu|}} + \mathcal{O}(m) \tag{3.116}$$

In regions B,C:

$$\frac{2\tilde{c}|\tau(z_{\mathrm{m}})|}{\sqrt{|\Delta|}} = \frac{2\tilde{c}|\tau(-1)|}{\sqrt{|\Delta|}} = \frac{p_0}{m(2k_0-q_z+\nu)}\sqrt{\frac{-q^2 k_0|2k_0'-\nu-q_z|}{|k_0'-\nu|(2k_0'+q_z-\nu)}} + \mathcal{O}(m^0) \tag{3.117}$$

In Section (g) of Appendix B it is shown how the above relations, inserted into eqs. (3.112) and (3.113), lead to the final results:

$$I\left(\frac{1}{st}\right) \simeq \frac{\pi}{q_z p_0 q^2} \times \begin{cases} \ln\left(\dfrac{p_0^4 (q^2)^2}{m^4 k_0 k_0' (k_0+\nu)|k_0'-\nu|}\right) & \text{in region A} \\ \ln\left(\dfrac{4p_0^4 (q^2)^2}{m^4 (k_0+\nu)|k_0'-\nu|(2k_0-q_z+\nu)(2k_0'+q_z-\nu)}\right) & \text{in region B} \\ \ln\left(\dfrac{-p_0^2 q^2 (2k_0-q_z+\nu)}{m^2 k_0 (k_0+\nu)(-2k_0'+q_z+\nu)}\right) & \text{in region C} \\ \ln\left(\dfrac{4p_0^2 (-q^2) k_0'}{m^2 (k_0+\nu)(2k_0'+q_z-\nu)(q_z+\nu-2k_0')}\right) & \text{in region D.} \end{cases} \tag{3.118}$$

The results in the latter equation is the explicit form of the result embodied by the first equation at line (D.16). This may be checked by making use of the expressions for A_4 in Table D.3, by noting that, according to Figure D.1, regions A,B,C and D are associated with classes 1,3,4 and 2, respectively, and by obtaining explicit expressions for A_4 from eqs. (D.12) and (D.1).

As an example, we discussed the derivation of the results in eq. (3.118) in detail. The other results given at line (D.16) are derived in a similar way. The way in which these results from four-particle processes contribute to the structure functions of the nucleon can be seen by considering eqs. (4.5), (4.6) and (4.9)–(4.12) and the discussions in Appendix D.

3.5 The Vertex Correction to a Quark

A correction of $\mathcal{O}(\alpha_S)$ arises from the interference between the lowest-order diagram and the vertex correction in Figure 3.1 represented by the amplitudes M_{3a} and M_{3b}, respectively, where

$$\begin{aligned} M_{3a} &= \bar{u}(k',s')(ie\gamma_\nu)\epsilon^\nu_{\gamma^*}(q)u(k,s) \\ M_{3b} &= \int \frac{d^4p}{(2\pi)^4}\bar{u}(k',s')(-ig\gamma_\mu)(-g^{\mu\sigma})iD^{11}(p)iS^{11}(k'-p), \\ &\quad (ie\gamma_\nu)\epsilon^\nu_{\gamma^*}(q)iS^{11}(k-p)(-ig\gamma_\sigma)u(k,s). \end{aligned} \tag{3.119}$$

and where we suppress reference to colour factors and fractional charges. In the following we shall make use of the notation appearing in Table 3.1, eqs. (3.7), (3.8), (3.2) and (3.3).

It is to be noted that $k' \equiv k + q$ for the three-particle process under consideration. (For four-particle processes we have $k' \equiv k + q - p$.) For the interference,

$$M_{3a}M_{3b}^* + M_{3b}M_{3a}^* = 2\mathrm{Re}M_{3a}M_{3b}^* \,, \tag{3.120}$$

we need to consider the real part of (quark mass = 0 ; gluon mass = m):

$$\begin{aligned}\sum_{\pm s,\pm s'} M_{3a}M_{3b}^* \;=\; & \int \frac{d^4p}{(2\pi)^4}\mathrm{Tr}\left\{ \not{k}' ie\gamma_\nu \epsilon^\nu_{\gamma^*}(q)\, \not{k} ig\gamma_\sigma (\not{k}-\not{p})[i\bar{S}^{11}(k-p)]^*[\epsilon^\rho_{\gamma^*}(q)]^* \right. \\ & \left. (-ie\gamma_\rho)(\not{k}'-\not{p})[i\bar{S}^{11}(k'-p)]^*(-g^{\mu\sigma})[iD^{11}(p)]^* ig\gamma_\mu \right\}. \end{aligned} \tag{3.121}$$

Since, as may be seen from their expressions in Table 3.1 and the identity in eq. (3.17), each propagator can be decomposed into two terms, one corresponding to off-mass shell propagation and the other one corresponding to on-mass shell propagation and containing a Dirac delta function, the expression in eq. (3.121) contains terms with zero, one, two and three Dirac delta functions. Terms with zero and two Dirac delta functions are pure imaginary and therefore does not contribute since the interference is real as may be seen in eq. (3.120). The term containing three Dirac delta functions also does not contribute due to conflicting constraints imposed by the Dirac delta functions. Thus we only need to consider the three terms containing one Dirac delta function each. According to whether this Dirac delta function refers to the internal boson, fermion or fermion primed line in the $\mathcal{O}(\alpha_S)$ vertex graph in Figure 3.1, we call it the bosonic, fermionic or fermionic primed part of the vertex correction, respectively. Thus we obtain (we drop the subscript (γ^*) of ϵ)

$$\begin{aligned} 2\mathrm{Re}\sum_{\pm s,\pm s'} M_{3a}M_{3b}^* \;=\; & ieig(-ie)(-g^{\mu\sigma})ig\int \frac{d^4p}{(2\pi)^4}\mathrm{Tr}\left\{ \not{k}'\, \not{\epsilon}(q)\, \not{k}\gamma_\sigma(\not{k}-\not{p})[\not{\epsilon}(q)]^*(\not{k}'-\not{p})\gamma_\mu \right\} \\ & \times \left\{ \left[\pi\delta\left((k-p)^2\right) - 2\pi n_{\mathrm{F}}(x_{k-p})\delta\left((k-p)^2\right)\right] \frac{-i}{(k'-p)^2}\frac{-i}{p^2-m^2} \right. \\ & + \frac{-i}{(k-p)^2}\left[\pi\delta\left((k'-p)^2\right) - 2\pi n_{\mathrm{F}}(x_{k'-p})\delta\left((k'-p)^2\right)\right]\frac{-i}{p^2-m^2} \\ & \left. + \frac{-i}{(k-p)^2}\frac{-i}{(k'-p)^2}\left[\pi\delta(p^2-m^2) + 2\pi n_{\mathrm{B}}(|p_0|)\delta(p^2-m^2)\right]\right\} + \text{c.c.} \\ = \; & e^2g^2\int \frac{d^4p}{(2\pi)^4}\mathrm{Tr}\left\{ \not{k}'\, \not{\epsilon}(q)\, \not{k}\gamma^\mu(\not{k}-\not{p})[\not{\epsilon}(q)]^*(\not{k}'-\not{p})\gamma_\mu \right\} \\ & \times \left\{ -\frac{\pi\delta\left((k-p)^2\right)}{(k'-p)^2(p^2-m^2)}[1-2n_{\mathrm{F}}(x_{k-p})] \right. \\ & \left. -\frac{\pi\delta\left((k'-p)^2\right)}{(k-p)^2(p^2-m^2)}[1-2n_{\mathrm{F}}(x_{k'-p})] \right. \end{aligned}$$

$$-\frac{\pi\delta(p^2-m^2)}{(k-p)^2(k'-p)^2}[1+2n_{\rm B}(|p_0|)]\Big\}+\text{c.c.} \tag{3.122}$$

In the evaluation of the trace we make use of the assumption of massless quarks embodied by $k^2=0$ and $k'.k'=0$, energy-momentum conservation ($k'=k+q$) and the fact that $q.\epsilon=0$ for each polarization state of the virtual photon [see eq. (2.5)] to obtain

$$\begin{aligned}\mathrm{Tr}\{\not k'\not\epsilon(q)\not k\gamma^\mu(\not k-\not p)[\not\epsilon(q)]^*(\not k'-\not p)\gamma_\mu\} &= -4\Big\{[(q^2)^2+2q^2(k+k').p-p^2q^2]\epsilon.\epsilon^*\\ &\quad +4(q^2-p^2)|\epsilon.k|^2-4q^2(\epsilon^*.k)(\epsilon.p)+2q^2|\epsilon.p|^2\\ &\quad +4p.(k+k')(\epsilon.k)(\epsilon^*.p)\Big\}.\end{aligned}$$

Inserting the latter expression into eq. (3.122) we obtain

$$\begin{aligned}2\mathrm{Re}\sum_{\pm s,\pm s'}M_{3a}M_{3b}^* &= 8\pi e^2g^2\int\frac{d^4p}{(2\pi)^4}\Big\{[(q^2)^2+2q^2(k+k').p-p^2q^2]\epsilon.\epsilon^*\\ &\quad +4(q^2-p^2)|\epsilon.k|^2+[2(k+k').p-2q^2][(\epsilon.k)(\epsilon^*.p)+(\epsilon^*.k)(\epsilon.p)]\\ &\quad +2q^2|\epsilon.p|^2\Big\}\Big\{\frac{\delta\left((k-p)^2\right)}{(k'-p)^2(p^2-m^2)}[1-2n_{\rm F}(x_{k-p})]\\ &\quad +\frac{\delta\left((k'-p)^2\right)}{(k-p)^2(p^2-m^2)}[1-2n_{\rm F}(x_{k'-p})]\\ &\quad +\frac{\delta(p^2-m^2)}{(k-p)^2(k'-p)^2}[1+2n_{\rm B}(|p_0|)]\Big\}.\end{aligned} \tag{3.123}$$

In the latter expression, the terms proportional to $\delta\left((k-p)^2\right)$, $\delta\left((k'-p)^2\right)$ and $\delta(p^2-m^2)$ are referred to as the fermionic, fermionic primed and bosonic contributions, respectively. In Section 3.5.1 we derive further expressions of this interference term for the cases of longitudinal and transverse polarization of the virtual photon after implementing the restriction on the angle between $\vec{k}$ and $\vec{q}$ due to energy-momentum conservation.

3.5.1 The Phase Space Integral for the Vertex Correction

By including the factor $d^4p/(2\pi)^4$ from the loop integration, the phase space integral for the vertex correction to a quark becomes

$$\int d\mu_{\rm V}\,n_{\rm F}(x_k)[1-n_{\rm F}(x_{k'})] \tag{3.124}$$

where

$$d\mu_{\rm V} \equiv \frac{d^3k}{(2\pi)^3 2k_0}\frac{d^3k'}{(2\pi)^3 2k_0'}(2\pi)^4\delta^4(k'-k-q)\frac{d^4p}{(2\pi)^4} \tag{3.125}$$

$$= \frac{1}{4(2\pi)^2}\int\frac{|\vec{k}|dk_0d\phi dz}{k_0'}\delta(k_0'-k_0-\nu)\frac{d^4p}{(2\pi)^4} \tag{3.126}$$

and where $k'_0 = |\vec{k'}| = |\vec{k} + \vec{q}|$.

We consider the integration over $\vec{k}$ for the time being in a reference frame with the z axis chosen along the direction of $\vec{q}$. This choice of reference frame is shown in Figure 3.9. Also shown in this figure are the vectors $\vec{k}$, $\vec{k'}$ and $\vec{q}$ lying in the same plane due to the relation $\vec{k'} = \vec{k} + \vec{q}$. The integration over the angle θ between $\vec{k}$ and $\vec{q}$, embodied by the integration $\int dz$ where $z = \cos\theta$ in eq. (3.126), is performed next. The Dirac delta function $\delta(k'_0 - k_0 - \nu)$ must be taken into consideration in the integration over z:

$$\delta(k'_0 - k_0 - \nu) = \delta\left(g(z)\right)$$

where

$$g(z) = k'_0 - k_0 - \nu = |\vec{k} + \vec{q}| - k_0 - \nu = \sqrt{|\vec{k}|^2 + 2|\vec{k}|q_z z + q_z^2} - |\vec{k}| - \nu.$$

But

$$\delta\left(g(z)\right) = \sum_i \frac{1}{|g'(z_i)|}\delta(z - z_i)$$

where the z_i are the roots of the equation $g(z) = 0$. In our case

$$z_0 = \frac{q^2 + 2k_0\nu}{2|\vec{k}|q_z} \tag{3.127}$$

is the only root. Since z_0 is the cosine of an angle, the restriction,

$$-1 \leq \frac{q^2 + 2k_0\nu}{2|\vec{k}|q_z} \leq 1\,, \tag{3.128}$$

is understood to hold from now on in further integrations. Now

$$\begin{aligned} \frac{\partial g(z)}{\partial z} &= \frac{|\vec{k}|q_z}{|\vec{k'}|} \\ \Rightarrow \quad d\mu_V &= \frac{1}{4(2\pi)^2 q_z}\int dk_0 d\phi\theta(1 - z_0)\theta(1 + z_0)\frac{d^4p}{(2\pi)^4} \end{aligned} \tag{3.129}$$

where the step functions introduced into eq. (3.129) embody the restriction given in eq. (3.128).

In order to continue with the integration over ϕ we need to be aware of the behaviour of the integrand. For this purpose we continue at this stage with the evaluation of the expression in eq. (3.123). The contribution of the latter expression in the case of the longitudinal polarization ϵ_0 of the virtual photon can be obtained by using the expression for ϵ_0 given in

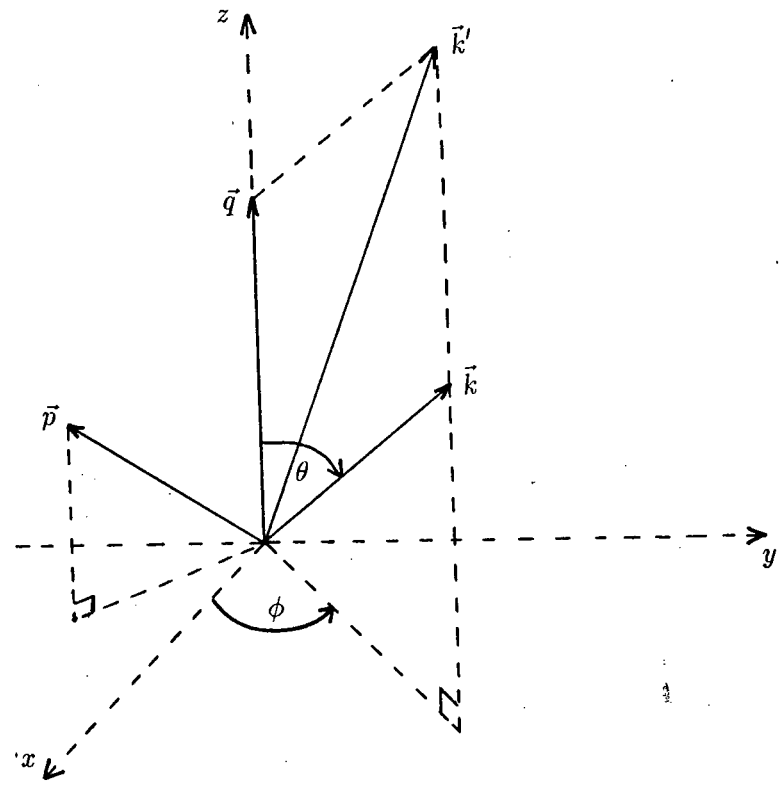

Figure 3.9: The reference frame in which we consider the integrations over the polar and azimuthal angles of $\vec{k}$. Subsequent integrations are considered in the reference frame shown in Figure 3.10.

eq. (2.4). This leads again to eqs. (3.19) and (3.20) as well as

$$(\epsilon_0.k)(\epsilon_0^*.p) = (\epsilon_0^*.k)(\epsilon_0.p) = -\frac{1}{q^2}(q_z k_0 - \nu k_z)(q_z p_0 - \nu p_z) \tag{3.130}$$

$$|\epsilon_0.p|^2 = -\frac{1}{q^2}(q_z p_0 - \nu p_z)^2 \,. \tag{3.131}$$

In order to write the expression in eq. (3.123) explicitly in terms of the quantities $(k'-p)^2$ and $(k-p)^2$ we make use of the following relations:

$$k.p = \frac{1}{2}[p^2 - (k-p)^2] \tag{3.132}$$

$$(k'-p)^2 = (k+q-p)^2 = q^2 + p^2 + 2k_0\nu - 2\vec{k}.\vec{q} - 2k.p - 2q.p \tag{3.133}$$

$$k'.p = \frac{1}{2}[p^2 - (k'-p)^2] \tag{3.134}$$

$$\vec{k}.\vec{q} = |\vec{k}||\vec{q}|z = k_0 q_z z = \frac{1}{2}(q^2 + 2k_0\nu) \tag{3.135}$$

where, in the last step of eq. (3.135), use has been made of eq. (3.127). Furthermore, since $q = (\nu, 0, 0, q_z)$,

$$q.p = \nu p_0 - q_z p_z \ . \tag{3.136}$$

From eqs. (3.133), (3.135), (3.132) and (3.136) there then follows that

$$p_z = \frac{(k'-p)^2 - (k-p)^2 + 2\nu p_0}{2q_z} .$$

Since $q = (\nu, 0, 0, q_z)$, eq. (3.135) can also be written as

$$\vec{k}.\vec{q} = k_z q_z = \frac{1}{2}(q^2 + 2k_0\nu)$$

from which it follows that

$$k_z = \frac{q^2 + 2k_0\nu}{2q_z} \ .$$

With these expressions for p_z and k_z inserted into eqs. (3.20), (3.130) and (3.131) and by using eqs. (3.132) and (3.134), we obtain from eq. (3.123):

$$\begin{aligned}
&\left[2\mathrm{Re}\sum_{\pm s,\pm s'} M_0 M_1^*\right]_{\epsilon=\epsilon_0} \\
= \ & \frac{8\pi e^2 g^2}{q_z^2}\int\frac{d^4p}{(2\pi)^4}\Big\{[(k-p)^2-(k'-p)^2]\nu[(2k_0+\nu)(p^2-q^2)+2p_0q^2]+(k-p)^2 2q^2\nu p_0 \\
& +[(k-p)^2+(k'-p)^2]q^2(2k_0p_0-1)+p^2q^2[\nu^2+q_z^2+4k_0^2+4\nu(k_0-p_0)] \\
& -\frac{4p^2k_0p_0}{q^2}[(q^2)^2+\nu^2q_z^2]-(q^2)^3-2(q^2)^2[\nu(2k_0-p_0)+k_0^2+(k_0-p_0)^2] \\
& -[(k-p)^2]^2\nu(k_0+\nu)+(k-p)^2(k'-p)^2\nu^2+[(k'-p)^2]^2k_0\nu\Big\} \\
& \times\left\{\frac{\delta\left((k-p)^2\right)}{(k'-p)^2(p^2-m^2)}[1-2n_{\mathrm{F}}(x_{k-p})]+\frac{\delta\left((k'-p)^2\right)}{(k-p)^2(p^2-m^2)}[1-2n_{\mathrm{F}}(x_{k'-p})]\right. \\
& \left.+\frac{\delta(p^2-m^2)}{(k-p)^2(k'-p)^2}[1+2n_{\mathrm{B}}(|p_0|)]\right\} .
\end{aligned} \tag{3.137}$$

By using eq. (2.6) we obtain from eq. (3.123)

$$\begin{aligned}
&\sum_{\lambda=\pm1,0}(-1)^{\lambda+1}\left[2\mathrm{Re}\sum_{\pm s,\pm s'} M_0 M_1^*\right]_{\epsilon=\epsilon_\lambda} \\
= \ & 8\pi e^2 g^2\int\frac{d^4p}{(2\pi)^4}\left\{[(q^2)^2+2q^2(k+k').p-p^2q^2](-4+1)+4(q^2-p^2)\frac{(q.k)^2}{q^2}\right. \\
& \left.+[2(k+k').p-2q^2]\left[-2k.p+2\frac{(q.k)(q.p)}{q^2}\right]+2q^2\left[-p^2+\frac{(q.p)^2}{q^2}\right]\right\}
\end{aligned}$$

$$\times\left\{\frac{\delta\left((k-p)^2\right)}{(k'-p)^2(p^2-m^2)}[1-2n_{\rm F}(x_{k-p})]+\frac{\delta\left((k'-p)^2\right)}{(k-p)^2(p^2-m^2)}[1-2n_{\rm F}(x_{k'-p})]\right.$$
$$\left.+\frac{\delta(p^2-m^2)}{(k-p)^2(k'-p)^2}[1+2n_{\rm B}(|p_0|)]\right\}$$
$$= -16\pi e^2g^2\int\frac{d^4p}{(2\pi)^4}\left\{(p^2+q^2)[p^2+q^2-(k'-p)^2-(k-p)^2]+(k'-p)^2(k-p)^2\right\}$$
$$\times\left\{\frac{\delta\left((k-p)^2\right)}{(k'-p)^2(p^2-m^2)}[1-2n_{\rm F}(x_{k-p})]+\frac{\delta\left((k'-p)^2\right)}{(k-p)^2(p^2-m^2)}[1-2n_{\rm F}(x_{k'-p})]\right.$$
$$\left.+\frac{\delta(p^2-m^2)}{(k-p)^2(k'-p)^2}[1+2n_{\rm B}(|p_0|)]\right\}. \qquad (3.138)$$

The interference term for the transverse polarizations of the virtual photon can be obtained from eqs. (3.137) and (3.138) by means of the analogous method used in eq. (3.27).

From the expressions in eqs. (3.137) and (3.138) we see that the only dependence of the integrands on the angle ϕ in eq. (3.129) is through the factors $(k'-p)^2$ and $(k-p)^2$. From the relations satisfied by the latter two factors in eqs. (3.132) and (3.134) and from Figure 3.9 it can be seen that the origin of any possible ϕ dependence can be further narrowed down to the quantity $k.p$. However, since the $\int d^4p$ loop integration covers all phase space, sufficient symmetry is provided for the $\int d\phi$ integration in the reference frame shown in Figure 3.9 to simply extract a factor of 2π from the $\int d\phi$ integration. Then eq. (3.129) becomes

$$d\mu_{\rm V}=\frac{1}{8\pi q_z}\int dk_0\theta(1-z_0)\theta(1+z_0)\int\frac{d^4p}{(2\pi)^4}.$$

3.5.2 The Bosonic Part of the Vertex Correction

In the last paragraph before Section 3.5.1 we mentioned the fermionic, fermionic primed and bosonic contributions. In this section we consider, as an example, the bosonic contribution in detail. Considerations in the cases of the fermionic and fermionic primed contributions are similar and the results of their evaluations are summarized in Appendix D.

By including the factor $\delta(p^2-m^2)$ from eq. (3.123), the phase space integral for the bosonic part of the vertex correction to a quark becomes

$$d\mu_{\rm B} = \frac{1}{8\pi q_z}\int dk_0\theta(1-z_0)\theta(1+z_0)\int\frac{d^4p}{(2\pi)^4}\delta(p^2-m^2)$$
$$= \frac{1}{8\pi q_z}\int_{(q_z-\nu)/2}^{\infty}dk_0\theta(1-z_0)\theta(1+z_0)\int_{-\infty}^{\infty}dp_0\int_0^{\infty}\frac{|\vec{p}|^2d|\vec{p}|d\Omega_p}{(2\pi)^4}$$
$$\times\frac{1}{2\sqrt{p_0^2-m^2}}\left[\delta\left(|\vec{p}|-\sqrt{p_0^2-m^2}\right)+\delta\left(|\vec{p}|+\sqrt{p_0^2-m^2}\right)\right]$$

$$= \frac{1}{8\pi q_z}\int_{(q_z-\nu)/2}^{\infty} dk_0\theta(1-z_0)\theta(1+z_0)\frac{1}{2(2\pi)^4}\int_{-\infty}^{\infty} dp_0\sqrt{p_0^2-m^2}d\Omega_p. \quad (3.139)$$

Since we are, for the moment, considering the vertex correction to a quark, k_0 is positive with a lower limit of $(q_z-\nu)/2$ due to $\theta(1-z_0)\theta(1+z_0)$.

As was already mentioned, the angular dependence of the integrand appears through the factors $(k'-p)^2$ and $(k-p)^2$. We must therefore take the angles between $\vec{k}'$ and $\vec{p}$ and between $\vec{k}$ and $\vec{p}$ into consideration when performing the $\int d\Omega_p$ integration. Since the reference frame shown in Figure 3.9 is not appropriate for this integration, we introduce the new frame of reference shown in Figure 3.10. This choice of frame can be justified as follows: For each fixed value of $\vec{k}$ and $\vec{k}'$ in the outer integrations shown in eq. (3.125), one is free to choose a new frame of reference for the inner $\int d^4p$ integration such that $\vec{k}$ is always along the z-axis and $\vec{k}'$ is always in the zx plane. It is to be noted that the way the angles ϕ and θ are defined in Figure 3.10 differs from the way they were defined in Figure 3.9. However, no confusion should arise in the following discussions since the angles ϕ and θ, as defined in Figure 3.9, have been integrated out. We define the angles between $\vec{k}'$ and $\vec{p}$ and between $\vec{k}$ and $\vec{p}$ on which the integrand depends as θ' and θ, respectively, according to Figure 3.10.

In the following we show how to transform from the ϕ variable in eq. (3.140) to the θ' variable. According to the angles defined in Figure 3.10 we have

$$\begin{aligned} d\Omega_p &= \sin\theta d\theta d\phi = dz d\phi \quad (3.140)\\ \vec{k}' &= |\vec{k}'|(\sin\alpha_B, 0, \cos\alpha_B)\\ \vec{p} &= |\vec{p}|(\sin\theta\cos\phi, \sin\theta\sin\phi, \cos\theta)\\ \Rightarrow \quad \frac{\vec{k}'.\vec{p}}{|\vec{k}'||\vec{p}|} &= \cos\theta' = \sin\alpha_B\sin\theta\cos\phi + \cos\alpha_B\cos\theta\\ \Rightarrow \quad \cos\phi &= \frac{\cos\theta' - \cos\alpha_B\cos\theta}{\sin\alpha_B\sin\theta} \quad (3.141)\\ \Rightarrow \quad \frac{d\cos\phi}{d\theta'} &= -\sin\phi\frac{d\phi}{d\theta'}\\ &= \frac{-\sin\theta'}{\sin\alpha_B\sin\theta} \quad (3.142) \end{aligned}$$

where, in the latter step, we differentiated only the first term in the right hand side of eq. (3.141) with respect to θ' since, as may be seen from Figure 3.10, when we vary ϕ, θ' will also vary while α_B and θ will remain constant. From eq. (3.142) there follows that

$$d\phi = \frac{-d(\cos\theta')}{\sin\phi\sin\alpha_B\sin\theta}. \quad (3.143)$$

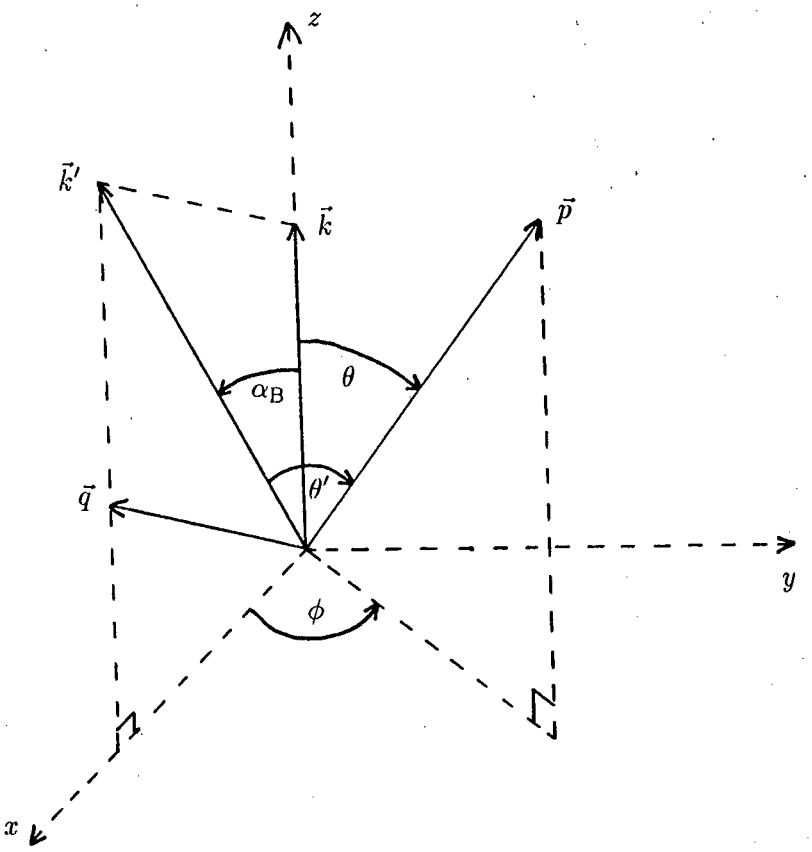

Figure 3.10: The reference frame in which we consider the $\int d\Omega_p$ integration appearing in eq. (3.139). It is to be noted that θ and ϕ, in this figure, are angles describing $\vec{p}$ relative to $\vec{k}$ as opposed to Figure 3.9 where they describe $\vec{k}$ relative to $\vec{q}$.

Since the $\int d\Omega_p$ integration is symmetric about the zx plane in Figure 3.10 we may write

$$\int_0^{2\pi} d\phi = 2\int_0^{\pi} d\phi. \tag{3.144}$$

Then, since $\phi \in [0,\pi]$, we have that $\sin\phi \in [0,1]$ which implies that we have a positive sign for the square root when expressing $\sin\phi$ as:

$$\begin{aligned} \sin\phi &= \sqrt{1-\cos^2\phi} \\ &= \sqrt{1-\frac{(\cos\theta' - \cos\alpha_B\cos\theta)^2}{\sin^2\alpha_B\sin^2\theta}} \end{aligned}$$

$$\begin{aligned} \Rightarrow \quad & \sin\alpha_B\sin\theta\sin\phi \\ = \; & \left[(1-\cos^2\alpha_B)(1-\cos^2\theta) - \cos^2\theta' + 2\cos\theta'\cos\alpha_B\cos\theta - \cos^2\alpha_B\cos^2\theta\right]^{1/2} \\ = \; & \sqrt{-\gamma(z,z',\cos\alpha_B)} \end{aligned} \tag{3.145}$$

where $z = \cos\theta$, $z' = \cos\theta'$ and γ is the function defined in eq. (3.43). From eqs. (3.144), (3.143) and (3.145) there follows that

$$d\phi = \frac{2dz'}{\sqrt{-\gamma(z, z', \cos\alpha_B)}}.$$

From the latter equation and eq. (3.140) there follows that

$$d\Omega_p = \frac{2dzdz'}{\sqrt{-\gamma(z, z', \cos\alpha_B)}}. \tag{3.146}$$

3.5.3 Performing the Angular Integration for the Bosonic Part of the Vertex Correction

In this section we focus on the $\int dz \int dz'$ part of the phase space integrations referred to in eqs. (3.139) and (3.146). In order to make the dependence of the integrand on z and z' explicit we define

$$s_B \equiv (k' - p)^2 = 2k'_0|\vec{p}|(z' - v_B) \tag{3.147}$$

$$t_B \equiv (k - p)^2 = 2k_0|\vec{p}|(z - u_B) \tag{3.148}$$

where

$$u_B \equiv \frac{2k_0p_0 - m^2}{2k_0|\vec{p}|} \tag{3.149}$$

$$v_B \equiv \frac{2k'_0p_0 - m^2}{2k'_0|\vec{p}|}. \tag{3.150}$$

The terms appearing in eqs. (3.137) and (3.138) depend on s_B and t_B through factors of the following types:

$$\frac{1}{s_B}\ ;\ \frac{1}{t_B}\ ;\ \frac{s_B}{t_B}\ ;\ \frac{t_B}{s_B}\ ;\ \frac{1}{s_Bt_B} \text{ and } (s_Bt_B)^0. \tag{3.151}$$

In addition, the argument of the square root in eq. (3.146) contributes to the z and z' dependence of the integrand. However it is to be noted that $\cos\alpha_B$ does not contribute to the z and z' dependence of the integrand:

$$\cos\alpha_B = \frac{\vec{k}.\vec{k'}}{|\vec{k}||\vec{k'}|} = \frac{\vec{k}.(\vec{q}+\vec{k})}{k_0k'_0} = \frac{k_0q_zz_0 + k_0^2}{k_0k'_0}.$$

By inserting the expression for z_0 in eq. (3.127) and by making use of the relation $k'_0 = \nu + k_0$, $\cos\alpha_B$ becomes

$$\cos\alpha_B = \frac{q^2}{2k_0k'_0} + 1. \tag{3.152}$$

Thus a typical integral has the form

$$\begin{aligned} I_{\rm B}(f) &\equiv \int\int f(z,z')d\Omega_p \\ &= 2\int_{-1}^{1} dz \int_a^b dz' \frac{f(z,z')}{\sqrt{-\gamma(z,z',\cos\alpha_{\rm B})}} \end{aligned} \tag{3.153}$$

where a and b are specified in (3.154) and where $f(z,z')$ could be any one of the factors listed in line (3.151).

As far as the integration over z' is concerned we need to evaluate

$$C_m \equiv \int_a^b dz' \frac{s_{\rm B}^m}{\sqrt{-\gamma(z,z',\cos\alpha_{\rm B})}}$$

where, as may be seen from line (3.151), the cases $m = 0, \pm 1$ need to be considered. We start by considering the case $m = -1$:

$$C_{-1} \equiv \int_a^b \frac{dz'}{2k_0'|\vec{p}|(z'-v_{\rm B})\sqrt{-\gamma(z,z',\cos\alpha_{\rm B})}}.$$

From eq. (3.145) there follows that

$$\begin{aligned} -\gamma(z,z',\cos\alpha_{\rm B}) &= \sin^2\alpha_{\rm B}\sin^2\theta\sin^2\phi \\ &\geq 0. \end{aligned}$$

By using an argument similar to the one used at Figure 3.7 we can deduce from the latter condition that

$$a \equiv z\cos\alpha_{\rm B} - \sqrt{1-z^2}\sin\alpha_{\rm B} \leq z' \leq z\cos\alpha_{\rm B} + \sqrt{1-z^2}\sin\alpha_{\rm B} \equiv b. \tag{3.154}$$

The change of variable

$$x = \frac{1}{z'-v_{\rm B}}$$

leads to

$$C_{-1} = \frac{-1}{2k_0'|\vec{p}|}\int_{(a-v_{\rm B})^{-1}}^{(b-v_{\rm B})^{-1}} \frac{dx}{x\sqrt{-\gamma(v_{\rm B}+1/x,z,\cos\alpha_{\rm B})}}. \tag{3.155}$$

Before we proceed we show the existence of the two possibilities, $z' > v_{\rm B}$ and $z' < v_{\rm B}$, which means that the two cases, $x = \sqrt{x^2}$ and $x = -\sqrt{x^2}$, repspectively, need to be considered in further calculations of C_{-1}. We shall show that

$$\begin{array}{llll} z' > v_{\rm B} & \text{always for} & p_0 < 0 & \\ z' < v_{\rm B} & \text{always for} & 0 < p_0 < k_0' & \\ z' < v_{\rm B} & \text{for} & p_0 > k_0' & \text{and } v_{\rm B} > b \\ z' > v_{\rm B} & \text{for} & p_0 > k_0' & \text{and } v_{\rm B} < z' < b \\ z' < v_{\rm B} & \text{for} & p_0 > k_0' & \text{and } z' < v_{\rm B} < b. \end{array} \tag{3.156}$$

Illustrations of the latter three cases for which $p_0 > k'_0$ appear in Figure 3.12.

In these discussions k_0 and k'_0 are both positive since we are considering the vertex correction to a quark. Consider

$$s_B = (k' - p)^2 = -2k'_0 p_0 + 2k'_0\sqrt{p_0^2 - m^2}z' + m^2. \tag{3.157}$$

For $p_0 > 0$ we obtain from eq. (3.157):

$$\begin{aligned} -2k'_0p_0 - 2k'_0p_0\sqrt{1 - m^2/p_0^2} + m^2 \;&\leq\; s_B \leq -2k'_0p_0 + 2k'_0p_0\sqrt{1 - m^2/p_0^2} + m^2 \\ \Rightarrow\quad -4k'_0p_0 + \left(\frac{k'_0 + p_0}{p_0}\right)m^2 + \mathcal{O}(m^4) \;&\leq\; s_B \leq \left(\frac{p_0 - k'_0}{p_0}\right)m^2 + \mathcal{O}(m^4) \end{aligned} \tag{3.158}$$

where, in the latter step, we have Taylor expanded the square root for $p_0^2 > m^2$.

For $p_0 < 0$ we obtain from eq. (3.157):

$$\begin{aligned} &2k'_0|p_0| - 2k'_0|p_0|\sqrt{1 - m^2/p_0^2} + m^2 \leq s_B \leq 2k'_0|p_0| + 2k'_0|p_0|\sqrt{1 - m^2/p_0^2} + m^2 \\ \Rightarrow\quad &\left(\frac{k'_0 + |p_0|}{|p_0|}\right)m^2 + \mathcal{O}(m^4) \leq s_B \leq 4k'_0|p_0| + \left(\frac{|p_0| - k'_0}{|p_0|}\right)m^2 + \mathcal{O}(m^4). \end{aligned} \tag{3.159}$$

From (3.159) we see that, in the case of $p_0 < 0$, $s_B > 0$ for $m^2 > 0$ and therefore, from eq. (3.147), that $z' > v_B$. In the case of $p_0 > 0$ we see from (3.158) that $s_B < 0$ for $m^2 > 0$ and $p_0 < k'_0$ and therefore, from eq. (3.147), that $z' < v_B$. For $p_0 > 0$, $m^2 > 0$ and $p_0 > k'_0$ we see from (3.158) that both the cases $s_B < 0$ and $s_B > 0$ are possible. The following analysis shows exactly when the corresponding $z' < v_B$ and $z' > v_B$ occur.

From eq. (3.150) there follows in the case of $p_0 > 0$ that

$$\begin{aligned} v_B = \frac{2k'_0p_0 - m^2}{2k'_0p_0\left(1 - \frac{m^2}{2p_0^2}\right)} + \mathcal{O}(m^4) \;&=\; \left(1 - \frac{m^2}{2k'_0p_0}\right)\left(1 + \frac{m^2}{2p_0^2}\right) + \mathcal{O}(m^4) \\ &=\; 1 - \left(\frac{p_0 - k'_0}{2k'_0p_0^2}\right)m^2 + \mathcal{O}(m^4). \end{aligned} \tag{3.160}$$

From the latter expression it can be seen that $v_B > 1$ for $p_0 < k'_0$ but for $p_0 > k'_0$, v_B becomes less than one although its value stays very close to one for $m^2 \to 0$. It is only in the latter case of $v_B < 1$ that $z' > v_B$ becomes a possibility for the case of $p_0 > 0$ but, since v_B is very close to one and the upper limit of z' is given in (3.154) as

$$z' \leq z\cos\alpha_B + \sqrt{1 - z^2}\sin\alpha_B = \cos(\alpha_B - \theta) \leq 1, \tag{3.161}$$

it is still a question whether $z' > v_B$ can obtain at all. From (3.161) it can be seen that the upper limit of z' becomes equal to one in only the case $\theta = \alpha_B$. Thus $z' > v_B$ is possible for $p_0 > k'_0$.

The Integration over z' and z in the case of $p_0 > 0$

In the following we consider the $\int dz \int dz'$ integration in the context of the $p_0 > 0$ part of the $\int_{-\infty}^{\infty} dp_0$ integration in eq. (3.139).

According to eq. (3.160) we have for $p_0 > 0$ that

$$v_B = 1 - \left(\frac{p_0 - k_0'}{2k_0' p_0^2}\right) m^2 + \mathcal{O}(m^4). \tag{3.162}$$

From eq. (3.149) there follows in the case of $p_0 > 0$ that

$$\begin{aligned} u_B &= \frac{2k_0 p_0 - m^2}{2k_0\sqrt{p_0^2 - m^2}} = \left(1 - \frac{m^2}{2k_0 p_0}\right)\left(1 + \frac{m^2}{2p_0^2}\right) + \mathcal{O}(m^4) \\ &= 1 - \left(\frac{p_0 - k_0}{2k_0 p_0^2}\right) m^2 + \mathcal{O}(m^4). \end{aligned} \tag{3.163}$$

From eqs. (3.162) and (3.163) we see that the following possibilities exist:

$$\begin{array}{lllll} \text{(i)} & p_0 > 0\ ;\ k_0 > p_0\ ;\ k_0' > p_0 & \Rightarrow & v_B > 1 \text{ and } u_B > 1 \\ \text{(ii)} & p_0 > 0\ ;\ k_0 > p_0\ ;\ k_0' < p_0 & \Rightarrow & v_B < 1 \text{ and } u_B > 1 \\ \text{(iii)} & p_0 > 0\ ;\ k_0 < p_0\ ;\ k_0' > p_0 & \Rightarrow & v_B > 1 \text{ and } u_B < 1 \\ \text{(iv)} & p_0 > 0\ ;\ k_0 < p_0\ ;\ k_0' < p_0 & \Rightarrow & v_B < 1 \text{ and } u_B < 1. \end{array} \tag{3.164}$$

Case (ii) must be ignored since for $k_0 > p_0$ one can only have $k_0' > p_0$ due to the relation $k_0' = k_0 + \nu$. Cases (i), (iii) and (iv) correspond to the regions shown in Figure 3.11. The origin of the line, $k_0 = (q_z - \nu)/2$, in the latter figure is explained in the sentence following on eq. (3.139).

For the $\int dz'$ integration we consider cases (i) and (iii) together but case (iv) separately. We do so because $v_B > 1$ in cases (i) and (iii) implies that $z' < v_B$ which in turn implies that x in eq. (3.155) becomes $x = -\sqrt{x^2}$. However, in case (iv) we have $p_0 > k_0'$ so that both the cases $z' < v_B$ and $z' > v_B$ ($x = -\sqrt{x^2}$ and $x = \sqrt{x^2}$) occur according to (3.156). Although we consider cases (i) and (iii) together for the $\int dz'$ integration, we shall distinguish between the two cases in the subsequent $\int dz$ integration since $u_B > 1$ in case (i) and $u_B < 1$ in case (iii).

So for cases (i) and (iii), eq. (3.155) becomes

$$\begin{aligned} C_{-1} &= \frac{1}{2k_0'|\vec{p}|} \int_{(a-v_B)^{-1}}^{(b-v_B)^{-1}} \frac{dx}{\sqrt{-x^2\gamma(v_B + 1/x, z, \cos\alpha_B)}} \\ &= \frac{1}{2k_0'|\vec{p}|} \int_{(a-v_B)^{-1}}^{(b-v_B)^{-1}} \frac{dx}{\sqrt{x^2(1 - \cos^2\alpha_B - z^2 - v_B^2 + 2zv_B\cos\alpha_B + 2x(z\cos\alpha_B - v_B) - 1}}. \end{aligned}$$

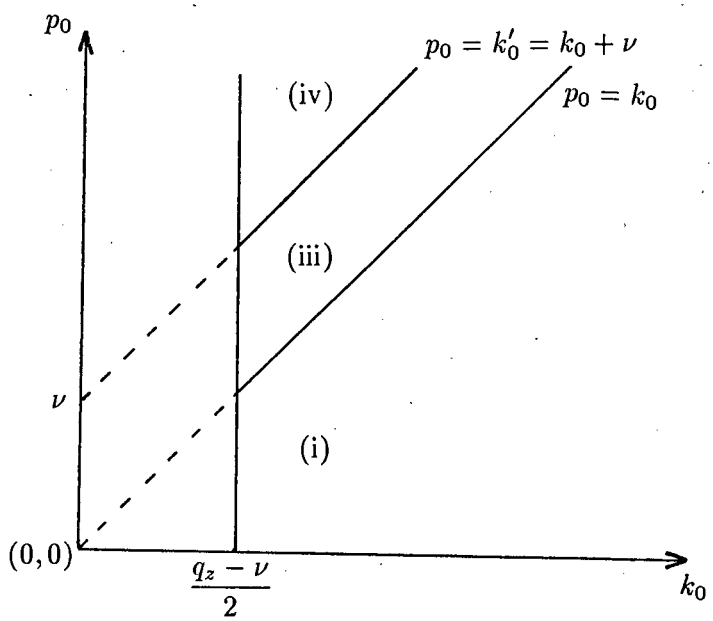

Figure 3.11: Three regions in the $p_0 k_0$ plane that need to be separately considered in the $p_0 > 0$ part of the $\int_{-\infty}^{\infty} dp_0$ integration in eq. (3.139).

But

$$1 - \cos^2\alpha_B - z^2 - v_B^2 + 2zv_B\cos\alpha_B = -\gamma(z, v_B, \cos\alpha_B) \leq 0$$

since the graph of $\gamma(z, v_B, \cos\alpha_B)$ versus z is always positive in cases (i) and (iii) as may be seen from the following analysis:

$$\frac{d\gamma}{dz} = 2z - 2v_B\cos\alpha_B$$

$$\Rightarrow \quad \frac{d\gamma}{dz} = 0 \quad \text{when} \quad z = v_B\cos\alpha_B.$$

But

$$\begin{aligned}
\gamma(z = v_B\cos\alpha_B, v_B, \cos\alpha_B) &= v_B^2 + \cos^2\alpha_B - v_B^2\cos^2\alpha_B - 1 \\
&= 1 + \left(\frac{k_0' - p_0}{k_0' p_0^2}\right) m^2 + \cos^2\alpha_B - \cos^2\alpha_B \\
&\quad - \left(\frac{k_0' - p_0}{k_0' p_0^2}\right) m^2\cos^2\alpha_B - 1 + \mathcal{O}(m^4) \\
&= m^2\left(\frac{k_0' - p_0}{k_0' p_0^2}\right)\sin^2\alpha_B + \mathcal{O}(m^4)
\end{aligned}$$

from which it can be seen that $[\gamma(z, v_B, \cos\alpha_B)]_{\text{minimum}} > 0$ for $m^2 \to 0$ and $k_0' > p_0$ which is the case in regions (i) and (iii).

Thus

$$C_{-1} = \frac{1}{2k_0'|\vec{p}|\sqrt{\gamma(z,v_B,\cos\alpha_B)}} \times \int_{(a-v_B)^{-1}}^{(b-v_B)^{-1}} dx \left[-x^2 + \frac{2x(z\cos\alpha_B - v_B)}{\gamma(z,v_B,\cos\alpha_B)} - \frac{1}{\gamma(z,v_B,\cos\alpha_B)}\right]^{-1/2}. \quad (3.165)$$

The derivation now follows exactly the same steps as those leading from eq. (B.7) to eq. (B.14). This may be seen by identifying the correspondences $l \to v_B$, $\cos\beta \to z$ and $\cos\rho \to \cos\alpha_B$ and by taking care that certain arguments which were used in the derivations leading to eq. (B.14) still hold in the present application. One such argument is the one leading from eq. (B.9) to eq. (B.10) which in the present application becomes

$$Q = \frac{(z\cos\alpha_B - v_B)^2 - G}{G^2} = \frac{(1-z^2)\sin^2\alpha_B}{G^2}$$
$$\Rightarrow \quad \sqrt{q} = +\frac{\sqrt{1-z^2}\sin\alpha_B}{G}$$

since one is free to choose, for each fixed value of $\vec{k}$ and $\vec{k}'$ in the outer integrations, the reference frame in Figure 3.10 in such a manner that $\alpha_B \in [0,\pi]$ so that $\sqrt{\sin^2\alpha_B} = +\sin\alpha_B$.

From eq. (B.14) we may therefore deduce that eq. (3.165) becomes

$$C_{-1} = \frac{-\pi}{2k_0'|\vec{p}|\sqrt{\gamma(z,v_B,\cos\alpha_B)}} \quad \text{for cases (i) and (iii).} \quad (3.166)$$

In case (iv) $v_B < 1$ so that both the cases $z' < v_B$ and $z' > v_B$ are possible as explained after eq. (3.160). Thus we shall encounter the pole at $z' = v_B$ in C_{-1} and we shall integrate over it in the principal value sense since its origin is $1/(k'-p)^2$ in eq. (3.122).

Before continuing we prove that the case $v_B < a$, where $a = \cos(\theta + \alpha_B)$ is the lower limit of the z' integration, need not concern us for the case of $p_0 > k_0'$ under consideration. From eq. (3.160) we have $v_B = 1 - \mathcal{O}(m^2)$ so that only for $\theta = -\alpha_B$ is $a = \cos(\theta+\alpha_B) = 1$ and therefore $v_B < a$ possible. But since $\theta \in [0,\pi]$ and $\alpha_B \in [0,\pi]$, $\theta = -\alpha_B$ is only possible for $\theta = 0$ **and** $\alpha_B = 0$. But $\alpha_B = 0$ implies $\cos\alpha_B = 1$ which, according to eq. (3.152) and the fact that $k_0' = k_0 + \nu$, only occurs in the special limit $k_0 \to \infty$. Any contribution that might have resulted in this limit is exponentially suppressed by the thermal distribution factor $n_F(x_k)$ in (3.124).

In the following we show that the occurence of $z' > v_B$ and therefore $z' = v_B$ (since $a \le v_B$ as explained in the previous paragraph) is determined by the values of z in the outer

integration. In order to have that $z' > v_B$, the upper limit b of the $\int dz'$ integration must satisfy $b > v_B$, i.e.,

$$b = \cos(\theta - \alpha_B) = z\cos\alpha_B + \sqrt{1-z^2}\sin\alpha_B > v_B \quad (3.167)$$

$$\Rightarrow \quad \sqrt{1-z^2}\sin\alpha_B > v_B - z\cos\alpha_B. \quad (3.168)$$

(Since the lower limit a of z' satisfies $a \leq v_B$, the occurence of $z' < v_B$ in addition to the occurence of $z' > v_B$ must be borne in mind when $b > v_B$.) Since $\alpha_B \in [0, \pi]$ we have that $\sqrt{1-z^2}\sin\alpha_B \geq 0$ and since $v_B = 1 - \mathcal{O}(m^2)$ and the case $\cos\alpha_B < 1$ is, as explained in the previous paragraph, of relevance, we also have that $v_B - z\cos\alpha_B \geq 0$ for all practical purposes. Since both the left and right hand sides of the inequality in (3.168) are positive, that condition becomes upon squaring:

$$(1-z^2)\sin^2\alpha_B > (v_B - z\cos\alpha_B)^2$$

$$\Rightarrow \quad z^2 - 2zv_B\cos\alpha_B + v_B^2 - \sin^2\alpha_B < 0.$$

The roots of the equation $z^2 - 2zv_B\cos\alpha_B + v_B^2 - \sin^2\alpha_B = 0$ are

$$\lambda_\pm = \frac{2v_B\cos\alpha_B \pm \sqrt{4v_B^2\cos^2\alpha_B - 4v_B^2 + 4\sin^2\alpha_B}}{2}$$

$$= v_B\cos\alpha_B \pm \sqrt{1-v_B^2}\sin\alpha_B \quad (3.169)$$

where the latter square root is real since $v_B < 1$ for the case (iv) under consideration. For the case (iv) we therefore express $\int_{-1}^{1} dz h(z) C_{-1}$, where $h(z)$ is any function that has to be taken into account in the $\int dz$ integration, as

$$\int_{-1}^{1} dz h(z) C_{-1} = \int_{-1}^{\lambda_-} dz h(z) C_{-1} + \int_{\lambda_-}^{\lambda_+} dz h(z) C_{-1} + \int_{\lambda_+}^{1} dz h(z) C_{-1}$$

$$\equiv I_1 + I_2 + I_3. \quad (3.170)$$

According to the above analyses, $z' - v_B < 0$ in I_1 and I_3 while both the cases $z' - v_B < 0$ and $z' - v_B > 0$ appear in I_2. It should also be borne in mind that the range of z' in C_{-1} is still given by

$$\cos(\theta + \alpha_B) = a \leq z' \leq b = \cos(\theta - \alpha_B)$$

in each of I_1, I_2 and I_3. The latter observations are represented by the sketches in Figure 3.12. According to eqs. (3.169) and (3.152), the positions of λ_+ and λ_- depend on the value of k_0 in the outer integration and are not shown in Figure 3.12.

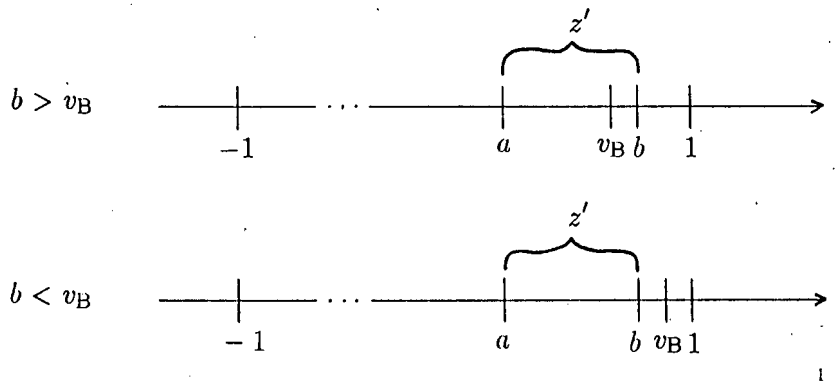

Figure 3.12: Sketches showing (for the case (iv) for which $p_0 > k_0' \geq 0$) the occurence of both $z' < v_B$ and $z' > v_B$ when $v_B < b = \cos(\theta - \alpha_B)$ and the occurence of only $z' < v_B$ when $v_B > b = \cos(\theta - \alpha_B)$

Since $z' - v_B < 0$ implies that $x = -\sqrt{x^2}$ in I_1 and I_3, the evaluation of C_{-1}, which is embedded in I_1 and I_3, follows exactly the same steps as those leading from eq. (3.155) to eq. (3.166) since all the arguments that were used in the cases (i) and (iii) depended on $z' - v_B < 0$ and $k_0' > p_0$ which also apply for I_1 and I_3. Thus we obtain

$$I_1 = -\frac{\pi}{2k_0'|\vec{p}|}\int_{-1}^{\lambda_-} dz \frac{h(z)}{\sqrt{\gamma(z, v_B, \cos\alpha_B)}} \tag{3.171}$$

$$I_3 = -\frac{\pi}{2k_0'|\vec{p}|}\int_{\lambda_+}^{1} dz \frac{h(z)}{\sqrt{\gamma(z, v_B, \cos\alpha_B)}}. \tag{3.172}$$

Next we evaluate I_2. Since both the cases $z' - v_B < 0$ (which implies that $x = -\sqrt{x^2}$) and $z' - v_B > 0$ (which implies that $x = \sqrt{x^2}$) occur for I_2, we perform the $\int dz'$ integration in C_{-1} over the pole at $z' = v_B$ in the principal value sense as was already envisaged in the paragraph following on eq. (3.166):

$$\begin{aligned} C_{-1} &= \lim_{\epsilon\to 0+}\left[\int_a^{v_B-\epsilon} + \int_{v_B+\epsilon}^{b}\right] \frac{dz'}{2k_0'|\vec{p}|(z' - v_B)\sqrt{\gamma(z, z', \cos\alpha_B)}} \\ &\equiv J_1 + J_2 \end{aligned}$$

$$\begin{aligned} \text{In } J_1: \quad & x = (z' - v_B)^{-1} < 0 \quad \Rightarrow \quad x = -\sqrt{x^2} \\ \text{In } J_2: \quad & x = (z' - v_B)^{-1} > 0 \quad \Rightarrow \quad x = \sqrt{x^2} \end{aligned}$$

The latter relations lead to

$$J_1 = \lim_{\epsilon\to 0+}\frac{1}{2k_0'|\vec{p}|}\int_{(a-v_B)^{-1}}^{-\epsilon^{-1}} \frac{dx}{\sqrt{x^2[-\gamma(z, v_B, \cos\alpha_B)] + 2x(z\cos\alpha_B - v_B) - 1}}$$

$$J_2 = -\lim_{\epsilon\to 0+}\frac{1}{2k_0'|\vec{p}|}\int_{\epsilon^{-1}}^{(b-v_B)^{-1}} \frac{dx}{\sqrt{x^2[-\gamma(z, v_B, \cos\alpha_B)] + 2x(z\cos\alpha_B - v_B) - 1}}.$$

Since J_1 and J_2 are imbedded in I_2 for which

$$\lambda_- = v_B \cos\alpha_B - \sqrt{1-v_B^2}\sin\alpha_B \le z \le v_B\cos\alpha_B + \sqrt{1-v_B^2}\sin\alpha_B = \lambda_+$$

$$\Rightarrow \quad \gamma(z, v_B, \cos\alpha_B) < 0\ , \tag{3.173}$$

we extract the factor $[-\gamma(z, v_B, \cos\alpha_B)]^{-1/2}$ [as opposed to the factor, $[\gamma(z, v_B, \cos\alpha_B)]^{-1/2}$, which was extracted in eq. (3.165)] to obtain

$$\begin{aligned} J_1 &= \lim_{\epsilon\to 0^+} \frac{1}{2k_0'|\vec{p}|\sqrt{-\gamma(z, v_B, \cos\alpha_B)}} \\ &\quad \times \int_{(a-v_B)^{-1}}^{-1/\epsilon} dx \left[x^2 - \frac{2x(z\cos\alpha_B - v_B)}{\gamma(z, v_B, \cos\alpha_B)} + \frac{1}{\gamma(z, v_B, \cos\alpha_B)}\right]^{-1/2} \end{aligned} \tag{3.174}$$

$$\begin{aligned} J_2 &= -\lim_{\epsilon\to 0^+} \frac{1}{2k_0'|\vec{p}|\sqrt{-\gamma(z, v_B, \cos\alpha_B)}} \\ &\quad \times \int_{1/\epsilon}^{(b-v_B)^{-1}} dx \left[x^2 - \frac{2x(z\cos\alpha_B - v_B)}{\gamma(z, v_B, \cos\alpha_B)} + \frac{1}{\gamma(z, v_B, \cos\alpha_B)}\right]^{-1/2}. \end{aligned} \tag{3.175}$$

In Subsection (a) of Appendix C it is proven that

$$J_1 = -J_2 = \lim_{\epsilon'\to 0^+} \frac{1}{2k_0'|\vec{p}|\sqrt{-\gamma(z, v_B, \cos\alpha_B)}} \left(-\operatorname{arccosh}\frac{1}{\epsilon'}\right). \tag{3.176}$$

Thus we have proven that $J_1 + J_2 = 0$ so that

$$I_2 = 0. \tag{3.177}$$

Thus far we may conclude from eqs. (3.166), (3.170), (3.171), (3.172) and (3.177) that

$$\int_{-1}^{1} dz h(z) C_{-1}$$

$$= \begin{cases} \displaystyle\int_{-1}^{1} dz \frac{-\pi h(z)}{2k_0'|\vec{p}|\sqrt{\gamma(z, v_B, \cos\alpha_B)}} & \text{for } p_0 > 0,\ k_0 > 0 \text{ and } p_0 < k_0', \\ & \text{i.e., for cases (i) and (iii)} \\ \left[\displaystyle\int_{-1}^{\lambda_-} dz + \int_{\lambda_+}^{1} dz\right] \frac{-\pi h(z)}{2k_0'|\vec{p}|\sqrt{\gamma(z, v_B, \cos\alpha_B)}} & \text{for } p_0 > 0,\ k_0 < 0 \text{ and } p_0 > k_0', \\ & \text{i.e., for case (iv).} \end{cases} \tag{3.178}$$

For $f(z, z')$ in eq. (3.153) equals to one of the factors proportional to s_B^{-1} in line (3.151), the cases $h(z) = 2t_B$; $2t_B^0$; $2t_B^{-1}$ need to be considered in eq. (3.178). We continue with the $\int dz$ integration by considering the most complicated case of $h(z) = 2t_B^{-1}$.

For cases (i) and (iii) we have from (3.178) and eq. (3.148) that

$$I\left(\frac{1}{s_B t_B}\right) = 2\int_{-1}^{1} dz t_B^{-1} C_{-1} = -\frac{\pi}{2k_0 k_0'|\vec{p}|^2} \int_{-1}^{1} \frac{dz}{(z-u_B)\sqrt{\gamma(z, v_B, \cos\alpha_B)}}. \tag{3.179}$$

However, since $u_B > 1$ in case (i) implies $z - u_B < 0$ only in case (i) while $u_B < 1$ in case (iii) implies both $z - u_B < 0$ and $z - u_B > 0$ in case (iii), we shall treat cases (i) and (iii) separately when performing the $\int dz$ integration. Case (iv) also requires special attention and we shall return to it after treating cases (i) and (iii) first.

For case (i) the $\int dz$ integration may be performed following the same steps as those leading from eq. (3.89) to eq. (3.91). The latter steps include those in Subsection (e) of Appendix B. We may do so by noticing that $z - u_B < 0$ implies that $(z-u_B)^{-1} \equiv \tau' = -\sqrt{\tau'^2}$ and by establishing the following correspondence between the symbols used to obtain eq. (3.91) and those involved in the evaluation of eq. (3.179):

$$d \to u_B \qquad H \to v_B \qquad J \to \cos\alpha_B$$

$$\Rightarrow \qquad HJ - d \to v_B \cos\alpha_B - u_B = -\frac{b}{2} \qquad \text{where} \qquad b \equiv 2(u_B - v_B \cos\alpha_B)$$

$$\tilde{c} \equiv \gamma(d,H,J) \;\to\; \gamma(v_B,u_B,\cos\alpha_B) \equiv c \tag{3.180}$$

$$\Delta \equiv -4(H^2-1)(J^2-1) \;\to\; -4(v_B^2-1)(\cos^2\alpha_B - 1) = 4\sin^2\alpha_B(v_B^2-1) \equiv \Delta. \tag{3.181}$$

Then the corresponding result in the present application becomes:

$$I\left(\frac{1}{s_B t_B}\right) = 2\int_{-1}^{1} dz t_B^{-1} C_{-1} = -\frac{\pi}{2k_0 k_0' |\vec{p}|^2} \int_{\tau(-1)}^{\tau(1)} d\tau \left[c\left(\tau^2 + \frac{\Delta}{4c^2}\right)\right]^{-1/2} \quad \text{for case (i)} \tag{3.182}$$

where

$$\tau(z) = \frac{1}{z - u_B} + \frac{b}{2c}. \tag{3.183}$$

At lines (C.7) and (C.10) it is proven that $c \geq 0$ and $\Delta > 0$ for case (i). The latter two inequalities are comparable to the situation in eq. (3.101) where we also had $\tilde{c} \geq 0$ and $\Delta > 0$ so that we may, in the evaluation of the expression in eq. (3.182), follow similar steps as those leading from eq. (3.101) to eq. (3.104). Thus

$$I\left(\frac{1}{s_B t_B}\right) = -\frac{\pi}{2k_0 k_0' |\vec{p}|^2 \sqrt{c}} \left[\operatorname{arcsinh}\left(\frac{2c}{\sqrt{\Delta}}\tau(1)\right) - \operatorname{arcsinh}\left(\frac{2c}{\sqrt{\Delta}}\tau(-1)\right)\right] \quad \text{for case (i).} \tag{3.184}$$

In case (iii) at line (3.164) we have $u_B < 1$ but $-1 \leq z \leq 1$ in the $\int dz$ integration so that we shall encounter the pole at $z = u_B$ in the evaluation of eq. (3.179). We integrate over this

pole in the principal value sense since its origin is $1/(k-p)^2$ in eq. (3.122):

$$I\left(\frac{1}{s_B t_B}\right) = -\frac{\pi}{2k_0k_0'|\vec{p}|^2}\lim_{\epsilon\to 0^+}\left[\int_{-1}^{u_B-\epsilon}+\int_{u_B+\epsilon}^{1}\right]\frac{dz}{(z-u_B)\sqrt{\gamma(z,v_B,\cos\alpha_B)}}$$
$$\equiv E_1+E_2. \tag{3.185}$$

The evaluation of E_1 follows the same steps as described for the derivation of eq. (3.184) in case (i) since, in E_1, we also have $z-u_B<0$, $c\geq 0$ and $\Delta>0$ [The proof of the latter two inequalities appears at lines (C.7) and (C.10).] Thus

$$E_1=-\frac{\pi}{2k_0k_0'|\vec{p}|^2\sqrt{c}}\lim_{\epsilon\to 0^+}\left[\operatorname{arcsinh}\left(\frac{2c}{\sqrt{\Delta}}\tau(u_B-\epsilon)\right)-\operatorname{arcsinh}\left(\frac{2c}{\sqrt{\Delta}}\tau(-1)\right)\right].$$

The evaluation of E_2 follows the same steps as those followed in the evaluation of E_1 except that an overall factor of (-1) must be taken into account since now $z-u_B>0$ for E_2. Thus we obtain from the result for E_1:

$$E_2=\frac{\pi}{2k_0k_0'|\vec{p}|^2\sqrt{c}}\lim_{\epsilon\to 0^+}\left[\operatorname{arcsinh}\left(\frac{2c}{\sqrt{\Delta}}\tau(1)\right)-\operatorname{arcsinh}\left(\frac{2c}{\sqrt{\Delta}}\tau(u_B+\epsilon)\right)\right]. \tag{3.186}$$

At eqs. (C.16) and (C.17) it is proven that

$$\lim_{\epsilon\to 0^+}\tau(u_B-\epsilon) = \lim_{\epsilon\to 0^+}\left(-\frac{1}{\epsilon}\right) \tag{3.187}$$
$$\lim_{\epsilon\to 0^+}\tau(u_B+\epsilon) = \lim_{\epsilon\to 0^+}\left(\frac{1}{\epsilon}\right). \tag{3.188}$$

Thus we obtain for case (iii):

$$\begin{aligned} I\left(\frac{1}{s_B t_B}\right) &= E_1+E_2 \\ &= -\frac{\pi}{2k_0k_0'|\vec{p}|^2\sqrt{c}}\lim_{\epsilon\to 0^+}\left[\operatorname{arcsinh}\left(-\frac{2c}{\sqrt{\Delta}}\frac{1}{\epsilon}\right)-\operatorname{arcsinh}\left(\frac{2c}{\sqrt{\Delta}}\tau(-1)\right)\right. \\ &\quad \left.-\operatorname{arcsinh}\left(\frac{2c}{\sqrt{\Delta}}\tau(1)\right)+\operatorname{arcsinh}\left(\frac{2c}{\sqrt{\Delta}}\frac{1}{\epsilon}\right)\right] \\ &= \frac{\pi}{2k_0k_0'|\vec{p}|^2\sqrt{c}}\left[\operatorname{arcsinh}\left(\frac{2c}{\sqrt{\Delta}}\tau(-1)\right)+\operatorname{arcsinh}\left(\frac{2c}{\sqrt{\Delta}}\tau(1)\right)\right] \quad \text{for case (iii)} \end{aligned}$$

where the latter step was obtained by making use of the property, $\operatorname{arcsinh}(-x)=-\operatorname{arcsinh}(x)$.

In case (iv) at line (3.164) we have from (3.178) and eq. (3.148) that

$$I\left(\frac{1}{s_B t_B}\right) = 2\int_{-1}^{1}dz t_B^{-1}C_{-1}$$
$$= -\frac{\pi}{2k_0k_0'|\vec{p}|^2}\left[\int_{-1}^{\lambda_-}+\int_{\lambda_+}^{1}\right]\frac{dz}{(z-u_B)\sqrt{\gamma(z,v_B,\cos\alpha_B)}} \tag{3.189}$$
$$\equiv D_1+D_2. \tag{3.190}$$

From (3.164) we see that $u_B < 1$ for the case (iv) under consideration. Similar to procedures we followed in previous examples, we require knowledge of the sign of $\tau' \equiv (z - u_B)^{-1}$ in D_1 and D_2 in order to determine the sign of the square root when we write $\tau' = \pm\sqrt{\tau'^2}$ in future calculations. According to eq. (3.163), $u_B = 1 - \mathcal{O}(m^2)$ so that we should keep in mind that u_B is only slightly less than one. Nevertheless we should check whether, in D_1, $1 > \lambda_- > u_B$ is a possibility: According to eqs. (3.169) and (3.162) we have

$$\begin{aligned} \lambda_- &= \left(1 + \frac{k_0' - p_0}{2k_0'p_0^2}m^2\right)\cos\alpha_B - \sqrt{\frac{p_0 - k_0'}{k_0'p_0^2}}m\sin\alpha_B \\ &= \cos\alpha_B - \mathcal{O}(m). \end{aligned}$$

Thus, in D_1, $\lambda_- > u_B$ only occurs when $\cos\alpha_B \simeq 1$ which, according to eq. (3.152) and the fact that $k_0' = k_0 + \nu$, only occurs in the special limit $k_0 \to \infty$. Any contribution that might have resulted in this special limit is exponentially suppressed by the thermal distribution factor $n_F(x_k)$ in (3.124). We may thus conclude that $u_B > \lambda_-$ for all practical purposes in D_1 and therefore $z - u_B < 0$ in D_1.

In D_2 we have, by a similar argument as the one in the case of λ_- above, that $u_B > \lambda_+$. Since $\lambda_+ \leq z \leq 1$ and $1 > u_B > \lambda_+$ in D_2, both the cases $z - u_B < 0$ and $z - u_B > 0$ occur in D_2.

In D_1, $z - u_B < 0$ implies that $(z - u_B)^{-1} \equiv \tau' = -\sqrt{\tau'^2}$ so that we may use the same steps as those leading from eq. (3.179) to eq. (3.182):

$$D_1 = -\frac{\pi}{2k_0k_0'|\vec{p}|^2}\int_{\tau(-1)}^{\tau(\lambda_-)} d\tau\left[c\left(\tau^2 + \frac{\Delta}{4c^2}\right)\right]^{-1/2} \quad \text{for case (iv)} \tag{3.191}$$

where

$$\tau(z) = \frac{1}{z - u_B} + \frac{b}{2c}$$

Further calculations depend on the signs of c and Δ. At lines (C.7) and (C.10) it is proven that $c \geq 0$ and $\Delta < 0$ in case (iv). Thus we write D_1 as

$$D_1 = -\frac{\pi}{2k_0k_0'|\vec{p}|^2\sqrt{c}}\int_{\tau(-1)}^{\tau(\lambda_-)} d\tau\left(\sqrt{\tau^2 - \frac{|\Delta|}{4c^2}}\right)^{-1} \tag{3.192}$$

$$= -\frac{\pi}{2k_0k_0'|\vec{p}|^2\sqrt{c}}\int_{x_1'}^{x_2'}\frac{dx'}{\sqrt{x'^2 - 1}} \tag{3.193}$$

where we changed variable:

$$x' = \frac{2c}{\sqrt{|\Delta|}}\tau$$

$$x_1' = \frac{2c}{\sqrt{|\Delta|}}\tau(-1) \qquad x_2' = \frac{2c}{\sqrt{|\Delta|}}\tau(\lambda_-).$$

The further change of variable, $x' = \cosh y'$, leads to

$$\begin{aligned} D_1 &= -\frac{\pi}{2k_0k_0'|\vec{p}|^2\sqrt{c}}\int_{\operatorname{arccosh} x_1'}^{\operatorname{arccosh} x_2'} dy' \\ &= -\frac{\pi}{2k_0k_0'|\vec{p}|^2\sqrt{c}}\left[\operatorname{arccosh}\left(\frac{2c}{\sqrt{|\Delta|}}\tau(\lambda_-)\right) - \operatorname{arccosh}\left(\frac{2c}{\sqrt{|\Delta|}}\tau(-1)\right)\right] \end{aligned} \tag{3.194}$$

where the latter expression is well defined since, at lines (C.20) and (C.13), it is shown that $\tau(\lambda_-) > 0$ and $\tau(-1) > 0$ so that the arguments of arccosh are positive.

As was already mentioned, both the cases $z - u_B < 0$ and $z - u_B > 0$ occur in D_2. We integrate over the pole at $z = u_B$ in the principal value sense since its origin is $1/(k-p)^2$ in eq. (3.122):

$$\begin{aligned} D_2 &= -\frac{\pi}{2k_0k_0'|\vec{p}|^2}\lim_{\epsilon\to 0+}\left[\int_{\lambda_+}^{u_B-\epsilon} + \int_{u_B+\epsilon}^{1}\right]\frac{dz}{(z-u_B)\sqrt{\gamma(z,v_B,\cos\alpha_B)}} \\ &\equiv F_1 + F_2. \end{aligned} \tag{3.195}$$

In F_1, $z - u_B < 0$ so that we may use the same steps as those leading from the expression for D_1 in eq. (3.189) to the expression for D_1 in eq. (3.192):

$$F_1 = -\frac{\pi}{2k_0k_0'|\vec{p}|^2\sqrt{c}}\lim_{\epsilon\to 0+}\int_{\tau(\lambda_+)}^{\tau(u_B-\epsilon)} d\tau\left(\sqrt{\tau^2 - \frac{|\Delta|}{4c^2}}\right)^{-1}. \tag{3.196}$$

However, at lines (C.19) and (C.16), it is shown that $\tau(\lambda_+) < 0$ and $\lim_{\epsilon\to 0+}\tau(u_B-\epsilon) < 0$ so that we introduce a minus sign in the change of variable,

$$x' = -\frac{2c}{\sqrt{|\Delta|}}\tau\,,$$

in order to ensure that the arguments of arccosh, appearing in the final result, will be positive. Thus

$$F_1 = \frac{\pi}{2k_0k_0'|\vec{p}|^2\sqrt{c}}\lim_{\epsilon\to 0+}\int_{x_1'}^{x_2'}\frac{dx'}{\sqrt{x'^2-1}}$$

where

$$x_1' = -\frac{2c}{\sqrt{|\Delta|}}\tau(\lambda_+) = \left|\frac{2c}{\sqrt{|\Delta|}}\tau(\lambda_+)\right| \qquad x_2' = -\frac{2c}{\sqrt{|\Delta|}}\tau(u_B-\epsilon) = \left|\frac{2c}{\sqrt{|\Delta|}}\tau(u_B-\epsilon)\right|.$$

The further change of variable, $x' = \cosh y'$, leads to

$$F_1 = \frac{\pi}{2k_0k_0'|\vec{p}|^2\sqrt{c}}\lim_{\epsilon\to 0+}\left[\operatorname{arccosh}\left(\left|\frac{2c}{\sqrt{|\Delta|}}\tau(u_B-\epsilon)\right|\right) - \operatorname{arccosh}\left(\left|\frac{2c}{\sqrt{|\Delta|}}\tau(\lambda_+)\right|\right)\right]. \tag{3.197}$$

In F_2, $z - u_B > 0$ as opposed to $z - u_B < 0$ in F_1 so that the intermediate result for F_2 is similar to that of F_1 in eq. (3.196) except for an overall factor of (-1) and different integration limits:

$$F_2 = \frac{\pi}{2k_0k_0'|\vec{p}|^2\sqrt{c}} \lim_{\epsilon\to 0^+} \int_{\tau(u_B+\epsilon)}^{\tau(1)} d\tau \left(\sqrt{\tau^2 - \frac{|\Delta|}{4c^2}}\right)^{-1}.$$

At lines (C.17) and (C.15) it is shown that $\lim_{\epsilon\to 0^+} \tau(u_B+\epsilon) > 0$ and $\tau(1) > 0$ in case (iv) so that we may follow the same steps as those leading from the expression in eq. (3.192) to the expression in eq. (3.194). Thus

$$F_2 = \frac{\pi}{2k_0k_0'|\vec{p}|^2\sqrt{c}} \lim_{\epsilon\to 0^+} \left[\operatorname{arccosh}\left(\frac{2c}{\sqrt{|\Delta|}}\tau(1)\right) - \operatorname{arccosh}\left(\frac{2c}{\sqrt{|\Delta|}}\tau(u_B+\epsilon)\right)\right]. \quad (3.198)$$

Thus, in case (iv), we obtain from eqs. (3.190), (3.194), (3.195), (3.197) and (3.198):

$$\begin{aligned} I\left(\frac{1}{s_Bt_B}\right) &= -\frac{\pi}{2k_0k_0'|\vec{p}|^2\sqrt{c}} \lim_{\epsilon\to 0^+} \left[\operatorname{arccosh}\left(\frac{2c}{\sqrt{|\Delta|}}\tau(\lambda_-)\right) - \operatorname{arccosh}\left(\frac{2c}{\sqrt{|\Delta|}}\tau(-1)\right)\right. \\ &\quad -\operatorname{arccosh}\left(\left|\frac{2c}{\sqrt{|\Delta|}}\tau(u_B-\epsilon)\right|\right) + \operatorname{arccosh}\left(\left|\frac{2c}{\sqrt{|\Delta|}}\tau(\lambda_+)\right|\right) \\ &\quad \left.-\operatorname{arccosh}\left(\frac{2c}{\sqrt{|\Delta|}}\tau(1)\right) + \operatorname{arccosh}\left(\frac{2c}{\sqrt{|\Delta|}}\tau(u_B+\epsilon)\right)\right] \\ &= -\frac{\pi}{2k_0k_0'|\vec{p}|^2\sqrt{c}} \left[\operatorname{arccosh}\left(\frac{2c}{\sqrt{|\Delta|}}\tau(\lambda_-)\right) - \operatorname{arccosh}\left(\frac{2c}{\sqrt{|\Delta|}}\tau(-1)\right)\right. \\ &\quad \left.+\operatorname{arccosh}\left(\left|\frac{2c}{\sqrt{|\Delta|}}\tau(\lambda_+)\right|\right) - \operatorname{arccosh}\left(\frac{2c}{\sqrt{|\Delta|}}\tau(1)\right)\right] \quad \text{in case (iv)} \end{aligned}$$

where the latter step follows from the fact that eqs. (3.187) and (3.188) enable one to write:

$$\begin{aligned} &\lim_{\epsilon\to 0^+} \left[-\operatorname{arccosh}\left(\left|\frac{2c}{\sqrt{|\Delta|}}\tau(u_B-\epsilon)\right|\right) + \operatorname{arccosh}\left(\frac{2c}{\sqrt{|\Delta|}}\tau(u_B+\epsilon)\right)\right] \\ = &\lim_{\epsilon\to 0^+} \left[-\operatorname{arccosh}\left(\frac{2c}{\sqrt{|\Delta|}}\frac{1}{\epsilon}\right) + \operatorname{arccosh}\left(\frac{2c}{\sqrt{|\Delta|}}\frac{1}{\epsilon}\right)\right] \\ = &\ 0. \end{aligned}$$

The Integration over z' and z in the case of $p_0 < 0$

In the following we consider the $\int dz \int dz'$ integration in the context of the $p_0 < 0$ part of the $\int_{-\infty}^{\infty} dp_0$ integration in eq. (3.139).

From eq. (3.150) there follows in the case of $p_0 < 0$ that

$$v_B = \frac{2k_0'p_0 - m^2}{2k_0'(-p_0)\left(1 - \frac{m^2}{2p_0^2}\right)} + \mathcal{O}(m^4) = \left(-1 + \frac{m^2}{2k_0'p_0}\right)\left(1 + \frac{m^2}{2p_0^2}\right) + \mathcal{O}(m^4)$$

$$= -1 + \left(\frac{p_0 - k_0'}{2k_0' p_0^2}\right) m^2 + \mathcal{O}(m^4) \tag{3.199}$$
$$\leq -1 \quad \text{for } p_0 < 0 \text{ and } k_0' > 0.$$

From eq. (3.149) there follows in the case of $p_0 < 0$ that

$$u_B = \frac{2k_0 p_0 - m^2}{2k_0(-p_0)\left(1 - \frac{m^2}{2p_0^2}\right)} + \mathcal{O}(m^4)$$
$$= \left(-1 + \frac{m^2}{2k_0 p_0}\right)\left(1 + \frac{m^2}{2p_0^2}\right) + \mathcal{O}(m^4)$$
$$= -1 - \left(\frac{k_0 - p_0}{2k_0 p_0^2}\right) m^2 + \mathcal{O}(m^4) \tag{3.200}$$
$$< -1 \quad \text{for } p_0 < 0 \text{ and } k_0 > 0. \tag{3.201}$$

Thus for $p_0 < 0$ we always have $u_B < -1$ and $v_B < -1$ which mean that we always have $z' - v_B > 0$ and $z - u_B > 0$ in integrations over z' and z since

$$z' \geq a = \cos(\theta + \alpha_B) \geq -1 > v_B$$

and

$$z \geq -1 > u_B.$$

Therefore we shall not encounter singularities at $z' = v_B$ and $z = u_B$ which circumvents the need in the present case of $p_0 < 0$ to separately consider regions in the $p_0 k_0$ plane as was needed in the case of $p_0 > 0$ shown in Figure 3.11.

The calculation of

$$I\left(\frac{1}{s_B t_B}\right) = 2\int_{-1}^{1} dz t_B^{-1} C_{-1} = \frac{1}{2k_0 k_0' |\vec{p}|^2} \int_{-1}^{1} dz \frac{1}{(z - u_B)} \int_a^b \frac{dz'}{(z' - v_B)\sqrt{-\gamma(z, z', \cos\alpha_B)}}, \tag{3.202}$$

where a and b are specified in (3.154), proceeds as follows in the case of $p_0 < 0$: In

$$C_{-1} = \int_a^b \frac{dz'}{2k_0' |\vec{p}|(z' - v_B)\sqrt{-\gamma(z, z', \cos\alpha_B)}}$$

we introduce the change of variable,

$$x = (z' - v_B)^{-1}$$

for which $x > 0$ implies that $x = +\sqrt{x^2}$ so that

$$C_{-1} = -\frac{1}{2k_0' |\vec{p}|} \int_{(a - v_B)^{-1}}^{(b - v_B)^{-1}} \frac{dx}{\sqrt{x^2[-\gamma(z, v_B, \cos\alpha_B)] + 2x(z\cos\alpha_B - v_B) - 1}}.$$

By considering $\gamma(z, v_B, \cos\alpha_B)$ as a quadratic function of v_B one can, similar to previous cases, determine that the roots, $v_B^{\pm}$, of the equation, $\gamma(z, v_B, \cos\alpha_B) = 0$, are at

$$v_B^- = \cos(\theta + \alpha_B) = a \quad \text{and} \quad v_B^+ = \cos(\theta - \alpha_B) = b$$

so that

$$\gamma(z, v_B, \cos\alpha_B) > 0 \quad \text{for} \quad v_B < a$$

which is always the case for $p_0 < 0$ since $v_B < -1 \leq a$. We therefore write C_{-1} in the form

$$C_{-1} = -\frac{1}{2k_0'|\vec{p}|\sqrt{\gamma(z, v_B, \cos\alpha_B)}} \times \int_{(a-v_B)^{-1}}^{(b-v_B)^{-1}} dx \left[-x^2 + \frac{2x(z\cos\alpha_B - v_B)}{\gamma(z, v_B, \cos\alpha_B)} - \frac{1}{\gamma(z, v_B, \cos\alpha_B)}\right]^{-1/2}.$$

The integral in the latter expression is identical to the integral in eq. (3.165). The result of the integral in eq. (3.165) appears in eq. (3.166) and can be taken over in the present application:

$$C_{-1} = \frac{\pi}{2k_0'|\vec{p}|\sqrt{\gamma(z, v_B, \cos\alpha_B)}} \quad \text{for} \quad p_0 < 0.$$

Therefore $I\,(1/(s_B t_B))$ in eq. (3.202) becomes

$$I\left(\frac{1}{s_B t_B}\right) = \frac{\pi}{2k_0 k_0'|\vec{p}|^2} \int_{-1}^{1} \frac{dz}{(z - u_B)\sqrt{\gamma(z, v_B, \cos\alpha_B)}}. \tag{3.203}$$

At line (3.201) it was proven that $u_B < -1$ for $p_0 < 0$ so that $z - u_B > 0$ in eq. (3.203). Except for the integration limits, the integral in eq. (3.203) is identical to the integral in the expression for E_2 in eq. (3.185) since $z - u_B > 0$ in E_2 too. The result for E_2 is given in eq. (3.186) and can be applied to eq. (3.203) by checking that c and Δ as defined in eqs. (3.180) and (3.181) are positive in the present case of $p_0 < 0$ too. This check is done at lines (C.22) and (C.24). Thus

$$I\left(\frac{1}{s_B t_B}\right) = -\frac{\pi}{2k_0 k_0'|\vec{p}|^2\sqrt{c}} \left[\operatorname{arcsinh}\left(\frac{2c}{\sqrt{\Delta}}\tau(1)\right) - \operatorname{arcsinh}\left(\frac{2c}{\sqrt{\Delta}}\tau(-1)\right)\right] \quad \text{for} \quad p_0 < 0 \tag{3.204}$$

where $\tau(z)$ is defined in eq. (3.183).

3.5.4 Summary of the Regularized Expressions for the Bosonic Part of the Vertex Correction

In this section we summarize the results obtained in the previous section for

$$I\left(\frac{1}{s_B t_B}\right) = \frac{1}{2k_0 k_0'|\vec{p}|^2} \int_{-1}^{1} dz \frac{1}{(z - u_B)} \int_a^b \frac{dz'}{(z' - v_B)\sqrt{-\gamma(z, z', \cos\alpha_B)}}.$$

We also derive regularized expressions for these results which enable us to treat the $m^2 \to 0$ limit.

For $k_0 > 0$, $k_0' > 0$ (i.e. for quarks as opposed to anti-quarks) and the $p_0 > 0$ part of the $\int_{-\infty}^{\infty} dp_0$ integration in eq. (3.139), we derived the following results for the regions (i), (iii) and (iv) indicated in Figure 3.11:

$$I\left(\frac{1}{s_B t_B}\right) = \frac{\pi}{2k_0 k_0' |\vec{p}|^2 \sqrt{c}} \times \begin{cases} \left[\operatorname{arcsinh}\left(\frac{2c}{\sqrt{\Delta}}\tau(-1)\right) - \operatorname{arcsinh}\left(\frac{2c}{\sqrt{\Delta}}\tau(1)\right)\right] & \text{for region (i)} \\ \left[\operatorname{arcsinh}\left(\frac{2c}{\sqrt{\Delta}}\tau(-1)\right) + \operatorname{arcsinh}\left(\frac{2c}{\sqrt{\Delta}}\tau(1)\right)\right] & \text{for region (iii)} \\ \left[\operatorname{arccosh}\left(\frac{2c}{\sqrt{|\Delta|}}\tau(-1)\right) + \operatorname{arccosh}\left(\frac{2c}{\sqrt{|\Delta|}}\tau(1)\right)\right. & \\ \left. -\operatorname{arccosh}\left(\frac{2c}{\sqrt{|\Delta|}}\tau(\lambda_-)\right) - \operatorname{arccosh}\left(\left|\frac{2c}{\sqrt{|\Delta|}}\tau(\lambda_+)\right|\right)\right] & \text{for region (iv).} \end{cases} \tag{3.205}$$

For $k_0 > 0$, $k_0' > 0$ and the $p_0 < 0$ part of the $\int_{-\infty}^{\infty} dp_0$ integration in eq. (3.139), we derived the following result:

$$I\left(\frac{1}{s_B t_B}\right) = \frac{\pi}{2k_0 k_0' |\vec{p}|^2 \sqrt{c}} \left[\operatorname{arcsinh}\left(\frac{2c}{\sqrt{\Delta}}\tau(-1)\right) - \operatorname{arcsinh}\left(\frac{2c}{\sqrt{\Delta}}\tau(1)\right)\right] \quad \text{for } p_0 < 0. \tag{3.206}$$

In Subsection (d) of Appendix C it is proven that all the expressions in eqs. (3.205) and (3.206) lead to the same single regularized expression in the $m^2 \to 0$ limit:

$$I\left(\frac{1}{s_B t_B}\right) = \frac{\pi}{p_0^2(-q^2)} \ln|A_B| \qquad \text{for both } p_0 < 0 \text{ and } p_0 > 0 \tag{3.207}$$

where

$$A_B = \frac{p_0^4 (q^2)^2}{m^4 k_0 k_0' (k_0 - p_0)(k_0' - p_0)}. \tag{3.208}$$

The results in the latter two equations is the explicit form of the result in the first equation at line (D.21).

As an example, we discussed the derivation of the result in eq. (3.207) in detail. The other results given at lines (D.21) and (D.22) are derived in a similar way. The way in which these results from three-particle processes contribute to the structure functions of the nucleon can be seen by considering eqs. (4.5), (4.6) and (4.9)–(4.12) and the discussions in Appendix D.

3.6 The Self-Energy Correction to a Quark

3.6.1 Introduction

The standard treatment of the fermion self-energy in conventional zero-temperature field theory must be modified in finite-temperature field theory which is no longer Lorentz covariant due to the preferred rest frame of the heat bath. This observation and the associated kinematic modifications which have to be introduced have been explained by Donoghue and Holstein in ref. [76]. The way these considerations have been applied by Cleymans and Dadić [15] in the analytical part of our calculations is outlined in this Section 3.6.

3.6.2 The Fermion Self-Energy and Thermal Spinors

In ref. [76] Donoghue and Holstein explained that, due to the lack of Lorentz covariance in finite-temperature field theory, the standard decomposition of the self-energy into a Lorentz invariant mass shift and a wave function renormalization proportional to $\not{p}-m$ is not obtained. In consequence they write the thermal self-energy in the form [76, p.240](b)

$$\Sigma_\beta(p) = B(p) + C(p)(\not{p} - m_{\rm phys}) + \not{D}(p) \tag{3.209}$$

where B, C and D_μ are not necessarily covariant functions of E_p and $\vec{p}$ and the meaning of $m_{\rm phys}$ is discussed below. One introduces thermal spinors which satisfy

$$\left[\not{p} - m_{\rm R} - \Sigma_\beta(p)|_{\not{p}=m_{\rm phys}}\right] u_\beta(p) = 0$$

and define for notational convenience

$$\not{\tilde{p}} - \tilde{m} = \not{p} - m_{\rm R} - \Sigma_\beta(p). \tag{3.210}$$

The particles which propagate freely in the heat bath at finite temperature are described by the thermal spinors which satisfy

$$(\not{\tilde{p}} - \tilde{m}) u_\beta(p) = 0. \tag{3.211}$$

If Σ_β were Lorentz invariant this would reduce to the Dirac equation with $\tilde{m}$ being the physical mass but, since the standard decomposition of the self-energy into a Lorentz invariant mass shift and a wave function renormalization proportional to $\not{p} - m$ is not obtained [see eq. (3.209)], one must be careful in defining what is meant by the term "mass".

Donoghue and Holstein define the "phase space mass" from the location of the pole of the propagator which occurs when $p^2 = m^2_{\rm phys}$ where an expression for $m_{\rm phys}$ is derived further on and differs from $\tilde{m}$ and $m_{\rm R}$ where $m_{\rm R}$ is the conventional renormalized mass at zero temperature ($m_{\rm R}$ is introduced to keep the discussion general for a while but further on we return to our consideration of massless quarks, i.e., $m_{\rm R} = 0$). As we shall see, $m_{\rm phys}$ is a function of T, μ and $|\vec{p}|$. According to Donoghue and Holstein the terminology, "phase space mass", arises from the direct association of $m_{\rm phys}$ with the kinematics of the particle in a heat bath and can be given an operational definition in terms of threshold and phase space behaviour for particle reactions. For this purpose they consider as an example the decay of a neutral Higgs boson (H^0) into an e^+e^- pair where the self-energy corrections to the leptons are considered in finite-temperature QED and state that the decay cannot take place if the H^0 mass is below $2m_{\rm phys}$ – even if the H^0 mass is above $2m_{\rm R} = 0$. They go on to state that one could imagine measuring the phase space mass by examining the threshold of various reactions or by a careful study of phase space distributions of a particular reaction. Both techniques are utilized in the search for the possible neutrino mass.

From eqs. (3.209) and (3.210) there follows that

$$\begin{aligned} \not{\tilde{p}} - \tilde{m} &= \not{p} - m_{\rm R} - B(p) - C(p)(\not{p} - m_{\rm R}) - \not{D}(p) \\ &= \gamma_0(p_0 - p_0 C - D_0) - \vec{\gamma}.[\vec{p} - \vec{p}C - \vec{D}] - m_{\rm R} - B + m_{\rm R}C \end{aligned} \tag{3.212}$$

where we replaced $m_{\rm phys}$ from eq. (3.209) by the renormalized mass at zero temperature, $m_{\rm R}$, since $m_{\rm phys} = m_{\rm R} + \mathcal{O}(\alpha_{\rm S})$ and the replacement occurs in the presence of the factor C which, due to its appearance in Σ_β, is already of $\mathcal{O}(\alpha_{\rm S})$ so that the replacement causes a difference of $\mathcal{O}(\alpha^2_{\rm S})$ which may be neglected since we work up to $\mathcal{O}(\alpha_{\rm S})$ only. From eq. (3.212) there follows that

$$\tilde{p}_0 = p_0(1 - C) - D_0 \tag{3.213}$$

$$\vec{\tilde{p}} = \vec{p}(1 - C) - \vec{D} \tag{3.214}$$

$$\tilde{m} = m_{\rm R}(1 - C) + B. \tag{3.215}$$

In analogy to the way that one obtains solutions to the free Dirac equation at zero temperature, one directly obtains solutions to eq. (3.211) by making the necessary substitutions in

the zero-temperature result:

$$u_\beta^{(s)}(p) = \sqrt{\tilde{E}+\tilde{m}} \begin{pmatrix} \chi^{(s)} \\ \frac{\vec{\sigma}.\vec{\tilde{p}}}{\tilde{E}+\tilde{m}}\chi^{(s)} \end{pmatrix} \tag{3.216}$$

where

$$\chi^{(1)} = \begin{pmatrix} 1 \\ 0 \end{pmatrix} \qquad \chi^{(2)} = \begin{pmatrix} 0 \\ 1 \end{pmatrix}$$

and, according to eq. (3.213), $\tilde{E} = E(1-C) - D_0$ with $E = \sqrt{|\vec{p}|^2 + m_{\rm phys}^2}$ and where the normalization of the spinors corresponds to having $2\tilde{E}$ particles per unit volume. Thus the renormalized thermal propagator is

$$\begin{aligned} & iS^{\rm R}(x-y) \\ = & \int \frac{d^3p}{(2\pi)^3 2\tilde{E}} \sum_{s=1,2} \left[\theta(x_0-y_0) u_\beta^{(s)}(p)\bar{u}_\beta^{(s)}(p) e^{-ip.(x-y)} + \theta(y_0-x_0) v_\beta^{(s)}(p)\bar{v}_\beta^{(s)}(p) e^{ip.(x-y)}\right] \\ = & \int \frac{d^3p}{(2\pi)^3 2\tilde{E}} \left[\theta(x_0-y_0)(\tilde{p}+\tilde{m}) e^{-ip.(x-y)} + \theta(y_0-x_0)(-\tilde{p}+\tilde{m}) e^{ip.(x-y)}\right] \end{aligned} \tag{3.217}$$

For later use, an expression for the wave function renormalization constant in terms of the newly introduced quantities is derived as follows: According to the definition of the wave function renormalization constant, the propagator in eq. (3.217) should be equal to

$$\begin{aligned} iS^{\rm R}(x-y) &= i\int \frac{d^4p}{(2\pi)^4} \frac{Z_2^{-1} e^{-ip.(x-y)}}{\not{p} - m_{\rm R} - \Sigma_\beta(p) + i\epsilon} \\ &= i\int \frac{d^4p}{(2\pi)^4} \frac{Z_2^{-1}(\tilde{p}+\tilde{m}) e^{-ip.(x-y)}}{\tilde{p}^2 - \tilde{m}^2 + i\epsilon} \end{aligned} \tag{3.218}$$

where, in the latter step, we made use of eq. (3.210). In order to perform the integration over p_0 in eq. (3.218) we write the denominator in the form:

$$\begin{aligned} \tilde{p}^2 - \tilde{m}^2 + i\epsilon &= [p_0(1-C) - D_0]^2 - [\vec{p}(1-C) - \vec{D}]^2 \\ &\quad -[m_{\rm R}(1-C) + B]^2 + i\epsilon \qquad (3.219) \\ &= \kappa\left(p_0^2 - \vec{p}^2 - m_{\rm phys}^2(|\vec{p}|) + i\epsilon\right) \qquad (3.220) \end{aligned}$$

where $m_{\rm phys}$ depends on $|\vec{p}|$ rather than $\vec{p}$ since in the rest frame of the heat bath the vectors $\vec{p}$ are distributed isotropically. The following mathematical trick can be used to obtain an expression for κ: Differentiate both the expressions in (3.219) and (3.220) *partially* with respect to p_0^2 and evaluate the result at the point $p_0^2 = m_{\rm phys}^2 + |\vec{p}|^2$ so that the coefficient of

$\partial\kappa/\partial p_0^2$ vanishes. Then, by making use of

$$\frac{\partial}{\partial p_0^2} = \frac{\partial p_0}{\partial p_0^2}\frac{\partial}{\partial p_0} = \frac{1}{2p_0}\frac{\partial}{\partial p_0} \qquad ; \qquad \frac{\partial m_R}{\partial p_0} = 0$$

one obtains

$$\begin{aligned}\kappa &= 1 - C - p_0\frac{\partial C}{\partial p_0} - \frac{\partial D_0}{\partial p_0} - C - \frac{D_0}{p_0} + \frac{|\vec{p}|^2}{p_0}\frac{\partial C}{\partial p_0} + \frac{1}{p_0}\vec{p}.\frac{\partial \vec{D}}{\partial p_0} + \frac{m_R^2}{p_0}\frac{\partial C}{\partial p_0} - \frac{m_R}{p_0}\frac{\partial B}{\partial p_0} \\ &= (1-C)\left[1 - C - \frac{1}{p_0}\frac{\partial}{\partial p_0}(m_R B + p.D)\right]\end{aligned}$$

where, in the latter step, use has been made of the fact that C, due to its appearance in Σ_β, is of $\mathcal{O}(\alpha_S)$ and that the coefficient of $\partial C/\partial p_0$ is equal to:

$$\begin{aligned}\frac{1}{p_0}(-p_0^2 + |\vec{p}|^2 + m_R^2) &= \frac{1}{p_0}(-p_0^2 + |\vec{p}|^2 + m_{\text{phys}}^2) + \mathcal{O}(\alpha_S) \\ &= 0 + \mathcal{O}(\alpha_S) \qquad \text{at} \qquad p_0^2 = |\vec{p}|^2 + m_{\text{phys}}^2,\end{aligned}$$

so that terms containing $\partial C/\partial p_0$ do not contribute to $\mathcal{O}(\alpha_S)$.

An expression for m_{phys} can also be derived as follows: From eq. (3.220) it follows that, at the point $p_0^2 = |\vec{p}|^2 + m_{\text{phys}}^2$, $\tilde{p}^2 - \tilde{m}^2 = 0$ will hold and therefore, from eqs. (3.213), (3.214) and (3.215), that

$$[p_0(1-C) - D_0]^2 - [\vec{p}(1-C) - \vec{D}]^2 - [m_R(1-C) + B]^2 = 0 \tag{3.221}$$

at $p_0^2 = |\vec{p}|^2 + m_{\text{phys}}^2$. By making use of the fact that B, C and D_μ, due to their appearances in Σ_β, are of $\mathcal{O}(\alpha_S)$, the result in eq. (3.221) becomes

$$p^2 - m_R^2 = 2m_R B + 2p.D + 2C(p^2 - m_R^2) + \mathcal{O}(\alpha_S^2) \tag{3.222}$$

$$= 2m_R B + 2p.D + \mathcal{O}(\alpha_S^2) \tag{3.223}$$

where the latter step follows since, as may be seen from line (3.222), $p^2 - m_R^2$ is of $\mathcal{O}(\alpha_S)$. Since the result in eq. (3.223) has been derived for $p_0^2 = |\vec{p}|^2 + m_{\text{phys}}^2$ one can conclude that

$$m_{\text{phys}}^2(|\vec{p}|) = m_R^2 + 2m_R B + 2p.D.$$

At this point we continue with the derivation of the wave function renormalization constant. The integration over p_0 in eq. (3.218) is performed by making use of eq. (3.220):

$$\begin{aligned}iS^R(x-y) &= i\int \frac{d^4p}{(2\pi)^4}\frac{Z_2^{-1}(\tilde{p}+\tilde{m})e^{-ip.(x-y)}}{\kappa\left(p_0^2 - \vec{p}^2 - m_{\text{phys}}^2(|\vec{p}|) + i\epsilon\right)} \\ &= \int \frac{d^3p}{(2\pi)^3 2\tilde{E}}\frac{Z_2^{-1}}{\kappa}\Big[\theta(x_0-y_0)(\tilde{p}+\tilde{m})e^{-ip.(x-y)} \\ &\quad + \theta(y_0-x_0)(-\tilde{p}+\tilde{m})e^{ip.(x-y)}\Big]\end{aligned} \tag{3.224}$$

where $E = |\vec{p}|^2 + m^2_{\rm phys}$. By comparing the expression in eq. (3.224) with the expression in (3.217), one obtains

$$\begin{aligned} Z_2^{-1} &= \frac{E\kappa}{\tilde{E}} = \frac{E(1-C)\left[1-C-\frac{1}{p_0}\frac{\partial}{\partial p_0}(m_{\rm R}B+p.D)\right]}{E(1-C)-D_0} \\ &= 1-C-\frac{1}{p_0}\frac{\partial}{\partial p_0}(m_{\rm R}B+p.D)+\frac{D_0}{E}+\mathcal{O}(\alpha_{\rm S}) \end{aligned} \tag{3.225}$$

3.6.3 Writing down the Self-Energy Contributions

Corrections of $\mathcal{O}(\alpha_{\rm S})$ arise from the interference of the lowest order diagram with the two self-energy diagrams in Figure 3.1 represented by the amplitudes M_{3a}, M_{3c} and M_{3d}, respectively, where M_{3a} is given in eq. (3.119) and

$$M_{3c} = \bar{u}(k',s')ie\gamma_\nu\epsilon^\nu_{\gamma^*}(q)iS^{11}(k)\left[-i\Sigma_\beta(k)\right]u(k,s) \tag{3.226}$$

$$M_{3d} = \bar{u}(k',s')\left[-i\Sigma_\beta(k')\right]iS^{11}(k')ie\gamma_\nu\epsilon^\nu_{\gamma^*}(q)u(k,s) \tag{3.227}$$

where colour factors are suppressed and where

$$-i\Sigma_\beta(k) \equiv \int\frac{d^4p}{(2\pi)^4}(-ig\gamma_\mu)(-g^{\mu\sigma})iD^{11}(p)iS^{11}(k-p)(-ig\gamma_\sigma) \tag{3.228}$$

where, in the latter expressions, only type 1 vertices are considered in accordance with discussions below. For the interference,

$$M_{3a}M^*_{3c}+M_{3c}M^*_{3a}+M_{3a}M^*_{3d}+M_{3d}M^*_{3a} = 2{\rm Re}\left[M_{3a}M^*_{3c}+M_{3a}M^*_{3d}\right], \tag{3.229}$$

we need to consider the real part of (quark mass = $m_{\rm R}$; gluon mass = m ; It is to be noted that $m_{\rm phys}$, $m_{\rm R}$ and the bare fermion mass all differ from each other by terms of $\mathcal{O}(\alpha_{\rm S})$ so that one may use anyone of them in expressions where they have coefficients which are already of $\mathcal{O}(\alpha_{\rm S})$ since their respective use causes differences of $\mathcal{O}(\alpha_{\rm S}^2)$ only.):

$$\begin{aligned} &\sum_{\pm s,\pm s'}(M_{3a}M^*_{3c}+M_{3a}M^*_{3d}) \\ =\ &\int\frac{d^4p}{(2\pi)^4}{\rm Tr}\Big\{(\not k'+m_{\rm R})ie\gamma_\nu\epsilon^\nu_{\gamma^*}(q)(\not k+m_{\rm R})ig\gamma_\sigma(\not k-\not p+m_{\rm R})[i\bar{S}^{11}(k-p)]^*[iD^{11}(p)]^* \\ &\times(-g^{\mu\sigma})ig\gamma_\mu(\not k+m_{\rm R})[i\bar{S}^{11}(k)]^*[\epsilon^\alpha_{\gamma^*}(q)]^*(-ie\gamma_\alpha) \\ &+(\not k'+m_{\rm R})ie\gamma_\nu\epsilon^\nu_{\gamma^*}(q)(\not k+m_{\rm R})[\epsilon^\alpha_{\gamma^*}(q)]^*(-ie\gamma_\alpha)(\not k'+m_{\rm R})[i\bar{S}^{11}(k')]^*ig\gamma_\sigma \\ &\times(\not k'-\not p+m_{\rm R})[i\bar{S}^{11}(k'-p)]^*[iD^{11}(p)]^*(-g^{\mu\sigma})ig\gamma_\mu\Big\}. \end{aligned} \tag{3.230}$$

Since the vertices marked with 1,2 in the self-energy diagrams in Figure 3.1 are connected to only internal lines, they may be of both types one and two according to the discussion in Section 1.3.1. For the terms containing only type one vertices one proceeds according to the following considerations:

Since, as may be seen from their expressions in Table 3.1 and the identity in eq. (3.17), each propagator can be decomposed into two terms, one corresponding to off-mass shell propagation and the other one corresponding to on-mass shell propagation and containing a Dirac delta function, the expression in eq. (3.230) contains terms with zero, one, two and three Dirac delta functions. Terms with zero and two Dirac delta functions are pure imaginary and therefore does not contribute since the interference is real as may be seen in eq. (3.229). Terms containing three Dirac delta functions contribute only to the ill-defined either $\delta^2(k^2 - m_{\rm R}^2)$ or $\delta^2(k'^2 - m_{\rm R}^2)$ expressions which arise from the fermion lines on both sides of the self-energy loop.

All the self-energy terms containing the internal type 2 vertex contain three Dirac delta functions which will, for the same reason as given in the sentence preceding this one, contribute only to the ill-defined expressions which cancel according to the mechanism provided by the real-time formalism.

Of the terms containing only one Dirac delta function, we consider only those with either the gluon on mass shell or the fermion line with momentum $k - p$ or $k' - p$ on mass shell since the terms with the internal fermion line between the gluon vertex and the photon vertex on mass shell also leads to ill-defined δ^2 expressions due to the presence of the mass shell Dirac delta function associated with an external fermion line when performing phase space integrations.

Thus we only need to consider the terms containing one Dirac delta function stemming from either the internal gluon, fermion with momentum $k - p$ or fermion primed with momentum $k' - p$ line in the $\mathcal{O}(\alpha_{\rm S})$ self-energy graph in Figure 3.1. We call it the bosonic, fermionic or fermionic primed part of the self-energy correction, respectively. Thus we obtain (we drop the subscript γ^* of ϵ):

$$
\begin{aligned}
& 2\mathrm{Re} \sum_{\pm s, \pm s'} (M_{3a} M_{3c}^* + M_{3a} M_{3d}^*) \\
= \; & e^2 g^2 \int \frac{d^4p}{(2\pi)^4} \Big[\mathrm{Tr} \left\{ (\not{k}' + m_{\rm R})\, \not{q}(q)(\not{k} + m_{\rm R}) \gamma^\mu (\not{k} - \not{p} + m_{\rm R}) \gamma_\mu (\not{k} + m_{\rm R}) [\not{q}(q)]^* \right\}
\end{aligned}
$$

$$\times\left\{-\frac{\pi\delta\left((k-p)^2\right)}{(p^2-m^2)(k^2-m_{\rm R}^2)}[1-2n_{\rm F}(x_{k-p})]-\frac{\pi\delta(p^2-m^2)}{((k-p)^2-m_{\rm R}^2))\,(k^2-m_{\rm R}^2)}\right.$$
$$\left.\times[1+2n_{\rm B}(|p_0|)]\right\}+{\rm Tr}\left\{(\not k'+m_{\rm R})\not q(q)(\not k+m_{\rm R})[\not q(q)]^*(\not k'+m_{\rm R})\gamma^\mu(\not k'-\not p+m_{\rm R})\gamma_\mu\right\}$$
$$\times\left\{-\frac{\pi\delta\left((k'-p)^2\right)}{(p^2-m^2)(k'^2-m_{\rm R}^2)}[1-2n_{\rm F}(x_{k'-p})]-\frac{\pi\delta(p^2-m^2)}{((k'-p)^2-m_{\rm R}^2))\,(k'^2-m_{\rm R}^2)}\right.$$
$$\left.[1+2n_{\rm B}(|p_0|)]\right\}\Bigg]+{\rm c.c.}$$

In accordance with our conclusion in the latter paragraph we only consider those terms in $-i\Sigma_\beta(k)$, as defined in eq. (3.228), containing one Dirac delta function stemming from either the on mass shell gluon or the on mass shell fermion with momentum $k-p$. For the same reason we only consider those terms in $-i\Sigma_\beta(k')$ containing one Dirac delta function stemming from either the on mass shell gluon or the on mass shell fermion primed with momentum $k'-p$. Thus the relevant contribution from e.g. $-i\Sigma(k)$ is $-i{\rm Re}\Sigma(k)$ where

$$\begin{aligned}{\rm Re}\Sigma(k) \;\equiv\; & 2\pi g^2\int\frac{d^4p}{(2\pi)^4}(\not k-\not p-2m_{\rm R})\left[\delta(p^2-m^2)\left((1+2n_{\rm B}(|p_0|)\right)\frac{1}{(k-p)^2-m_{\rm R}^2}\right.\\ & \left.+\delta\left((k-p)^2-m_{\rm R}^2\right)(1-2n_{\rm F}(x_{k-p}))\frac{1}{p^2-m^2}\right].\end{aligned}\tag{3.231}$$

By defining the quantities B, C and D_μ in eq. (3.209) as

$$\begin{aligned}B(k) &= -m_{\rm R}C(k)\\ C(k) &= \frac{g^2}{(2\pi)^3}{\rm P}\int d^4p c(k,p)\\ D_\mu(k) &= -\frac{g^2}{(2\pi)^3}{\rm P}\int d^4p p_\mu c(k,p)\end{aligned}$$

where

$$\begin{aligned}c(k,p) \;\equiv\; & -\frac{1}{\pi}{\rm Im}\left\{\left(\frac{1+n_{\rm B}(|p_0|)}{p^2-m^2+i\epsilon}-\frac{n_{\rm B}(|p_0|)}{p^2-m^2-i\epsilon}\right)\right.\\ & \left.\times\left(\frac{1-n_{\rm F}(x_{k-p})}{(k-p)^2-m_{\rm R}^2+i\epsilon}+\frac{n_{\rm F}(x_{k-p})}{(k-p)^2-m_{\rm R}^2-i\epsilon}\right)\right\}\\ =\; & \delta(p^2-m^2)\left(1+2n_{\rm B}(|p_0|)\right)\frac{1}{(k-p)^2-m_{\rm R}^2}\\ & +\delta\left((k-p)^2-m_{\rm R}^2\right)(1-2n_{\rm F}(x_{k-p}))\frac{1}{p^2-m^2},\end{aligned}$$

the expression on the right hand side of eq. (3.209) exactly reproduces the expression on the right hand side of eq. (3.231).

In writing down the amplitude squared $|M_{3a}|^2$ for the "lowest order diagram" in Figure 3.1, an $\mathcal{O}(\alpha_S)$ contribution arising from the use of the thermal spinor is to be noted:

$$\begin{aligned} M_{3a} &= \bar{u}_\beta(k')ie\gamma_\nu\epsilon^\nu_{\gamma^*}(q)u_\beta(k) \\ \sum_{\pm s,\pm s'}|M_{3a}|^2 &= \mathrm{Tr}\left\{(\tilde{\not{k}}' + \tilde{m})ie\gamma_\nu\epsilon^\nu_{\gamma^*}(q)(\tilde{\not{k}} + \tilde{m})(-ie\gamma_\sigma)[\epsilon^\sigma_{\gamma^*}(q)]^*\right\} \\ &= \sum_{\pm s,\pm s'}|M_{\mathrm{Born}}|^2\left[1 - C(k) - C(k')\right] + 4e^2\left\{[k'.D(k) + k.D(k')]\epsilon.\epsilon^*\right. \\ &\quad \left. -k'.\epsilon[D(k).\epsilon^*] - k.\epsilon^*[D(k').\epsilon] - k'.\epsilon^*[D(k).\epsilon] - k.\epsilon[D(k').\epsilon^*]\right\} \quad (3.232) \end{aligned}$$

where

$$\sum_{\pm s,\pm s'}|M_{\mathrm{Born}}|^2 = 4e^2\left\{(k'.\epsilon)(k.\epsilon) + (k'.\epsilon^*)(k.\epsilon) - (k.k')(\epsilon.\epsilon^*)\right\}$$

is the zeroth order in α_S Born term contribution.

Since C and D_μ are of $\mathcal{O}(\alpha_S)$ we see from eq. (3.232) that the "lowest order diagram" contains both zeroth and first order in α_S contributions.

Other $\mathcal{O}(\alpha_S)$ contributions are from self-energy and counter term contributions:

$$2\mathrm{Re}\sum_{\pm s,\pm s'}[M_{3a}(M_{3c} + M_{3e})^*] = -2\sum_{\pm s,\pm s'}|M_{\mathrm{Born}}|^2\left(Z_2^{-1}(k) - 1\right) \quad (3.233)$$

$$2\mathrm{Re}\sum_{\pm s,\pm s'}[M_{3a}(M_{3d} + M_{3f})^*] = -2\sum_{\pm s,\pm s'}|M_{\mathrm{Born}}|^2\left(Z_2^{-1}(k') - 1\right). \quad (3.234)$$

All the contributions so far must be divided by $\sqrt{Z_2(k)}\sqrt{Z_2(k')}$ due to the wave function renormalization. Since $Z_2 = 1 + \mathcal{O}(\alpha_S)$, the only $\mathcal{O}(\alpha_S)$ contribution from wave function renormalization is from

$$\begin{aligned} \sum_{\pm s,\pm s'}\left|\frac{1}{\sqrt{Z_2(k)}\sqrt{Z_2(k')}}M_{\mathrm{Born}}\right|^2 &= \sum_{\pm s,\pm s'}|M_{\mathrm{Born}}|^2 + 2\sum_{\pm s,\pm s'}|M_{\mathrm{Born}}|^2\left[\left(\sqrt{Z_2^{-1}(k)} - 1\right)\right. \\ &\quad \left. + \left(\sqrt{Z_2^{-1}(k')} - 1\right)\right]. \quad (3.235) \end{aligned}$$

Another source of $\mathcal{O}(\alpha_S)$ contributions is from $\tilde{E}$ and $\tilde{E}'$ appearing in the phase space factors

$$\frac{d^3k}{(2\pi)^3 2\tilde{E}}\frac{d^3k'}{(2\pi)^3 2\tilde{E}'} = \frac{d^3k}{(2\pi)^3 2k_0}\frac{d^3k'}{(2\pi)^3 2k_0'}\left[1 + \mathcal{O}(\alpha_S)\right] \quad (3.236)$$

where, e.g.,

$$\begin{aligned} \tilde{E}' &= E'\left(1 - C(k')\right) - D_0(k') \\ E' &= \sqrt{k_0'^2 + m^2_{\mathrm{phys}}} \qquad ; \qquad k_0' = |\vec{k} + \vec{q}| \end{aligned} \quad (3.237)$$

and where the use of $2\tilde{E}2\tilde{E}'$ in the denominators on the left hand side of eq. (3.236) stems from the normalization of thermal spinors which, as mentioned just after eq. (3.216), corresponds to having $2\tilde{E}$ particles per unit volume. Since we are working to $\mathcal{O}(\alpha_S)$ only, the $\mathcal{O}(\alpha_S)$ terms in eq. (3.236) contribute, as in the case of the wave function renormalization constant, only as factors of zeroth order in α_S contributions:

$$\begin{aligned}
&\int \frac{d^3k}{(2\pi)^3 2\tilde{E}} \frac{d^3k'}{(2\pi)^3 2\tilde{E}'} \sum_{\pm s,\pm s'} |M_{\rm Born}|^2 \\
&= \int \frac{d^3k}{(2\pi)^3 2E} \frac{d^3k'}{(2\pi)^3 2E'} \sum_{\pm s,\pm s'} |M_{\rm Born}|^2 \left(1 + C(k) + C(k') + \frac{D_0(k)}{k_0} + \frac{D_0(k')}{k_0'}\right) + \mathcal{O}(\alpha_S^2) \\
&= \int \frac{d^3k}{(2\pi)^3 2k_0} \frac{d^3k'}{(2\pi)^3 2k_0'} \sum_{\pm s,\pm s'} |M_{\rm Born}|^2 \left(1 + C(k) + C(k') + \frac{D_0(k)}{k_0} + \frac{D_0(k')}{k_0'}\right) \\
&\quad + \mathcal{O}(\alpha_S^2) \qquad (3.238)
\end{aligned}$$

where the replacement of E and E' with k_0 and k_0' [Line (3.237) shows the difference between E' and k_0'.] in the latter step can be shown to lead to no additional $\mathcal{O}(\alpha_S)$ corrections.

For convenience we include the $\mathcal{O}(\alpha_S)$ contribution from eq. (3.238) in the expression for $\sum_{\pm s,\pm s'} |M_{3a}|^2$ in eq. (3.232) and redefine the latter as a primed quantity:

$$\begin{aligned}
&\sum_{\pm s,\pm s'} |M'_{3a}|^2 \\
&= \sum_{\pm s,\pm s'} |M_{\rm Born}|^2 + \sum_{\pm s,\pm s'} |M_{\rm Born}|^2 \left[\frac{D_0(k)}{k_0} + \frac{D_0(k')}{k_0'}\right] + 4e^2 \left\{[k'.D(k) + k.D(k')]\epsilon.\epsilon^* \right. \\
&\left. -k'.\epsilon[D(k).\epsilon^*] - k.\epsilon^*[D(k').\epsilon] - k'.\epsilon^*[D(k).\epsilon] - k.\epsilon[D(k').\epsilon^*]\right\}. \qquad (3.239)
\end{aligned}$$

In Section (a) of Appendix E it is proven that Z_2^{-1} in eq. (3.225) can be written as

$$Z_2^{-1}(k) = 1 + \frac{D_0(k)}{k_0} + \mathcal{O}(\alpha_S^2). \qquad (3.240)$$

By using the latter expression for Z_2^{-1} in the addition of the self-energy contributions from eqs. (3.239), (3.233), (3.234) and the second term on the right hand side of eq. (3.235), one obtains:

$$\begin{aligned}
&\sum_{\pm s,\pm s'} |M_{\rm Born}|^2 \left\{1 + \frac{D_0(k)}{k_0} + \frac{D_0(k')}{k_0'} - 2\left[Z_2^{-1}(k) - 1\right] - 2\left[Z_2^{-1}(k') - 1\right]\right. \\
&\left. +2\left[\sqrt{Z_2^{-1}(k)} - 1 + \sqrt{Z_2^{-1}(k')} - 1\right]\right\} + 4e^2 \left\{[k'.D(k) + k.D(k')]\epsilon.\epsilon^* \right. \\
&\left. -k'.\epsilon[D(k).\epsilon^*] - k.\epsilon^*[D(k').\epsilon] - k'.\epsilon^*[D(k).\epsilon] - k.\epsilon[D(k').\epsilon^*]\right\} + \mathcal{O}(\alpha_S^2)
\end{aligned}$$

$$= \sum_{\pm s,\pm s'} |M_{\rm Born}|^2 + 4e^2 \{[k'.D(k) + k.D(k')]\epsilon.\epsilon^* - k'.\epsilon[D(k).\epsilon^*] - k.\epsilon^*[D(k').\epsilon] - k'.\epsilon^*[D(k).\epsilon] - k.\epsilon[D(k').\epsilon^*]\} + \mathcal{O}(\alpha_S^2). \quad (3.241)$$

The $\mathcal{O}(\alpha_S)$ second term of the latter expression can be written in a convenient form for angular integrations. To do so we write D_μ in the form (we consider massless quarks, i.e., $m_R = 0$):

$$D_\mu(k) = -\frac{g^2}{(2\pi)^3} \int d^4p p p_\mu (k'-p)^2 \Delta$$
$$D_\mu(k') = -\frac{g^2}{(2\pi)^3} \int d^4p p p_\mu (k-p)^2 \Delta$$

where $\Delta = \Delta_B + \Delta_F + \Delta_{F'}$ and

$$\Delta_B = \frac{1 + 2n_B(|p_0|)}{(k-p)^2(k'-p)^2} \delta(p^2 - m^2) \quad (3.242)$$

$$\Delta_F = \frac{1 - 2n_F(x_{k-p})}{(k'-p)^2(p^2-m^2)} \delta\left((k-p)^2\right) \quad (3.243)$$

$$\Delta_{F'} = \frac{1 - 2n_F(x_{k'-p})}{(k-p)^2(p^2-m^2)} \delta\left((k'-p)^2\right). \quad (3.244)$$

The first term in eq. (3.241) is of zeroth order in α_S and is considered in Chapter 4 where it contributes to the structure function F_2 according to eq. (4.7). For the present discussion we consider only the $\mathcal{O}(\alpha_S)$ second term in eq. (3.241):

$$E_\epsilon \equiv 4e^2 \{[k'.D(k) + k.D(k')]\epsilon.\epsilon^* - k'.\epsilon[D(k).\epsilon^*] - k.\epsilon^*[D(k').\epsilon] - k'.\epsilon^*[D(k).\epsilon] - k.\epsilon[D(k').\epsilon^*]\}.$$

By making use of eqs. (2.6), (3.132) and (3.134) and the relations

$$k.q = -\frac{1}{2}q^2 \quad ; \quad p.q = \frac{1}{2}\left[(k-p)^2 - (k'-p)^2\right]$$

one obtains

$$\sum_{\lambda=\pm1,0} (-1)^{\lambda+1} E_{\epsilon=\epsilon_\lambda} = -8e^2g^2\pi \int \frac{d^4p}{(2\pi)^4} \left\{-\frac{1}{2}p^2(k'-p)^2 + \left[(k'-p)^2\right]^2 - \frac{1}{2}p^2(k-p)^2 + \left[(k-p)^2\right]^2 - (k-p)^2(k'-p)^2\right\} \Delta.$$

3.7 Summary of Expressions Obtained after the Addition of Self-Energy- and Vertex Corrections to a Quark

By adding the latter self-energy corrections to the vertex correction given in eq. (3.138) one obtains

$$\begin{aligned}
&\sum_{\lambda=\pm1,0}(-1)^{\lambda+1}\left\{\left[2\mathrm{Re}\sum_{\pm s,\pm s'}M_{3a}M_{3b}^{*}\right]_{\epsilon=\epsilon_\lambda}+E_{\epsilon=\epsilon_\lambda}\right\}\\
&= -4e^2g^2\pi\int\frac{d^4p}{(2\pi)^4}\left\{4(p^2)^2+2q^2[4p^2-2(k'-p)^2-2(k-p)^2]+2[(k-p)^2]^2\right.\\
&\quad\left.+2[(k'-p)^2]^2+4(q^2)^2+2(k-p)^2(k'-p)^2-5p^2[(k'-p)^2+(k-p)^2]\right\}\Delta \quad (3.245)\\
&= 8e^2g^2\pi\int\frac{d^4p}{(2\pi)^4}\left\{-2(q^2)^2+2q^2(k-p)^2\left(1-\frac{p_0}{2k_0'}\right)+2q^2(k'-p)^2\left(1-\frac{p_0}{2k_0}\right)\right.\\
&\quad -4p^2q^2\left[\frac{3}{4}+\frac{(k_0+k_0')(k_0+k_0'-2p_0)}{4q_z^2}\right]-(k-p)^2(k'-p)^2\left(1+\frac{k_0}{k_0'}+\frac{k_0'}{k_0}\right.\\
&\quad \left.+\frac{q^2}{2k_0^2}+\frac{q^2}{2{k_0'}^2}\right)+p^2(k-p)^2\left(\frac{1}{2}-\frac{{k_0'}^2}{q_z^2}+\frac{k_0^2}{q_z^2}+\frac{q^2}{2{k_0'}^2}+\frac{k_0}{k_0'}\right)\\
&\quad \left.+p^2(k'-p)^2\left(\frac{1}{2}+\frac{{k_0'}^2}{q_z^2}-\frac{k_0^2}{q_z^2}+\frac{q^2}{2{k_0}^2}+\frac{k_0'}{k_0}\right)\right\}\Delta \quad (3.246)
\end{aligned}$$

where the latter step follows by making use of the following relations which can be considered as effective equalities valid under the three-particle phase space integrations (Their derivations appear in Section (b) of Appendix E.):

$$\begin{aligned}
(k'-p)^4\Delta &= (k'-p)^2\left\{(k-p)^2\left(\frac{q^2}{2k_0^2}+\frac{k_0'}{k_0}\right)+p^2\left(-\frac{q^2}{2k_0^2}-\frac{\nu}{k_0}\right)+\frac{q^2p_0}{k_0}\right\}\Delta \quad (3.247)\\
p^4\Delta &= p^2\left\{(k'-p)^2\left(-\frac{q^2}{2q_z^2}-\frac{k_0\nu}{q_z^2}\right)+(k-p)^2\left(-\frac{q^2}{2q_z^2}+\frac{k_0'\nu}{q_z^2}\right)\right.\\
&\quad \left.+\frac{q^2}{q_z^2}\left[-\frac{q_z^2}{2}+\frac{1}{2}(k_0+k_0')(k_0+k_0'-p_0)\right]\right\}\Delta \quad (3.248)\\
(k-p)^4\Delta &= (k-p)^2\left\{(k'-p)^2\left(\frac{q^2}{2{k_0'}^2}+\frac{k_0}{k_0'}\right)+p^2\left(-\frac{q^2}{2{k_0'}^2}+\frac{\nu}{k_0'}\right)\right.\\
&\quad \left.+\frac{q^2p_0}{k_0'}\right\}\Delta. \quad (3.249)
\end{aligned}$$

Similarly one obtains for longitudinally polarized photons:

$$\left[2\mathrm{Re}\sum_{\pm s,\pm s'}M_{3a}M_{3b}^{*}\right]_{\epsilon=\epsilon_0}+E_{\epsilon=\epsilon_0}$$

$$
\begin{aligned}
= \; & 8e^2g^2\pi \int \frac{d^4p}{(2\pi)^4}\Bigg\{-\frac{(q^2)^2}{q_z^2}[q^2+(2k_0+\nu-p_0)^2+p_0^2-\nu^2] \\
& +\frac{2q^2(k-p)^2}{q_z^2}\left[\frac{q^2-2\nu k_0'}{2}-p_0\left(\frac{q^2}{4k_0'}-\nu\right)\right]+\frac{2q^2(k'-p)^2}{q_z^2}\left[\frac{q^2+2\nu k_0}{2}\right. \\
& \left.-p_0\left(\frac{q^2}{4k_0}+\nu\right)\right]-4p^2q^2\left[-\frac{1}{4}-\frac{(k_0+k_0')(k_0+k_0'-2p_0)}{4q_z^2}\right] \\
& -\frac{(k-p)^2(k'-p)^2}{q_z^2}\left[-\nu^2+\frac{q^2}{2}\left(\frac{k_0}{k_0'}+\frac{k_0'}{k_0}+\frac{q^2}{2k_0^2}+\frac{q^2}{2k_0'^2}\right)\right] \\
& +\frac{p^2(k-p)^2}{q_z^2}\left[-\frac{\nu^2}{2}+k_0'^2-k_0^2+\frac{q^2}{2}\left(\frac{k_0}{k_0'}+\frac{q^2}{2k_0'^2}\right)\right] \\
& +\frac{p^2(k'-p)^2}{q_z^2}\left[-\frac{\nu^2}{2}-k_0'^2+k_0^2+\frac{q^2}{2}\left(\frac{k_0'}{k_0}+\frac{q^2}{2k_0^2}\right)\right]\Bigg\}\Delta. \qquad (3.250)
\end{aligned}
$$

The expressions in eqs. (3.246) and (3.250) exclude phase space integrations associated with the external quark lines. Such integrations have been discussed in detail for the example of a contribution to the bosonic part of the vertex correction in Section 3.5. The results from such phase space integrations of all the other three-particle contributions are summarized in Section D.4.

3.8 The Cancellation of Collinear Singularities

3.8.1 Introduction

So far we have discussed the derivation of expressions for examples of four- and three-particle processes. The results for *all* four- and three-particle processes are summarized in Appendix D. The expressions for four- and three-particle processes given in eqs. (D.17),(D.18) and (D.23)–(D.25) contain collinear singularities due to the presence of factors of m in the arguments of some of the ln functions. In ref. [24, p.387] it is mentioned that these singularities cancel separately in four groups of contributions according to the scheme shown in Figure 3.13. It is also mentioned that the principle of detailed balance existing for thermal equilibrium is responsible for the cancellations. In Sections 3.8.2 and 3.8.3 we discuss explicit examples of the cancellations which lead to the final expressions for four-particle processes given by eqs. (D.19) and (D.20) and for three-particle processes given by eqs. (D.27) and (D.28). In Section 3.8.4 we explain how the principle of detailed balance underlies the cancellations.

In Appendix D it is mentioned that, for the purpose of the cancellation of collinear

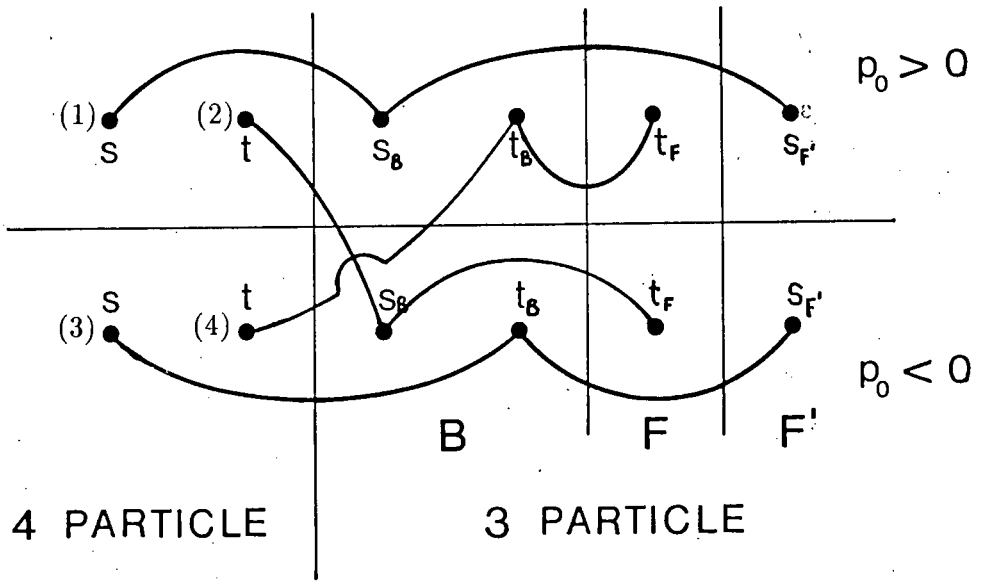

Figure 3.13: The scheme according to which collinear singularities cancel

singularities, one transforms from the variables (k_0, p_0) to the variables (K, p_0) where K is defined in eq. (D.1). The resulting regions of support in the K, p_0 plane for four- and three-particle processes are shown in Figures D.1 and D.2, respectively. The necessity for the transformation from k_0 to K is explained in Section 3.8.3.

3.8.2 A First Example

We start by discussing an example of cancellation according to the group of contributions containing s^{-1} type singularities with $p_0 > 0$ (This group is denoted by the label (1) in Figure 3.13.) The meaning of the group of contributions as described in the latter sentence should become clear in the detailed discussions below.

In the following we discuss cancellations in the context of expressions for the sum over all polarizations of the virtual photon, i.e., eqs. (D.17) and (D.23)–(D.25). According to the results of angular integrations in (D.16) and Table D.3, the s^{-1} singularity for four-particle processes is associated with B_4 in classes 1,2,3 and 4 which specifies the term proportional to $\ln|B_4|$ to be considered in eq. (D.17). According to the results of angular integrations in (D.21) the s_B^{-1} singularity for the bosonic three-particle contribution (to be considered according to group (1) of the scheme for cancellations in Figure 3.13) is associated with B_B which specifies the term proportional to $\ln|B_B|$ to be considered in eq. (D.23). According

to the results of angular integrations in (D.22) the $s_{F'}^{-1}$ singularity for the fermionic three-particle contribution (to be considered according to group (1) of the scheme for cancellations in Figure 3.13) is associated with $B_{F'}$ which specifies the term proportional to $\ln|B_{F'}|$ to be considered in eq. (D.25). In order to show the cancellation of collinear singularities, we consider the latter three contributions in isolation in the following. Adding them up and suppressing common factors in their coefficients as they appear in eqs. (D.17),(D.23) and (D.25), one obtains

$$\begin{aligned} E \equiv\ & S_4|q^2|\left[\frac{|p_0|}{4A^2}-\frac{\epsilon(p_0)}{2A}\right]\ln|B_4| - S_{3B}|q^2|\left[\frac{|p_0|}{4A^2}-\frac{\epsilon(p_0)}{2A}\right]\ln|B_B| \\ & -S_{3F'}\epsilon(B)|q^2|\left[\frac{p_0}{4A^2}-\frac{1}{2A}\right]\ln|B_{F'}| \end{aligned}$$

where the K, p_0 support of all these terms overlap exactly since we are considering the $\ln|B_4|$ term from four-particle processes only in classes 1,2,3 and 4 (where it contributes to collinear singularities according to Table D.3) which, according to Figure D.1, have support on exactly the same region of the K, p_0 plane that the three-particle terms have their support according to Figure D.2.

According to the definitions of the quantities B_4, B_B and $B_{F'}$ we can write (For the sake of brevity we consider only the examples of classes 1 and 4.):

$$\begin{aligned} \ln|B_4| &= \begin{cases} \ln\left|\frac{4p_0^2A}{B}\right|+\ln\frac{1}{m^2} & \text{in class 1} \\ \ln\left|\frac{4p_0Ac}{E}\right|+\ln\frac{1}{m^2} & \text{in class 4} \end{cases} \\ \ln|B_B| &= \ln\left|\frac{4p_0^2A}{B}\right|+\ln\frac{1}{m^2} \\ \ln|B_{F'}| &= \ln|4AB|+\ln\frac{1}{m^2}. \end{aligned}$$

Then

$$E = |q^2|\left[\frac{|p_0|}{4A^2}-\frac{\epsilon(p_0)}{2A}\right]\left[R_1\ln\frac{1}{m^2}+R_2\right]$$

where, in order to prove the cancellation of collinear singularities we need to prove that

$$R_1 \equiv S_4 - S_{3B} - \epsilon(p_0)\epsilon(B)S_{3F'}$$

is zero and where

$$R_2 \equiv \begin{cases} S_4 \ln\left|\frac{4p_0^2A}{B}\right| - S_{3B}\ln\left|\frac{4p_0^2A}{B}\right| - \epsilon(p_0)\epsilon(B)S_{3F'}\ln|4AB| & \text{in class 1} \\ S_4 \ln\left|\frac{4p_0Ac}{E}\right| - S_{3B}\ln\left|\frac{4p_0^2A}{B}\right| - \epsilon(p_0)\epsilon(B)S_{3F'}\ln|4AB| & \text{in class 4.} \end{cases}$$

According to the regions of support under consideration according to the above discussions, we have to prove that R_1 is zero for the cases ($p_0 > 0$ is fixed according to group (1) in Figure 3.13):

$$\begin{array}{llllll} \text{(i)} & p_0 > 0 & k_0 > 0 & B = k_0 + \nu - p_0 > 0 & k_0 + \nu > 0 \\ \text{(ii)} & p_0 > 0 & k_0 > 0 & B = k_0 + \nu - p_0 < 0 & k_0 + \nu > 0 \\ \text{(iii)} & p_0 > 0 & k_0 < 0 & B = k_0 + \nu - p_0 > 0 & k_0 + \nu < 0 \\ \text{(iv)} & p_0 > 0 & k_0 < 0 & B = k_0 + \nu - p_0 < 0 & k_0 + \nu < 0. \end{array}$$

According to the definitions of S_4, S_{3B} and $S_{3F'}$ we have for case (i):

$$\begin{aligned} & R_1[(\text{i}):\ p_0 > 0\ ;\ k_0 > 0\ ;\ B = k_0 + \nu - p_0 > 0\ ;\ k_0 + \nu > 0] \\ = \ & \frac{1}{e^{\beta(k_0-\mu)}+1}\left\{\frac{1}{e^{\beta p_0}-1}\left[\frac{1}{e^{\beta(k_0+\nu-\mu)}+1} - \frac{1}{e^{\beta(k_0+\nu-p_0-\mu)}+1}\right]\right. \\ & \left. + \frac{1}{e^{\beta(k_0+\nu-\mu)}+1}\left[1 - \frac{1}{e^{\beta(k_0+\nu-p_0-\mu)}+1}\right]\right\} = 0 \end{aligned}$$

where the latter expression in curly brackets can be algebraically shown to be zero and where the same expression in curly brackets can be written, for the purpose of discussions in Section 3.8.4, in the form:

$$\begin{aligned} A_1[(i)] \ &\equiv \ n_B(|p_0|)[n_F(x_{k+q}) - n_F(x_{k+q-p})] + n_F(x_{k+q})[1 - n_F(x_{k+q-p})] \\ &= \ n_F(x_{k+q})[1 - n_F(x_{k+q-p})][1 + n_B(|p_0|)] \\ &\quad -n_F(x_{k+q-p})[1 - n_F(x_{k+q})]n_B(|p_0|). \end{aligned} \tag{3.251}$$

According to the definitions of S_4, S_{3B} and $S_{3F'}$ we have for case (ii):

$$\begin{aligned} & R_1[(\text{ii}):\ p_0 > 0\ ;\ k_0 > 0\ ;\ B = k_0 + \nu - p_0 < 0\ ;\ k_0 + \nu > 0] \\ = \ & \frac{1}{e^{\beta(k_0-\mu)}+1}\left\{\frac{1}{e^{\beta p_0}-1}\left[\frac{1}{e^{\beta(k_0+\nu-\mu)}+1} + \frac{1}{e^{\beta(-k_0-\nu+p_0+\mu)}+1} - 1\right]\right. \\ & \left. + \frac{1}{e^{\beta(k_0+\nu-\mu)}+1}\frac{1}{e^{\beta(-k_0-\nu+p_0+\mu)}+1}\right\} = 0 \end{aligned}$$

where the latter expression in curly brackets can be algebraically shown to be zero and where the same expression in curly brackets can be written, for the purpose of discussions in

Section 3.8.4, in the form:

$$\begin{aligned} A_2[(ii)] &\equiv n_{\rm B}(|p_0|)[n_{\rm F}(x_{k+q}) + n_{\rm F}(x_{k+q-p}) - 1] + n_{\rm F}(x_{k+q})n_{\rm F}(x_{k+q-p}) \\ &= n_{\rm F}(x_{k+q})n_{\rm F}(x_{k+q-p})[1 + n_{\rm B}(|p_0|)] \\ &\quad -n_{\rm B}(|p_0|)[1 - n_{\rm F}(x_{k+q})][1 - n_{\rm F}(x_{k+q-p})] \end{aligned} \tag{3.252}$$

Similarly one can show that $R_1 = 0$ for cases (iii) and (iv). Thus we have proven that collinear singularities cancel for the group (1) of contributions in Figure 3.13.

The fact that $R_1 = 0$ can also be used to prove the cancellation of some kinematical factors: Substituting S_4 by $S_{3\rm B} + \epsilon(p_0)\epsilon(B)S_{3\rm F'}$ in class 1 and $S_{3\rm B}$ by $S_4 + \epsilon(p_0)\epsilon(B)S_{3\rm F'}$ in class 4 one obtains for R_2:

$$R_2 \equiv \begin{cases} -\epsilon(p_0)\epsilon(B)S_{3\rm F'} \ln\left|\dfrac{B^2}{p_0^2}\right| & \text{in class 1} \\ S_4 \ln|\bar{B}_4| - S_{3\rm B}\ln|\bar{B}_{\rm B}| - \epsilon(p_0)\epsilon(B)S_{3\rm F'}\ln|\bar{B}_{\rm F'}| & \text{in class 4} \end{cases}$$

where

$$\bar{B}_4 = \begin{cases} 1 & \text{in class 1} \\ \dfrac{Bc}{Ep_0} & \text{in class 4} \end{cases}$$

$$\bar{B}_{\rm B} = 1 \qquad \bar{B}_{\rm F'} = \frac{B^2}{p_0^2}$$

in agreement with eqs. (D.27) and (D.26) and Table D.4.

3.8.3 A Second Subtler Example

As our final example we consider the cancellation of collinear singularities according to the group (4) of contributions in Figure 3.13 which is subtler in that one cancels four-particle contributions with $p_0 < 0$ against three-particle contributions with $p_0 > 0$ as indicated in Figure 3.13. According to group (4) we consider t^{-1} type singularities. These arise from both t^{-1} type and $s^{-1}t^{-1}$ type terms. Here we shall present only the example of the cancellation of singularities arising from the t^{-1} part of $s^{-1}t^{-1}$ type terms as explained in the following.

In the following we again discuss cancellations in the context of expressions for the sum over all polarizatifilelons of the virtual photon, i.e., eqs. (D.17) and (D.23)–(D.25). According to the results of angular integrations in (D.16) and Table D.3 the $s^{-1}t^{-1}$ type term for four-particle processes is associated with A_4 which specifies the term proportional to $\ln|A_4|$ to be considered in eq. (D.17). According to Table D.3, A_4 is proportional to either m^0, m^{-2} or

m^{-4} depending on the class for which it is defined. This fact has its roots in the fact that the s^{-1} part of the $s^{-1}t^{-1}$ type term associated with A_4 contributes a factor of m^{-2} to A_4 in classes 1,2,3 and 4 since z_U is, according to Table D.1, the upper limit of the z integration in the latter classes and $s(z_U)\ \alpha\ m^2$ according to the second paragraph of Section D.3. The t^{-1} part of the $s^{-1}t^{-1}$ type term also contributes a factor of m^{-2} to A_4 in classes 1,3,5 and 7 since z'_U is, according to Table D.1, the upper limit of the z' integration in the latter classes and $t(z'_U)\ \alpha\ m^2$ according to the second paragraph of Section D.3. At present we consider only the singularities due to the t^{-1} part of the $s^{-1}t^{-1}$ type term according to the group (4) of contributions in Figure 3.13. The singularities due to the s^{-1} part of the $s^{-1}t^{-1}$ type term cancel separately according to a group of contributions associated with s in Figure 3.13 and their cancellation is not discussed here.

In accordance with the latter discussion we separate only the singular terms due to the t^{-1} part of the $s^{-1}t^{-1}$ type term:

$$\ln|A_4| = \begin{cases} \ln\left|\dfrac{p_0^4q^4}{m^2AaBb}\right| + \ln\dfrac{1}{m^2} & \text{in class 1} \\ \ln\left|\dfrac{p_0^4q^4}{m^2AbcD}\right| + \ln\dfrac{1}{m^2} & \text{in class 3} \\ \ln\left|\dfrac{p_0^2q^2D}{BbC}\right| + \ln\dfrac{1}{m^2} & \text{in class 5} \\ \ln\left|\dfrac{p_0^2q^2a}{bCc}\right| + \ln\dfrac{1}{m^2} & \text{in class 7.} \end{cases} \tag{3.253}$$

The latter singularities are to be cancelled by singularities due to the t_B^{-1} part of the $s_B^{-1}t_B^{-1}$ type term [associated, according to the results in (D.21), with the term proportional to $\ln|A_B|$ in eq. (D.23)] and singularities due to the t_F^{-1} part of the $t_F^{-1}[(k'-p)^2]^{-1}$ type term [associated, according to the results in (D.21), with the term proportional to $\ln|A_F|$ in eq. (D.24)]. For this purpose we separate the singular terms as before:

$$\ln|A_B| = \ln\left|\frac{p_0^4q^4}{m^2AaBb}\right| + \ln\frac{1}{m^2} \tag{3.254}$$

$$\ln|A_F| = \ln\left|\frac{q^2p_0^2b}{aDd}\right| + \ln\frac{1}{m^2} \tag{3.255}$$

where it is to be noted that we do not separate the factor m^{-2} due to the s_B^{-1} part of

$\ln|A_B|$ since the latter singularity will cancel separately according to a group of contributions associated with s in Figure 3.13.

The three-particle contributions as given as given in eqs. (3.254) and (3.255) contribute to singularities everywhere where three-particle processes have their support as indicated in Figure D.2. This seems to lead to a complication since the singularities stemming from the four-particle contribution $\ln|A_4|$ in (3.253) have support in classes 1,3,5 and 7 but, as may be seen from Figure D.1, classes 5 and 7 lie in regions which do not have any overlap with the regions of support for three-particle processes shown in Figure D.2. Thus it appears that the possibility for the cancellation of singularities between four- and three-particle processes exists only in regions associated with classes 1 and 3 for four-particle processes while in regions associated with classes 5 and 7 singularities will remain.

The resolution to this potential problem is obtained by crossing the line between $p_0 < 0$ and $p_0 > 0$ as shown in Figure 3.13 when comparing four- and three-particle contributions associated with the group (4) of contributions. From Figure D.1 it can be seen that, when we turn the whole diagram for four-particle processes through one hundred and eighty degrees around the axis defined by $p_0 = 0$, all the regions of support for classes 1,3,5 and 7 overlap exactly with the regions of support for three-particle processes shown in Figure D.2. Thus, in the example under consideration, we shall cancel singularities from four-particle contributions at a negative value of p_0 with singularities from three-particle contributions with the same magnitude of p_0 but opposite sign of p_0.

Adding up the contributions in (3.253),(3.254) and (3.255) and suppressing common factors in their coefficients as they appear in eqs. (D.17),(D.23) and (D.25), one obtains

$$\begin{aligned} F_1 &\equiv S_4 \ln|A_4| - S_{3B} \ln|A_B| - \epsilon(p_0)\epsilon(b) S_{3F} \ln|A_F| \\ &\equiv F_2 \ln\frac{1}{m^2} + F_3 \end{aligned}$$

where, in order to prove the cancellation of collinear singularities due to the t^{-1} part of $s^{-1}t^{-1}$ type terms, we need to prove that

$$F_2 \equiv S_4 - S_{3B} - \epsilon(p_0)\epsilon(b) S_{3F} \tag{3.256}$$

is zero and where F_3 contains the remaining terms of F_1 which we need not consider further for the example under consideration. According to the discussions in the previous two paragraphs, the support of all these terms overlap exactly if we view the term containing S_4 at a

$p_0 < 0$ value while viewing the terms containing S_{3B} and S_{3F} at a $p_0 > 0$ value but with $|p_0|$ the same. Another requirement for the cancellation of singularities will be that one compare terms at a fixed value of K as opposed to a fixed value of k_0. The implementation of the latter prescriptions will become clear in the following where we prove that F_2 is zero.

The exact expression for F_2 depends on the signs of $k_0, k_0 + \nu, k_0 + \nu - p_0, p_0$ and $b = (2K - p_0 - \nu)/2 = k_0 - p_0$. In consequence we must prove that F_2 is zero for each of the regions labelled (a),(b) and (c) in Figures 3.14 and 3.15. The signs of the relevant quantities in each of these regions are given in Table 3.2.

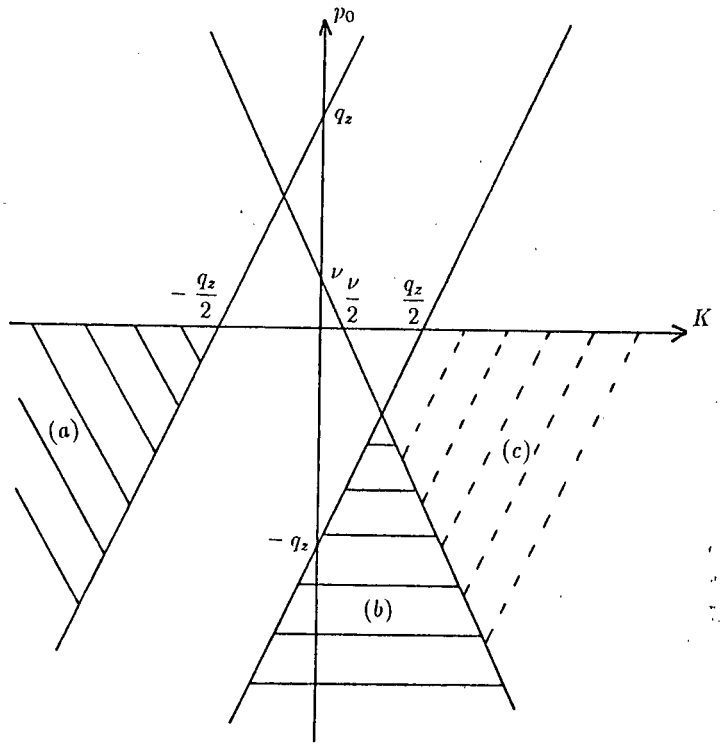

Figure 3.14: Regions with $p_0 < 0$ for four-particle processes considered according to our discussions on the group (4) of contributions shown in Figure 3.13

In region (a) of Figure 3.14 one has according to the definition of S_4 and Table 3.2:

$$\begin{aligned} S_4 &= \left[1 - \frac{1}{e^{\beta(-k_0+\mu)}+1}\right] \frac{1}{e^{\beta(-k_0-\nu+p_0+\mu)}+1} \frac{1}{e^{-\beta p_0}-1} \\ &= \left[1 - \frac{1}{e^{\beta(-K+(\nu-p_0)/2+\mu)}+1}\right] \frac{1}{e^{\beta(-K-(\nu-p_0)/2+\mu)}+1} \frac{1}{e^{-\beta p_0}-1} \\ &= \left[1 - \frac{1}{e^{\beta(-K+(\nu+|p_0|)/2+\mu)}+1}\right] \frac{1}{e^{\beta(-K-(\nu+|p_0|)/2+\mu)}+1} \frac{1}{e^{\beta|p_0|}-1} \end{aligned}$$

where we first transformed from k_0 to K according to eq. (D.1) and, in the final step, wrote

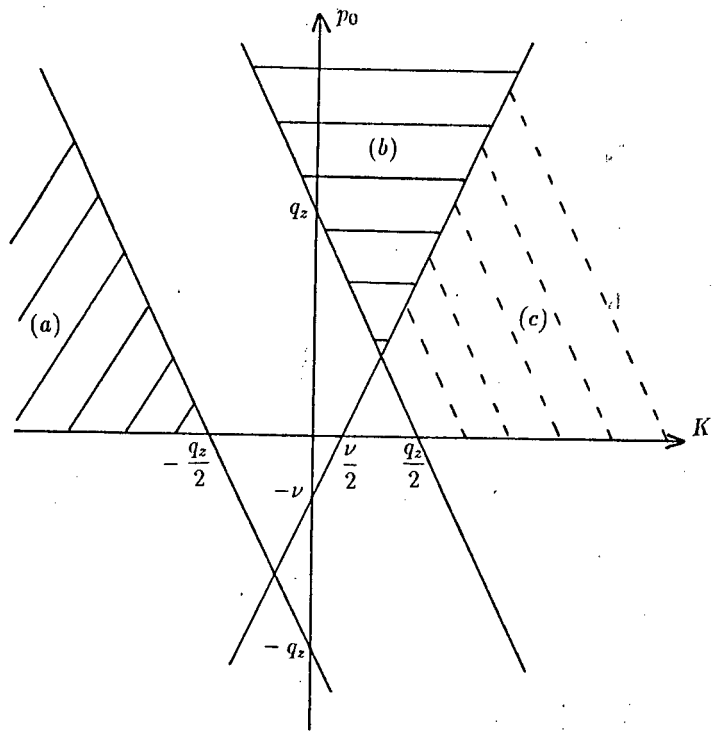

Figure 3.15: Regions with $p_0 > 0$ for three-particle processes considered according to our discussions on the group (4) of contributions shown in Figure 3.13

p_0 as $-|p_0|$ for reasons to be explained shortly.

In region (a) of Figure 3.15 one has according to the definitions of S_{3B} and S_{3F} and Table 3.2:

$$
\begin{aligned}
-S_{3B} &= -\left[1-\frac{1}{e^{\beta(-K+(\nu-|p_0|)/2+\mu)}+1}\right]\frac{1}{e^{\beta(-K-(\nu+|p_0|)/2+\mu)}+1}\left[\frac{1}{2}+\frac{1}{e^{\beta|p_0|}-1}\right] \\
-\epsilon(p_0)\epsilon(b)S_{3F} &= \left[1-\frac{1}{e^{\beta(-K+(\nu-|p_0|)/2+\mu)}+1}\right]\frac{1}{e^{\beta(-K-(\nu+|p_0|)/2+\mu)}+1} \\
&\quad \times\left[\frac{1}{2}-\frac{1}{e^{\beta(-K+(\nu+|p_0|)/2+\mu)}+1}\right]
\end{aligned}
$$

where we wrote down only the final step in each case since intermediate steps are similar to those shown for S_4.

By directly adding up the latter final expressions for each of the three terms of F_2 in eq. (3.256), one obtains zero after some algebra. Thereby the cancellation of collinear singularities for the case under consideration is proven.

It is to be noted that, after transforming from k_0 to K, we added the first term in eq. (3.256) evaluated at a value of $p_0 < 0$ to the second and third terms in eq. (3.256) evaluated

Table 3.2: Signs of quantities in regions labelled (a),(b) and (c) in Figures 3.14 and 3.15. These signs are used in the discussions on the cancellation of collinear singularities.

Process:	Four-particle			Three-particle		
Figure number:	3.14			3.15		
Label of region:	(a)	(b)	(c)	(a)	(b)	(c)
Sign of						
p_0	<0	<0	<0	>0	>0	>0
k_0	<0	<0	>0	<0	>0	>0
$k_0+\nu$		n.a.		<0	>0	>0
$k_0+\nu-p_0$	<0	>0	>0		n.a.	
$b=k_0-p_0$		n.a.		<0	<0	>0

at the same value of $|p_0|$ but with $p_0 > 0$. For the latter reason we expressed the latter three terms in terms of $\mp|p_0|$ and not p_0 in order to make them directly comparable for addition. The consequence of the latter treatment, for the case under consideration, is that one adds the four- and three-particle terms at the same value of K (not the same value of k_0) and $|p_0|$ with p_0 having opposite signs between four- and three-particle terms. Had we not transformed from k_0 to K but attempted to prove that F_2 is zero when we perform the addition of four- and three-particle terms at the same value of k_0 (not the same value of K) and $|p_0|$ with p_0 having, as before, opposite signs between four- and three-particle terms, we would have failed.

The proof that F_2 is also zero for the other regions (b) and (c) in Figures 3.14 and 3.15 is similar. Thereby the proof that collinear singularities due to the t^{-1} part of $s^{-1}t^{-1}$ type terms cancel according to the group (4) of contributions shown in Figure 3.13 can be completed. Similarly all the collinear singularities stemming from the t^{-1} part of terms cancel according to the groups (2) and (4) of contributions shown in Figure 3.13.

It is to be noted that, in the case of the groups (1) and (3) of contributions in Figure 3.13 (associated with the s^{-1} part of terms), it is all the same, as far as the cancellation of collinear

singularities is concerned, whether one transforms from k_0 to K or not. The reason for this is that, in these cases, p_0 has the same sign in the four- and three-particle terms which cancel each other. An example of this was discussed in Section 3.8.2 where the cancellation of singularities was proven without transforming from k_0 to K. Thus, as opposed to the groups (2) and (4) in Figure 3.13, collinear singularities cancel in the cases of groups (1) and (3) when one adds four- and three-particle terms at the same value of k_0 (and for that matter the same value of K) and $|p_0|$ with p_0 having the same sign in four- and three-particle terms.

The cancellation of collinear singularities leads to the final expressions for four-particle processes given by eqs. (D.19) and (D.20) and for three-particle processes given by eqs. (D.27) and (D.28). Due to the accompanying cancellation of kinematical factors, these expressions are now also devoid of infrared ($p_0 \to 0$) singularities.

3.8.4 The Principle of Detailed Balance Underlying the Cancellation of Collinear Singularities

In Section 3.8.2 we discussed examples of the cancellation of collinear singularities. In this section we explain how the principle of detailed balance existing for thermal equilibrium underlies these cancellations. For this purpose we consider the processes depicted in Figure 3.16 which are examples of some of the $\mathcal{O}(\alpha_S)$ processes occurring in the heat bath of quarks and gluons.

In the figure labelled (a) we have gluon emission from a quark, i.e.,

$$k_0 > 0 \qquad p_0 > 0 \qquad k_0 - p_0 > 0. \tag{3.257}$$

The inverse reaction, namely gluon absorption by a quark, is depicted in Figure 3.16(b). The four-momenta in (b) are equal to those in (a) and therefore also satisfy the relations in (3.257). The rates at which the processes in (a) and (b) occur are proportional to

$$|M_{(a)}|^2 n_F(x_k)[1 - n_F(x_{k-p})][1 + n_B(|p_0|)] \tag{3.258}$$

and

$$|M_{(b)}|^2 n_F(x_{k-p}) n_B(|p_0|)[1 - n_F(x_k)], \tag{3.259}$$

respectively, where the accompanying thermal distribution-, Pauli-blocking- and stimulated emission factors have also been written down.

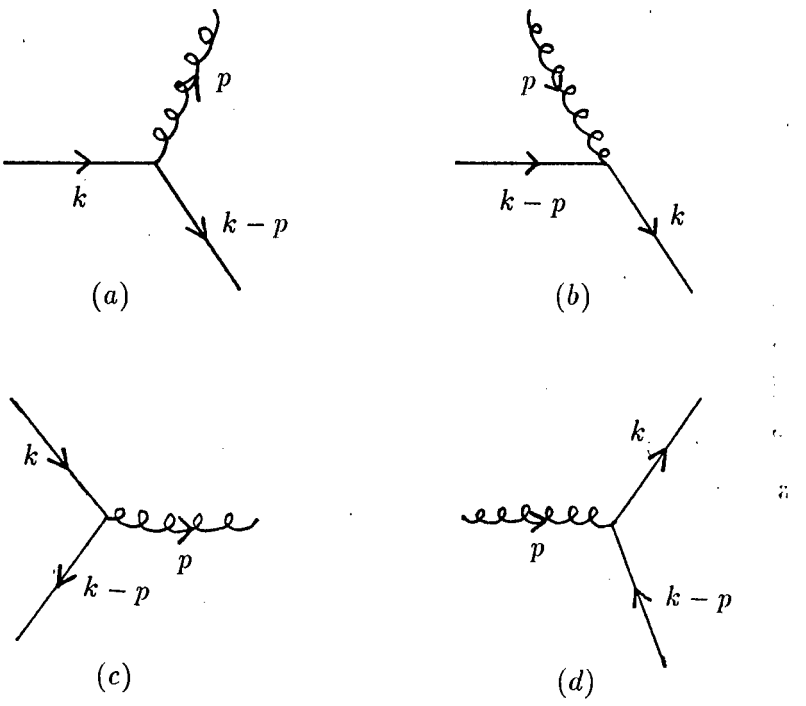

Figure 3.16: Examples of some of the $\mathcal{O}(\alpha_S)$ processes occurring in the heat bath of quarks and gluons. The reactions labelled (b) and (d) are the inverse of the reactions labelled (a) and (c), repectively.

The principle of detailed balance requires that the rate at which reaction (a) takes place must be equal to the rate at which reaction (b) takes place. This requires equality between the expressions in (3.258) and (3.259). Since the respective matrix elements squared in (3.258) and (3.259) are equal, the principle of detailed balance requires that

$$n_F(x_k)[1 - n_F(x_{k-p})][1 + n_B(|p_0|)] = n_F(x_{k-p})n_B(|p_0|)[1 - n_F(x_k)]. \tag{3.260}$$

By observing that the replacement of k by $k + q$ in eq. (3.260) is equivalent to the requirement that the expression in eq. (3.251) is zero, we see that the condition for the cancellation of collinear singularities (embodied by $A_1[(i)] = 0$) is the same as the condition derived from the principle of detailed balance.

As another example of how the principle of detailed balance underlies the cancellation of collinear singularities, we consider Figure 3.16(c) which depicts quark-antiquark pair annihilation into a gluon, i.e.,

$$k_0 > 0 \qquad k_0 - p_0 < 0 \qquad p_0 > 0. \tag{3.261}$$

The inverse reaction, namely quark-antiquark pair creation by a gluon, is depicted in Figure (d). The four-momenta in (d) are equal to those in (c) and therefore also satisfy the relations in (3.261). The rates at which the processes in (c) and (d) occur are proportional to

$$|M_{(c)}|^2 n_{\rm F}(x_k) n_{\rm F}(x_{k-p})[1 + n_{\rm B}(|p_0|)] \tag{3.262}$$

and

$$|M_{(d)}|^2 n_{\rm B}(|p_0|)[1 - n_{\rm F}(x_k)][1 - n_{\rm F}(x_{k-p})], \tag{3.263}$$

respectively, where, due to $k_0 > 0$, $k_0 - p_0 < 0$ and the definition of the thermal distribution function for fermions in eqs. (3.1) and (3.2), one has for example

$$\begin{aligned} n_{\rm F}(x_k) &= \frac{1}{e^{\beta(k_0-\mu)}+1} \\ n_{\rm F}(x_{k-p}) &= \frac{1}{e^{\beta(|k_0-p_0|+\mu)}+1}. \end{aligned}$$

The principle of detailed balance requires that the rate at which reaction (c) takes place must be equal to the rate at which reaction (d) takes place. This requires equality between the expressions in (3.262) and (3.263). Since the respective matrix elements squared in (3.262) and (3.263) are equal, the principle of detailed balance requires that

$$n_{\rm F}(x_k) n_{\rm F}(x_{k-p})[1 + n_{\rm B}(|p_0|)] = n_{\rm B}(|p_0|)[1 - n_{\rm F}(x_k)][1 - n_{\rm F}(x_{k-p})]. \tag{3.264}$$

By observing that the replacement of k by $k + q$ in eq. (3.264) is equivalent to the requirement that the expression in eq. (3.252) is zero, we see that, in this case too, the condition for the cancellation of collinear singularities (embodied by $A_2[(ii)] = 0$) is the same as the condition derived from the principle of detailed balance.

3.9 The Cancellation of Ultraviolet Divergences

The final expressions for three-particle processes in eqs. (D.27) and (D.28) contain terms which give rise to ultraviolet (UV) divergences in the $p_0 \to \pm\infty$ limits encountered when performing the K, p_0 integrations. These divergences cancel when contributions at a positive and negative value of p_0 (but with $|p_0|$ fixed) are added. In this section we discuss explicit examples of such cancellations.

As an example, we discuss cancellations in the context of the expression in eq. (D.27) and restrict our attention to the quark side of the K, p_0 integration region, i.e., $K \geq (q_z - p_0)/2$

in Figure D.2. By transforming from the K variable to the k_0 variable according to eq. (D.1), the quark side of the k_0, p_0 integration region becomes that shown in Figure 3.17. By transforming from p_0 to $-p_0$ in the $\int_{-\infty}^{0}$ part of the $\int_{-\infty}^{\infty} dp_0$ integration and adding the result to the $\int_{0}^{\infty}$ part, the quark side of the k_0, p_0 integration region becomes that $[(a)+(b)]$ shown in Figure 3.18.

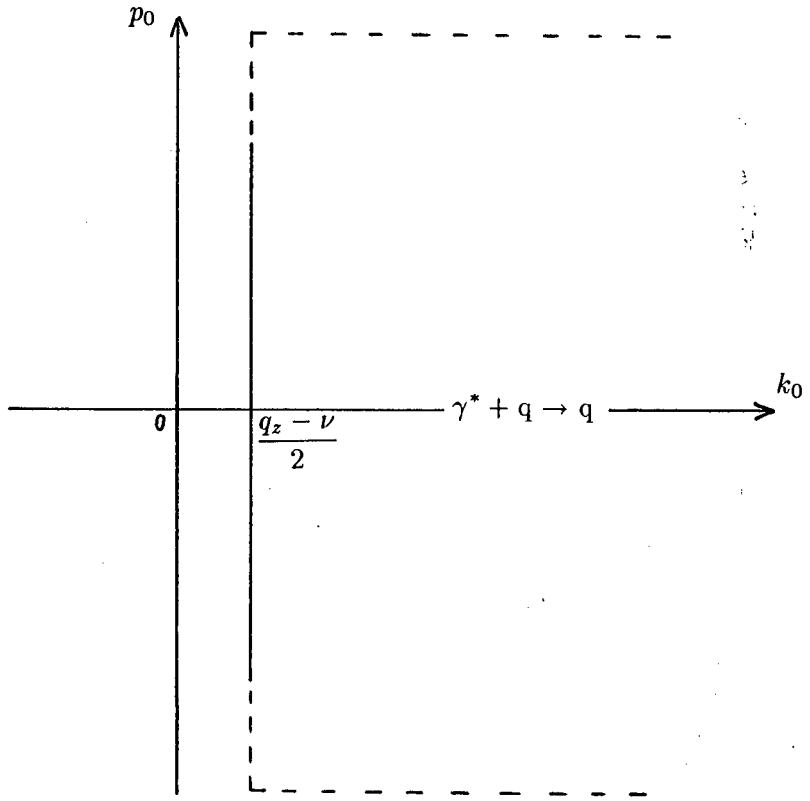

Figure 3.17: The quark side of the k_0, p_0 integration region obtained after transforming back from K to k_0 on the quark side of the K, p_0 integration region in Figure D.2.

It is sufficient to prove the cancellation of UV divergences in region (a) of Figure 3.18. In region (b) of Figure 3.18 it is only possible to reach the $p_0 \to \infty$ limit by letting $k_0 \to \infty$ too, but then any UV divergence will be exponentially suppressed by the overall factor $n_F(x_k)$ appearing in the statistical factors in eq. (D.27). By introducing the line $p_0 = k_0 + (\nu + q_z)/2$ which separate regions (a) and (b) in Figure 3.18, the discussion about the cancellation of UV divergences can be simplified since, for region (a), the absolute value signs appearing in the integrand in eq. (D.27) can then be removed.

As a first example we show how the UV divergence in the terms proportional to S_{3B}

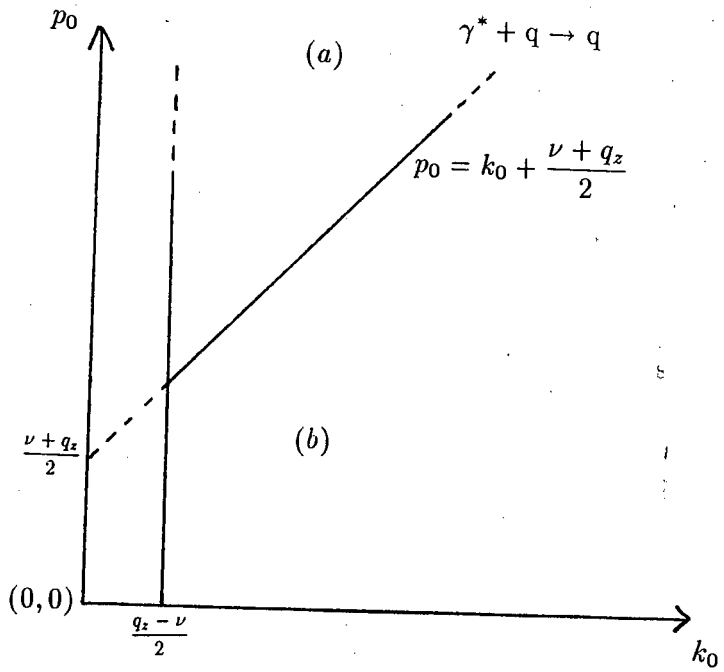

Figure 3.18: The k_0, p_0 integration region $[(a) + (b)]$ obtained after transforming from p_0 to $-p_0$ in the $p_0 < 0$ part of the integration region shown in Figure 3.17.

cancels against UV divergences in terms proportional to S_{3F} and $S_{3F'}$ in eq. (D.27). After the transformations explained in the previous paragraph, the contribution of terms proportional to S_{3B} in eq. (D.27) is as follows *in region* (a):

$$I^{3B} = \frac{1}{4\pi^3 q_z}\int_{q_z}^{\infty} dp_0 \int_{(q_z-\nu)/2}^{p_0-(\nu+q_z)/2} dk_0 \frac{-2p_0}{e^{\beta(k_0-\mu)}+1}\left(1-\frac{1}{e^{\beta(k_0'-\mu)}+1}\right) \times \left(\frac{1}{2}+\frac{1}{e^{\beta p_0}-1}\right)\left[1+\frac{k_0}{k_0'}+\frac{k_0'}{k_0}+\frac{q^2}{2}\left(\frac{1}{k_0^2}+\frac{1}{k_0'^2}\right)\right]$$

where $k_0' = k_0 + \nu$. The term proportional to

$$-2p_0\left(1-\frac{1}{e^{\beta(k_0'-\mu)}+1}\right)\frac{1}{2}\left[1+\frac{k_0}{k_0'}+\frac{k_0'}{k_0}+\frac{q^2}{2}\left(\frac{1}{k_0^2}+\frac{1}{k_0'^2}\right)\right] \tag{3.265}$$

gives rise to an UV divergence when $p_0 \to \infty$ in the p_0 integration.

The contribution of terms proportional to S_{3F} in eq. (D.27) is as follows *in region* (a):

$$I^{3F} = I_a^{3F} + I_b^{3F}$$

where I_a^{3F} and I_b^{3F} originate from the $\int_{-\infty}^{0}$ and $\int_0^{\infty}$ parts of the $\int_{-\infty}^{\infty} dp_0$ integration, respectively, and where

$$I_{a\atop b}^{3F} = \frac{1}{4\pi^3 q_z}\int_{q_z}^{\infty} dp_0 \int_{(q_z-\nu)/2}^{p_0-(\nu+q_z)/2} dk_0 \frac{1}{e^{\beta(k_0-\mu)}+1}\left(1-\frac{1}{e^{\beta(k_0+\nu-\mu)}+1}\right)$$

$$\times\left(\frac{1}{2}-\frac{1}{e^{\beta(\pm k_0+p_0\mp\mu)}+1}\right)\left\{\frac{-q^2}{2p_0}\ln\left[\frac{(k_0\pm p_0)^2}{(k_0\pm p_0)^2+(k_0\pm p_0)\nu+q^2/4}\right]\right.$$
$$\pm q^2\left(\frac{\mp p_0}{4k_0^2}-\frac{1}{2k_0}\right)\ln\frac{(k_0\pm p_0)^2}{p_0^2}\mp\frac{q^2}{q_z}\left[\frac{3}{4}+\frac{(2k_0+\nu)(2k_0+\nu\pm 2p_0)}{4q_z^2}\right]$$
$$\left.\times\ln\frac{(q_z+\nu)(2k_0\pm 2p_0-q_z+\nu)}{(q_z-\nu)(2k_0\pm 2p_0+q_z+\nu)}+(p_0\pm k_0)\left(\frac{1}{2}+\frac{{k_0'}^2-k_0^2}{q_z^2}+\frac{q^2}{2k_0^2}+\frac{k_0'}{k_0}\right)\right\}.$$

The contribution of terms proportional to $S_{3F'}$ in eq. (D.27) is as follows *in region* (a):

$$I^{3F'}=I_a^{3F'}+I_b^{3F'}$$

where $I_a^{3F'}$ and $I_b^{3F'}$ originate from the $\int_{-\infty}^{0}$ and $\int_0^{\infty}$ parts of the $\int_{-\infty}^{\infty}dp_0$ integration, respectively, and where

$$I_{\substack{a\\b}}^{3F'} = \frac{1}{4\pi^3 q_z}\int_{q_z}^{\infty}dp_0\int_{(q_z-\nu)/2}^{p_0-(\nu+q_z)/2}dk_0\frac{1}{e^{\beta(k_0-\mu)}+1}\left(1-\frac{1}{e^{\beta(k_0+\nu-\mu)}+1}\right)$$
$$\times\left(\frac{1}{2}-\frac{1}{e^{\beta(\pm k_0\pm\nu+p_0\mp\mu)}+1}\right)\left\{\frac{-q^2}{2p_0}\ln\left[\frac{(k_0+\nu\pm p_0)^2}{(k_0\pm p_0)^2+(k_0\pm p_0)\nu+q^2/4}\right]\right.$$
$$+q^2\left(\frac{\mp p_0}{4{k_0'}^2}-\frac{1}{2k_0'}\right)\ln\frac{(k_0+\nu\pm p_0)^2}{p_0^2}\mp\frac{q^2}{q_z}\left[\frac{3}{4}+\frac{(2k_0+\nu)(2k_0+\nu\pm 2p_0)}{4q_z^2}\right]$$
$$\left.\times\ln\frac{(q_z+\nu)(2k_0\pm 2p_0+q_z+\nu)}{(q_z-\nu)(2k_0\pm 2p_0-q_z+\nu)}+(p_0\pm k_0\pm\nu)\left(\frac{1}{2}-\frac{{k_0'}^2-k_0^2}{q_z^2}+\frac{q^2}{2{k_0'}^2}+\frac{k_0}{k_0'}\right)\right\}.$$

The UV divergence from I^{3B} mentioned at line (3.265) cancels against similar UV divergent terms in I^{3F} and $I^{3F'}$ which are not proportional to ln functions. The terms proportional to ln functions in I^{3F} and $I^{3F'}$, however, also contain UV divergences but they cancel amongst themselves since I^{3B} does not contain terms proportional to ln functions. Examples of the latter type of cancellations are discussed after the following discussion on the cancellation of divergences from terms which are not proportional to ln functions.

By adding the coefficients of the common factor,

$$\frac{1}{4\pi^3 q_z}\frac{1}{e^{\beta(k_0-\mu)}+1}\left(1-\frac{1}{e^{\beta(k_0'-\mu)}+1}\right)\frac{1}{2}p_0,$$

present in terms not proportional to ln functions in I^{3B}, I_a^{3F},$I_a^{3F'}$,I_b^{3F} and $I_b^{3F'}$, in that order, one obtains

$$C_1 \equiv \left(-2-\frac{2k_0}{k_0'}-\frac{2k_0'}{k_0}-\frac{q^2}{k_0^2}-\frac{q^2}{{k_0'}^2}\right)+\left(\frac{1}{2}+\frac{{k_0'}^2-k_0^2}{q_z^2}+\frac{q^2}{2k_0^2}+\frac{k_0'}{k_0}\right)$$
$$+\left(\frac{1}{2}-\frac{{k_0'}^2-k_0^2}{q_z^2}+\frac{q^2}{2{k_0'}^2}+\frac{k_0}{k_0'}\right)+\left(\frac{1}{2}+\frac{{k_0'}^2-k_0^2}{q_z^2}+\frac{q^2}{2k_0^2}+\frac{k_0'}{k_0}\right)$$

$$+\left(\frac{1}{2}-\frac{k_0'^2-k_0^2}{q_z^2}+\frac{q^2}{2k_0'^2}+\frac{k_0}{k_0'}\right)$$
$$= 0.$$

Thereby we have proven the cancellation of UV divergences in terms not proportional to ln functions.

It is to be noted that the cancellation of the above terms have been proven for region (a) in Figure 3.18. In subregions of region (b) in Figure 3.18 these terms have relative sign differences due to the absolute value signs in the original eq. (D.27) which leads to their non-cancellation in parts of region (b) so that these terms cannot be disregarded entirely in eq. (D.27). This observation, however, has no consequence on the UV finiteness of our expressions since, due to the reason given in the latter half of the second paragraph of this section, it is unnecessary to prove their cancellation in region (b).

Next we consider the cancellation of UV divergences in terms proportional to ln functions appearing only in $I^{3\mathrm{F}}$ and $I^{3\mathrm{F}'}$. By adding the coefficients of the common factor,

$$\frac{1}{4\pi^3 q_z}\frac{1}{e^{\beta(k_0-\mu)}+1}\left(1-\frac{1}{e^{\beta(k_0'-\mu)}+1}\right)\frac{1}{2},$$

present in terms proportional to ln functions in $I_a^{3\mathrm{F}}$,$I_a^{3\mathrm{F}'}$,$I_b^{3\mathrm{F}}$ and $I_b^{3\mathrm{F}'}$, in that order, one obtains the following UV divergent terms:

$$\begin{aligned}
C_2 \equiv\ & \left\{q^2\left(\frac{-p_0}{4k_0^2}-\frac{1}{2k_0}\right)\ln\frac{(k_0+p_0)^2}{p_0^2}-\frac{q^2}{q_z}\left[\frac{3}{4}+\frac{(2k_0+\nu)(2k_0+\nu+2p_0)}{4q_z^2}\right]\right.\\
&\left.\times\ln\frac{(q_z+\nu)(2k_0+2p_0-q_z+\nu)}{(q_z-\nu)(2k_0+2p_0+q_z+\nu)}\right\}+\left\{q^2\left(\frac{-p_0}{4k_0'^2}-\frac{1}{2k_0'}\right)\ln\frac{(k_0+\nu+p_0)^2}{p_0^2}\right.\\
&\left.+\frac{q^2}{q_z}\left[\frac{3}{4}+\frac{(2k_0+\nu)(2k_0+\nu+2p_0)}{4q_z^2}\right]\ln\frac{(q_z+\nu)(2k_0+2p_0+q_z+\nu)}{(q_z-\nu)(2k_0+2p_0-q_z+\nu)}\right\}\\
&+\left\{-q^2\left(\frac{p_0}{4k_0^2}-\frac{1}{2k_0}\right)\ln\frac{(k_0-p_0)^2}{p_0^2}+\frac{q^2}{q_z}\left[\frac{3}{4}+\frac{(2k_0+\nu)(2k_0+\nu-2p_0)}{4q_z^2}\right]\right.\\
&\left.\times\ln\frac{(q_z+\nu)(2k_0-2p_0-q_z+\nu)}{(q_z-\nu)(2k_0-2p_0+q_z+\nu)}\right\}+\left\{-q^2\left(\frac{p_0}{4k_0'^2}-\frac{1}{2k_0'}\right)\ln\frac{(k_0+\nu-p_0)^2}{p_0^2}\right.\\
&\left.-\frac{q^2}{q_z}\left[\frac{3}{4}+\frac{(2k_0+\nu)(2k_0+\nu-2p_0)}{4q_z^2}\right]\ln\frac{(q_z+\nu)(2k_0-2p_0+q_z+\nu)}{(q_z-\nu)(2k_0-2p_0-q_z+\nu)}\right\}
\end{aligned}$$

where

$$\lim_{p_0\to\infty}\ln\frac{(k_0\pm p_0)^2}{p_0^2} = \lim_{p_0\to\infty}\left(\pm 2\frac{k_0}{p_0}-\frac{k_0^2}{p_0^2}+\cdots\right)$$

$$\lim_{p_0\to\infty} \ln \frac{(k_0+\nu\pm p_0)^2}{p_0^2} = \lim_{p_0\to\infty}\left(\pm 2\frac{k_0+\nu}{p_0} - \frac{(k_0+\nu)^2}{p_0^2} + \cdots\right)$$
$$\lim_{p_0\to\infty} \ln \frac{2k_0\pm 2p_0 - q_z + \nu}{2k_0\pm 2p_0 + q_z + \nu} = \lim_{p_0\to\infty}\left(\mp\frac{q_z}{p_0} + \frac{2q_z(2k_0+\nu)}{4p_0^2} + \cdots\right).$$

By inserting the expressions for the latter limits into the expression for C_2, one notices terms proportional to p_0^{-1}, p_0^0 and p_0 in C_2 which give rise to UV divergences under the $\int_{q_z}^{\infty} dp_0$ integral. Each of these types of divergences cancel separately amongst themselves in the expression for C_2.

As was mentioned at the beginning of the second paragraph of this section, we discussed the cancellation of UV divergences for the example of the quark side of the integration region and in the context of the expression in eq. (D.27). The cancellation of UV divergences can also be shown for the antiquark side of the integration region and in the context of the expression in eq. (D.28).

Chapter 4

Numerical Calculation of the Structure Functions of the Nucleon in the Statistical Model

4.1 Introduction

In this chapter we present the results from the numerical calculations of the structure functions F_2 and R [defined in eqs. (2.10) and (2.11)]. So far we have considered deep inelastic scattering of leptons off a heat bath of quarks and gluons to first order in the strong coupling constant α_S. The numerical calculation was performed in two parts. The numerical calculations of the zeroth order in α_S and $\mathcal{O}(\alpha_S)$ contributions are discussed in Sections 4.2 and 4.3, respectively. Results from the total calculation, i.e., zeroth order plus $\mathcal{O}(\alpha_S)$ results are presented in Section 4.3.3.

We chose to fit to a plot of F_2 versus x, where

$$x = \frac{Q^2}{2M\nu},$$

which is determined by parton distributions which reproduce a wide range of experimental data. Such parton distributions were published in 1990 by Kwiecinski et al. in ref. [77]. They decide on a parametrization of the parton distributions at $Q_0^2 \equiv -q^2 = 4$ GeV^2 and evolve up in Q^2 in order to test their parton distributions against experimental data. According to their so-called B_- fit, one obtains:

$$x[u_v(x) + d_v(x)] = 0.38x^{0.27}(1-x)^{3.93}(1 + 9.9x^{1/2} + 17.7x) \quad (4.1)$$

$$xd_v(x) = 1.50x^{0.61}(1-x)^{4.68}(1 + 1.08x^{1/2}) \quad (4.2)$$

$$\begin{aligned} xS &\equiv 2x(\bar{u}+\bar{d}+\bar{s}) \\ &= 0.0168x^{-1/2}(1+27.4x^{1/2}+263x)(1-x)^{9.9} \end{aligned} \tag{4.3}$$

where the sea quark distributions are related by

$$u_s = \bar{u}_s = d_s = \bar{d}_s = 2s_s = 2\bar{s}_s.$$

We express F_2 for a proton in terms of the latter parton distributions as follows:

$$\begin{aligned} F_2 &= \left(\frac{2}{3}\right)^2 x[u_v+u_s+\bar{u}_s] + \left(\frac{1}{3}\right)^2 x[d_v+d_s+\bar{d}_s] + \left(\frac{1}{3}\right)^2 x[s_s+\bar{s}_s] \\ &= \frac{4}{9}x[u_v+d_v] - \frac{3}{9}xd_v + \frac{2}{9}xS + \frac{2}{90}xS. \end{aligned} \tag{4.4}$$

Figure 4.1 shows the plot of F_2 in eq. (4.4) versus x [plot (a)]. In the same figure it is shown that by dropping the contribution from strange sea quarks, embodied by the very last term in eq. (4.4), one obtains slightly different values of F_2 at small values of x only . Strictly speaking we should fit the results from our calculations, which involve only up and down quarks in our model of the proton, to plot (b) but, due to the small difference between plots (a) and (b), we keep plot (a) as our reference in this chapter.

The values for temperature and chemical potential which give the best fit for F_2 versus x are used to calculate the corresponding plot of R versus x which we compare with experimental data given by Whitlow [78] (Figure 4.2).

The zeroth order in α_S contributions are calculated with ease. The numerical calculation of $\mathcal{O}(\alpha_S)$ contributions requires much effort. In our discussions of the analytical calculations of the $\mathcal{O}(\alpha_S)$ contributions we saw in the previous chapter that phase space and loop integrations could be analytically reduced to an integration over the two energy variables K and p_0 as shown in the final expressions for four-particle processes given by eqs. (D.19) and (D.20) and for three-particle processes given by eqs. (D.27) and (D.28). These double integrals cannot be analytically calculated. Their numerical calculation is discussed in Section 4.3.2.

We distinguish between the zeroth and first order in α_S contributions by writing:

$$F_2^{\rm th} = F_2^{(0)} + F_2^{(1)}. \tag{4.5}$$

Since we are also interested in the structure function R which is expressible in terms of F_2 and F_1 according to eq. (2.14), we also calculate

$$F_1^{\rm th} = F_1^{(0)} + F_1^{(1)}. \tag{4.6}$$

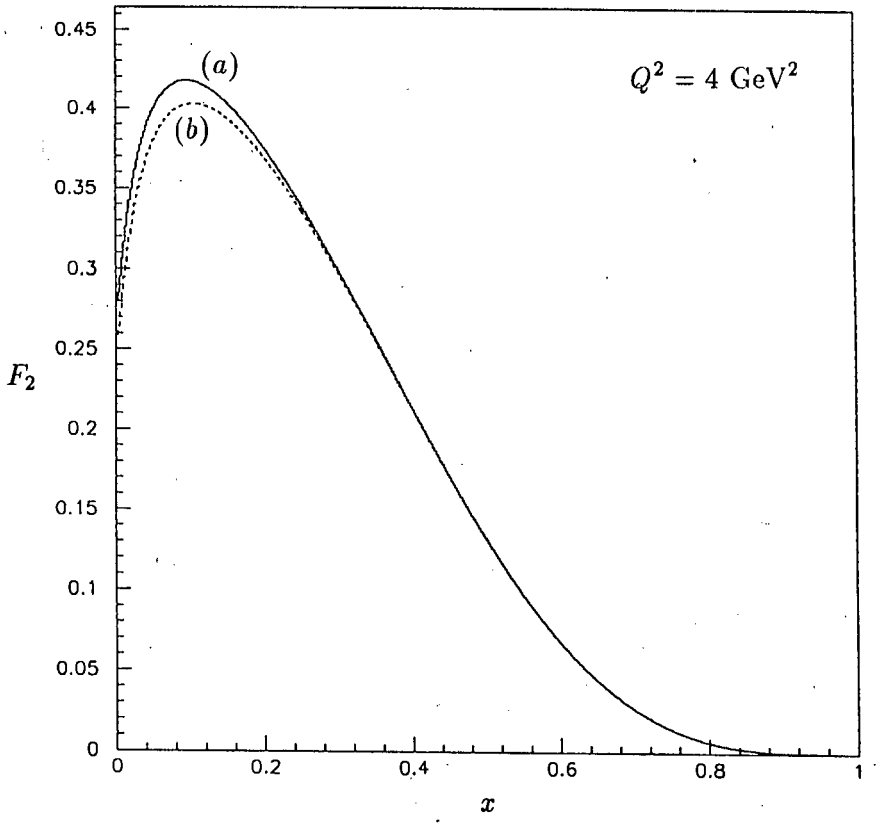

Figure 4.1: Plots of F_2 versus x for a proton at $Q^2 = 4$ GeV^2. Plot (a) corresponds exactly to eq. (4.4). Plot (b) is the same as plot (a) except for the exclusion of the contributions from strange sea quarks embodied by the very last term in eq. (4.4).

Zeroth order in α_S expressions for F_2 and F_1 in the statistical model are given by Cleymans and Thews in ref. [71]:

$$F_2^{(0)} = \frac{3M^2x^2VT}{2\pi^2}\frac{(1+Mx/2)^2}{(1+Mx/\nu)^5}\sum_q e_q^2\left\{\left[\frac{3}{2}\left(1+\frac{2\mu_q}{\nu}\right)^2-\frac{1}{2}\left(1+\frac{Mx}{\nu}\right)^2\right]f_0(z_q)\right.$$
$$\left.+\frac{6T}{\nu}\left(1+\frac{2\mu_q}{\nu}\right)f_1(z_q)+\frac{6T^2}{\nu^2}f_2(z_q)+\mu_q\to-\mu_q, z_q\to\bar{z}_q\right\} \quad (4.7)$$

$$F_1^{(0)} = \frac{3M^2x^2VT}{8\pi^2}\frac{(1+Mx/2)}{(1+Mx/\nu)^3}\sum_q e_q^2\left\{\left[\left(1+\frac{2\mu_q}{\nu}\right)^2+\left(1+\frac{Mx}{\nu}\right)^2\right]f_0(z_q)\right.$$
$$\left.+\frac{4T}{\nu}\left(1+\frac{2\mu_q}{\nu}\right)f_1(z_q)+\frac{4T^2}{\nu^2}f_2(z_q)+\mu_q\to-\mu_q, z_q\to\bar{z}_q\right\} \quad (4.8)$$

where the sum over q is over quark flavours only and where

$$z_q \equiv \frac{Mx}{2T}-\frac{\mu_q}{T} \qquad \bar{z}_q \equiv \frac{Mx}{2T}+\frac{\mu_q}{T}$$

$$f_n(z) \equiv \int_z^\infty \frac{y^n dy}{e^y+1} \qquad \text{with} \qquad n = 0;1;2.$$

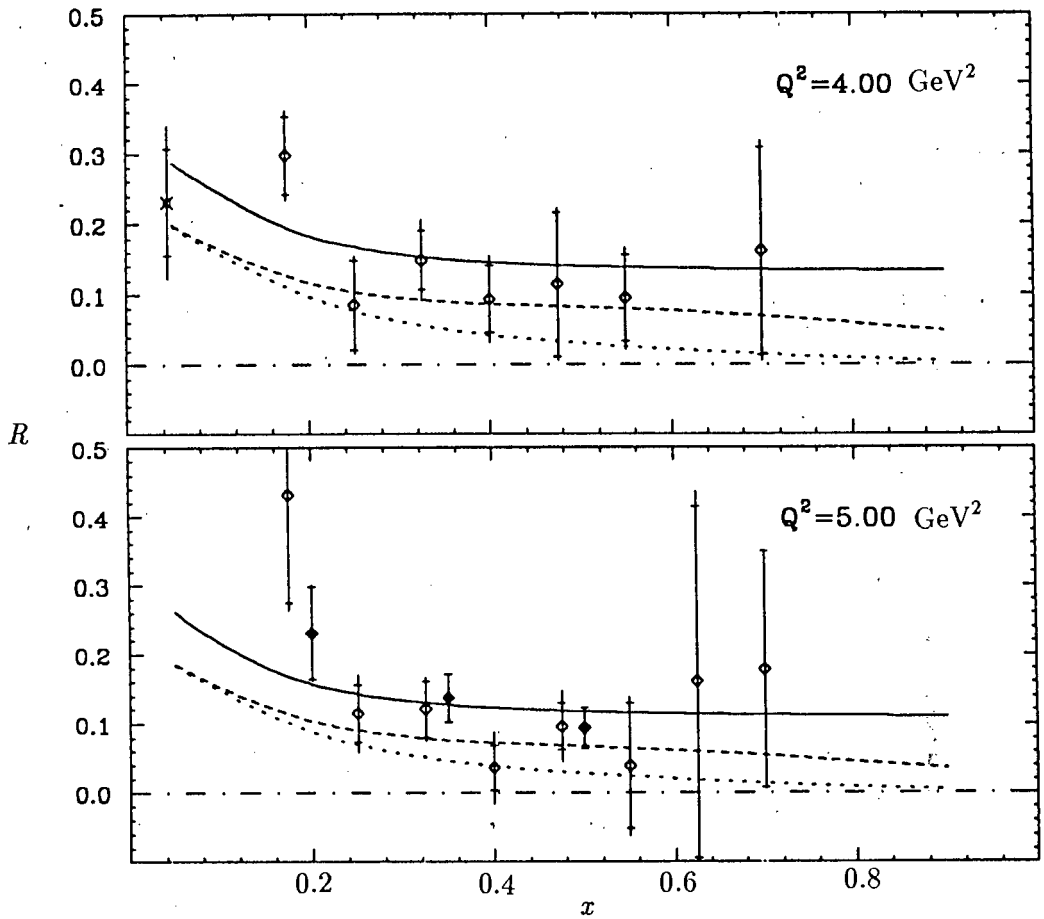

Figure 4.2: Plots of $R = \sigma_L/\sigma_T$ versus x at $Q^2 = 4$ GeV^2 and $Q^2 = 5$ GeV^2 as presented by Whitlow [78, p.106]. The discrete points are experimental data. The curves are some theoretical fits discussed in ref. [78]. They are not our fits.

According to the discussions in Chapter 2 the $O(\alpha_S)$ part of expressions for F_2 and F_1 in the statistical model are:

$$F_2^{(1)} = \frac{K}{4\pi^2\alpha}(\sigma_T^{(\alpha_S)} + \sigma_L^{(\alpha_S)})\frac{-q^2\nu}{q_z^2} \tag{4.9}$$

$$F_1^{(1)} = \frac{K}{4\pi^2\alpha}M\sigma_T^{(\alpha_S)} \tag{4.10}$$

where

$$\sigma_T^{(\alpha_S)} = \frac{1}{2}\frac{V}{2K}\frac{N_C^2-1}{2}4\pi\alpha_S 4\pi\alpha\sum_q e_q^2\left\{\int \bar{M}_\Sigma S_4 d\mu + \sum_{W=B,F,F'}\int \bar{M}_\Sigma^{3W} S_{3W} d\mu_W \right.$$
$$\left. + \int \bar{M}_0 S_4 d\mu + \sum_{W=B,F,F'}\int \bar{M}_0^{3W} S_{3W} d\mu_W\right\} \tag{4.11}$$

$$\sigma_L^{(\alpha_S)} = \frac{V}{2K}\frac{N_C^2-1}{2}4\pi\alpha_S 4\pi\alpha\sum_q e_q^2\left\{\int \bar{M}_0 S_4 d\mu + \sum_{W=B,F,F'}\int \bar{M}_0^{3W} S_{3W} d\mu_W\right\} \quad (4.12)$$

with the expressions in curly brackets exactly as given in eqs. (D.27), (D.28), (D.19) and (D.20) and where the expressions in curly brackets has to be evaluated for each flavour of quark, since the chemical potential appearing in the statistical factors S_4 and S_{3W} differ for each flavour as we sum over the flavours of quarks. As explained in Appendix D, the K, p_0 integration regions for three- and four-particle processes is as given in Figures D.2 and D.1, respectively, and the integrand for four-particle processes is different in each subregion shown in Figure D.1.

In all the numerical calculations we use fixed values for the quantities given in Table 4.1.

Table 4.1: Quantities for which fixed values are assigned in all our numerical calculations

Quantity	Symbol	Value
$-q^2$ of virtual photon	Q^2	4 GeV^2
Proton mass	M	0.94 GeV
Radius of proton	R	5.07 GeV^{-1} (= 1 fermi)
Volume of proton	V	$\frac{4}{3}\pi R^3$
Number of colours	N_C	3
Strong coupling constant	α_S	0.2

4.2 The Zeroth Order in α_S Calculation

4.2.1 Introduction

In this section we discuss the numerical calculation of the zeroth order in α_S contributions at $Q^2 = 4$ GeV^2. We calculate the structure function $F_2^{(0)}$ for different values of temperature and chemical potential in order to determine the zeroth order in α_S fit to the plot of F_2 versus x given in Figure 4.1(a). The fit which takes the $\mathcal{O}(\alpha_S)$ corrections into account too is discussed in Section 4.3.3.

In ref. [71] Cleymans and Thews presented results of the zeroth order in α_S calculation of F_2. In the deep-inelastic scattering limit, x, T, μ_q finite with ν going to infinity, the expression for $F_2^{(0)}$ in eq. (4.7) is dominated by the f_0 term which can be evaluated analytically. The result is

$$F_2^{(0)}(x) \overset{\nu\to\infty}{\longrightarrow} \frac{3}{2\pi^2} M^2 V T x^2 \sum_q e_q^2 \left[\ln(1+\mathrm{e}^{-z_q}) + \ln(1+\mathrm{e}^{-\bar{z}_q})\right].$$

Cleymans and Thews used the latter expression to fit to the experimental data published in 1981 by Aubert et al. [79].

In this work we keep the full expression for $F_2^{(0)}$ as given in eq. (4.7) and fit to a recent plot of F_2 versus x which is determined by the parton distributions published in 1990 by Kwiecinski et al. in ref. [77] [see eq. (4.4)]. The values for temperature and chemical potential which produce the best fit to the plot of F_2 versus x of Kwiecinski et al. are used to calculate $F_1^{(0)}$ in eq. (4.8) too. Then the structure function R which is expressible in terms of $F_2^{(0)}$ and $F_1^{(0)}$ according to eq. (2.14) can be calculated and compared to the experimental data in Figure 4.2.

4.2.2 Results and Conclusions

We obtained plots of F_2 versus x according to the zeroth order in α_S expression given in eq. (4.7) for different combinations of values for the temperature and the chemical potential for the up quarks and with the quantities given in Table 4.1 kept fixed throughout. The chemical potential for the down quarks was kept fixed in terms of the chemical potential for the up quarks according to

$$\mu_{\mathrm{down}} = \frac{\mu_{\mathrm{up}}}{2^{1/3}} \tag{4.13}$$

(as was done in ref. [71]) in order to reproduce the ratio of up to down quarks as being 2 to 1. This is approximately the case for a quark gas at very low temperatures.

As opposed to the f_0 function, the functions f_1 and f_2, which also appear in the expression for $F_2^{(0)}$ in eq. (4.7), cannot be evaluated analytically. They were numerically calculated by means of a Gauss-Legendre integration technique.

For $x \geq 0.4$, the zeroth order in α_S calculation produced a good fit to the $Q^2 = 4$ GeV^2 data of Kwiecinski et al. as shown in Figure 4.3. The plots in Figure 4.4 show that other combinations of values for T and μ_{up} do not produce an improved fit to the data of Kwiecinski et al.

According to the following rough estimates, the failure of the zeroth order in α_S theory of the statistical model to reproduce the low x behaviour of F_2 could be understood from a finite-size effect due to the finite volume of the nucleon.

From the mass shell condition on the four-momentum $k' = k + q$ of the outgoing quark in the zeroth order in α_S Feynman diagram M_{3a} in Figure 3.1, one obtains a lower limit on $|\vec{k}|$ of the incoming quark as follows. From the mass shell condition for *massless* quarks $[(k+q)^2 = 0]$ and the relation $x = Q^2/(2M\nu)$ one obtains

$$-1 \quad \leq \quad \cos\theta_{\vec{k}\vec{q}} = \frac{2|\vec{k}|\nu - Q^2}{2|\vec{k}|\sqrt{\nu^2 + 2M\nu x}} \quad \leq \quad 1.$$

The first inequality in the latter line produces

$$\begin{aligned} |\vec{k}| \quad &\geq \quad \frac{Q^2}{2\nu + 2\nu\sqrt{1 + \frac{2Mx}{\nu}}} = \frac{2M\nu x}{2\nu + 2\nu\left[1 + \mathcal{O}\left(\frac{x}{\nu}\right)\right]} \\ &= \quad \frac{Mx}{2} + \mathcal{O}\left(\frac{x}{\nu}\right). \end{aligned} \tag{4.14}$$

Another lower limit on $|\vec{k}|$ is obtainable from the Heisenberg uncertainty principle of the general form $\Delta x \Delta k \geq 1$. Taking Δx equal to the diameter of the nucleon (2 fermi = 10.14 GeV^{-1}), one obtains $\Delta k \geq (10.14)^{-1}$. From this and the value of the lower limit on $|\vec{k}|$ in eq. (4.14) one could deduce that our theory is only valid for x values satisfying

$$\frac{Mx}{2} \geq (10.14)^{-1},$$

i.e.,

$$x \geq 0.21.$$

The zeroth order in α_S calculation, however, was only able to reproduce the data of Kwiecinski et al. for values of $x \geq 0.4$. In Section 4.3 we investigate to what extent the $\mathcal{O}(\alpha_S)$ corrections are able to extend the reproduction of the data of Kwiecinski et al. to values of x smaller than 0.4.

The zeroth order in α_S results for the structure function R are shown on plot (a) in Figure 4.5. For $x \geq 0.25$ these results are consistent with the $Q^2 = 4$ GeV^2 experimental data in Figure 4.2. The way the unexpected almost linear behaviour of the zeroth order in α_S results for R versus x comes about can be seen from the plots of $Mq_z^2/(-q^2\nu)$ and $F_2^{(0)}/F_1^{(0)}$ [which are quantities appearing in the expression for R in eq. (2.14)] in Figure 4.6. Plot (b) in Figure 4.5 is discussed in Section 4.3.3.

4.3 The Zeroth- Plus First Order in α_S Calculation

4.3.1 Introduction

In this section we take the $\mathcal{O}(\alpha_S)$ corrections into account by numerically calculating the quantities given in eqs. (4.9) and (4.10) and adding them to zeroth order in α_S results according to eqs. (4.5) and (4.6). The zeroth order in α_S quantities given in eqs. (4.7) and (4.8) are calculated in the manner discussed in Section 4.2. Due to the modifications introduced by the $\mathcal{O}(\alpha_S)$ contributions, we search for new values of temperature and chemical potential which will produce a fit to the plot of F_2 versus x of Kwiecinski et al. given in Figure 4.1(a).

We include only up and down quarks in our statistical model. We keep the chemical potential of the down quarks fixed in terms of the chemical potential of the up quarks according to eq. (4.13). The values for temperature and chemical potential which produce the best fit to the plot of F_2 versus x of Kwiecinski et al. are used to calculate F_1^{th} in eq. (4.6) too. Then the structure function R which is expressible in terms of F_2 and F_1 according to eq. (2.14) can be calculated and compared to the experimental data in Figure 4.2.

4.3.2 Technicalities of the Numerical Calculation of the $\mathcal{O}(\alpha_S)$ Contributions

According to the $\mathcal{O}(\alpha_S)$ expressions, $F_2^{(1)}$ and $F_1^{(1)}$ in eqs. (4.9) and (4.10), one needs to numerically calculate the double integrals in eqs. (D.19), (D.20), (D.27) and (D.28). The K, p_0 integration regions for four- and three-particle processes are shown in Figures D.1 and D.2, respectively. These integrals are finite according to discussions in Sections 3.8 and 3.9. However, individual terms in the integrands can still become infinite along certain lines in the K, p_0 integration regions. This happens when factors in denominators or arguments of ln functions in some terms become equal to zero along certain lines (see Figure 4.7).

As an example we consider singularities which arise along the line along which the quantity b is equal to zero. The latter singularity arises in the terms proportional to $\ln|C_4|$ and $|G_4|$ in eq. (D.19).

One of the subregions which contain the line along which b is equal to zero is subregion D in Figure D.1 (Compare Figures D.1 and 4.7 to see this.). In region D the terms proportional

to $\ln|C_4|$ and $|G_4|$ in eq. (D.19) are as follows:

$$\begin{aligned}
&\frac{1}{4\pi^3 q_z}\int_{(q_z+\nu)/2}^{\infty} dp_0 \int_{(p_0-\nu)/2}^{(p_0+q_z)/2} dK\; S_4 \left\{ |q^2| \left(\frac{|p_0|}{4b^2} + \frac{\epsilon(p_0)}{2b} \right) \ln|\bar{C}_4| \right. \\
&\left. + \frac{(a+p_0)(d+e)(D+E)}{2b} |G_4| \right\} \\
= \;& \frac{1}{4\pi^3 q_z}\int_{(q_z+\nu)/2}^{\infty} dp_0 \int_{(p_0-\nu)/2}^{(p_0+q_z)/2} dK\; S_4 \left\{ -q^2 \left(\frac{p_0}{4b^2} + \frac{1}{2b} \right] \ln\left(\frac{q^2}{4dD} \right) \right. \\
&\left. - \frac{(a+p_0)B}{2b} \right\}
\end{aligned}$$

where the unique signs of quantities in region D (defined by the integration limits in the above expressions) allowed the removal of absolute value signs in the latter step.

The argument of the ln function is expressible as follows:

$$\frac{q^2}{4dD} = \frac{q^2}{4b^2 + 4b\nu + q^2} = \frac{1}{1 + 4b\nu/q^2 + 4b^2/q^2}.$$

Therefore we have that

$$\lim_{b\to 0} \ln \frac{q^2}{4dD} = \lim_{b\to 0} \ln\left(1 - \frac{4\nu}{q^2} b\right) = \lim_{b\to 0} \left(-\frac{4\nu}{q^2} b \right)$$

which leads to

$$\begin{aligned}
\lim_{b\to 0} T_1 &\equiv \lim_{b\to 0} \left(-q^2 \frac{p_0}{4b^2} \ln \frac{q^2}{4dD} \right) = \lim_{b\to 0} \frac{p_0 \nu}{b} \\
\lim_{b\to 0} T_2 &\equiv \lim_{b\to 0} \left(-q^2 \frac{1}{2b} \ln \frac{q^2}{4dD} \right) = 2\nu \\
\lim_{b\to 0} T_3 &\equiv \lim_{b\to 0} \frac{-(a+p_0)B}{2b} = \lim_{b\to 0} \frac{-p_0\nu}{b}.
\end{aligned}$$

The term T_2 is finite in the $b \to 0$ limit. The singularities from the terms T_1 and T_3 cancel each other. Even though they cancel, the terms T_1 and T_3 individually give rise to singularities. Therefore one should take care not to approach the line along which $b = 0$ too closely in the numerical integration. For the same reason one should steer clear of other lines along which other individual terms in expressions for three- and four-particel processes are singular. This is accomplished by implementing a two-dimensional lattice constructed in such a way that the two nearest successive lattice points to any of the lines with non-zero slope in Figure 4.7 are always located an equal distance on both sides of the relevant line. Such a lattice is shown in Figure 4.10 for one quadrant. Before we discuss its construction, we consider the following.

For the reasons given in the latter paragraph, we have decided on a trapesium integration method whereby the integrand is evaluated at discrete lattice points. The value of the integral is the stable value attained in successive numerical integrations in which, independently and in steps, the density of lattice points is increased and the range of integration is extended (The presence of thermal distribution factors in terms suppresses contributions at large values of the integration variables.).

Since these integrals in the $\mathcal{O}(\alpha_S)$ contributions to the structure functions have to be calculated for many independent values of x, T, μ_{up} and of parameters determining the density of lattice points and the range of integration, it is necessary to find ways to reduce the time it takes to evaluate one integral. In the following we discuss two techniques each of which reduces the duration of calculation.

The first technique involves the use of crossing properties of the three- and four-particle processes to map the second, third and fourth quadrants of integration regions onto the first quadrant. The resultant integration region is shown in Figure 4.8. Taking into account the effect that the mapping has on signs of quantities and extending the definition of statistical factors, one can in effect integrate over all four quadrants by evaluating the suitably defined integrand at lattice points located only in the first quadrant.

As a simple example we show how the integration region Y for the four-particle process of gluon emission from an *antiquark* can be mapped onto the integration region X for gluon emission from a *quark* as shown in Figure 4.9. In the following discussions we let $K' > 0$ always and consider only points K' which lie in region X. From Figure 4.9 it then follows that all the points $-K'$ lie in region Y. From

$$k_0(K, p_0) \equiv K - \frac{\nu - p_0}{2}$$

and

$$k_0'(K, p_0) \equiv k_0 + \nu - p_0 = K + \frac{\nu - p_0}{2}$$

we see that

$$k_0(K = -K', p_0) = -k_0'(K = K', p_0) < 0$$

$$k_0'(K = -K', p_0) = -k_0(K = K', p_0) < 0$$

and from Table D.2(b) we see that

$$S_4(K = -K' < 0, p_0)$$

$$= \frac{1}{e^{\beta[-k_0'(K=-K',p_0)+\mu]}+1}\left[1-\frac{1}{e^{\beta[-k_0(K=-K',p_0)+\mu]}+1}\right]\left[1+\frac{1}{e^{\beta p_0}-1}\right]$$
$$= \frac{1}{e^{\beta[k_0(K=K',p_0)+\mu]}+1}\left[1-\frac{1}{e^{\beta[k_0'(K=K',p_0)+\mu]}+1}\right]\left[1+\frac{1}{e^{\beta p_0}-1}\right]. \qquad (4.15)$$

We also have that

$$\sum_{\text{spins}}\left|M_{\substack{\gamma^* \\ \nu>0}} + {}_{\substack{\bar{q} \\ k_0'<0}} \rightarrow {}_{\substack{\bar{q} \\ k_0<0}} + {}_{\substack{g \\ p_0>0}} (K=-K',p_0)\right|^2$$
$$= \sum_{\text{spins}}\left|M_{\substack{\gamma^* \\ \nu>0}} + {}_{\substack{q \\ k_0>0}} \rightarrow {}_{\substack{q \\ k_0'>0}} + {}_{\substack{g \\ p_0>0}} (K=K',p_0)\right|^2.$$

Thus the contribution from gluon emission from an *antiquark*, obtained by integrating over region Y, can be determined by integrating the expression for gluon emission from a *quark* over region X except that the statistical factor in line 4.15 is to be used. Thus *both* the contributions from gluon emission from an *antiquark* and from a *quark* can be taken into account by using the integrand for gluon emission from a *quark*, integrating only once over the region X and, instead of using the statistical factor

$$\frac{1}{e^{\beta(k_0-\mu)}+1}\left(1-\frac{1}{e^{\beta(k_0'-\mu)}+1}\right)\left(1+\frac{1}{e^{\beta p_0}-1}\right)$$

associated with gluon emission from a *quark*, using the extended statistical factor

$$\frac{1}{e^{\beta(k_0-\mu)}+1}\left(1-\frac{1}{e^{\beta(k_0'-\mu)}+1}\right)\left(1+\frac{1}{e^{\beta p_0}-1}\right)$$
$$+\ \frac{1}{e^{\beta(k_0+\mu)}+1}\left(1-\frac{1}{e^{\beta(k_0'+\mu)}+1}\right)\left(1+\frac{1}{e^{\beta p_0}-1}\right).$$

From Figure D.2 it can be seen that three-particle processes will provide additional contributions at each lattice point in region X. According to similar considerations as above, the part of the contribution from the three-particle process in Figure 2.2(h) which has support in region Y can be mapped so that it contributes together with the part of the contribution from the three-particle process in Figure 2.2(g) which has support in region X at each lattice point in region X.

Continuing according to similar considerations we obtain expressions for both four- and three-particle processes which have support in all the regions (other than region X too) in the first quadrant and which represent contributions from all the quadrants shown in Figures D.1 and D.2. For each lattice point (K,P) in Figure 4.10 we let $p_0 = P$ and $p_0 = -P$ in the

computer program in order to add contributions from positive and negative p_0, respectively, at each lattice point.

A second technique which reduces the duration of integration on the computer is as follows: In practice we found that, by only taking into account lattice points which lie on certain strips in the first quadrant shown in Figure 4.10, the same result could be obtained as that obtained when all the lattice points in Figure 4.10 are taken into consideration. These strips, each of width $2r$ and centered on the lines in the first quadrant, are shown in Figure 4.11. This technique is implemented by using program statements which filter out points which do not lie on these strips. The durability of the fact that the same result could be obtained by only taking into account lattice points which lie on certain strips as that obtained when all the lattice points are taken into consideration, was checked at some of the points in parameter space encountered as we moved through parameter space. Once the final results were obtained, the latter check was also performed on them.

Next we discuss how a lattice can be constructed in such a way that the two nearest successive lattice points to any of the lines with non-zero slope in Figure 4.10 are always located an equal distance on both sides of the relevant line as referred to earlier in this section.

We employ a trick which guarantees the latter requirement even when the positions of the lines in Figure 4.10 shift as a result of the variations of q_z and ν when we consider different values of x at fixed Q^2. From Figure 4.10 it can be seen that such a lattice can be constructed by choosing ν and q_z to be integer multiples n_ν and n_{q_z}, respectively, of the same quantity Δ

$$\nu = n_\nu \Delta \qquad \text{and} \qquad q_z = n_{q_z} \Delta, \tag{4.16}$$

by letting the increment size in the K and P directions be

$$\delta_K = \frac{\Delta}{2m} \qquad \text{and} \qquad \delta_P = \frac{\Delta}{m},$$

respectively, where m is an integer by means of which increment sizes can be varied independently of the other numerical parameters and by choosing the leftmost point in the bottom row of the lattice so as to lie on the coordinate

$$(K, P) = \left(\frac{\Delta}{2m}, \frac{\Delta}{2m}\right).$$

The expression for the quantity Δ can be derived from the expressions in eq. (4.16) and $Q^2 = q_z^2 - \nu^2$ and is as follows:

$$\Delta = \sqrt{\frac{Q^2}{n_{q_z}^2 - n_\nu^2}}.$$

Values for n_ν, n_{q_z}, ν, q_z and Δ corresponding to each of the values of x for which data points are plotted in Figure 4.12 are given in Table 4.2. It is to be noted that for each set of fixed

Table 4.2: Values of quantities involved in numerical calculations corresponding to each of a discrete set of x values at fixed $Q^2 = 4$ GeV^2.

x	n_ν	n_{q_z}	ν(GeV)	q_z(GeV)	Δ(GeV)
0.02	5659	5660	106.38	106.40	0.019
0.06	629	630	35.45	35.51	0.056
0.10	226	227	21.24	21.33	0.094
0.20	57	58	10.63	10.82	0.187
0.25	73	75	8.49	8.72	0.116
0.30	25	26	7.00	7.28	0.280
0.41	14	15	5.20	5.57	0.371
0.50	19	21	4.25	4.70	0.224
0.60	27	31	3.55	4.07	0.131
0.71	5	6	3.02	3.62	0.603
0.80	4	5	2.67	3.33	0.667
0.90	13	17	2.37	3.10	0.183
1.00	43	59	2.13	2.92	0.050

values for Q^2, n_ν and n_{q_z} which determine unique values for Δ, ν, q_z and x, the parameter m which controls the density of lattice points can be freely varied.

4.3.3 Results of the Total Calculation, i.e., Zeroth Order Plus $\mathcal{O}(\alpha_S)$ Contributions and Conclusions

In Section 4.2.2 it was mentioned that the zeroth order in α_S calculation is able to reproduce the data of Kwiecinski et al. on F_2 versus x for values of $x \geq 0.4$ only. From Figure 4.12 it can be seen that, by including $\mathcal{O}(\alpha_S)$ corrections, the reproduction of the data of Kwiecinski et al. could be extended to values of x smaller than 0.4. A reasonable fit could be obtained for values of $x \geq 0.25$. This is compatible with our estimate for the limited range of validity

of our theory ($x \geq 0.21$ as derived in Section 4.2.2) due to a finite-size effect arising from the finite volume of the nucleon.

For the fixed values of the quantities in Table 4.1 and the fixed expression for the chemical potential of the down quarks in terms of the chemical potential of the up quarks in eq. (4.13), a fit to the data of Kwiecinki et al. is possible for values of temperature and chemical potential in the immediate vicinity of $T = 0.067$ GeV and $\mu_{\rm up} = 0.133$ GeV only.

Figures 4.13 and 4.14 show how the results for F_2 versus x from the calculation including zeroth order plus $\mathcal{O}(\alpha_S)$ contributions vary as a function of temperature at fixed chemical potential and as a function of chemical potential at fixed temperature, respectively.

From Figure 4.12 it can be seen that the $\mathcal{O}(\alpha_S)$ corrections to F_2 is negative for large x. Such negative values could in principle arise from interference terms from three-particle processes since, by neglecting the $\mathcal{O}(\alpha_S^2)$ contributions to the amplitude squared corresponding to the $\mathcal{O}(\alpha_S^0)$ and $\mathcal{O}(\alpha_S)$ Feynman diagrams for three-particle processes (see Figure 3.10, the positive definiteness of the amplitude squared is lost.

Results of the calculation of the structure function R with zeroth order plus $\mathcal{O}(\alpha_S)$ expressions for F_2 and F_1, as they appear in the expression for R in eq. (2.14) appear in Figure 4.15. In the $x \geq 0.25$ region of interest the results typically lie a factor of 6 above the experimental data for R shown in Figure 4.2. The absence of data for $x \geq 0.8$ in Figure 4.15 is due to numerical instability encountered as F_1, appearing in a denominator in the expression for R in eq. (2.14), goes to zero at large x. A comparison of the plot for R in Figure 4.15 with the corresponding zeroth order in α_S plot for R [labelled (b) in Figure 4.5] shows the large effect Feynman diagrams containing gluons have on results when $\mathcal{O}(\alpha_S)$ contributions are included.

Even when taking into account the fact that all measurements of R suffer from large experimental errors due to the weak dependence of the deep inelastic cross section for charged leptons on R [as discussed at eq. (2.11)], the factor of 6 misfit remains unacceptable. It indicates a shortcoming of the statistical model in its present form to reproduce the spin structure of the proton.

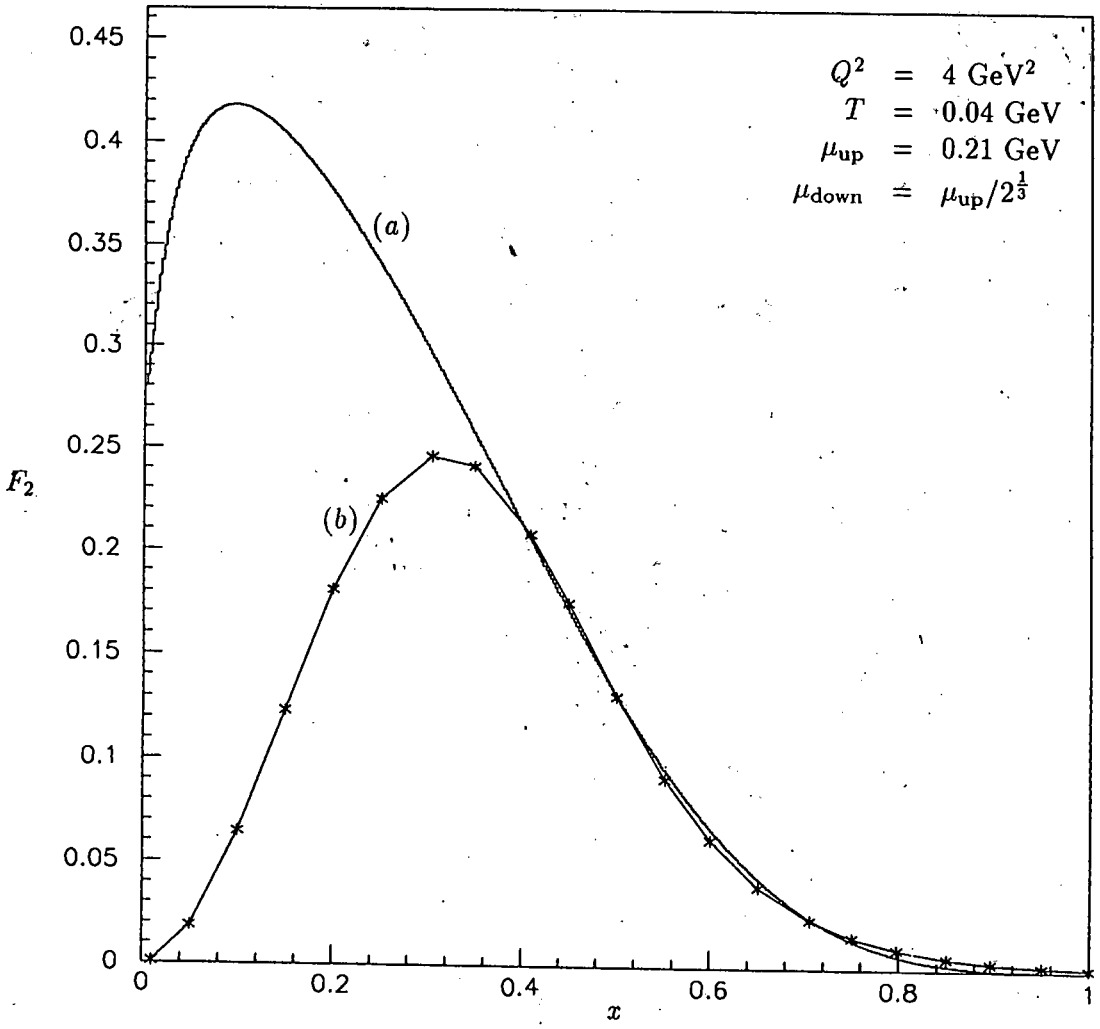

Figure 4.3: Plots of F_2 versus x at $Q^2 = 4$ GeV^2; (a): in terms of the parton distributions of Kwiecinski et al. as given in eq. (4.4) and (b): according to the zeroth order in α_S expression given in eq. (4.7).

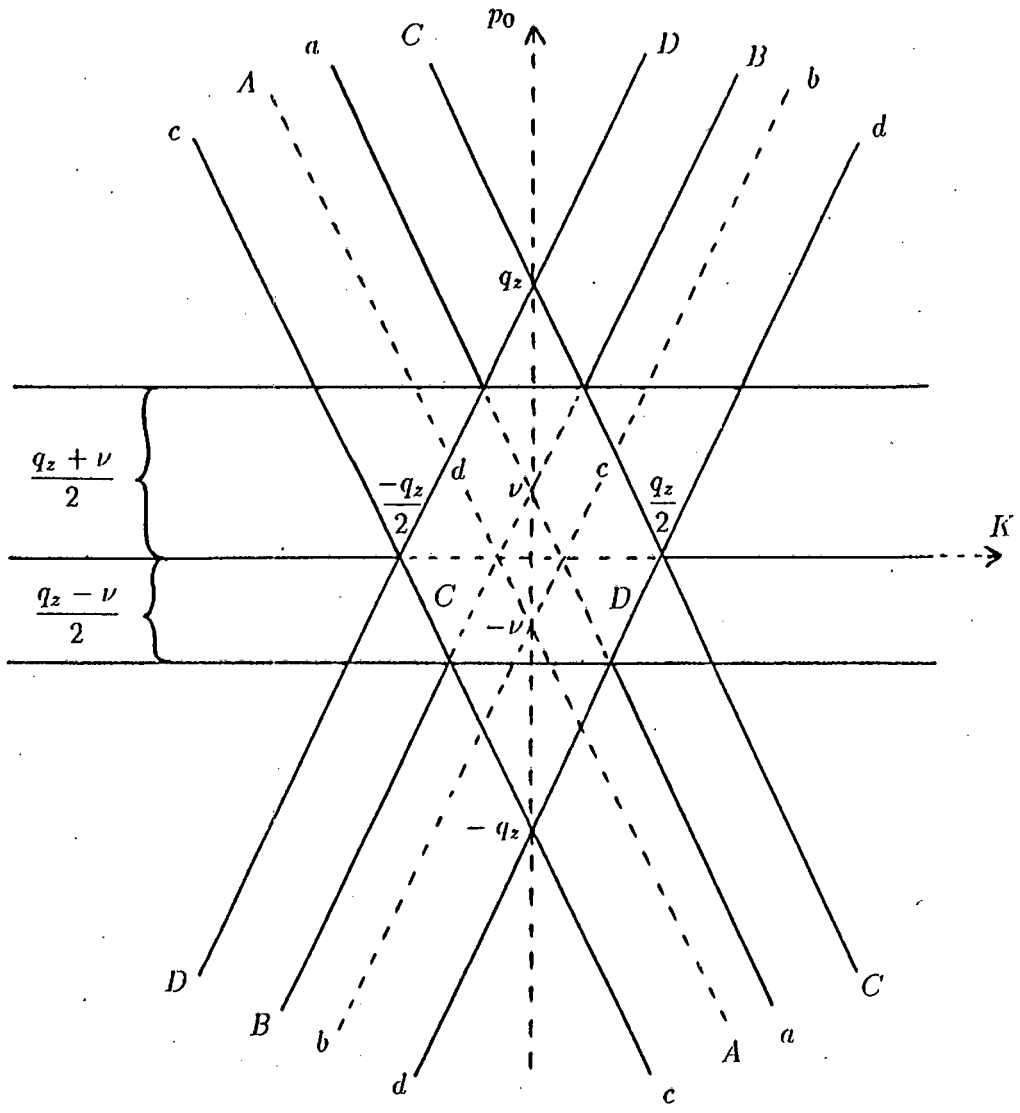

Figure 4.7: Lines in the K, p_0 plane along which the quantities defined at line (D.12) are equal to zero. It is to be noted that the presence of sign functions in the definitions of some of the quantities at line (D.12) causes those quantities to be zero only along segments of lines and not along entire lines.

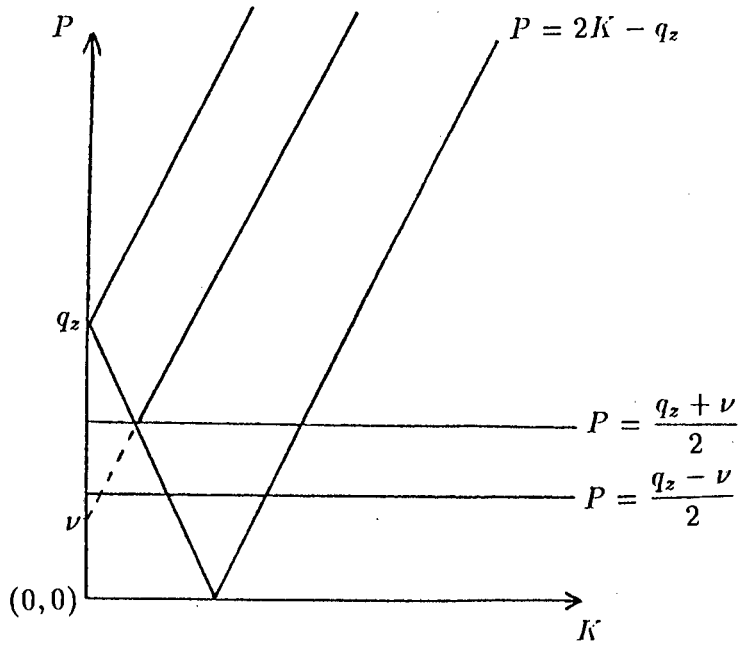

Figure 4.8: The integration region for the numerical integration obtained after mapping the second, third and fourth quadrants onto the first quadrant in Figures D.2 *and* D.1

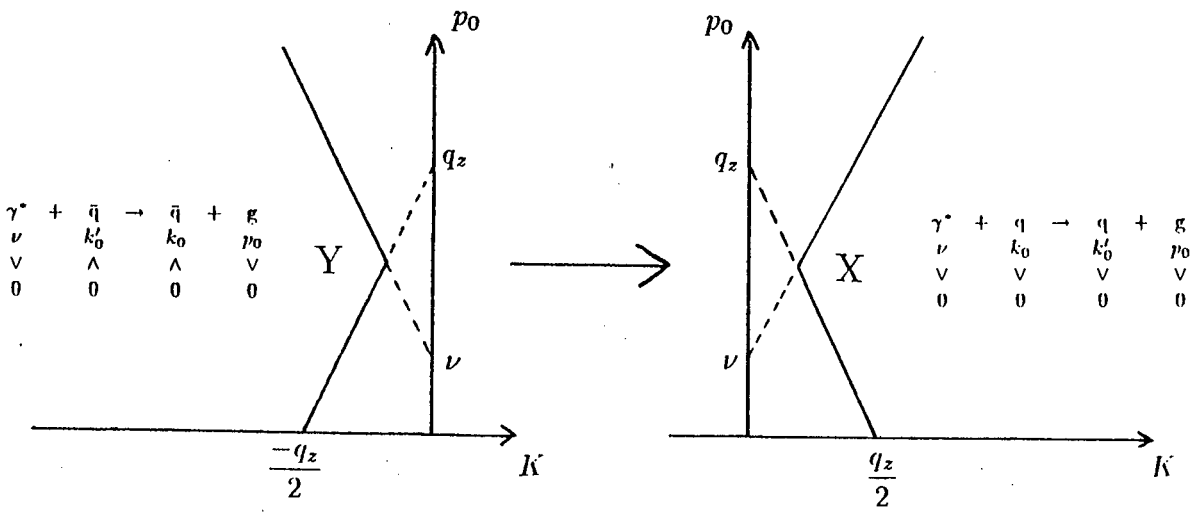

Figure 4.9: The mapping of the integration region Y for gluon emission from an *antiquark* onto the integration region X for gluon emission from a *quark*

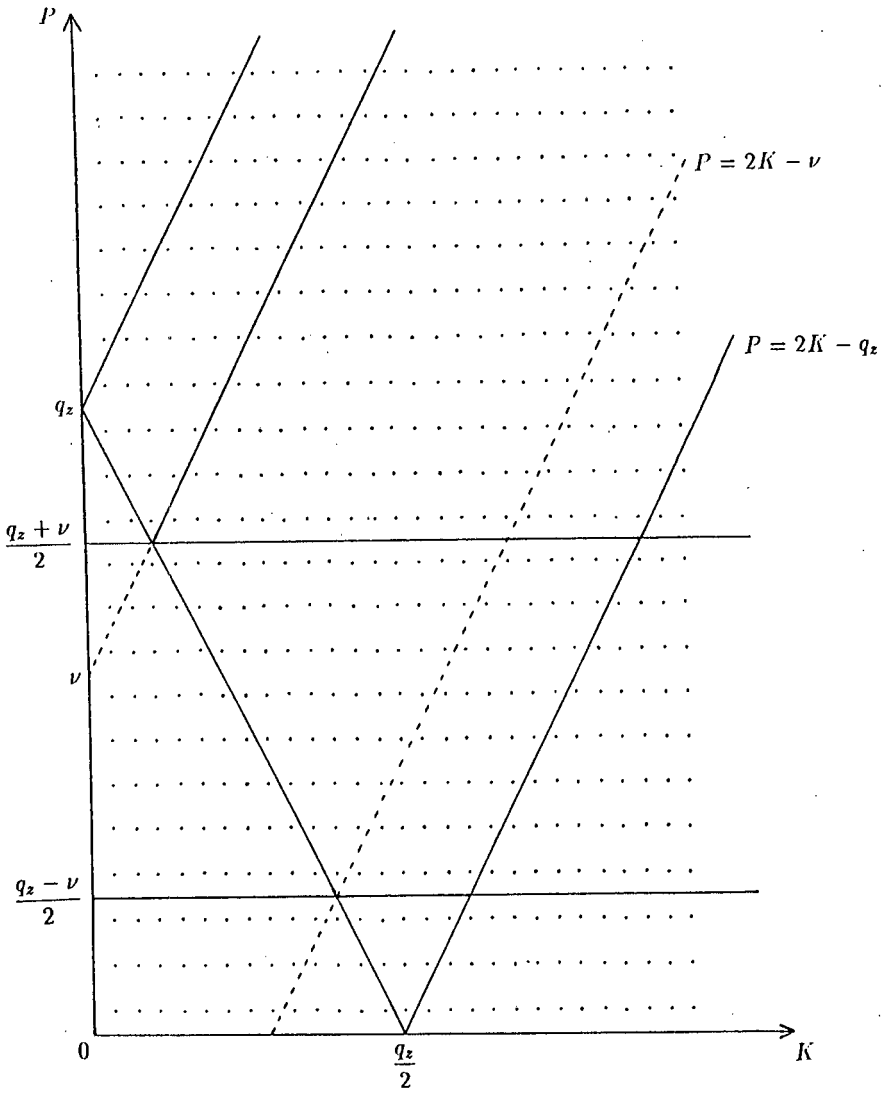

Figure 4.10: Lattice points at which the integrand is evaluated in the numerical integration.

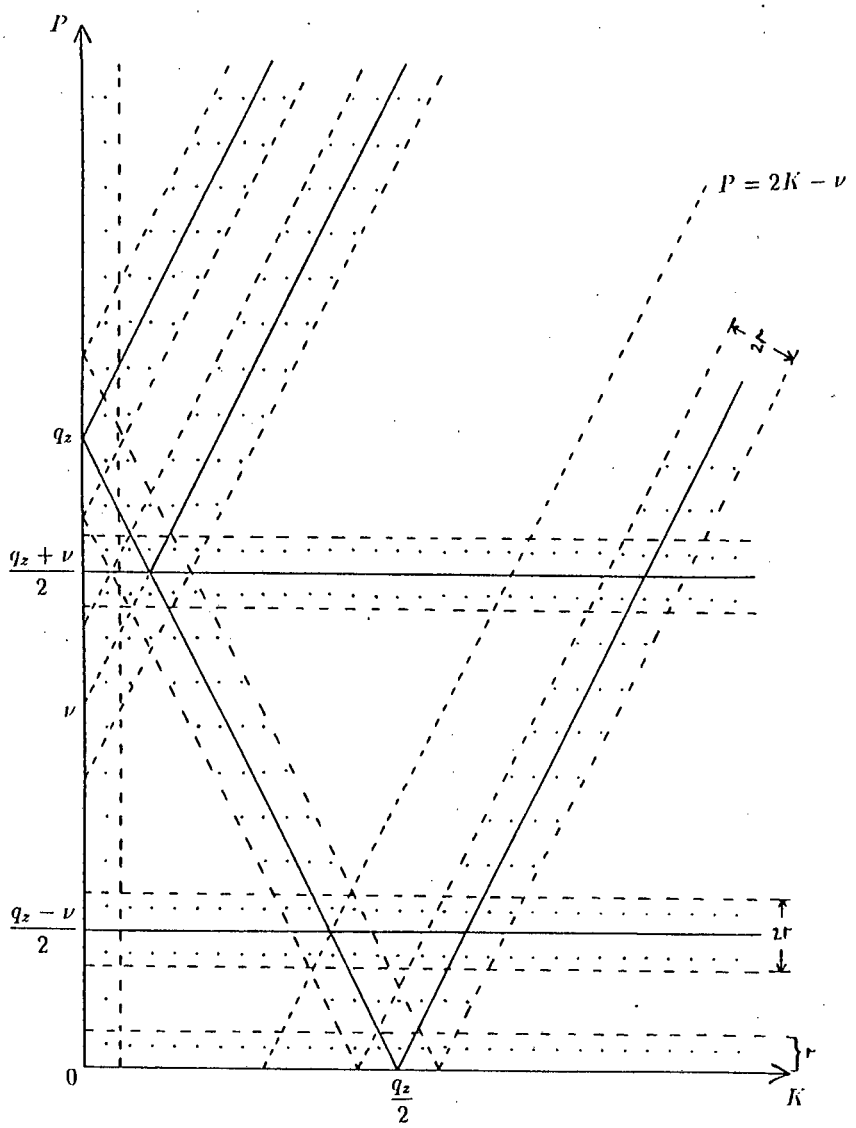

Figure 4.11: Strips containing lattice points which determine the values of the integrals under consideration. By increasing the density of lattice points, more points can be made to fall on strips of a given width.

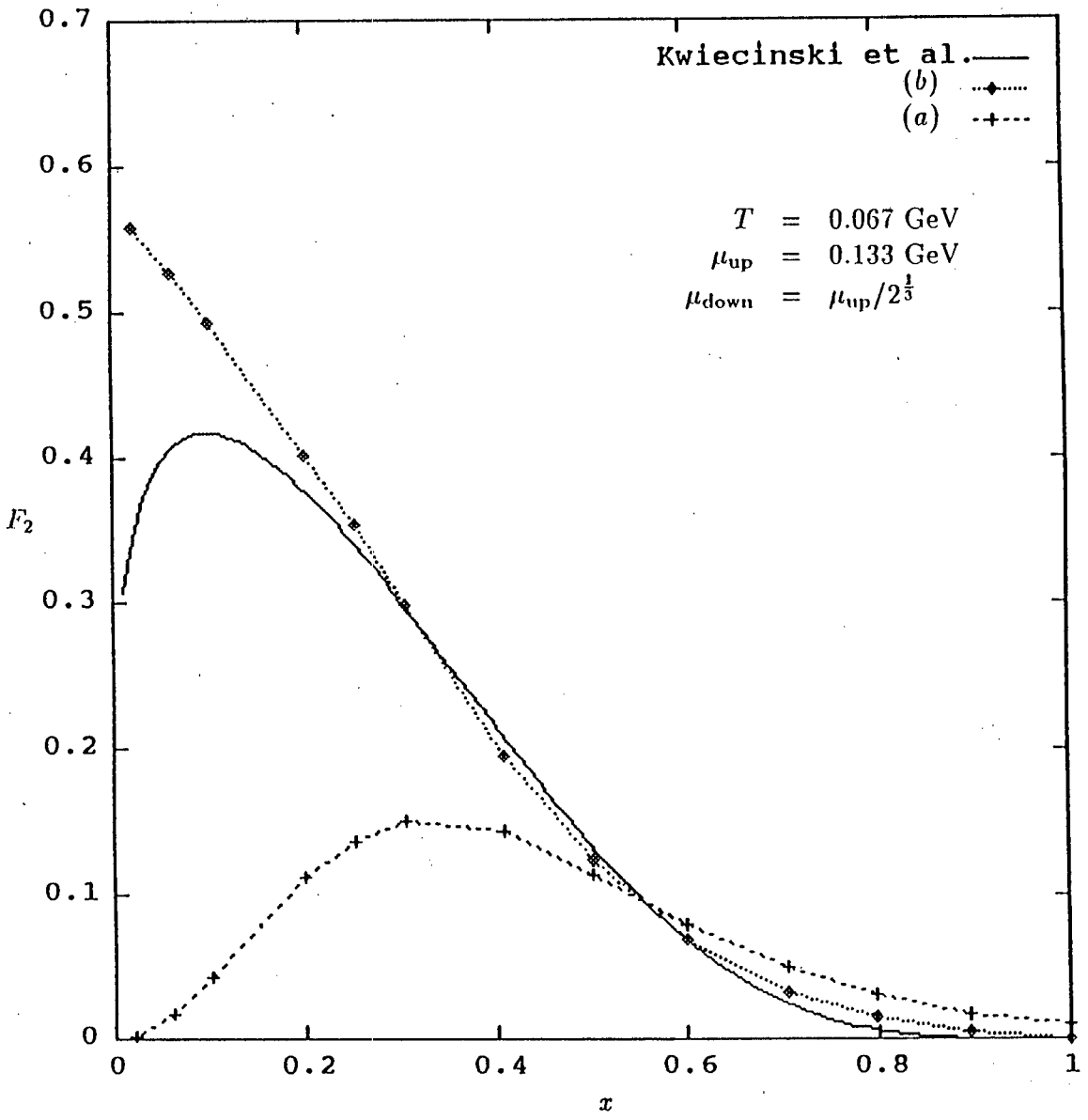

Figure 4.12: Plots of F_2 versus x at $Q^2 = 4$ GeV^2; (a): according to the zeroth order in α_S expression given in eq. (4.7) and (b): according to the zeroth order plus $\mathcal{O}(\alpha_S)$ expression given in eqs. (4.5) and (4.9) with $\alpha_S = 0.2$.

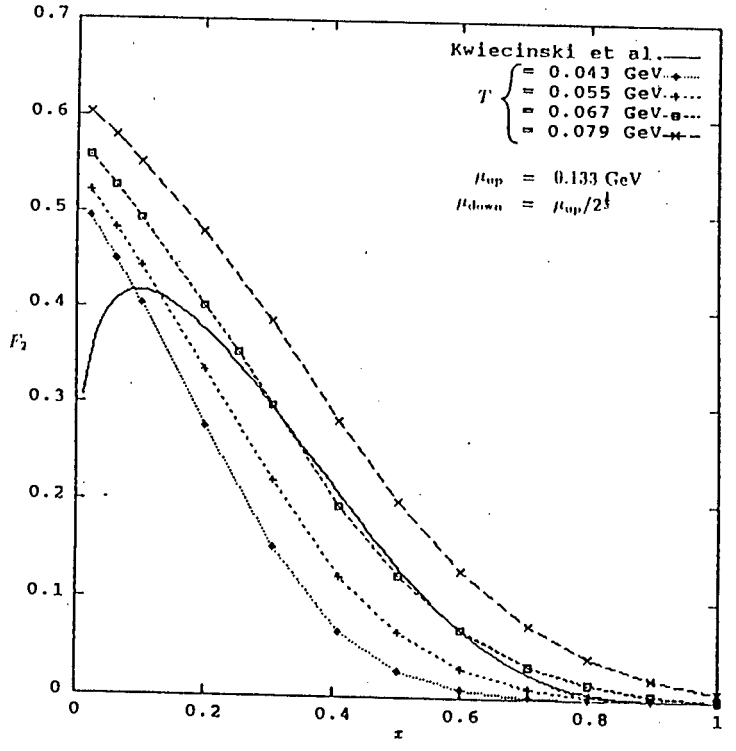

Figure 4.13: Plots of F_2 versus x at $Q^2 = 4$ GeV^2 as a function of temperature at fixed chemical potential according to the zeroth order plus $\mathcal{O}(\alpha_S)$ expression given in eqs. (4.5) and (4.9) with $\alpha_S = 0.2$.

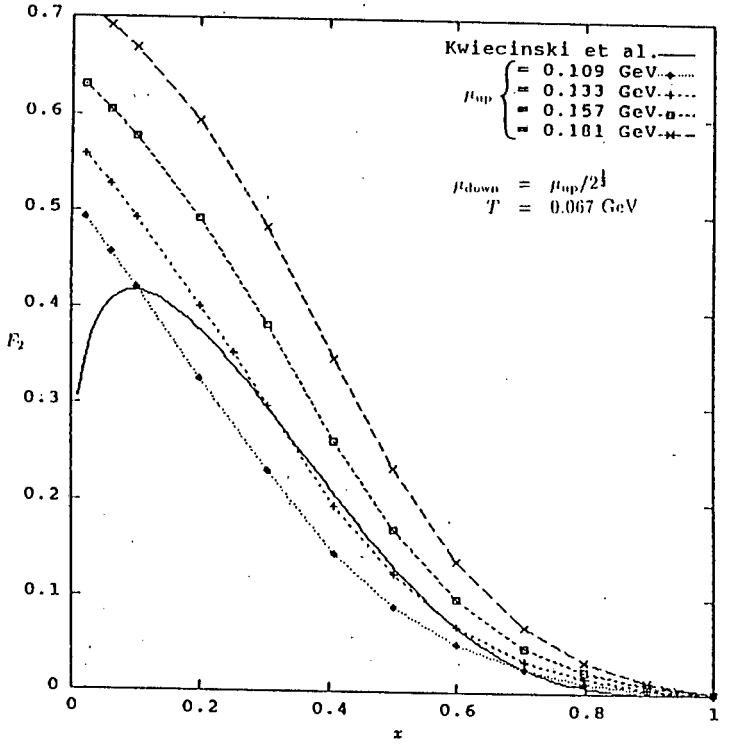

Figure 4.14: Plots of F_2 versus x at $Q^2 = 4$ GeV^2 as a function of chemical potential at fixed temperature according to the zeroth order plus $\mathcal{O}(\alpha_S)$ expression given in eqs. (4.5) and (4.9) with $\alpha_S = 0.2$.

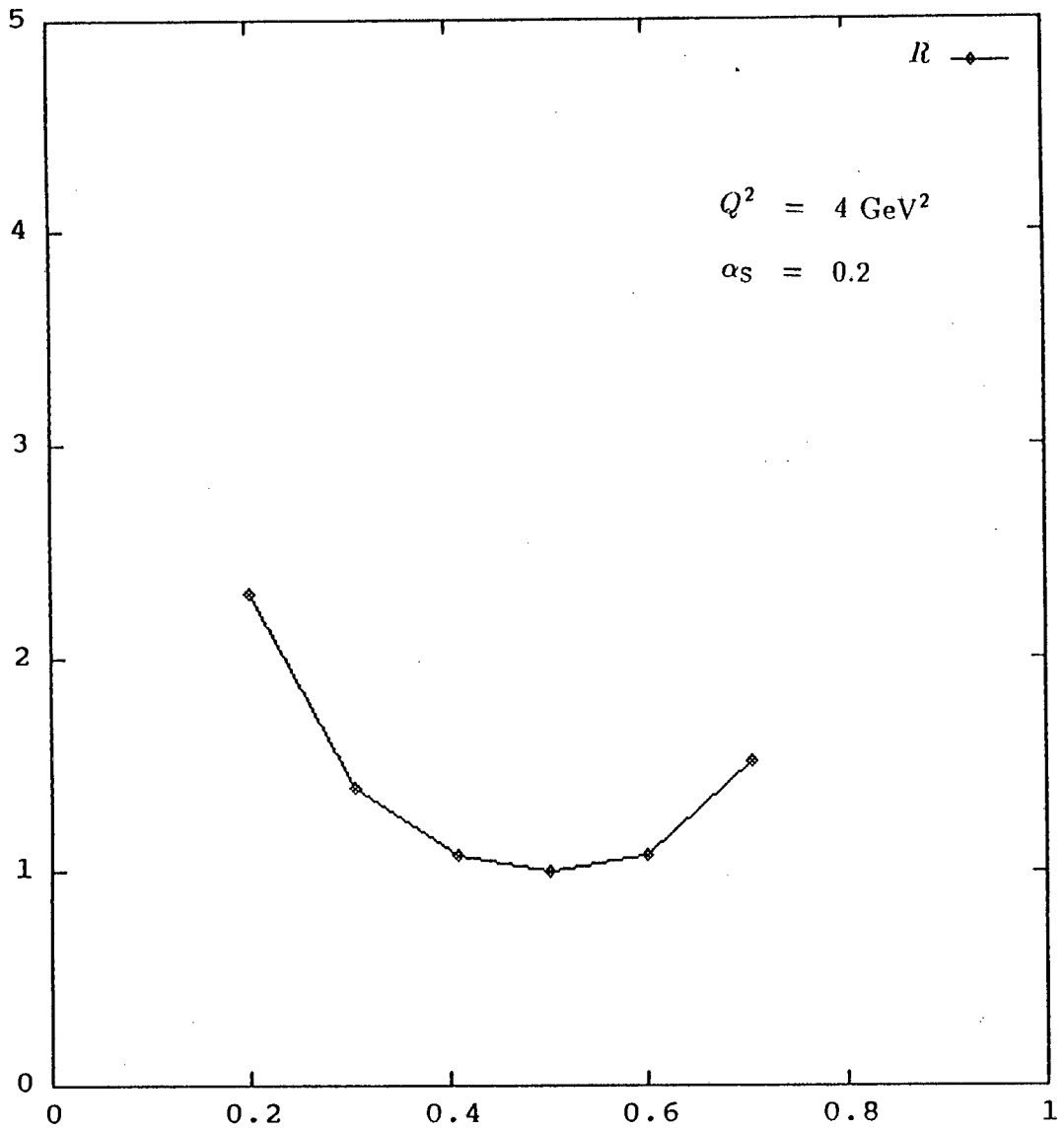

Figure 4.15: Plot of R versus x at $Q^2 = 4$ GeV^2 with $\alpha_S = 0.2$, $T = 0.067$ GeV, $\mu_{up} = 0.133$ GeV and $\mu_{down} = \mu_{up}/2^{\frac{1}{3}}$

Chapter 5

Summary

In this work, we considered deep inelastic scattering of leptons off a proton in the statistical model first proposed by Cleymans and Thews [71]. The interior of the nucleon is viewed as a thermalized assembly of up and down quarks and gluons. This enables one to incorporate features which are absent in the parton model. They include the presence of identical quarks and gluons in initial and final states and of quantum statistical correlations which also have a role to play in the propagation of particles when considering Feynman diagrams containing internal lines in next-to-leading-order calculations. These features are incorporated through the use of Fermi-Dirac and Bose-Einstein distributions for quarks and gluons, respectively. Stimulated emission factors for final-state gluons and Pauli-blocking factors for final-state quarks are incorporated. The propagation of particles through a many-body medium is taken into account by using thermal Feynman rules for propagators and vertices. The statistical model could also be seen as an attempt to describe the interior of the nucleon at a more fundamental level than that attained through the use of arbitrary parton distributions containing many parameters in the parton model.

We chose to fit to a plot of F_2 versus x, where

$$x = \frac{Q^2}{2M\nu},$$

which is determined by parton distributions which reproduce a wide range of experimental data. Such parton distributions were published in 1990 by Kwiecinski et al. in ref. [77]. They decide on a parametrization of the parton distributions at $Q_0^2 \equiv -q^2 = 4$ GeV^2 and evolve up in Q^2 in order to test their parton distributions against experimental data.

Our zeroth order in the strong coupling constant α_S calculation of the structure function F_2 versus x at $Q^2 = 4$ GeV^2 produced a good fit to the data of J. Kwiecinski et al. for

$x \geq 0.4$. The values for temperature and chemical potential which give the best fit are $T = 0.04$ GeV and $\mu_{\rm up} = 0.21$ GeV (with $\mu_{\rm down} = \mu_{\rm up}/2^{\frac{1}{3}}$). Other combinations of values for T and $\mu_{\rm up}$ do not produce an improved fit to the data of Kwiecinski et al. In consequence, we investigated to what extent $\mathcal{O}(\alpha_{\rm S})$ corrections are able to extend the reproduction of the data of Kwiecinski et al. to values of x smaller than 0.4. The corresponding zeroth order in $\alpha_{\rm S}$ results for the structure function R are consistent with experimental data.

The analytical calculations by Cleymans and Dadić [15] of the $\mathcal{O}(\alpha_{\rm S})$ corrections are discussed in this work. They took all processes contributing to order $\alpha_{\rm S}$ exactly into account and were able to cancel all infrared, collinear and ultraviolet divergences in the framework provided by the real-time formalism of finite-temperature quantum field theory (reviewed in Chapter 1).

Finite-temperature quantum field theory takes into account thermal effects in fields of physics ranging from solid state physics to particle physics in the early universe and in ultra-relativistic heavy ion collisions. Physical processes no longer take place in the ordinary vacuum, but in a heat bath. In the imaginary-time formulation of finite-temperature quantum field theory, direct calculation of static thermodynamic quantities, such as energy density, pressure, entropy and number densities, is possible, while the calculation of dynamic quantities, associated with time-dependent phenomena, is only indirectly possible through a process of analytic continuation to real time. An example of a time-dependent phenomenon which intrinsically involve real time is a scattering process in a heat bath. Propagators express the presence of a particle at one position and time in terms of its presence at another position and another time. Since these times assume values on the continuous real axis, we need, after a Fourier transformation to momentum space, Feynman diagrams with continuous real energies on external lines. The imaginary-time Green functions can be extended from the discrete imaginary energies to real continuous energies through a process of analytic continuation. But, for n-point functions with $n > 2$ or for graphs beyond the one-loop level, the analytic continuation becomes impracticable [12, p.329], [2, p.144]. In recent years, a real-time formulation has been developed, which makes direct calculation of time-dependent quantities possible. Additional advantages of the real-time formulation are also discussed in Section 1.4.

Research projects which are the most closely related to ours, in that next-to-leading-order

contributions are considered in the framework provided by the real-time formalism of finite-temperature quantum field theory too, have been reported on by groups working in Nice [17] and Annecy [20] in France and Bielefeld [14] in West Germany. The main difference between our project and the latter projects, besides being on different but related physical processes, is the kinematics involved. The fact that the Lorentz invariance property, which is used in the usual zero temperature calculations, is lost due to the preferred frame of reference defined by the heat bath, has the immediate consequence that the number of calculations required is increased dramatically. For this reason all the above-mentioned groups reduce the complexity of their calculations significantly by using special kinematics [e.g. in lepton pair production from a thermalized quark gluon plasma they would use a virtual photon with zero spatial momentum: $q = (q_0, \vec{q} = 0)$]. In our case we perform calculations for the case of general kinematics [i.e. $q = (q_0, \vec{q} \neq 0)$].

The inclusion of the $\mathcal{O}(\alpha_S)$ corrections in our numerical calculations allowed the extension of the reproduction of the data of Kwiecinski et al. to values of x smaller than 0.4. A fit could be obtained for values of $x \geq 0.25$. This is compatible with our estimate for the limited range of validity of our theory ($x \geq 0.21$) due to a finite-size effect arising from the finite volume of the nucleon. The latter fit is possible for values of temperature and chemical potential in the immediate vicinity of $T = 0.067$ GeV and $\mu_{\mathrm{up}} = 0.133$ GeV only (with $\mu_{\mathrm{down}} = \mu_{\mathrm{up}}/2^{\frac{1}{3}}$ and $\alpha_S = 0.2$).

The latter values of parameters, however, give rise to a large misfit of the structure function $R = \sigma_L/\sigma_T$ to the experimental data of L.W. Whitlow [78]. Even when taking into account the fact that all measurements of R suffer from large experimental errors due to the weak dependence of the deep inelastic cross section for charged leptons on R, the size of the misfit remains unacceptable. It indicates a shortcoming of the statistical model in its present form to reproduce the spin structure of the proton.

Appendix A

Kinematics for Gluon Emission from a Quark

In this appendix we introduce kinematical quantities for the specific process of gluon emission from a quark. In Section D.2 some of these quantities are written in a generalized form in order to be in accordance with our convention for treating the general four-particle process.

According to the momentum assignments in Figure 3.2 one has

$$\gamma^*(q) + q(k) \rightarrow q(k') + g(p).$$

In this work we have

$$q^2 < 0,\ k^2 = k'^2 = 0 \quad \text{and} \quad p^2 = m^2. \tag{A.1}$$

The latter two relations regularize both infrared and collinear singularities. In the rest frame of the heat bath we choose the z axis to be along the direction of the virtual photon:

$$q = (\nu, 0, 0, q_z) \tag{A.2}$$

and

$$q^2 \equiv -Q^2 = \nu^2 - q_z^2 < 0 \tag{A.3}$$

The momenta of the other particles are

$$\begin{aligned} k &= (k_0, \vec{k}) \\ k' &= (k'_0, \vec{k'}) \\ p &= (p_0, \vec{p}) \end{aligned} \tag{A.4}$$

where, due to the assumption of masslessness for the quarks,

$$k_0 = |\vec{k}| \quad \text{and} \quad k'_0 = |\vec{k'}|.$$

The conservation laws are

$$\nu + k_0 = k'_0 + p_0 \tag{A.5}$$

and

$$\vec{q} + \vec{k} = \vec{k'} + \vec{p}. \tag{A.6}$$

The invariant variables are

$$s = (k+q)^2 = (k'+p)^2$$

$$t = (k'-q)^2 = (k-p)^2.$$

Inequalities can be derived in the center-of-mass frame which show that s and t are always not equal to zero for $m^2 > 0$ (However, it has to be taken into account that, for some of the other four-particle processes, s and t can become equal to zero as shown in Section D.2):

$$s = (k'+p)^2 \overset{\text{c.m.}}{=} 2k'_0(p_0 + |\vec{p}|) + m^2 > 0, \tag{A.7}$$

trivially. The proof that $t < 0$ is somewhat longer:

$$q_0 \overset{\text{c.m.}}{=} \frac{s+q^2}{2\sqrt{s}}$$

$$|\vec{q}| \overset{\text{c.m.}}{=} \frac{s-q^2}{2\sqrt{s}}$$

and

$$s = (k'+p)^2 \overset{\text{c.m.}}{=} (k'_0 + p_0)^2 \tag{A.8}$$

but

$$|\vec{p}| \overset{\text{c.m.}}{=} |\vec{k'}| = k'_0$$

From the latter equation and eq. (A.7) we can write

$$s \overset{\text{c.m.}}{=} 2k'_0(p_0 + k'_0) + m^2.$$

The latter equation and eq. (A.8) lead to

$$k'_0 \overset{\text{c.m.}}{=} \frac{s-m^2}{2\sqrt{s}}.$$

Now

$$t = (q-k')^2 = q^2 - 2k'_0 q_0 + 2k'_0|\vec{q}|\cos\theta_{\vec{k'}\vec{q}}$$

and therefore

$$t_{\max} = q^2 - 2k'_0(q_0 - |\vec{q}|) \stackrel{\text{c.m.}}{=} q^2 - \frac{s - m^2}{\sqrt{s}}\left(\frac{q^2}{\sqrt{s}}\right) = \frac{m^2 q^2}{s} < 0$$

from which the strict inequality, $t < 0$, follows.

The cosines of the angles of the quark directions relative to that of the virtual photon as shown in Figure 3.3 are

$$z \equiv \frac{\vec{k}.\vec{q}}{k_0 q_z} = \cos\theta$$

$$z' \equiv \frac{\vec{k}'.\vec{q}}{k'_0 q_z} = \cos\theta'$$

For the purpose of angular integration, the invariants s and t in terms of these angles are

$$s = -2k_0 q_z(z - d) \tag{A.9}$$

$$t = 2k'_0 q_z(z' - l) \tag{A.10}$$

where

$$d \equiv \frac{q^2 + 2k_0\nu}{2k_0 q_z} \tag{A.11}$$

$$l \equiv \frac{-q^2 + 2k'_0\nu}{2k'_0 q_z}. \tag{A.12}$$

Appendix B

More Details on the Integration over Polar Angles for Gluon Emission from a Quark

In Subsections (a),(b),(c),(d) and (e) of this appendix we prove eqs. (3.69), (3.81), (3.83), (3.85) and (3.91) , respectively. In Subsection (f) we prove the relations in (3.105), (3.106), (3.114), (3.116) and (3.117). In Subsection (g) we prove all the relations in (3.118).

(a) Eq. (3.69) is derived from eq. (3.67) as follows:

$$A_0 = \int_a^b dz' \frac{1}{\sqrt{(z' - \cos\theta_+)(\cos\theta_- - z')}}$$

but

$$(z' - \cos\theta_+)(\cos\theta_- - z') = -\left[z' - \frac{\cos\theta_+ + \cos\theta_-}{2}\right]^2 + \frac{(\cos\theta_+ - \cos\theta_-)^2}{4}. \quad \text{(B.1)}$$

Let

$$x = z' - \frac{\cos\theta_+ + \cos\theta_-}{2} = z' - \cos\rho\cos\beta \quad \text{(B.2)}$$

$$x_1 = a - \cos\rho\cos\beta \quad ; \quad x_2 = b - \cos\rho\cos\beta \quad \text{(B.3)}$$

$$c = \frac{\cos\theta_+ - \cos\theta_-}{2} = \sin\rho\sin\beta. \quad \text{(B.4)}$$

Then

$$A_0 = \int_{x_1}^{x_2} \frac{dx}{\sqrt{c^2 - x^2}} = \int_{x_1/c}^{x_2/c} \frac{dy}{\sqrt{1 - y^2}} \quad \text{(B.5)}$$

where $y = x/c$ so that

$$A_0 = \arcsin y\Big|_{x_1/c}^{x_2/c} = \arcsin\left[\frac{z' - \cos\rho\cos\beta}{\sin\rho\sin\beta}\right]\Bigg|_{z'=a}^{z'=b} \tag{B.6}$$

which is the result given in eq. (3.69).

(b) Eq. (3.81) is derived from eq. (3.77) as follows: Let

$$x = \frac{1}{z' - l}$$

in eq. (3.77). Then

$$\begin{aligned} A_{-1} &= \frac{1}{2k_0' q_z}\int_{(a-l)^{-1}}^{(b-l)^{-1}} \frac{-x^{-2}dx}{x^{-1}\sqrt{-\gamma(l+\frac{1}{x},\cos\beta,\cos\rho)}} \\ &= \frac{-1}{2k_0' q_z}\int_{(a-l)^{-1}}^{(b-l)^{-1}} \frac{dx}{x\sqrt{-\gamma(l+\frac{1}{x},\cos\beta,\cos\rho)}} \end{aligned}$$

but, since we have from (3.80) that $z' < l$, we can deduce that

$$\begin{aligned} x &= \frac{1}{z'-l} < 0 \\ \Rightarrow \quad x &= -\sqrt{x^2}. \end{aligned}$$

The latter equation enables us to write

$$\begin{aligned} A_{-1} &= \frac{1}{2k_0' q_z}\int_{(a-l)^{-1}}^{(b-l)^{-1}} dx \\ &\quad \times \left[\sqrt{x^2(1-\cos^2\beta-\cos^2\rho-l^2+2l\cos\beta\cos\rho)+2x(\cos\beta\cos\rho-l)-1}\right]^{-1} \\ &= \frac{1}{2k_0' q_z\sqrt{\gamma(l,\cos\beta,\cos\rho)}}\int_{(a-l)^{-1}}^{(b-l)^{-1}} dx \\ &\quad \times \left[-x^2+\frac{2x(\cos\beta\cos\rho-l)}{\gamma(l,\cos\beta,\cos\rho)}-\frac{1}{\gamma(l,\cos\beta,\cos\rho)}\right]^{-1/2} \end{aligned} \tag{B.7}$$

where the factor $[\gamma(l,\cos\beta,\cos\rho)]^{-1/2}$ has been moved to the left of the integral sign in the latter step. This factor is well defined since

$$\gamma(l,\cos\beta,\cos\rho) > 0 \tag{B.8}$$

which follows from the fact that [see (3.78)] $l > \cos(\rho-\beta)$ as may be seen from Figure 3.7 if we were to redraw the graph as $-\gamma(l,\cos\beta,\cos\rho)$ versus l instead of $-\gamma(z',\cos\beta,\cos\rho)$ versus z'.

For convenience we define

$$G = \gamma(l, \cos\beta, \cos\rho).$$

Then

$$\begin{aligned} A_{-1} &= \frac{1}{2k_0' q_z \sqrt{G}} \int_{(a-l)^{-1}}^{(b-l)^{-1}} \frac{dx}{\sqrt{(-1)\,[x^2 - 2x(\cos\beta\cos\rho - l)/G + 1/G]}} \\ &= \frac{1}{2k_0' q_z \sqrt{G}} \int_{y_1}^{y_2} \frac{dy}{\sqrt{(-1)\,[y^2 - Q]}} \end{aligned}$$

where

$$\begin{aligned} y &= x - \frac{(\cos\beta\cos\rho - l)}{G} \\ Q &= \frac{(\cos\beta\cos\rho - l)^2 - G}{G^2} \\ &= \frac{\sin^2\rho\sin^2\beta}{G^2}. \end{aligned} \tag{B.9}$$

But

$$\sqrt{Q} = \sqrt{\frac{\sin^2\rho\sin^2\beta}{G^2}} = +\frac{\sin\rho\sin\beta}{G} \tag{B.10}$$

since $G > 0$ [see (B.8)] and $\sin\rho\sin\beta \geq 0$ as may be seen from (3.71) and (3.72). Thus

$$\begin{aligned} A_{-1} &= \frac{1}{2k_0' q_z \sqrt{G}} \int_{y_1}^{y_2} dy \left\{ \sqrt{(-1)\frac{\sin^2\rho\sin^2\beta}{G^2}\left[\frac{y^2G^2}{\sin^2\rho\sin^2\beta} - 1\right]} \right\}^{-1} \\ &= \frac{1}{2k_0' q_z \sqrt{G}} \frac{G}{\sin\rho\sin\beta} \int_{y_1}^{y_2} dy \left\{ \sqrt{1 - \frac{y^2G^2}{\sin^2\rho\sin^2\beta}} \right\}^{-1} \\ &= \frac{1}{2k_0' q_z \sqrt{G}} \int_{y_1'}^{y_2'} \frac{dy'}{\sqrt{1 - y'^2}} \end{aligned} \tag{B.11}$$

where

$$y' = yG/(\sin\rho\sin\beta) \tag{B.12}$$

and, since

$$\begin{aligned} G &= l^2 + \cos^2\rho + \cos^2\beta - 2l\cos\rho\cos\beta - 1 \\ &= -(1 - \cos^2\beta)(1 - \cos^2\rho) + (l - \cos\rho\cos\beta)^2 \\ &= -\sin^2\beta\sin^2\rho + (l - \cos\rho\cos\beta)^2, \end{aligned}$$

$$\begin{aligned} y_1' &= \frac{G}{\sin\rho\sin\beta}\left\{\frac{1}{\cos(\rho+\beta) - l} - \frac{\cos\beta\cos\rho - l}{G}\right\} \\ &= \frac{-\sin^2\beta\sin^2\rho + (l - \cos\rho\cos\beta)^2 + (l - \cos\rho\cos\beta)(\cos\rho\cos\beta - \sin\rho\sin\beta - l)}{\sin\rho\sin\beta(\cos\rho\cos\beta - \sin\rho\sin\beta - l)} \\ &= 1 \end{aligned} \tag{B.13}$$

and, similarly, $y'_2 = -1$. Thus

$$\begin{aligned} A_{-1} &= \frac{-1}{2k'_0 q_z \sqrt{G}} \int_{-1}^{1} \frac{dy'}{\sqrt{1-y'^2}} \\ &= \frac{-\pi}{2k'_0 q_z \sqrt{\gamma(l, \cos\beta, \cos\rho)}} \end{aligned} \tag{B.14}$$

which is the result given in eq. (3.81).

(c) Eq. (3.83) is derived from eq. (3.82) as follows:

$$A_1 = 2k'_0 q_z (A_{1a} - l A_{1b})$$

where

$$\begin{aligned} A_{1a} &= \int_a^b dz' \frac{z'}{\sqrt{-\gamma(z', \cos\beta, \cos\rho)}} \\ A_{1b} &= \int_a^b dz' \frac{1}{\sqrt{-\gamma(z', \cos\beta, \cos\rho)}}. \end{aligned}$$

The result for A_{1b} is the same as that for A_0 as may be seen from eqs. (3.66) and (3.76):

$$A_{1b} = A_0 = \pi.$$

The result for A_{1a} is obtained by making use in line (B.15) of the same step that led from eq. (3.66) to eq. (3.67) and, in line (B.16), using eq. (B.1) and the same change of variables as used at eq. (B.2):

$$A_{1a} = \int_a^b dz' \frac{z'}{\sqrt{(z' - \cos\theta_+)(\cos\theta_- - z')}} \tag{B.15}$$

$$= \int_{x_1}^{x_2} dx \frac{x + (\cos\theta_+ + \cos\theta_-)/2}{\sqrt{c^2 - x^2}} \tag{B.16}$$

where x_1, x_2 and c are given in (B.3) and (B.4). Eqs. (3.68), (B.5) and (3.76) enable us to write

$$\frac{\cos\theta_+ + \cos\theta_-}{2} \int_{x_1}^{x_2} dx \frac{1}{\sqrt{c^2 - x^2}} = \pi \cos\rho \cos\beta.$$

Furthermore,

$$\int_{x_1}^{x_2} dx \frac{x}{\sqrt{c^2 - x^2}} = 0$$

since $x_1 = -\sin\rho\sin\beta$, $x_2 = \sin\rho\sin\beta$ and the integrand is an odd function of x. Thus,

$$\begin{aligned} A_{1a} &= \pi\cos\rho\cos\beta \\ \Rightarrow \quad A_1 &= 2k_0' q_z (A_{1a} - lA_{1b}) \\ &= 2k_0' q_z \pi(\cos\rho\cos\beta - l) \end{aligned}$$

which is the result given in eq. (3.83).

(d) In the following, we sketch the proof of the identity in eq. (3.85).

We first prove that all the z dependence can be shuffled into the arguments of the gamma function:

$$|\vec{q}+\vec{k}|^2\gamma(z',\cos\beta,\cos\rho) = k_0^2\gamma(z',z,\cos\alpha) \tag{B.17}$$

where, at this intermediate step, it is to be noted that the left hand side of eq. (B.17) has a z' where that of eq. (3.85) has an l and where $\cos\alpha$ is given in eqs. (B.19) and (B.20). From eq. (3.42) there follows that

$$|\vec{q}+\vec{k}|^2\gamma(z',\cos\beta,\cos\rho) = -|\vec{q}+\vec{k}|^2\sin^2\phi^-\sin^2\beta\sin^2\theta'. \tag{B.18}$$

By following steps similar to those surrounding eq. (3.40) we have, in the reference frame shown in Figure 3.4,

$$\begin{aligned} \vec{k}' &= k_0'(\sin\theta', 0, \cos\theta') \\ \vec{k} &= k_0(\sin\theta\cos\phi^-, \sin\theta\sin\phi^-, \cos\theta) \\ \Rightarrow \quad \cos\alpha &\equiv \frac{\vec{k}.\vec{k}'}{k_0 k_0'} = \sin\theta'\sin\theta\cos\phi^- + \cos\theta\cos\theta' \qquad \text{(B.19)} \\ \Rightarrow \quad \cos\phi^- &= \frac{\cos\alpha - \cos\theta\cos\theta'}{\sin\theta'\sin\theta} \\ \Rightarrow \quad \sin^2\phi^- &= 1 - \cos^2\phi^- \\ &= \frac{-\gamma(\cos\theta,\cos\theta',\cos\alpha)}{\sin^2\theta\sin^2\theta'} \end{aligned}$$

where the latter step is the same as the one leading to eq. (3.42). The right hand side of eq. (B.18) becomes

$$-|\vec{q}+\vec{k}|^2\sin^2\phi^-\sin^2\beta\sin^2\theta' = |\vec{q}+\vec{k}|^2\gamma(z',\cos\theta,\cos\alpha)\frac{\sin^2\beta}{\sin^2\theta}.$$

But, as may be seen from Figure 3.4,

$$\frac{\sin^2\beta}{\sin^2\theta} = \frac{|\vec{k}|^2}{|\vec{q}+\vec{k}|^2}$$

so that we obtain ($|\vec{k}| = k_0$):

$$-|\vec{q}+\vec{k}|^2 \sin^2\phi^- \sin^2\beta \sin^2\theta' = k_0^2\gamma(z', \cos\theta, \cos\alpha)$$

and, thereby, eq. (B.17) is proven.

From eq. (B.19) and

$$\begin{aligned} |\vec{p}|^2 &= |\vec{q}+\vec{k}-\vec{k}'|^2 = q_z^2 + k_0^2 + {k_0'}^2 + 2\vec{q}.\vec{k} - 2\vec{q}.\vec{k}' - 2\vec{k}.\vec{k}' \\ &= q_z^2 + k_0^2 + {k_0'}^2 + 2q_z k_0 z - 2q_z k_0' z' - 2k_0 k_0' \cos\alpha \end{aligned}$$

there follows that

$$\cos\alpha = \frac{k_0^2 + {k_0'}^2 + q_z^2 - |\vec{p}|^2}{2k_0k_0'} + z\frac{q_z}{k_0'} - z'\frac{q_z}{k_0}. \tag{B.20}$$

By substituting z' by l in eq. (B.17) we obtain

$$|\vec{q}+\vec{k}|^2\gamma(l, \cos\beta, \cos\rho) = k_0^2\gamma(l, z, \cos\alpha_l) \tag{B.21}$$

where $\cos\alpha_l$ is obtained by replacing z' by l in eq. (B.20):

$$\cos\alpha_l = \frac{k_0^2 + {k_0'}^2 + q_z^2 - |\vec{p}|^2}{2k_0k_0'} + z\frac{q_z}{k_0'} - l\frac{q_z}{k_0}. \tag{B.22}$$

The identity in eq. (3.85) can now be proven by algebraic manipulations which involve replacing, in the right hand side of eq. (B.21), l by its expression given in eq. (A.12), $\cos\alpha_l$ by its expression given in eq. (B.22) and subsequently substituting l and $|\vec{p}|^2$ appearing in $\cos\alpha_l$ by the expression in eq. (A.12) and $|\vec{p}|^2 = p_0^2 - m^2 = (\nu + k_0 - k_0')^2 - m^2$, respectively.

(e) Eq. (3.91) is derived from eq. (3.89) as follows: Let

$$\tau' \equiv \frac{1}{z-d}$$

$$\Rightarrow \quad z = \frac{1}{\tau'} + d \quad ; \quad dz = \frac{-d\tau'}{\tau'^2}$$

$$\begin{aligned} \Rightarrow \quad E &\equiv \int_{z_m}^{z_M} \frac{dz}{(z-d)\sqrt{\gamma(z,H,J)}} \\ &= \int_{\tau'(z_m)}^{\tau'(z_M)} \frac{-d\tau'}{\tau'^2}\tau' \left\{\frac{1}{\tau'^2} + \frac{2d}{\tau'} + d^2 + H^2 + J^2 - \frac{2HJ}{\tau'} - 2dHJ - 1\right\}^{-\frac{1}{2}} \\ &= \int_{\tau'(z_m)}^{\tau'(z_M)} d\tau' \left[1 + 2d\tau' + (d^2 + H^2 + J^2)\tau'^2 - 2HJ\tau' - 2dHJ\tau'^2 - \tau'^2\right]^{-\frac{1}{2}} \end{aligned}$$

where, in the latter step, we made use of the fact that

$$\frac{1}{\tau'} = -\sqrt{\frac{1}{\tau'^2}}$$

since we have from eqs. (A.7) and (A.9) that

$$\frac{1}{\tau'} = z - d < 0.$$

The gamma function defined in eq. (3.43) can be identified in the expression for E:

$$\begin{aligned} E &= \int_{\tau'(z_m)}^{\tau'(z_M)} d\tau' \left[\tau'^2\gamma(d,H,J) + 2\tau'(d-HJ) + 1\right]^{-\frac{1}{2}} \\ &= \int_{\tau'(z_m)}^{\tau'(z_M)} d\tau' \left(\gamma(d,H,J)\left\{\left[\tau' - \frac{HJ-d}{\gamma(d,H,J)}\right]^2 - \frac{(d-HJ)^2}{[\gamma(d,H,J)]^2} + \frac{1}{\gamma(d,H,J)}\right\}\right)^{-\frac{1}{2}} \\ &= \int_{\tau(z_m)}^{\tau(z_M)} d\tau \left\{\tilde{c}\left(\tau^2 - \frac{(d-HJ)^2 - \tilde{c}}{\tilde{c}^2}\right)\right\}^{-\frac{1}{2}} \end{aligned}$$

where, in the latter step, $\tilde{c}$ is the gamma function as defined in eq. (3.92) and we introduced the change of variables [see eq. (3.90)]:

$$\tau = \tau' - \frac{HJ-d}{\tilde{c}} = \frac{1}{z-d} - \frac{HJ-d}{\tilde{c}}.$$

But

$$\frac{(d-HJ)^2 - \tilde{c}}{\tilde{c}^2} = \frac{H^2J^2 - H^2 - J^2 + 1}{\tilde{c}^2} = \frac{-\triangle}{4\tilde{c}^2}$$

with $\triangle$ defined in eq. (3.93) so that

$$E = \int_{\tau(z_m)}^{\tau(z_M)} d\tau \left[\tilde{c}\left(\tau^2 + \frac{\triangle}{4\tilde{c}^2}\right)\right]^{-\frac{1}{2}}.$$

Thereby the derivation of eq. (3.91) from eq. (3.89) is completed.

(f) In this subsection we prove the relations in (3.105), (3.106) and (3.114)– (3.117).

We start by proving eq. (3.115). From the last paragraph before Section 3.4.4 we have $z_M = z_U$ in regions A, B, C, and D and from eqs. (3.90), (3.49) and (A.11) we have that

$$\begin{aligned} \tau(z_U) &= \frac{1}{z_U - d} - \frac{HJ-d}{\tilde{c}} \\ &= \frac{2k_0q_z}{\left(k_0' + \sqrt{p_0^2 - m^2}\right)^2 - k_0^2 - q_z^2 - q^2 - 2k_0\nu} - \frac{HJ-d}{\tilde{c}}. \end{aligned} \tag{B.23}$$

But

$$\begin{aligned}
&\left(k_0' + \sqrt{p_0^2 - m^2}\right)^2 - k_0^2 - q_z^2 - q^2 - 2k_0\nu \\
&= \left(k_0' + p_0\sqrt{1 - \frac{m^2}{p_0^2}}\right)^2 - (k_0 + \nu)^2 \\
&= \left[k_0' + p_0\left(1 - \frac{m^2}{2p_0^2}\right)\right]^2 - (k_0' + p_0)^2 + \mathrm{O}(m^4) \\
&= -m^2\frac{k_0' + p_0}{p_0} + \mathcal{O}(m^4) \qquad \text{(B.24)}
\end{aligned}$$

where the penultimate step was obtained by means of a Taylor expansion in the limit $m \to 0$ and $k_0 + \nu = k_0' + p_0$.

We also obtain by making use of, amongst others, eq. (3.98),

$$\begin{aligned}
\tilde{c} &= d^2 + H^2 + J^2 - 1 - 2dHJ \\
&= \frac{(q^2)^2 + 4k_0\nu q^2 + 4k_0^2\nu^2}{4k_0^2q_z^2} + 1 + \frac{m^2}{2k_0(k_0' - \nu)} \\
&\quad + \frac{m^4}{4k_0^2(k_0' - \nu)^2} + \frac{q^2(2k_0' - \nu - q_z)(2k_0' - \nu + q_z)}{4q_z^2(k_0' - \nu)^2} \\
&\quad - \frac{q^2 + 2k_0\nu}{k_0q_z}\left(1 + \frac{m^2}{2k_0(k_0' - \nu)}\right)\left(\frac{q^2}{2q_z(k_0' - \nu)} + \frac{\nu}{q_z}\right) \\
&\equiv f_{\tilde{c}}(m^2) \\
&= f_{\tilde{c}}(0) + \mathcal{O}(m^2)
\end{aligned}$$

where

$$\begin{aligned}
f_{\tilde{c}}(0) &= \frac{(q^2)^2 + 4k_0\nu q^2 + 4k_0^2\nu^2}{4k_0^2q_z^2} + 1 + \frac{q^2(2k_0' - \nu - q_z)(2k_0' - \nu + q_z)}{4q_z^2(k_0' - \nu)^2} \\
&\quad - \frac{q^2 + 2k_0\nu}{k_0q_z}\left(\frac{q^2}{2q_z(k_0' - \nu)} + \frac{\nu}{q_z}\right).
\end{aligned}$$

Substitution of k_0' by $k_0' = \nu + k_0 - p_0$ in the numerators of the latter expression leads to

$$f_{\tilde{c}}(0) = \frac{(-p_0q^2)^2}{4k_0^2q_z^2(k_0' - \nu)^2}$$

$$\Rightarrow \quad \tilde{c} = \left(\frac{-q^2p_0}{2q_zk_0(k_0' - \nu)}\right)^2 + \mathcal{O}(m^2). \qquad \text{(B.25)}$$

Thereby eq. (3.115) is proven.

Next we prove eq. (3.114). We have that

$$\begin{aligned} HJ - d &= \left(1 + \frac{m^2}{2k_0(k_0' - \nu)}\right)\left(\frac{q^2}{2q_z(k_0' - \nu)} + \frac{\nu}{q_z}\right) - \frac{q^2 + 2k_0\nu}{2k_0 q_z} \\ &= \frac{p_0 q^2}{2k_0 q_z(k_0' - \nu)} + \mathcal{O}(m^2). \end{aligned} \tag{B.26}$$

From eqs. (B.23)–(B.26) it follows that

$$\tau(z_U) = \frac{-2k_0 q_z p_0}{m^2(k_0' + p_0)} + \mathcal{O}(m^0). \tag{B.27}$$

From eqs. (3.95), (3.96) and (3.98) it follows that

$$\begin{aligned} \triangle &= -4\frac{m^2}{2k_0(k_0' - \nu)}\left(2 + \frac{m^2}{2k_0(k_0' - \nu)}\right)\frac{q^2(2k_0' - \nu - q_z)(2k_0' - \nu + q_z)}{4q_z^2(k_0' - \nu)^2} \\ &= -\frac{m^2 q^2(2k_0' - \nu - q_z)(2k_0' - \nu + q_z)}{k_0(k_0' - \nu)^3 q_z^2} + \mathcal{O}(m^4). \end{aligned} \tag{B.28}$$

Thus, from eqs. (B.25), (B.27) and (B.28), it follows that

$$\begin{aligned} \frac{2\tilde{c}|\tau(z_U)|}{\sqrt{|\triangle|}} &= 2\left(\frac{-q^2 p_0}{2q_z k_0(k_0' - \nu)}\right)^2 \left|\frac{-2k_0 q_z p_0}{m^2(k_0' + p_0)}\right| \\ &\quad \times \left|-\frac{m^2 q^2(2k_0' - \nu - q_z)(2k_0' - \nu + q_z)}{k_0(k_0' - \nu)^3 q_z^2}\right|^{-1/2} + \mathcal{O}(m^{-1}). \end{aligned} \tag{B.29}$$

In order to simplify the latter expression further we bear in mind, in the following derivations, that

$$(2k_0' - \nu - q_z) \begin{cases} > 0 & \text{in regions A,B} \\ < 0 & \text{in regions C,D} \end{cases}$$

$$2k_0' - \nu + q_z > 0 \text{ in regions A,B,C,D (since } q_z > \nu)$$

$$(k_0' - \nu) \begin{cases} > 0 & \text{in regions A,B and in regions C,D if } k_0' > \nu \\ < 0 & \text{in regions C,D if } k_0' < \nu \end{cases}$$

$$k_0' + p_0 = k_0 + \nu$$

k_0, ν, k_0', p_0, q_z and m are each ≥ 0 for the process under consideration.

Thus, in regions A,B,C,D, we have

$$\begin{aligned} \frac{2\tilde{c}|\tau(z_U)|}{\sqrt{|\triangle|}} &= 2\frac{(-q^2)^2 p_0^2}{4q_z^2 k_0^2(k_0' - \nu)^2}\frac{2k_0 q_z p_0}{m^2(k_0' + p_0)} \\ &\quad \times \left(\frac{k_0(k_0' - \nu)^2|k_0' - \nu|q_z^2}{-q^2 m^2|2k_0' - \nu - q_z|(2k_0' - \nu + q_z)}\right)^{1/2} + \mathcal{O}(m^{-1}) \end{aligned}$$

$$
\begin{aligned}
&= \frac{-q^2 p_0^3}{(k_0+\nu)m^3}\left(\frac{(-q^2)^2 k_0^2 q_z^2}{q_z^4 k_0^4 (k_0'-\nu)^4}\frac{k_0(k_0'-\nu)^2|k_0'-\nu|q_z^2}{(-q^2)|2k_0'-\nu-q_z|(2k_0'-\nu+q_z)}\right)^{1/2} \\
&\quad +\mathcal{O}(m^{-1}) \\
&= \frac{-q^2 p_0^3}{(k_0+\nu)m^3}\left(\frac{-q^2}{k_0(2k_0'-\nu+q_z)|k_0'-\nu||q_z+\nu-2k_0'|}\right)^{1/2}+\mathcal{O}(m^{-1}).
\end{aligned}
$$

Thereby eq. (3.114) is proven.

Next we prove eq. (3.116). From the last paragraph before Section 3.4.4 we have $z_{\rm m} = z_{\rm L}$ in regions A,D. Following steps similar to those followed in order to obtain eqs. (B.23) and (B.24), we obtain

$$
\tau(z_{\rm L}) = \frac{2k_0 q_z}{\left(k_0' - \sqrt{p_0^2-m^2}\right)^2 - k_0^2 - q_z^2 - q^2 - 2k_0\nu} - \frac{HJ-d}{\tilde{c}} \tag{B.30}
$$

and

$$
\begin{aligned}
&\left(k_0' - \sqrt{p_0^2-m^2}\right)^2 - k_0^2 - q_z^2 - q^2 - 2k_0\nu \\
&= {k_0'}^2 - 2k_0'p_0 + 2k_0'\frac{m^2}{p_0} + p_0^2 - {k_0'}^2 - 2k_0'p_0 - p_0^2 + \mathcal{O}(m^4) \\
&= -4k_0'p_0 + \mathcal{O}(m^2).
\end{aligned} \tag{B.31}
$$

From eqs. (B.30), (B.31), (B.25) and (B.26) it follows that

$$
\begin{aligned}
\tau(z_{\rm L}) &= \frac{2k_0q_z}{-4k_0'p_0} - \frac{p_0q^2}{2k_0q_z(k_0'-\nu)}\left(\frac{2q_zk_0(k_0'-\nu)}{-q^2p_0}\right)^2 + \mathcal{O}(m^2) \\
&= \frac{k_0q_zq^2 + 4k_0'q_zk_0(k_0'-\nu)}{-2k_0'p_0q^2} + \mathcal{O}(m^2).
\end{aligned} \tag{B.32}
$$

Thus, from eqs. (B.25), (B.32) and (B.28), it follows that

$$
\begin{aligned}
\frac{2\tilde{c}|\tau(z_{\rm L})|}{\sqrt{|\triangle|}} &= 2\left(\frac{-q^2p_0}{2q_zk_0(k_0'-\nu)}\right)^2\left|\frac{k_0q_zq^2+4k_0'q_zk_0(k_0'-\nu)}{-2k_0'p_0q^2}\right| \\
&\quad \times\left|-\frac{m^2q^2(2k_0'-\nu-q_z)(2k_0'-\nu+q_z)}{k_0(k_0'-\nu)^3q_z^2}\right|^{-1/2} + \mathcal{O}(m) \\
&= \frac{(q^2)^2p_0}{4q_zk_0(k_0'-\nu)^2}\left(\frac{[q^2+4k_0'(k_0'-\nu)]^2}{{k_0'}^2(q^2)^2}\right)^{1/2} \\
&\quad \times\left(\frac{k_0(k_0'-\nu)^2|k_0'-\nu|q_z^2}{-q^2m^2|2k_0'-\nu-q_z|(2k_0'-\nu+q_z)}\right)^{1/2} + \mathcal{O}(m) \\
&= \mathcal{O}(m) + \frac{p_0}{4mk_0'}\left(\frac{(q^2)^4}{q_z^2k_0^2(k_0'-\nu)^4}\right)^{1/2}
\end{aligned}
$$

$$\times \left(\frac{[q^2 + 4k_0'(k_0' - \nu)]^2}{(q^2)^2} \frac{k_0(k_0' - \nu)^2 |k_0' - \nu| q_z^2}{-q^2 |2k_0' - \nu - q_z|(2k_0' - \nu + q_z)} \right)^{1/2}$$

But

$$q^2 + 4k_0'(k_0' - \nu) = (2k_0' - \nu + q_z)(2k_0' - \nu - q_z)$$

$$\begin{aligned} \Rightarrow \quad \frac{2\tilde{c}|\tau(z_L)|}{\sqrt{|\Delta|}} &= \frac{p_0}{4mk_0'} \left(\frac{-q^2}{k_0|k_0' - \nu|} \frac{(2k_0' - \nu + q_z)^2 |2k_0' - \nu - q_z|^2}{|2k_0' - \nu - q_z|(2k_0' - \nu + q_z)} \right)^{1/2} + \mathcal{O}(m) \\ &= \frac{p_0}{4mk_0'} \left(\frac{-q^2(2k_0' + q_z - \nu)|q_z + \nu - 2k_0'|}{k_0|k_0' - \nu|} \right)^{1/2} + \mathcal{O}(m). \end{aligned}$$

Thereby eq. (3.116) is proven.

Next we prove eq. (3.117). From the last paragraph before Section 3.4.4 we have $z_m = -1$ in regions B,C. From eqs. (3.90), (A.11), (B.25) and (B.26) we have that

$$\begin{aligned} \tau(-1) &= \frac{1}{-1-d} - \frac{HJ - d}{\tilde{c}} \\ &= \frac{2k_0 q_z}{-2k_0 q_z - q^2 - 2k_0\nu} - \frac{p_0 q^2}{2k_0 q_z (k_0' - \nu)} \frac{4q_z^2 k_0^2 (k_0' - \nu)^2}{(q^2)^2 p_0^2} + \mathcal{O}(m^2) \\ &= 2k_0 q_z \frac{q^2 p_0 - (k_0' - \nu)(-2k_0 q_z - q^2 - 2k_0\nu)}{(-2k_0 q_z - q^2 - 2k_0\nu) q^2 p_0} + \mathcal{O}(m^2) \end{aligned} \tag{B.33}$$

$$\begin{aligned} \Rightarrow \quad \frac{2\tilde{c}|\tau(-1)|}{\sqrt{|\Delta|}} &= 2 \frac{(q^2)^2 p_0^2}{4q_z^2 k_0^2 (k_0' - \nu)^2} 2k_0 q_z \left| \frac{q^2 p_0 - (k_0' - \nu)(-2k_0 q_z - q^2 - 2k_0\nu)}{(-2k_0 q_z - q^2 - 2k_0\nu) q^2 p_0} \right| \\ &\quad \times \left| - \frac{k_0 (k_0' - \nu)^3 q_z^2}{m^2 q^2 (2k_0' - \nu - q_z)(2k_0' - \nu + q_z)} \right|^{1/2} + \mathcal{O}(m^0) \\ &= \frac{(q^2)^2 p_0}{k_0 (k_0' - \nu)^2} \left| \frac{q^2 p_0 - (k_0' - \nu)(-2k_0 q_z - q^2 - 2k_0\nu)}{(-2k_0 q_z - q^2 - 2k_0\nu) q^2} \right| \\ &\quad \times \left| - \frac{k_0 (k_0' - \nu)^3}{m^2 q^2 (2k_0' - \nu - q_z)(2k_0' - \nu + q_z)} \right|^{1/2} + \mathcal{O}(m^0). \end{aligned}$$

The substitution of p_0 by $p_0 = \nu + k_0 - k_0'$ in one of the latter factors and the use of $q^2 = (\nu + q_z)(\nu - q_z)$ lead to

$$\left| \frac{q^2 p_0 - (k_0' - \nu)(-2k_0 q_z - q^2 - 2k_0\nu)}{(-2k_0 q_z - q^2 - 2k_0\nu) q^2} \right| = \left| \frac{q^2 k_0 - (k_0' - \nu) k_0 (-2q_z - 2\nu)}{(-2k_0 q_z - q^2 - 2k_0\nu) q^2} \right| \tag{B.34}$$

$$= \frac{k_0 (q_z + \nu)}{(q_z + \nu)} \left| \frac{(\nu - q_z) + 2(k_0' - \nu)}{(-2k_0 - \nu + q_z) q^2} \right| \tag{B.35}$$

and, since $k_0 \geq (q_z - \nu)/2$ as may be seen from Figure 3.6, we have that $2k_0 - q_z + \nu \geq 0$ so that we can write

$$\begin{aligned}
\frac{2\tilde{c}|\tau(-1)|}{\sqrt{|\triangle|}} &= \mathcal{O}(m^0) + \frac{p_0}{m(2k_0 - q_z + \nu)} \\
&\quad \times \left| \frac{(q^2)^4}{k_0^2(k_0' - \nu)^4} \frac{k_0^2(2k_0' - \nu - q_z)^2}{(q^2)^2} \frac{k_0(k_0' - \nu)^3}{(-q^2)(2k_0' - \nu - q_z)(2k_0' - \nu + q_z)} \right|^{1/2} \\
&= \frac{p_0}{m(2k_0 - q_z + \nu)} \left| \frac{-q^2 k_0(2k_0' - \nu - q_z)}{(k_0' - \nu)(2k_0' - \nu + q_z)} \right|^{1/2} + \mathcal{O}(m^0) \\
&= \frac{p_0}{m(2k_0 - q_z + \nu)} \left(\frac{-q^2 k_0 |2k_0' - \nu - q_z|}{|k_0' - \nu|(2k_0' + q_z - \nu)} \right)^{1/2} + \mathcal{O}(m^0).
\end{aligned}$$

Thereby eq. (3.117) is proven.

Next we prove the relations in (3.105) and (3.106).

From eq. (B.27) we immediately see that $\tau(z_{\mathrm{U}}) < 0$ and since $z_{\mathrm{M}} = z_{\mathrm{U}}$ in regions A,B,C,D we have proven that $\tau(z_{\mathrm{M}}) < 0$ in regions A,B,C,D.

To prove that $\tau(z_{\mathrm{m}}) > 0$ in regions A,B and $\tau(z_{\mathrm{m}}) < 0$ in regions C,D we must bear in mind that $z_{\mathrm{m}} = z_{\mathrm{L}}$ in regions A,D and that $z_{\mathrm{m}} = -1$ in regions B,C. Thus we have to prove that

$$\tau(z_{\mathrm{L}}) \begin{cases} > 0 & \text{in region A} \\ < 0 & \text{in region D} \end{cases} \tag{B.36}$$

$$\tau(-1) \begin{cases} > 0 & \text{in region B} \\ < 0 & \text{in region C.} \end{cases} \tag{B.37}$$

According to eq. (B.32) we have in regions A,D:

$$\tau(z_{\mathrm{L}}) = \frac{k_0 q_z [q^2 + 4k_0'(k_0' - \nu)]}{-2k_0' p_0 q^2} + \mathcal{O}(m^2) \tag{B.38}$$

but

$$\frac{k_0 q_z}{-2k_0' p_0 q^2} > 0 \quad \text{in regions A,B,C,D} \tag{B.39}$$

and

$$q^2 + 4k_0'(k_0' - \nu) = 4\left({k_0'}^2 - k_0'\nu + \frac{q^2}{4} \right)$$

where the roots of the equation, ${k_0'}^2 - k_0'\nu + (q^2/4) = 0$, are ${k_0'}^{\pm} = (\nu \pm q_z)/2$. Thus

$$q^2 + 4k_0'(k_0' - \nu) \begin{cases} > 0 & \text{if } k_0' \geq \frac{\nu + q_z}{2} \text{ which is the case for region A} \\ < 0 & \text{if } \frac{\nu - q_z}{2} \leq k_0' \leq \frac{\nu + q_z}{2} \text{ which is the case for region D} \end{cases} \tag{B.40}$$

and the relations in (B.36) may be seen to follow from the relations in (B.38), (B.39) and (B.40).

Next we prove the relations in (B.37). According to eqs. (B.33) and (B.35) we have in regions B,C:

$$\tau(-1) = 2k_0 q_z \frac{k_0}{p_0} \frac{2k_0' - \nu - q_z}{(-q^2)(2k_0 + \nu - q_z)} + \mathcal{O}(m^2) \tag{B.41}$$

But, as was motivated just after eq. (B.35), $2k_0 + \nu - q_z \geq 0$ and therefore

$$2k_0 q_z \frac{k_0}{p_0} \frac{1}{(-q^2)(2k_0 + \nu - q_z)} > 0. \tag{B.42}$$

But

$$2k_0' - \nu - q_z \quad \begin{cases} > 0 & \text{in region B} \\ < 0 & \text{in region C.} \end{cases} \tag{B.43}$$

Thus the relations in (B.37) may be seen to follow from the relations in (B.41), (B.42) and (B.43).

Thereby the proof of the relations in (3.105) and (3.106) is completed.

(g) The relations in (3.118) are derived from eqs. (3.112)- (3.117) as follows:

From eq. (3.115) we obtain for the common factor in eqs. (3.112) and (3.113):

$$\frac{-\pi}{2k_0 q_z^2 |k_0' - \nu| \sqrt{\tilde{c}}} = \frac{-\pi}{2k_0 q_z^2 |k_0' - \nu|} \frac{2q_z k_0 |k_0' - \nu|}{(-q^2) p_0} = \frac{\pi}{q_z p_0 q^2}. \tag{B.44}$$

In regions A and B we have, according to the relations in (3.112) and (3.105):

$$\begin{aligned} & \operatorname{arcsinh}\left(\frac{2\tilde{c}}{\sqrt{|\Delta|}}\tau(z_{\mathrm{m}})\right) - \operatorname{arcsinh}\left(\frac{2\tilde{c}}{\sqrt{|\Delta|}}\tau(z_{\mathrm{M}})\right) \\ = \; & \operatorname{arcsinh}\left(\frac{2\tilde{c}}{\sqrt{|\Delta|}}|\tau(z_{\mathrm{m}})|\right) - \operatorname{arcsinh}\left(-\frac{2\tilde{c}}{\sqrt{|\Delta|}}|\tau(z_{\mathrm{M}})|\right) \\ = \; & \operatorname{arcsinh}\left(\frac{2\tilde{c}}{\sqrt{|\Delta|}}|\tau(z_{\mathrm{m}})|\right) + \operatorname{arcsinh}\left(\frac{2\tilde{c}}{\sqrt{|\Delta|}}|\tau(z_{\mathrm{M}})|\right). \end{aligned} \tag{B.45}$$

Now

$$\begin{aligned} \mathrm{e}^x &= \sinh x + \cosh x = \sinh x + \sqrt{1 + \sinh^2 x} \\ \Rightarrow \quad x &= \ln\left(\sinh x + \sqrt{1 + \sinh^2 x}\right) \end{aligned}$$

and by letting x =arcsinh$y$ in the latter equation, we obtain a useful identity:

$$\operatorname{arcsinh} y = \ln\left(y + \sqrt{1 + y^2}\right). \tag{B.46}$$

This enables us to write the expression in eq. (B.45) in the form:

$$\begin{aligned}
&\operatorname{arcsinh}\left(\frac{2\tilde{c}}{\sqrt{|\Delta|}}|\tau(z_{\rm m})|\right)+\operatorname{arcsinh}\left(\frac{2\tilde{c}}{\sqrt{|\Delta|}}|\tau(z_{\rm M})|\right)\\
&= \ln\left\{\left(\frac{2\tilde{c}}{\sqrt{|\Delta|}}|\tau(z_{\rm m})|+\sqrt{1+\left(\frac{2\tilde{c}}{\sqrt{|\Delta|}}|\tau(z_{\rm m})|\right)^2}\right)\right.\\
&\quad\left.\times\left(\frac{2\tilde{c}}{\sqrt{|\Delta|}}|\tau(z_{\rm M})|+\sqrt{1+\left(\frac{2\tilde{c}}{\sqrt{|\Delta|}}|\tau(z_{\rm M})|\right)^2}\right)\right\}. \qquad \text{(B.47)}
\end{aligned}$$

From this point onwards we distinguish betweem the cases of region A and region B.

For region A the derivation proceeds as follows: By bearing in mind that the expressions in eqs. (3.114) and (3.116) are proportional to m^{-3} and m^{-1}, respectively, the expression in eq. (B.47) becomes

$$\begin{aligned}
&\operatorname{arcsinh}\left(\frac{2\tilde{c}}{\sqrt{|\Delta|}}|\tau(z_{\rm m})|\right)+\operatorname{arcsinh}\left(\frac{2\tilde{c}}{\sqrt{|\Delta|}}|\tau(z_{\rm M})|\right)\\
&= \ln\left(2\frac{2\tilde{c}}{\sqrt{|\Delta|}}|\tau(z_{\rm m})|2\frac{2\tilde{c}}{\sqrt{|\Delta|}}|\tau(z_{\rm M})|\right)\\
&= \ln\left(\frac{p_0}{2mk_0'}\sqrt{\frac{-q^2(2k_0'+q_z-\nu)|q_z+\nu-2k_0'|}{k_0|k_0'-\nu|}}\right.\\
&\quad\left.\times\frac{(-2)q^2p_0^3}{(k_0+\nu)m^3}\sqrt{\frac{-q^2}{k_0(2k_0'+q_z-\nu)|k_0'-\nu||q_z+\nu-2k_0'|}}\right)\\
&= \ln\left(\frac{p_0^4(q^2)^2}{m^4k_0k_0'(k_0+\nu)|k_0'-\nu|}\right). \qquad \text{(B.48)}
\end{aligned}$$

Thus the result for region A in eq. (3.118) follows from eqs. (3.112), (B.44), (B.45) and (B.48).

For region B we obtain, from eq. (B.47) and by bearing in mind that the expressions in eqs. (3.114) and (3.117) are proportional to m^{-3} and m^{-1}, respectively:

$$\begin{aligned}
&\operatorname{arcsinh}\left(\frac{2\tilde{c}}{\sqrt{|\Delta|}}|\tau(z_{\rm m})|\right)+\operatorname{arcsinh}\left(\frac{2\tilde{c}}{\sqrt{|\Delta|}}|\tau(z_{\rm M})|\right)\\
&= \ln\left(2\frac{2\tilde{c}}{\sqrt{|\Delta|}}|\tau(z_{\rm m})|2\frac{2\tilde{c}}{\sqrt{|\Delta|}}|\tau(z_{\rm M})|\right)\\
&= \ln\left(\frac{2p_0}{m(2k_0-q_z+\nu)}\sqrt{\frac{-q^2k_0|2k_0'-q_z-\nu|}{|k_0'-\nu|(2k_0'+q_z-\nu)}}\right.\\
&\quad\left.\times\frac{(-2)q^2p_0^3}{(k_0+\nu)m^3}\sqrt{\frac{-q^2}{k_0(2k_0'+q_z-\nu)|k_0'-\nu||q_z+\nu-2k_0'|}}\right)
\end{aligned}$$

$$= \ln\left(\frac{4p_0^4(q^2)^2}{m^4(k_0+\nu)|k_0'-\nu|(2k_0-q_z+\nu)(2k_0'+q_z-\nu)}\right). \qquad \text{(B.49)}$$

Thus the result for region B in eq. (3.118) follows from eqs. (3.112), (B.44), (B.45) and (B.49).

To prove the results for regions C and D in eq. (3.118) we have to, according to eqs. (3.112) and (3.113), contend with expressions in terms of arcsinh or arccosh according to whether $k_0' < \nu$ or $k_0' > \nu$, respectively.

For $k_0' < \nu$ in regions C and D we have, according to the relations in (3.112) and (3.106):

$$\begin{aligned} & \operatorname{arcsinh}\left(\frac{2\tilde{c}}{\sqrt{|\Delta|}}\tau(z_{\mathrm{m}})\right) - \operatorname{arcsinh}\left(\frac{2\tilde{c}}{\sqrt{|\Delta|}}\tau(z_{\mathrm{M}})\right) \\ = \; & \operatorname{arcsinh}\left(-\frac{2\tilde{c}}{\sqrt{|\Delta|}}|\tau(z_{\mathrm{m}})|\right) - \operatorname{arcsinh}\left(-\frac{2\tilde{c}}{\sqrt{|\Delta|}}|\tau(z_{\mathrm{M}})|\right) \\ = \; & -\operatorname{arcsinh}\left(\frac{2\tilde{c}}{\sqrt{|\Delta|}}|\tau(z_{\mathrm{m}})|\right) + \operatorname{arcsinh}\left(\frac{2\tilde{c}}{\sqrt{|\Delta|}}|\tau(z_{\mathrm{M}})|\right). \end{aligned} \qquad \text{(B.50)}$$

The latter expression becomes, by means of the identity in eq. (B.46),

$$\begin{aligned} & -\operatorname{arcsinh}\left(\frac{2\tilde{c}}{\sqrt{|\Delta|}}|\tau(z_{\mathrm{m}})|\right) + \operatorname{arcsinh}\left(\frac{2\tilde{c}}{\sqrt{|\Delta|}}|\tau(z_{\mathrm{M}})|\right) \\ = \; & \ln\left\{\left(\frac{2\tilde{c}}{\sqrt{|\Delta|}}|\tau(z_{\mathrm{m}})| + \sqrt{1+\left(\frac{2\tilde{c}}{\sqrt{|\Delta|}}|\tau(z_{\mathrm{m}})|\right)^2}\right)^{-1}\right. \\ & \left.\times\left(\frac{2\tilde{c}}{\sqrt{|\Delta|}}|\tau(z_{\mathrm{M}})| + \sqrt{1+\left(\frac{2\tilde{c}}{\sqrt{|\Delta|}}|\tau(z_{\mathrm{M}})|\right)^2}\right)\right\}. \end{aligned} \qquad \text{(B.51)}$$

From this point onwards we distinguish between the cases of region C and region D.

For region C the derivation proceeds as follows: By bearing in mind that the expressions in eqs. (3.114) and (3.117) are proportional to m^{-3} and m^{-1}, respectively, the expression in eq. (B.51) becomes

$$\begin{aligned} & -\operatorname{arcsinh}\left(\frac{2\tilde{c}}{\sqrt{|\Delta|}}|\tau(z_{\mathrm{m}})|\right) + \operatorname{arcsinh}\left(\frac{2\tilde{c}}{\sqrt{|\Delta|}}|\tau(z_{\mathrm{M}})|\right) \\ = \; & \ln\left\{\left(2\frac{2\tilde{c}}{\sqrt{|\Delta|}}|\tau(z_{\mathrm{m}})|\right)^{-1}\left(2\frac{2\tilde{c}}{\sqrt{|\Delta|}}|\tau(z_{\mathrm{M}})|\right)\right\}. \\ = \; & \ln\left(\frac{2m(2k_0-q_z+\nu)}{p_0}\sqrt{\frac{|k_0'-\nu|(2k_0'+q_z-\nu)}{-q^2k_0|2k_0'-q_z-\nu|}}\right. \end{aligned}$$

$$\times \frac{(-2)q^2p_0^3}{(k_0+\nu)m^3}\sqrt{\frac{-q^2}{k_0(2k_0'+q_z-\nu)|k_0'-\nu||q_z+\nu-2k_0'|}}\Bigg)$$
$$= \ln\left(\frac{-p_0^2q^2(2k_0-q_z+\nu)}{m^2k_0(k_0+\nu)(-2k_0'+q_z+\nu)}\right). \qquad \text{(B.52)}$$

Thus the result for region C in eq. (3.118) follows, for the case of $k_0' < \nu$ under consideration, from eqs. (3.112), (B.44), (B.50) and (B.52).

For region D we obtain, from eq. (B.51) and by bearing in mind that the expressions in eqs. (3.114) and (3.116) are proportional to m^{-3} and m^{-1}, respectively:

$$-\text{arcsinh}\left(\frac{2\tilde{c}}{\sqrt{|\Delta|}}|\tau(z_{\rm m})|\right) + \text{arcsinh}\left(\frac{2\tilde{c}}{\sqrt{|\Delta|}}|\tau(z_{\rm M})|\right)$$
$$= \ln\left\{\left(2\frac{2\tilde{c}}{\sqrt{|\Delta|}}|\tau(z_{\rm m})|\right)^{-1}\left(2\frac{2\tilde{c}}{\sqrt{|\Delta|}}|\tau(z_{\rm M})|\right)\right\}$$
$$= \ln\left(\frac{2mk_0'}{p_0}\sqrt{\frac{k_0|k_0'-\nu|}{-q^2(2k_0'+q_z-\nu)|q_z+\nu-2k_0'|}}\right.$$
$$\left.\times \frac{(-2)q^2p_0^3}{(k_0+\nu)m^3}\sqrt{\frac{-q^2}{k_0(2k_0'+q_z-\nu)|k_0'-\nu||q_z+\nu-2k_0'|}}\right)$$
$$= \ln\left(\frac{4p_0^2(-q^2)k_0'}{m^2(k_0+\nu)(2k_0'+q_z-\nu)(q_z+\nu-2k_0')}\right). \qquad \text{(B.53)}$$

Thus the result for region D in eq. (3.118) follows, for the case of $k_0' < \nu$ under consideration, from eqs. (3.112), (B.44), (B.50) and (B.53).

For $k_0' > \nu$ in regions C and D we have, according to the relations in (3.113), (3.94) and (3.106):

$$-\text{arccosh}\left(\left|\frac{2\tilde{c}}{\sqrt{|\Delta|}}\tau(z_{\rm m})\right|\right) + \text{arccosh}\left(\left|\frac{2\tilde{c}}{\sqrt{|\Delta|}}\tau(z_{\rm M})\right|\right)$$
$$= -\text{arccosh}\left(-\frac{2\tilde{c}}{\sqrt{|\Delta|}}|\tau(z_{\rm m})|\right) + \text{arccosh}\left(-\frac{2\tilde{c}}{\sqrt{|\Delta|}}|\tau(z_{\rm M})|\right)$$
$$= -\text{arccosh}\left(\frac{2\tilde{c}}{\sqrt{|\Delta|}}|\tau(z_{\rm m})|\right) + \text{arccosh}\left(\frac{2\tilde{c}}{\sqrt{|\Delta|}}|\tau(z_{\rm M})|\right). \qquad \text{(B.54)}$$

Now

$$e^x = \sinh x + \cosh x = \cosh x + \sqrt{\cosh^2 x - 1}$$
$$\Rightarrow \quad x = \ln\left(\cosh x + \sqrt{\cosh^2 x - 1}\right)$$

and by letting x =arccosh$y$ in the latter equation, we obtain another useful identity:

$$\text{arccosh}y = \ln\left(y + \sqrt{y^2 - 1}\right). \tag{B.55}$$

This enables us to write the expression in eq. (B.54) in the form:

$$\begin{aligned} & -\text{arccosh}\left(\frac{2\tilde{c}}{\sqrt{|\Delta|}}|\tau(z_{\rm m})|\right) + \text{arccosh}\left(\frac{2\tilde{c}}{\sqrt{|\Delta|}}|\tau(z_{\rm M})|\right) \\ = \ & \ln\left\{\left(\frac{2\tilde{c}}{\sqrt{|\Delta|}}|\tau(z_{\rm m})| + \sqrt{\left(\frac{2\tilde{c}}{\sqrt{|\Delta|}}|\tau(z_{\rm m})|\right)^2 - 1}\right)^{-1}\right. \\ & \left. \times\left(\frac{2\tilde{c}}{\sqrt{|\Delta|}}|\tau(z_{\rm M})| + \sqrt{\left(\frac{2\tilde{c}}{\sqrt{|\Delta|}}|\tau(z_{\rm M})|\right)^2 - 1}\right)\right\}. \end{aligned} \tag{B.56}$$

From this point onwards we distinguish betweem the cases of region C and region D.

For region C the derivation proceeds as follows: By bearing in mind that the expressions in eqs. (3.114) and (3.117) are proportional to m^{-3} and m^{-1}, respectively, the expression in eq. (B.56) becomes

$$\begin{aligned} & -\text{arcsinh}\left(\frac{2\tilde{c}}{\sqrt{|\Delta|}}|\tau(z_{\rm m})|\right) + \text{arcsinh}\left(\frac{2\tilde{c}}{\sqrt{|\Delta|}}|\tau(z_{\rm M})|\right) \\ = \ & \ln\left\{\left(2\frac{2\tilde{c}}{\sqrt{|\Delta|}}|\tau(z_{\rm m})|\right)^{-1}\left(2\frac{2\tilde{c}}{\sqrt{|\Delta|}}|\tau(z_{\rm M})|\right)\right\} \\ = \ & \ln\left(\frac{2m(2k_0 - q_z + \nu)}{p_0}\sqrt{\frac{|k_0' - \nu|(2k_0' + q_z - \nu)}{-q^2 k_0|2k_0' - q_z - \nu|}}\right. \\ & \left. \times\frac{(-2)q^2 p_0^3}{(k_0 + \nu)m^3}\sqrt{\frac{-q^2}{k_0(2k_0' + q_z - \nu)|k_0' - \nu||q_z + \nu - 2k_0'|}}\right) \\ = \ & \ln\left(\frac{-p_0^2 q^2(2k_0 - q_z + \nu)}{m^2 k_0(k_0 + \nu)(-2k_0' + q_z + \nu)}\right). \end{aligned} \tag{B.57}$$

Thus the result for region C in eq. (3.118) follows, for the case of $k_0' > \nu$ under consideration, from eqs. (3.113), (B.44), (B.54) and (B.57) and is exactly the same result as was obtained for region C in the case when $k_0' < \nu$.

For region D we obtain, from eq. (B.56) and by bearing in mind that the expressions in eqs. (3.114) and (3.116) are proportional to m^{-3} and m^{-1}, respectively:

$$-\text{arccosh}\left(\frac{2\tilde{c}}{\sqrt{|\Delta|}}|\tau(z_{\rm m})|\right) + \text{arccosh}\left(\frac{2\tilde{c}}{\sqrt{|\Delta|}}|\tau(z_{\rm M})|\right)$$

$$
\begin{aligned}
&= \ln\left\{\left(2\frac{2\tilde{c}}{\sqrt{|\Delta|}}|\tau(z_{\rm m})|\right)^{-1}\left(2\frac{2\tilde{c}}{\sqrt{|\Delta|}}|\tau(z_{\rm M})|\right)\right\} \\
&= \ln\left(\frac{2mk_0'}{p_0}\sqrt{\frac{k_0|k_0'-\nu|}{-q^2(2k_0'+q_z-\nu)|q_z+\nu-2k_0'|}}\right. \\
&\quad \left.\times\frac{(-2)q^2p_0^3}{(k_0+\nu)m^3}\sqrt{\frac{-q^2}{k_0(2k_0'+q_z-\nu)|k_0'-\nu||q_z+\nu-2k_0'|}}\right) \\
&= \ln\left(\frac{4p_0^2(-q^2)k_0'}{m^2(k_0+\nu)(2k_0'+q_z-\nu)(q_z+\nu-2k_0')}\right). \qquad \text{(B.58)}
\end{aligned}
$$

Thus the result for region D in eq. (3.118) follows, for the case of $k_0' > \nu$ under consideration, from eqs. (3.113), (B.44), (B.54) and (B.58) and is exactly the same result as was obtained for region D in the case when $k_0' < \nu$.

Thereby the proof of all the relations in (3.118) is completed.

Appendix C

More Details on the Angular Integrations for the Bosonic Part of the Vertex Correction to a Quark

In Subsection (a) of this appendix we prove eq. (3.176). In Subsections (b) and (c) we present, for the cases of the $p_0 > 0$ and $p_0 < 0$ parts of the $\int_{-\infty}^{\infty} dp_0$ integration in eq. (3.139), respectively, the Taylor expansions of certain quantities which are required to write results in their regularized forms. The results of Subsections (b) and (c) are used in Subsection (d) to prove that all the expressions in eqs. (3.205) and (3.206) lead, in the $m^2 \to 0$ limit, to the same single regularized expression given in eq. (3.207).

(a) Eq. (3.176) is derived from eqs. (3.174) and (3.175) as follows: Follow the same steps as those leading from eq. (B.7) to eq. (B.11) but keep in mind the following:

(i) The correspondences $l \to v_B$, $\cos\beta \to z$ and $\cos\rho \to \cos\alpha_B$ must be identified.

(ii) There is an overall factor of -1 in the argument of each of the two square roots in eq. (B.7) relative to that of each of eqs. (3.174) and (3.175).

(iii) One of the two integration limits is not the same when we compare the integration in eq. (B.7) with the integration in each of eqs. (3.174) and (3.175).

The result we obtain from eq. (B.11) by keeping in mind the above three points is

$$J_1 = \lim_{\epsilon \to 0^+} \frac{1}{2k_0'|\vec{p}|\sqrt{-\gamma(z, v_B, \cos\alpha_B)}} \int_{y_1'}^{y_2'} \frac{dy'}{\sqrt{y'^2 - 1}} \tag{C.1}$$

$$J_2 = -\lim_{\epsilon\to 0^+} \frac{1}{2k_0'|\vec{p}|\sqrt{-\gamma(z,v_B,\cos\alpha_B)}} \int_{y_3'}^{y_4'} \frac{dy'}{\sqrt{y'^2-1}} \tag{C.2}$$

where

$$y' = \left[x - \frac{(z\cos\alpha_B - v_B)}{\gamma(z,v_B,\cos\alpha_B)}\right] \frac{[-\gamma(z,v_B,\cos\alpha_B)]}{\sqrt{1-z^2\sin\alpha_B}}. \tag{C.3}$$

It is to be noted that the latter change of variable has an overall factor of (-1) relative to that in eq. (B.12) since in the present case of J_1 and J_2 we have [compare with eq. (B.10)]

$$\sqrt{Q} = \sqrt{\frac{(1-z^2)\sin^2\alpha_B}{G^2}} = -\frac{\sqrt{1-z^2}\sin\alpha_B}{G}$$

where the latter minus sign appears due to the fact that now $G \equiv \gamma(z,v_B,\cos\alpha_B) < 0$ as may be seen from line (3.173).

The integration limits, $x = (a-v_B)^{-1}$ in eq. (3.174) and $x = (b-v_B)^{-1}$ in eq. (3.175), become, under the change of variable in eq. (C.3), $y_1' = -1$ and $y_4' = 1$, respectively [see eq. (B.13)]. For y_2' and y_3' we have:

$$\begin{aligned} y_2' &= \left[-\frac{1}{\epsilon} - \frac{(z\cos\alpha_B - v_B)}{\gamma(z,v_B,\cos\alpha_B)}\right] \frac{[-\gamma(z,v_B,\cos\alpha_B)]}{\sqrt{1-z^2\sin\alpha_B}} \\ &= \frac{-\gamma(z,v_B,\cos\alpha_B)}{\sqrt{1-z^2\sin\alpha_B}}\left(-\frac{1}{\epsilon}\right) + \frac{(z\cos\alpha_B - v_B)}{\sqrt{1-z^2\sin\alpha_B}} \qquad \text{(C.4)} \\ y_2' &= \frac{-\gamma(z,v_B,\cos\alpha_B)}{\sqrt{1-z^2\sin\alpha_B}}\left(\frac{1}{\epsilon}\right) + \frac{(z\cos\alpha_B - v_B)}{\sqrt{1-z^2\sin\alpha_B}}. \qquad \text{(C.5)} \end{aligned}$$

The inequality in line (3.173) leads to

$$\begin{aligned} & z\cos\alpha_B - \sqrt{1-z^2}\sin\alpha_B < v_B < z\cos\alpha_B + \sqrt{1-z^2}\sin\alpha_B \\ \Rightarrow \qquad & -1 < \frac{v_B - z\cos\alpha_B}{\sqrt{1-z^2}\sin\alpha_B} < 1 \end{aligned}$$

so that the second term in each of eqs. (C.4) and (C.5) is finite even when $z \to 1$. The inequality in line (3.173) also ensures that

$$\frac{-\gamma(z,v_B,\cos\alpha_B)}{\sqrt{1-z^2}\sin\alpha_B} > 0$$

so that, with the definition

$$\frac{1}{\epsilon'} \equiv \frac{-\gamma(z,v_B,\cos\alpha_B)}{\sqrt{1-z^2}\sin\alpha_B}\frac{1}{\epsilon},$$

we have

$$\lim_{\epsilon\to 0+} y_2' = \lim_{\epsilon'\to 0+}\left(-\frac{1}{\epsilon'}\right)$$
$$\lim_{\epsilon\to 0+} y_3' = \lim_{\epsilon'\to 0+}\left(\frac{1}{\epsilon'}\right).$$

In order to ensure that the argument of arccosh in the final results will be positive, we introduce a further transformation, $y'' = -y'$, in J_1 but not in J_2 and obtain

$$\begin{aligned} J_1 &= \lim_{\epsilon'\to 0+} \frac{1}{2k_0'|\vec{p}|\sqrt{-\gamma(z,v_B,\cos\alpha_B)}}(-1)\int_1^{1/\epsilon'} \frac{dy''}{\sqrt{y''^2-1}} \\ &= \lim_{\epsilon'\to 0+} \frac{1}{2k_0'|\vec{p}|\sqrt{-\gamma(z,v_B,\cos\alpha_B)}}\left(-\operatorname{arccosh}\frac{1}{\epsilon'} + \operatorname{arccosh} 1\right) \\ J_2 &= -\lim_{\epsilon'\to 0+} \frac{1}{2k_0'|\vec{p}|\sqrt{-\gamma(z,v_B,\cos\alpha_B)}}\int_{1/\epsilon'}^{1} \frac{dy'}{\sqrt{y'^2-1}} \\ &= \lim_{\epsilon'\to 0+} \frac{1}{2k_0'|\vec{p}|\sqrt{-\gamma(z,v_B,\cos\alpha_B)}}\left(-\operatorname{arccosh} 1 + \operatorname{arccosh}\frac{1}{\epsilon'}\right) \end{aligned}$$

which, due to $\operatorname{arccosh} 1 = 0$, are the results given in eq. (3.176).

(b) In this subsection we present, for the case of the $p_0 > 0$ part of the $\int_{-\infty}^{\infty} dp_0$ integration in eq. (3.139), the Taylor expansions of certain quantities which are used in Subsection (d) of this appendix to write results in their regularized forms.

From eqs. (3.162), (3.163) and (3.152) there follows that

$$\begin{aligned} c &= v_B^2 + u_B^2 + \cos^2\alpha_B - 2u_Bv_B\cos\alpha_B - 1 \\ &= (u_B - \cos\alpha_B)^2 + \mathcal{O}(m^2) \\ &= \frac{(q^2)^2}{4k_0^2k_0'^2} + \mathcal{O}(m^2) \qquad \text{(C.6)} \\ &\geq 0 \qquad \text{in cases (i), (iii) and (iv).} \qquad \text{(C.7)} \end{aligned}$$

From eqs. (3.162) and (3.152) there follows that

$$\begin{aligned} \Delta &= 4\sin^2\alpha_B(v_B^2 - 1) \\ &= \left(-\frac{(q^2)^2}{k_0^2k_0'^2} - \frac{4q^2}{k_0k_0'}\right)\frac{k_0' - p_0}{p_0^2k_0'}m^2 + \mathcal{O}(m^4) \\ &= \frac{-q^2(k_0' - p_0)}{k_0k_0'^2p_0^2}\left(\frac{q^2}{k_0k_0'} + 4\right)m^2 + \mathcal{O}(m^4). \qquad \text{(C.8)} \end{aligned}$$

The factor $q^2/(k_0k_0')+4$ in the latter expression is positive as may be seen by making use of $k_0'=k_0+\nu$ and determining the roots, $k_0^{\pm}$, of the equation $k_0^2+k_0\nu+q^2/4=0$:

$$\begin{aligned} k_0^{\pm} &= \frac{-\nu\pm\sqrt{\nu^2-(\nu^2-q_z^2)}}{2} \\ &= \frac{q_z-\nu}{2} \quad ; \quad -\frac{q_z+\nu}{2} \end{aligned}$$

$$\Rightarrow \qquad \frac{q^2}{k_0k_0'}+4\geq 0 \qquad \text{for} \qquad k_0\geq\frac{q_z-\nu}{2} \tag{C.9}$$

where the inequality, $k_0\geq(q_z-\nu)/2$, holds for all the cases under consideration (see Figure 3.11). Thus we may conclude from eq. (C.8) that

$$\Delta\begin{cases} >0 & \text{in cases (i) and (iii) at line (3.164)} \\ <0 & \text{in case (iv).} \end{cases} \tag{C.10}$$

From eqs. (3.183) and (C.6) there follows that

$$\begin{aligned} \tau(-1) &= \frac{1}{-1-u_B}+\frac{2(u_B-v_B\cos\alpha_B)}{2\gamma(v_B,u_B,\cos\alpha_B)} \\ &= \frac{1}{-1-1+\mathcal{O}(m^2)}+\frac{1-\cos\alpha_B+\mathcal{O}(m^2)}{\left[(q^2)^2/(4k_0^2k_0'^2)\right]+\mathcal{O}(m^2)} \\ &= -\frac{1}{2}-\frac{2k_0k_0'}{q^2}+\mathcal{O}(m^2) \qquad (C.11) \\ &\geq 0 \qquad \text{for } k_0\geq\frac{q_z-\nu}{2} \qquad (C.12) \end{aligned}$$

where the latter inequality follows from (C.9). Since $k_0\geq(q_z-\nu)/2$ holds for all the cases under consideration (see Figure 3.11) we may conclude that

$$\tau(-1)\geq 0 \qquad \text{in cases (i), (iii) and (iv) at line (3.164).} \tag{C.13}$$

From eqs. (3.183), (C.6), (3.152) and (3.163) there follows that

$$\begin{aligned} \tau(1) &= \frac{1}{1-u_B}+\frac{u_B-v_B\cos\alpha_B}{\gamma(v_B,u_B,\cos\alpha_B)} \\ &= -\frac{k_0p_0^2}{m^2(k_0-p_0)}-\frac{2k_0k_0'}{q^2}+\mathcal{O}(m^2). \end{aligned} \tag{C.14}$$

In the limit $m^2\to 0$ the first term in eq. (C.14) determines the sign of $\tau(1)$. Therefore

$$\tau(1)\begin{cases} <0 & \text{in case (i) at line (3.164)} \\ >0 & \text{in cases (iii) and (iv).} \end{cases} \tag{C.15}$$

Similarly we can prove eqs. (3.187) and (3.188):

$$\begin{aligned}\lim_{\epsilon\to 0^+}\tau(u_B-\epsilon) &= \lim_{\epsilon\to 0^+}\frac{1}{u_B-\epsilon-u_B}+\frac{u_B-v_B\cos\alpha_B}{\gamma(v_B,u_B,\cos\alpha_B)}\\ &= \lim_{\epsilon\to 0^+}\left[-\frac{1}{\epsilon}-\frac{2k_0k_0'}{q^2}+\mathcal{O}(m^2)\right]\\ &= \lim_{\epsilon\to 0^+}\left(-\frac{1}{\epsilon}\right)\end{aligned} \tag{C.16}$$

and

$$\begin{aligned}\lim_{\epsilon\to 0^+}\tau(u_B+\epsilon) &= \lim_{\epsilon\to 0^+}\left[\frac{1}{\epsilon}-\frac{2k_0k_0'}{q^2}+\mathcal{O}(m^2)\right]\\ &= \lim_{\epsilon\to 0^+}\frac{1}{\epsilon}.\end{aligned} \tag{C.17}$$

From eq. (3.169) and the fact that $\lambda_\pm$ are the roots of the equation,

$$\gamma(v_B,u_B,\cos\alpha_B)=0,$$

there follows that

$$\begin{aligned}\tau(\lambda_\pm) &= \frac{1}{\lambda_\pm-u_B}+\frac{u_B-v_B\cos\alpha_B}{\gamma(v_B,u_B,\cos\alpha_B)}\\ &= \frac{1}{\lambda_\pm-u_B}+\frac{u_B-v_B\cos\alpha_B}{(u_B-\lambda_+)(u_B-\lambda_-)}\\ &= \frac{-(u_B-\lambda_\mp)+u_B-v_B\cos\alpha_B}{(u_B-\lambda_+)(u_B-\lambda_-)}\\ &= \frac{\mp\sqrt{1-v_B^2}\sin\alpha_B}{\gamma(u_B,v_B,\cos\alpha_B)}.\end{aligned}$$

By making use of eqs. (3.162), (3.152) and (C.6) we can write the latter expression in the form

$$\begin{aligned}\tau(\lambda_\pm) &= \mp\sqrt{\frac{p_0-k_0'}{k_0'p_0^2}}m\sqrt{1-\cos^2\alpha_B}\frac{4k_0^2k_0'^2}{(q^2)^2}+\mathcal{O}(m^2)\\ &= \mp\sqrt{\frac{p_0-k_0'}{k_0'p_0^2}}m\sqrt{\frac{-q^2}{k_0k_0'}}\sqrt{\frac{4k_0k_0'+q^2}{4k_0k_0'}}\frac{4k_0^2k_0'^2}{(q^2)^2}+\mathcal{O}(m^2)\\ &= \mp\sqrt{\frac{(p_0-k_0')(4k_0k_0'+q^2)4k_0^2k_0'}{p_0^2(-q^2)^3}}\,m+\mathcal{O}(m^2).\end{aligned} \tag{C.18}$$

where the argument of the square root is positive since we consider $\tau(\lambda_\pm)$ only in the case of (iv) at line (3.164) for which $p_0 > k_0'$ and since $(4k_0k_0'+q^2) \geq 0$ for $k_0 \geq (q_z-\nu)/2$. Therefore, in the limit $m^2 \to 0$, we have

$$\tau(\lambda_+) < 0 \qquad \text{in case (iv)} \tag{C.19}$$

$$\tau(\lambda_-) > 0 \qquad \text{in case (iv).} \tag{C.20}$$

(c) In this subsection we present, for the case of the $p_0 < 0$ part of the $\int_{-\infty}^{\infty} dp_0$ integration in eq. (3.139), the Taylor expansions of certain quantities which are used in Subsection (d) of this appendix to write results in their regularized forms.

From eqs. (3.199), (3.200) and (3.152) there follows that

$$\begin{aligned} c &= v_B^2 + u_B^2 + \cos^2\alpha_B - 2u_B v_B \cos\alpha_B - 1 \\ &= (u_B + \cos\alpha_B)^2 + \mathcal{O}(m^2) \\ &= \frac{(q^2)^2}{4k_0^2 k_0'^2} + \mathcal{O}(m^2) \qquad \text{(C.21)} \\ &\geq 0 \qquad \text{for } p_0 < 0. \qquad \text{(C.22)} \end{aligned}$$

From eqs. (3.199) and (3.152) there follows that

$$\begin{aligned} \Delta &= 4\sin^2\alpha_B(v_B^2 - 1) \\ &= \frac{-q^2(k_0' - p_0)}{k_0 k_0'^2 p_0^2}\left(\frac{q^2}{k_0 k_0'} + 4\right) m^2 + \mathcal{O}(m^4). \qquad \text{(C.23)} \end{aligned}$$

By following steps similar to those leading from eq. (C.8) to (C.10), we can prove from the expression in eq. (C.23) that

$$\Delta > 0 \qquad \text{for } p_0 < 0. \qquad \text{(C.24)}$$

From eqs. (3.183) and (C.21) there follows that

$$\begin{aligned} \tau(-1) &= \frac{-1}{-1-u_B} + \frac{u_B - v_B\cos\alpha_B}{c} \\ &= \frac{1}{-1+1+m^2(k_0-p_0)/(2k_0p_0^2)} + \mathcal{O}(m^0) \\ &= \frac{2k_0p_0^2}{m^2(k_0-p_0)} + \mathcal{O}(m^0) \qquad \text{(C.25)} \end{aligned}$$

and

$$\begin{aligned} \tau(1) &= \frac{1}{1-u_B} + \frac{u_B - v_B\cos\alpha_B}{c} \\ &= \frac{1}{2} + \frac{-1 + q^2/(2k_0k_0') + 1}{(q^2)^2/(4k_0^2k_0'^2)} + \mathcal{O}(m^2) \\ &= \frac{q^2 + 4k_0k_0'}{2q^2} + \mathcal{O}(m^2). \qquad \text{(C.26)} \end{aligned}$$

(d) In this subsection we prove that all the expressions in eqs. (3.205) and (3.206) lead, in the $m^2 \to 0$ limit, to the same single regularized expression given in eq. (3.207).

Wherever square roots appear in the following expressions their arguments are positive. This may be checked by referring to the way these expressions were derived in foregoing discussions.

We start by simplifying the expression for the coefficient appearing in eqs. (3.144) and (3.145). By replacing $|\vec{p}|^2$ by p_0^2 and c by its expression for the $m^2 \to 0$ limit, given in eq. (C.6), we obtain

$$\frac{\pi}{2k_0k_0'|\vec{p}|^2\sqrt{c}} = \frac{\pi}{p_0^2(-q^2)}. \tag{C.27}$$

The results for regions (i) and (iii) in eq. (3.205) can be written as one expression by taking into consideration the results in lines (C.7), (C.10), (C.15) and (C.27) and making use of the property, $\operatorname{arcsinh}(-x) = -\operatorname{arcsinh} x$:

$$I\left(\frac{1}{s_B t_B}\right) = \frac{\pi}{p_0^2(-q^2)}\left[\operatorname{arcsinh}\left(\frac{2c}{\sqrt{\Delta}}\tau(-1)\right) + \operatorname{arcsinh}\left(\left|\frac{2c}{\sqrt{\Delta}}\tau(1)\right|\right)\right]. \tag{C.28}$$

The $m^2 \to 0$ limit of the latter expression is obtained as follows: From eqs. (C.6), (C.8), (C.11) and (C.14) there follows that

$$\begin{aligned} \frac{2c}{\sqrt{\Delta}}\tau(-1) &= \frac{1}{m}\frac{\sqrt{-q^2}}{4k_0\sqrt{k_0'}}\frac{p_0\sqrt{q^2+4k_0k_0'}}{\sqrt{k_0'-p_0}} \qquad (C.29)\\ &> 0 \quad \text{for regions (i) and (iii)} \\ \frac{2c}{\sqrt{\Delta}}\tau(1) &= \frac{1}{m^3}\frac{(-q^2)\sqrt{-q^2}}{\sqrt{k_0'}}\frac{(-p_0)^3}{\sqrt{(k_0'-p_0)(q^2+4k_0k_0')(k_0-p_0)}} \qquad (C.30)\\ &\begin{cases} < 0 & \text{for region (i)} \\ > 0 & \text{for region (iii).} \end{cases} \end{aligned}$$

By making use of the identity in eq. (B.46) and by noticing that the expressions in eqs. (C.29) and (C.30) are proportional to m^{-1} and m^{-3}, respectively, we obtain for region (i):

$$\begin{aligned} &\left[\operatorname{arcsinh}\left(\frac{2c}{\sqrt{\Delta}}\tau(-1)\right) + \operatorname{arcsinh}\left(\left|\frac{2c}{\sqrt{\Delta}}\tau(1)\right|\right)\right] \\ &= \left[\operatorname{arcsinh}\left(\frac{2c}{\sqrt{\Delta}}\tau(-1)\right) + \operatorname{arcsinh}\left(-\frac{2c}{\sqrt{\Delta}}\tau(1)\right)\right] \\ &= \ln\left\{2\frac{2c}{\sqrt{\Delta}}\tau(-1)\right\} + \ln\left\{-2\frac{2c}{\sqrt{\Delta}}\tau(1)\right\} \\ &= \ln\left\{-4\left(\frac{1}{m}\frac{\sqrt{-q^2}}{4k_0\sqrt{k_0'}}\frac{p_0\sqrt{q^2+4k_0k_0'}}{\sqrt{k_0'-p_0}}\right)\right. \end{aligned}$$

$$\times \left(\frac{1}{m^3} \frac{(-q^2)\sqrt{-q^2}}{\sqrt{k_0'}} \frac{(-p_0)^3}{\sqrt{(k_0'-p_0)(q^2+4k_0k_0')(k_0-p_0)}} \right) \Bigg\}$$

$$= \ln \left\{ \left| \frac{1}{m^4} \frac{p_0^4 (q^2)^2}{k_0 k_0' (k_0-p_0)(k_0'-p_0)} \right| \right\} \quad \text{in region (i).} \tag{C.31}$$

Thus our results in eqs. (C.28) and (C.31) for region (i) give exactly the result in eq. (3.207).

The $m^2 \to 0$ limit of the expression in eq. (C.28) for the case of region (iii) is derived similarly and leads to exactly the same final result as given in eq. (3.207).

The $m^2 \to 0$ limit of the expression for region (iv) in eq. (3.205) is obtained as follows: From eqs. (C.6), (C.8), (C.11) and (C.14) there follows that [Use is made of, e.g., the fact that $|\Delta| = -\Delta$ in region (iv).]:

$$\begin{aligned} \frac{2c}{\sqrt{|\Delta|}}\tau(-1) &= \frac{(q^2)^2}{2k_0^2 {k_0'}^2} \left[\frac{q^2(k_0'-p_0)}{k_0 {k_0'}^2 p_0^2} \left(\frac{q^2}{k_0 k_0'} + 4 \right) m^2 \right]^{-1/2} \left(-\frac{1}{2} - \frac{2k_0 k_0'}{q^2} \right) \\ &= \frac{1}{m} \frac{\sqrt{-q^2}}{4k_0\sqrt{k_0'}} \frac{p_0\sqrt{q^2+4k_0k_0'}}{\sqrt{p_0-k_0'}} \qquad \text{(C.32)} \\ &> 0 \qquad \text{in region (iv)} \end{aligned}$$

$$\begin{aligned} \frac{2c}{\sqrt{|\Delta|}}\tau(1) &= \frac{1}{m^3} \frac{(-q^2)\sqrt{-q^2}}{\sqrt{k_0'}} \frac{(-p_0)^3}{\sqrt{(p_0-k_0')(q^2+4k_0k_0')(k_0-p_0)}} \qquad \text{(C.33)} \\ &> 0 \qquad \text{in region (iv).} \end{aligned}$$

From eqs. (C.6), (C.8) and (C.18) there follows that

$$\begin{aligned} \frac{2c}{\sqrt{|\Delta|}}\tau(\lambda_-) &= -\frac{2c}{\sqrt{|\Delta|}}\tau(\lambda_+) \\ &= \frac{(q^2)^2}{2k_0^2 {k_0'}^2} \left[\frac{q^2(k_0'-p_0)}{k_0 {k_0'}^2 p_0^2} \left(\frac{q^2}{k_0 k_0'} + 4 \right) m^2 \right]^{-1/2} \\ &\quad \times \sqrt{\frac{(p_0-k_0')(q^2+4k_0k_0')4k_0^2k_0'}{p_0^2(-q^2)^3}}\, m \\ &= 1 \qquad \text{in region (iv).} \end{aligned}$$

By making use of the identity in eq. (B.55) and by noticing that the expressions in eqs. (C.32) and (C.33) are proportional to m^{-1} and m^{-3}, respectively, we obtain for region (iv):

$$\left[\arccosh\left(\frac{2c}{\sqrt{|\Delta|}}\tau(-1) \right) + \arccosh\left(\frac{2c}{\sqrt{|\Delta|}}\tau(1) \right) \right.$$

$$
\begin{aligned}
& -\operatorname{arccosh}\left(\frac{2c}{\sqrt{|\Delta|}}\tau(\lambda_-)\right) - \operatorname{arccosh}\left(\left|\frac{2c}{\sqrt{|\Delta|}}\tau(\lambda_+)\right|\right)\Bigg] \\
&= \ln\left\{2\frac{2c}{\sqrt{|\Delta|}}\tau(-1)\right\} + \ln\left\{2\frac{2c}{\sqrt{|\Delta|}}\tau(1)\right\} - \ln 1 - \ln(|-1|) \\
&= \ln\left\{\left|\frac{1}{m^4}\frac{p_0^4(q^2)^2}{k_0k_0'(k_0-p_0)(k_0'-p_0)}\right|\right\} \qquad \text{in region (iv).} \qquad \text{(C.34)}
\end{aligned}
$$

Thus our results for region (iv) in eqs. (3.205), (C.27) and (C.34) give exactly the result in eq. (3.207).

By following steps similar to those followed above it can be proven that the $m^2 \to 0$ limit of the expression for $p_0 < 0$ in eq. (3.206) also gives exactly the same result as given in eq. (3.207). For this proof one must use the results for the case of $p_0 < 0$ in Subsection (c) of this appendix.

Thereby we have proven that the $m^2 \to 0$ limit of all the expressions in eqs. (3.205) and (3.206) lead to exactly the same final regularized expression as given in eq. (3.207).

Appendix D

Summary of Expressions Frequently Referred to

D.1 Introduction

In this appendix we summarize expressions derived for the phase space integrations of the matrix element squared from four- and three-particle processes given in ref. [24](b) including some expressions which have not appeared in publications, which are frequently referred to in this work. The expressions given in this appendix include corrections to writing errors observed in the expressions given in ref. [24](b). These corrections are explicitly pointed out at the relevant places in this appendix.

The way in which the final expressions for four-particle processes in eqs. (D.19) and (D.20) and for three-particle processes in eqs. (D.27) and (D.28) contribute to the structure functions of the nucleon can be seen by considering eqs. (4.5), (4.6) and (4.9)–(4.12).

D.2 Kinematics for All the Four-Particle Processes

The final forms of the expressions for the matrix element squared for gluon emission from a quark (diagram (a) in Figure 2.2) are given for the sum over all polarizations and for the longitudinal polarization of the virtual photon in eqs. (3.26) and (3.23), respectively. These expressions (which exclude integrations over phase space) can be considered as valid for all the other four-particle processes (diagrams (b) to (f) in Figure 2.2) too {with the exceptions that considerations, as discussed below for the processes of quark-antiquark pair annihilation and pair creation for which $s = 0$ and $t = 0$ are possible, are taken into account and that an overall factor of $\epsilon(k_0 k'_0)$ [see eq. (D.15)] is implicit in order to take into account

the sign difference resulting from the sums over spins for the massless quarks and antiquarks, respectively} through the following convention: To each of the diagrams (a) to (f) in Figure 2.2 there correspond the two Feynman diagrams in Figure 3.2. These two Feynman diagrams, as drawn in Figure 3.2 with exactly the same four-momentum assignments and directions of arrows, are used for each of the processes (a) to (f) in Figure 2.2. When the energy components of the latter four-momenta are all positive the two Feynman diagrams refer to process (a) in Figure 2.2 and the energy of a particle in diagrams (b) to (f) in Figure 2.2 is considered to be negative when it changes from the left hand to the right hand side or vice versa relative to diagram (a) in Figure 2.2. The signs of k_0, k_0' and p_0 resulting from this convention are given in Table D.2.

The result discussed in Section 3.4 for gluon emission from a quark that the integrations over phase space could be analytically reduced to integrations over only the two energy variables k_0 and p_0 applies to all the other four-particle processes as well. According to the mechanism by means of which collinear and infrared divergences cancel (as discussed in Section 3.8) it is appropriate to transform from these variables (k_0, p_0) to the variables (K, p_0) where

$$K = k_0 + \frac{\nu - p_0}{2} \tag{D.1}$$

The convention discussed in the first paragraph of this section enables one to view all contributing four-particle processes simultaneously in the two-dimensional energy plane shown in Figure D.1.

In Appendix A kinematical quantities for the specific four-particle process of gluon emission from a quark were introduced. According to the way we implement the convention for the signs of energies of particles as discussed above for the general four-particle process in Figure 2.2, the quantities as defined in eqs. (A.1)–(A.6) remain the same while other kinematical quantities are generalized as follows [24](b):

$$\begin{aligned}
z &\equiv \cos\theta = \frac{\vec{k}.\vec{q}}{|\vec{k}|q_z}\epsilon(k_0'p_0) \\
z' &\equiv \cos\theta' = \frac{\vec{k}'.\vec{q}}{|\vec{k}'|q_z}\epsilon(k_0p_0) \\
s &\equiv (k+q)^2 = -2|\vec{k}|q_z(z\epsilon(k_0'p_0) - d) \qquad \text{(D.2)} \\
t &\equiv (q-k')^2 = 2|\vec{k}'|q_z(z'\epsilon(k_0p_0) - d') \qquad \text{(D.3)}
\end{aligned}$$

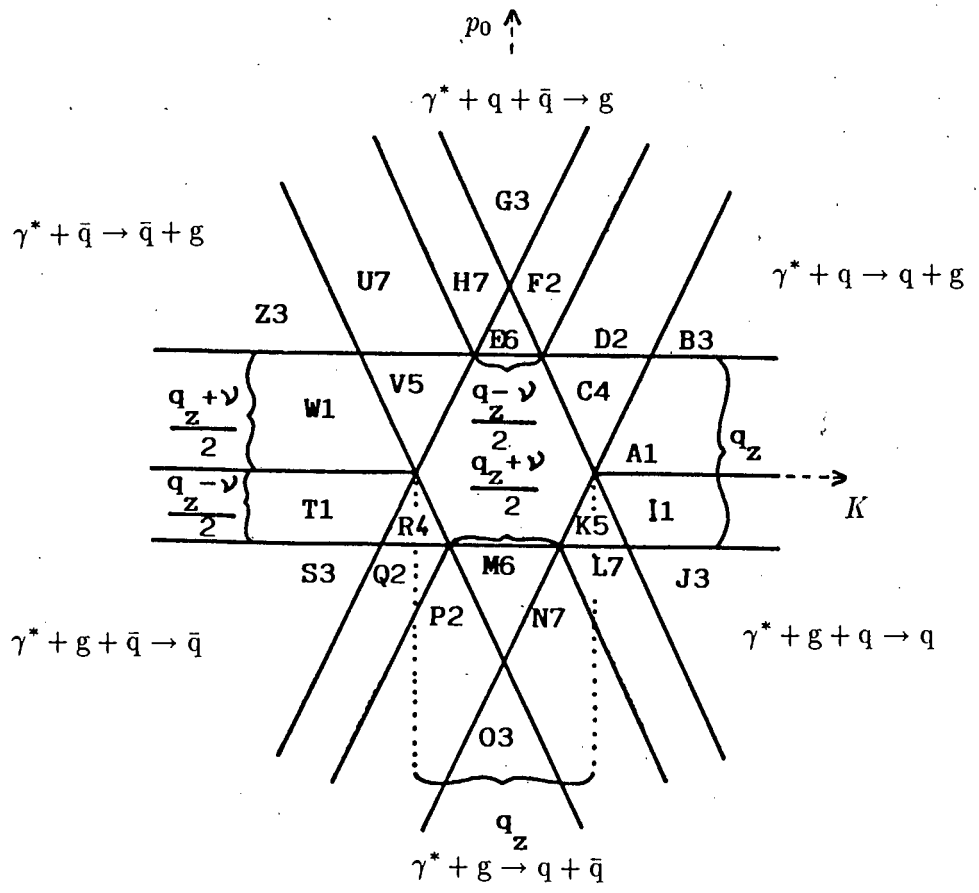

Figure D.1: Regions of support for all four-particle processes in the K, p_0 plane [24, p.381](b).

$$d \equiv \frac{2k_0\nu + q^2}{2|\vec{k}|q_z} \tag{D.4}$$

$$d' \equiv \frac{2k'_0\nu - q^2}{2|\vec{k}'|q_z}. \tag{D.5}$$

It is to be noted that the variables s and t can become equal to zero (even when $m^2 > 0$) in some of the subregions for the processes of pair annihilation

$$\gamma^* + q + \bar{q} \to g \tag{D.6}$$

and pair creation

$$\gamma^* + g \to q + \bar{q} \tag{D.7}$$

depicted in Figure D.1. However, for the remaining four-particle processes it can be shown that s and t are always not equal to zero for $m^2 > 0$ (see the proof for the example of gluon emission from a quark in Appendix A). A faster and somewhat more physical way of proving

that s and t can become equal to zero for the processes in (D.6) and (D.7) than the way followed to prove the opposite for the process considered in Appendix A is as follows:

According to our convention the two Feynman diagrams in Figure 3.2, with exactly the same four-momentum assignments and directions of arrows but appropriate signs of energies of particles, are used for each of the processes in (D.6) and (D.7).

We consider the process in (D.6) as the first example. We check whether the assumption that $s = (k+q)^2 = 0$ for the internal line of the Feynman diagram on the left in Figure 3.2 leads to a contradiction or not. According to this assumption one has an on mass shell quark on the latter internal line. For the process under consideration we have $k_0 > 0$, $q_0 > 0$ (and therefore $k_0 + q_0 > 0$ on the internal line), $p_0 > 0$ and $k'_0 < 0$. This information tells us that we have deep inelastic scattering at the left hand vertex which has two on mass shell quark lines attached to it and quark-antiquark pair annihilation into a positive-energy on mass shell gluon at the right hand vertex. Since both the subprocesses at the two vertices are kinematically allowed there is no contradiction and it can be concluded that $s = 0$ is possible. Using similar arguments one can show that $t = (q - k')^2 = 0$ is possible for the Feynman diagram on the right in Figure 3.2 and also that $s = 0$ and $t = 0$ are possible for the process in (D.7).

The ill-defined squares of Dirac delta functions with coinciding arguments resulting from the on mass shell internal lines when $s = 0$ or $t = 0$ cancel with contributions from self-energy diagrams. The corresponding s and t singularities from the principal value part of propagators are integrated over in the principal value sense in angular integrations.

Other generalized kinematical quantities are as follows: In Section 3.4.2 we proved for the case of gluon emission from a quark that

$$\begin{aligned} d\mu &= \frac{d^3k}{(2\pi)^3 2k_0}\frac{d^3k'}{(2\pi)^3 2k'_0}\frac{d^3p}{(2\pi)^3 2p_0}(2\pi)^4\delta^4(q+k-k'-p) \\ &= \frac{1}{8(2\pi)^4}dk_0 dk'_0 d\Omega \end{aligned}$$

with $d\Omega$ given in eq. (3.48). A more symmetric expression than the latter for $d\Omega$ is obtained by using the identity [15, p.66]

$$|\vec{k}+\vec{q}|^2\gamma(z',\cos\beta,\cos\rho) = k_0^2\gamma(z,z',\cos\alpha)$$

where $\cos\alpha$ is given in ref. [15, p.66] for the specific case of gluon emission from a quark. The generalized expression for $d\mu$, valid for any four-particle process, is given in ref. [24,

p.378](a) as

$$\begin{aligned} d\mu &= \frac{d^3k}{(2\pi)^3 2|k_0|}\frac{d^3k'}{(2\pi)^3 2|k'_0|}\frac{d^3p}{(2\pi)^3 2|p_0|}(2\pi)^4\delta^4(q+k-k'-p) \\ &= \frac{1}{8(2\pi)^4}dk_0 dp_0 d\Omega \end{aligned} \tag{D.8}$$

where

$$d\Omega = 2dzdz'[-\gamma(z,z',\cos\alpha)]^{-1/2}$$

with $\gamma(x,y,z)$ still as defined in eq. (3.43) but with $\cos\alpha$ generalized to

$$\begin{aligned} \cos\alpha &\equiv \frac{\vec{k}.\vec{k'}}{|\vec{k}||\vec{k'}|}\epsilon(k_0k'_0) \\ &= \frac{[k'^2_0 + k_0^2 - |\vec{p}|^2 + q_z^2 + 2|\vec{k}|q_z z\epsilon(k'_0p_0) - 2|\vec{k'}|q_z z'\epsilon(k_0p_0)]\epsilon(k_0k'_0)}{2|\vec{k}||\vec{k'}|} \end{aligned}$$

As was mentioned in the first paragraph of Section 3.4.3, one obtains in general different analytical results according to the combination of upper and lower limits for z and z' for each subregion shown in Figure D.1. Relevant to the discussions in Section 3.4.3 was the derivation of expressions for $z_{\mathrm{U,L}}$ and $z'_{\mathrm{U,L}}$ [eqs. (3.49) and (3.50), respectively] for the case of gluon emission from a quark. Their generalized expressions, valid for all the four-particle processes, are as follows [24, p.380](a):

$$z_{\mathrm{U,L}} = \frac{[(|\vec{k'}| \pm \epsilon(k'_0p_0)|\vec{p}|)^2 - |\vec{k}|^2 - q_z^2]\epsilon(k'_0p_0)}{2|\vec{k}|q_z} \tag{D.9}$$

$$z'_{\mathrm{U,L}} = \frac{-[(|\vec{k}| \mp \epsilon(k_0p_0)|\vec{p}|)^2 - |\vec{k'}|^2 - q_z^2]\epsilon(k_0p_0)}{2|\vec{k'}|q_z} \tag{D.10}$$

(D.11)

In the next section we mention how the latter quantities determine the collinear singularity structure.

D.3 Summary of Final Expressions for Four-Particle Processes

In Section 3.4.3 we explained how the choice of expressions for $(z_{\mathrm{M}}, z_{\mathrm{m}}, z'_{\mathrm{M}}, z'_{\mathrm{m}})$ determines the four subregions for the process of gluon emission from a quark shown in Figure 3.6. The corresponding choice of expressions for *all* the four-particle processes is given in Table D.1.

There the Latin letters label the subregions and the numbers label the class of the contribution. The class enters the discussion on the cancellation of collinear singularities in Section 3.8

Table D.1: Classes of contributions for four-particle processes [24, p.381](a).

Class	(z_M, z_m, z'_M, z'_m)	Subregion
1	(z_U, z_L, z'_U, z'_L)	A,I,T,W
2	$(z_U, z_L, 1, -1)$	D,F,P,Q
3	$(z_U, -1, z'_U, -1)$	B,G,O,J,S,Z
4	$(z_U, -1, 1, z'_L)$	C,R
5	$(1, z_L, z'_U, -1)$	K,V
6	$(1, z_L, 1, z'_L)$	M,E
7	$(1, -1, z'_U, z'_L)$	H,L,N,U

Similar to the way we proved that $s(z_U)\ \alpha\ m^2$ and $t(z'_U)\ \alpha\ m^2$ in Section 3.4.4, it can be shown that

$$s(z_U)\ \alpha\ m^2$$

and

$$t(z'_U)\ \alpha\ m^2$$

also hold for the generalized s, t, z_U and z'_U given in eqs. (D.2), (D.3), (D.9) and (D.10). Thus, collinear singularities arise from integrals containing s or t in the denominator in subregions for which $z_M = z_U$ or $z'_M = z'_U$, respectively. From Table D.1 it can then be seen that the s singularity appears in classes 1,2,3 and 4 and the t singularity appears in classes 1,3,5 and 7. The presence of these singularities in final expressions are pointed out explicitly in Section 3.8.

In the following we write down the final expressions for all the four-particle processes including statistical factors and integrations over phase space. In order to write the expressions

in a simplified form, the abbreviations

$$\begin{array}{ll} A=(2K+p_0+\nu)/2 & a=(2K+p_0-\nu)/2 \\ B=(2K-p_0+\nu)/2 & b=(2K-p_0-\nu)/2 \\ C=(2K+p_0+q_z\epsilon(k_0k_0'p_0))/2 & c=(2K+p_0-q_z\epsilon(k_0k_0'p_0))/2 \\ D=(2K-p_0+q_z\epsilon(k_0k_0'p_0))/2 & d=(2K-p_0-q_z\epsilon(k_0k_0'p_0))/2 \\ E=(\nu+q_z\epsilon(k_0k_0'p_0))/2 & e=(\nu-q_z\epsilon(k_0k_0'p_0))/2 \end{array} \tag{D.12}$$

are first introduced [24, p.382]. The lines along which these quantities are equal to zero in the K, p_0 integration region are shown in Figure 4.5.

We use the symbols

$$\int M_i S_4 d\mu \tag{D.13}$$

in the general context in the sense that they represent all the four-particle processes. The general phase space factor $d\mu$ is given in eq. (D.8). The explicit expressions for the various four-particle processes of the general statistical factor

$$S_4=\left[\frac{1}{2}-\frac{\epsilon(k_0)}{2}(1-2n_{\rm F}(x_k))\right]\left[\frac{1}{2}+\frac{\epsilon(k_0')}{2}(1-2n_{\rm F}(x_k'))\right]\left[\frac{1+\epsilon(p_0)}{2}+n_{\rm B}(|p_0|)\right] \tag{D.14}$$

are given in Table D.2. The symbol M_i in (D.13) stands for the general matrix element squared of a four-particle processes. Under the provisions explained in the first paragraph of Section D.2 its expression is given by eq. (3.26) or (3.23). The latter two equations express the matrix element squared for the sum over all polarizations ($i=\sum$) and the longitudinal polarization ($i=0$) of the virtual photon, respectively, where i is the index of M_i.

Angular integrals are defined as

$$I(f(\Omega))=\epsilon(k_0k_0')\int f(\Omega)d\Omega \tag{D.15}$$

where the origin of the factor $\epsilon(k_0k_0')$ is explained in the first paragraph of Section D.2. The results for terms encountered in the angular integrations are as follows [24, p.382]:

$$\begin{array}{ll} I\left(\frac{1}{st}\right)=\frac{-\pi}{|q_zp_0q^2|}\ln|A_4| & I(1)=\frac{4\pi|E_4|\epsilon(k_0k_0')}{q_z} \\ I\left(\frac{1}{s}\right)=\frac{\pi\epsilon(p_0)}{q_zA}\ln|B_4| & I\left(\frac{1}{t}\right)=-\frac{\pi\epsilon(p_0)}{q_zb}\ln|C_4| \\ I\left(\frac{t}{s}\right)=-\frac{1}{2}I(1)+\frac{q^2p_0}{A}I\left(\frac{1}{s}\right)-\frac{B-p_0}{2A}(c-E)(C-e)I\left(\frac{1}{|\vec{q}+\vec{k}|^2}\right) & \\ I\left(\frac{s}{t}\right)=-\frac{1}{2}I(1)-\frac{q^2p_0}{b}I\left(\frac{1}{t}\right)-\frac{a+p_0}{2b}(d+e)(D+E)I\left(\frac{1}{|\vec{q}-\vec{k}'|^2}\right) & \\ I\left(\frac{1}{|\vec{q}+\vec{k}|^2}\right)=\frac{4\pi\epsilon(k_0k_0')|F_4|}{q_z} & I\left(\frac{1}{|\vec{q}-\vec{k}'|^2}\right)=\frac{4\pi\epsilon(k_0k_0')|G_4|}{q_z} \end{array} \tag{D.16}$$

Table D.2: Signs of energy variables according to the convention described in the first paragraph of Section D.2 and explicit expressions for statistical factors of four-particle processes.

Process in Figure 2.2	Sign of k_0, k_0', p_0	Explicit expression of S_4 in eq. (D.14)
(a)	$k_0 > 0\ k_0' > 0\ p_0 > 0$	$\frac{1}{e^{\beta(k_0-\mu)}+1}\left(1-\frac{1}{e^{\beta(k_0'-\mu)}+1}\right)\left(1+\frac{1}{e^{\beta p_0}-1}\right)$
(b)	$k_0 < 0\ k_0' < 0\ p_0 > 0$	$\left(1-\frac{1}{e^{\beta(-k_0+\mu)}+1}\right)\frac{1}{e^{\beta(-k_0'+\mu)}+1}\left(1+\frac{1}{e^{\beta p_0}-1}\right)$
(c)	$k_0 > 0\ k_0' > 0\ p_0 < 0$	$\frac{1}{e^{\beta(k_0-\mu)}+1}\left(1-\frac{1}{e^{\beta(k_0'-\mu)}+1}\right)\frac{1}{e^{-\beta p_0}-1}$
(d)	$k_0 < 0\ k_0' < 0\ p_0 < 0$	$\left(1-\frac{1}{e^{\beta(-k_0+\mu)}+1}\right)\frac{1}{e^{\beta(-k_0'+\mu)}+1}\frac{1}{e^{-\beta p_0}-1}$
(e)	$k_0 > 0\ k_0' < 0\ p_0 > 0$	$\frac{1}{e^{\beta(k_0-\mu)}+1}\frac{1}{e^{\beta(-k_0'+\mu)}+1}\left(1+\frac{1}{e^{\beta p_0}-1}\right)$
(f)	$k_0 < 0\ k_0' > 0\ p_0 < 0$	$\left(1-\frac{1}{e^{\beta(-k_0+\mu)}+1}\right)\left(1-\frac{1}{e^{\beta(k_0'-\mu)}+1}\right)\frac{1}{e^{-\beta p_0}-1}$

where the results for $1/s^2$ and $1/t^2$ type terms are not given since they disappear according to the mechanism mentioned in ref. [24, pp.388,389]. The different analytical expressions resulting from different choices of angular integration limits are classified according to class and these differences appear in the quantities given in Table D.3. An example of the derivation of the first result in (D.16) is discussed in Section 3.4.5 and some of its explicit expressions are given in eq. (3.118).

By inserting the above results from angular integrations into eqs. (3.26) and (3.23) and ignoring only the overall factors e^2g^2 in the latter equations, one obtains:

$$\begin{aligned}\int M_\Sigma S_4 d\mu \;=\; & \frac{1}{4\pi^3 q_z}\int dK dp_0 S_4 \left\{\left|\frac{q^2}{2p_0}\right|\ln|A_4| + |q^2|\left[\frac{|p_0|}{4A^2}-\frac{\epsilon(p_0)}{2A}\right]\ln|B_4|\right. \\ & +|q^2|\left[\frac{|p_0|}{4b^2}+\frac{\epsilon(p_0)}{2b}\right]\ln|C_4| + \epsilon(k_0k_0')\left[|E_4| + \frac{(B-p_0)(c-E)(C-e)}{2A}|F_4|\right. \\ & \left.\left. +\frac{(a+p_0)(d+e)(D+E)}{2b}|G_4|\right]\right\} \qquad \text{(D.17)}\end{aligned}$$

Table D.3: Definitions of the quantities $A_4, B_4, \ldots, G_4$ appearing in eqs. (D.16)–(D.18) [24]

Class	A_4	B_4	C_4	E_4	F_4	G_4
1	$\frac{p_0^4 q^4}{m^4 AaBb}$	$\frac{4p_0^2 A}{m^2 B}$	$\frac{4p_0^2 b}{m^2 a}$	p_0	$\frac{p_0}{A(B-p_0)}$	$\frac{p_0}{b(a+p_0)}$
2	$\frac{p_0^2 q^2 B}{m^2 ADd}$	$\frac{4AB}{m^2}$	$\frac{q^2}{4dD}$	B	$\frac{B}{A(B-p_0)}$	$\frac{B}{(d+e)(D+E)}$
3	$\frac{p_0^4 q^4}{m^4 AbcD}$	$\frac{4p_0 EA}{m^2 c}$	$\frac{4p_0 Eb}{m^2 D}$	E	$\frac{E}{A(c-E)}$	$\frac{E}{b(D+E)}$
4	$\frac{p_0^2 q^2 c}{m^2 Aad}$	$\frac{4p_0 Ac}{m^2 E}$	$\frac{p_0 e}{ad}$	c	$\frac{c}{A(c-E)}$	$\frac{c}{(d+e)(a+p_0)}$
5	$\frac{p_0^2 q^2 D}{m^2 BbC}$	$\frac{p_0 e}{BC}$	$\frac{4p_0 bD}{m^2 E}$	D	$\frac{D}{(B-p_0)(C-e)}$	$\frac{D}{b(D+E)}$
6	$\frac{aB}{Cd}$	$\frac{eB}{p_0 C}$	$\frac{ea}{p_0 d}$	$p_0 - e$	$\frac{p_0 - e}{(C-e)(B-p_0)}$	$\frac{p_0 - e}{(a+p_0)(d+e)}$
7	$\frac{p_0^2 q^2 a}{m^2 bCc}$	$\frac{q^2}{4Cc}$	$\frac{4ab}{m^2}$	a	$\frac{a}{(C-e)(c-E)}$	$\frac{a}{b(a+p_0)}$

and

$$\begin{aligned}\int M_0 S_4 d\mu \;=\; & \frac{1}{4\pi^3 q_z}\int dK\, dp_0 S_4 \left\{ \frac{|q^2|}{2A}\left[\frac{|p_0|q^2}{4q_z^2 A} - \epsilon(p_0)\frac{q^2 - 2B\nu}{2q_z^2}\right]\ln|B_4| \right. \\ & + \left|\frac{q^2}{2p_0}\right| \frac{Cc+Dd}{q_z^2}\ln|A_4| + \frac{|q^2|}{2b}\left[\frac{|p_0|q^2}{4bq_z^2} + \epsilon(p_0)\frac{q^2+2a\nu}{2q_z^2}\right]\ln|C_4| \\ & + \epsilon(k_0 k_0')\frac{q^2}{2q_z^2}\left[|E_4| + \frac{(B-p_0)(c-E)(C-e)}{2A}|F_4| \right. \\ & \left.\left. + \frac{(a+p_0)(d+e)(D+E)}{2b}|G_4|\right]\right\}, \end{aligned} \tag{D.18}$$

respectively. These expressions are valid for all the four-particle processes with the K, p_0 integration region given in Figure D.1.

The expression for the coefficient of $\ln|C_4|$ in ref. [24, p.385] contains writing errors and is corrected in eq. (D.17).

The expressions in eqs. (D.17) and (D.18) with the quantities $A_4, B_4, \ldots, G_4$ as defined in Table D.3 are the final results for four-particle processes *before* the cancellation of collinear singularities. The final results for four-particle processes *after* the cancellation of collinear singularities, as discussed in Section 3.8, are given by the same expressions in eqs. (D.17) and (D.18) but with only the quantities A_4, B_4 and C_4 replaced by the quantities $\bar{A}_4, \bar{B}_4$ and $\bar{C}_4$ as defined in Table D.4:

$$\begin{aligned}\int \bar{M}_\Sigma S_4 d\mu \;=\; & \frac{1}{4\pi^3 q_z}\int dK dp_0 S_4 \left\{ \left|\frac{q^2}{2p_0}\right| \ln|\bar{A}_4| + |q^2| \left[\frac{|p_0|}{4A^2} - \frac{\epsilon(p_0)}{2A}\right] \ln|\bar{B}_4| \right. \\ & + |q^2| \left[\frac{|p_0|}{4b^2} + \frac{\epsilon(p_0)}{2b}\right] \ln|\bar{C}_4| + \epsilon(k_0 k_0') \left[|E_4| + \frac{(B-p_0)(c-E)(C-e)}{2A}|F_4| \right. \\ & \left. \left. + \frac{(a+p_0)(d+e)(D+E)}{2b}|G_4| \right] \right\} \end{aligned} \tag{D.19}$$

and

$$\begin{aligned}\int \bar{M}_0 S_4 d\mu \;=\; & \frac{1}{4\pi^3 q_z}\int dK dp_0 S_4 \left\{ \frac{|q^2|}{2A} \left[\frac{|p_0| q^2}{4q_z^2 A} - \epsilon(p_0)\frac{q^2 - 2B\nu}{2q_z^2}\right] \ln|\bar{B}_4| \right. \\ & + \left|\frac{q^2}{2p_0}\right| \frac{Cc + Dd}{q_z^2} \ln|\bar{A}_4| + \frac{|q^2|}{2b} \left[\frac{|p_0| q^2}{4bq_z^2} + \epsilon(p_0)\frac{q^2 + 2a\nu}{2q_z^2}\right] \ln|\bar{C}_4| \\ & + \epsilon(k_0 k_0')\frac{q^2}{2q_z^2} \left[|E_4| + \frac{(B-p_0)(c-E)(C-e)}{2A}|F_4| \right. \\ & \left. \left. + \frac{(a+p_0)(d+e)(D+E)}{2b}|G_4| \right] \right\}, \end{aligned} \tag{D.20}$$

D.4 Summary of Final Expressions for Three-Particle Processes

The final forms of the expressions for the matrix element squared for the three-particle process involving quarks (including vertex and self-energy corrections) are given for the sum over all polarizations and for the longitudinal polarization of the virtual photon in eqs. (3.246) and (3.250), respectively. These expressions (which exclude phase space integrations associated with the external quark lines) can be considered as valid for the three-particle process involving antiquarks (diagram (h) in Figure 2.2) too through the convention that to each of the diagrams (g) and (h) in Figure 2.2 there corresponds the six Feynman diagrams in Figure 3.1. These six Feynman diagrams, as drawn in Figure 3.1 with exactly the same four-momentum assignments and directions of arrows, are used for each of the processes (g)

Table D.4: Definitions of the quantities $\bar{A}_4, \bar{B}_4$ and $\bar{C}_4$ which replace the quantities A_4, B_4 and C_4 in eqs. (D.17) and (D.18) *after* the cancellation of collinear singularities [24]

Class	1	2	3	4	5	6	7
$\bar{A}_4$	1	$\frac{B^2}{Dd}$	$\frac{aB}{cD}$	$\frac{cB}{ad}$	$\frac{aD}{BC}$	$\frac{aB}{Cd}$	$\frac{a^2}{Cc}$
$\bar{B}_4$	1	$\frac{B^2}{p_0^2}$	$\frac{EB}{p_0 c}$	$\frac{Bc}{p_0 E}$	$\frac{p_0 e}{BC}$	$\frac{eB}{p_0 C}$	$\frac{q^2}{4Cc}$
$\bar{C}_4$	1	$\frac{q^2}{4dD}$	$\frac{Ea}{p_0 D}$	$\frac{p_0 e}{ad}$	$\frac{aD}{p_0 E}$	$\frac{ea}{p_0 d}$	$\frac{a^2}{p_0^2}$

and (h) in Figure 2.2. For $k_0 > 0$ and $k_0' > 0$ we are considering the three-particle process (g) involving quarks and for $k_0 < 0$ and $k_0' < 0$ we are considering the three-particle process (h) involving antiquarks.

The result discussed in Section 3.5 for a typical contribution to the vertex correction of a quark that the integrations over phase space, including the loop integration, could be analytically reduced to integrations over only the two energy variables k_0 and p_0 applies to all the other $\mathcal{O}(\alpha_S)$ contributions to three-particle processes as well. According to the mechanism by means of which collinear and infrared divergences cancel (as discussed in Section 3.8) it is appropriate to transform from these variables (k_0, p_0) to the variables (K, p_0) where K is defined in eq. (D.1).

The above convention enables one to view both the quark and antiquark three-particle processes simultaneously in the two-dimensional energy plane shown in Figure D.2.

In Sections 3.5.3 and 3.5.4 we derived, for the case of the bosonic part of the vertex correction to a quark, that

$$\begin{aligned} I_B\left(\frac{1}{s_B t_B}\right) &\equiv \int \frac{1}{s_B t_B} d\Omega_B \\ &= \frac{\pi}{p_0^2(-q^2)} \ln |A_B| \end{aligned}$$

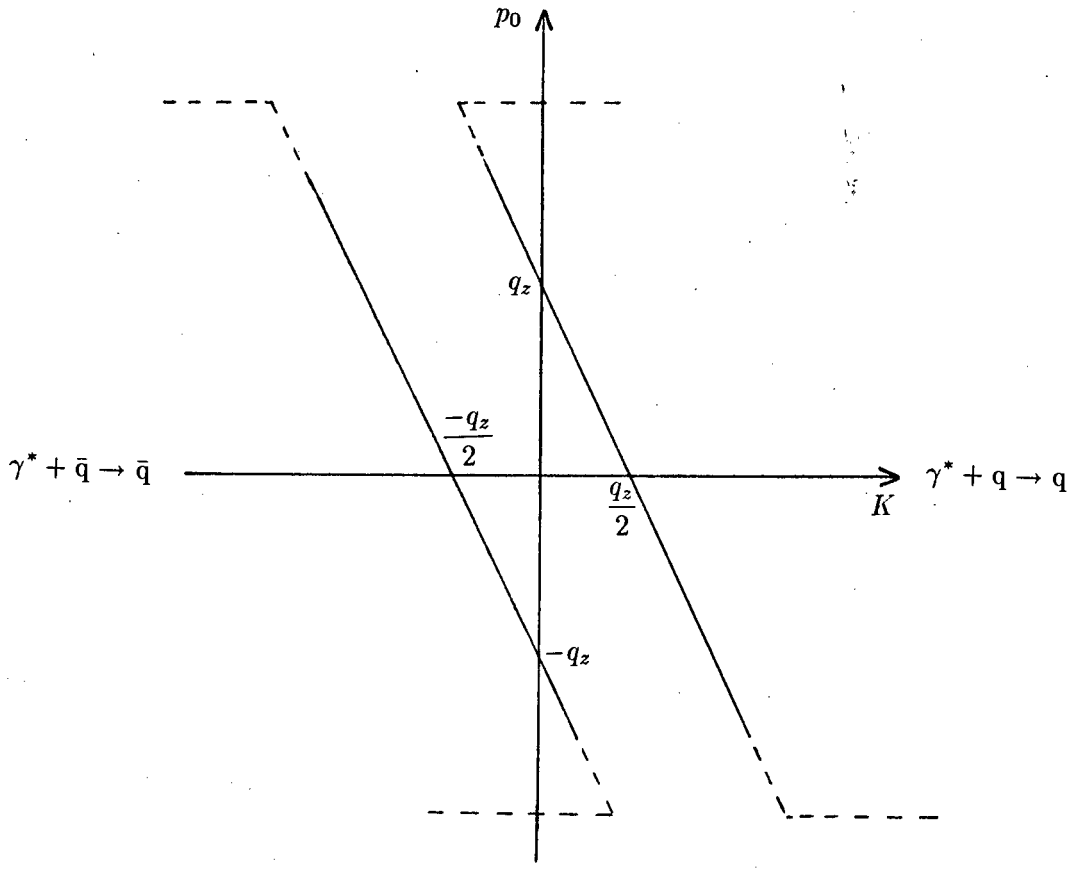

Figure D.2: Regions of support for all three-particle processes in the K,p_0 plane

where I_B is defined in eq. (3.153), $d\Omega_B$ is given as $d\Omega_p$ in eq. (3.146), A_B is given in eq. (3.208) and

$$s_B = (k' - p)^2 \qquad t_B = (k - p)^2.$$

The above-mentioned contribution is one example of the so-called bosonic contributions from the phase space and loop integrations associated with three-particle processes and which are characterized by the terms proportional to Δ_B in eqs. (3.246) and (3.250). One can define similar angular integrals for the so-called fermionic and fermionic primed contributions from three-particle processes which are characterized by the terms proportional to Δ_F and $\Delta_{F'}$, respectively, in eqs. (3.246) and (3.250).

Thus we define the general angular integral for three-particle processes as

$$I_W\left(f(\Omega)\right) = \int f(\Omega) d\Omega_W$$

with W=B,F or F′ denoting bosonic, fermionic or fermionic primed contributions, respec-

tively, and $d\Omega_B$ given by the expression for $d\Omega_p$ in eq. (3.146). Expressions for $d\Omega_F$ and $d\Omega_{F'}$ are the same as that for $d\Omega_B$ except that $\cos\alpha_B$ in eq. (3.146) is replaced by $\cos\alpha_F$ and $\cos\alpha_{F'}$, respectively, and except for different meanings attached to the variables $z \equiv \cos\theta$ and $z' \equiv \cos\theta'$ in eq. (3.146) according to the following arrangement: In the case of the bosonic (W=B) contributions the meanings of α_B, θ and θ' are shown in Figure 3.10. In the case of the F and F′ contributions the meanings of $\alpha_F, \theta, \theta'$ and $\alpha_{F'}, \theta, \theta'$ are shown in Figures E.1 and E.2, respectively. The latter two figures are considered since we temporarily transform from p to $h \equiv k - p$ and $h' \equiv k' - p$ in the angular integrations of F and F′ contributions, respectively. After the angular integrations we transform back to p in order to express the final results in terms of K and p_0.

More details on the distinction between the cases W=B,F and F′ appear in the text surrounding the appearances of Figures 3.10, E.1 and E.2, respectively.

In order to facilitate discussions on the cancellation of collinear singularities according to the cancellation scheme shown in Figure 3.13, we refer to s_B and t_B as defined above in integrals appearing in bosonic contributions. For the same reason we refer to $s_{F'}$ and t_F in integrals appearing in F′ and F contributions, respectively by letting

$$p^2 - m^2 = \begin{cases} s_{F'} & \text{for F' contributions} \\ t_F & \text{for F contributions.} \end{cases}$$

It is to be noted that we do not define quantities s_F and $t_{F'}$ since, afile1s may be seen from the following results, the quantities $s_B, t_B, s_{F'}$ and t_F are sufficient to parametrize singularities due to the $m \to 0$ limit in three-particle processes.

Results from angular integrations are [24, p.386]

$$I_B\left(\frac{1}{s_B t_B}\right) = \frac{\pi}{p_0^2|q^2|}\ln|A_B| \qquad I_B(1) = 4\pi$$

$$I_B\left(\frac{1}{s_B}\right) = \frac{-\pi}{p_0 A}\ln|B_B| \qquad I_B\left(\frac{1}{t_B}\right) = -\frac{\pi}{p_0 a}\ln|C_B|$$

$$I_B\left(\frac{s_B}{t_B}\right) = 4\pi\frac{A}{a}\left[1 + \frac{q^2}{2Aa}(1 + \ln|C_B|)\right] \qquad I_B\left(\frac{t_B}{s_B}\right) = 4\pi\frac{A}{a}\left[1 + \frac{q^2}{2Aa}(1 + \ln|B_B|)\right]$$

$$I_F\left(\frac{1}{t_F(k'-p)^2}\right) = \frac{\pi}{p_0^2|q^2|b}\ln|A_F| \qquad I_F(1) = 4\pi$$

$$I_F\left(\frac{1}{(k'-p)^2}\right) = \frac{\pi}{q_z b}\ln|K_F| \qquad I_F\left(\frac{1}{t_F}\right) = -\frac{\pi}{ab}\ln|C_F|$$

(D.21)

$$
\begin{aligned}
I_{\mathrm{F}}\left(\frac{(k'-p)^2}{t_{\mathrm{F}}}\right) &= \frac{2\pi}{a^2}\left[-q^2-2\nu a+\frac{p_0q^2}{|b|}\ln|C_{\mathrm{F}}|\right] \\
I_{\mathrm{F}}\left(\frac{t_{\mathrm{F}}}{(k'-p)^2}\right) &= -\frac{2\pi}{q_z^2}\left[-q^2-2\nu a+\frac{q^2(q^2+4\nu b+4ab)}{4ab}\ln|K_{\mathrm{F}}|\right] \\
I_{\mathrm{F}'}\left(\frac{1}{s_{\mathrm{F}'}(k-p)^2}\right) &= \frac{\pi}{p_0^2|q^2|B}\ln|A_{\mathrm{F}'}| \quad I_{\mathrm{F}'}(1)=4\pi \\
I_{\mathrm{F}'}\left(\frac{1}{(k-p)^2}\right) &= -\frac{\pi}{q_zB}\ln|K_{\mathrm{F}'}| \qquad I_{\mathrm{F}'}\left(\frac{1}{s_{\mathrm{F}'}}\right) = -\frac{\pi}{AB}\ln|B_{\mathrm{F}'}| \\
I_{\mathrm{F}'}\left(\frac{(k-p)^2}{s_{\mathrm{F}'}}\right) &= \frac{2\pi}{A^2}\left[-q^2+2\nu A+\frac{p_0q^2}{|B|}\ln|B_{\mathrm{F}'}|\right] \\
I_{\mathrm{F}'}\left(\frac{s_{\mathrm{F}'}}{(k-p)^2}\right) &= -\frac{2\pi}{q_z^2}\left[-q^2+2\nu A+\frac{q^2(q^2-4\nu B+4AB)}{4AB}\ln|K_{\mathrm{F}'}|\right]
\end{aligned}
\tag{D.22}
$$

where

$$
\begin{aligned}
A_{\mathrm{B}} &= \frac{p_0^4q^4}{m^4AaBb} \quad B_{\mathrm{B}} = \frac{4p_0^2A}{m^2B} & C_{\mathrm{B}} &= \frac{4p_0^2a}{m^2b} \\
A_{\mathrm{F}} &= \frac{q^2p_0^2b}{m^2aDd} \quad K_{\mathrm{F}} = \frac{(q_z+\nu)(2K-p_0-q_z)}{(q_z-\nu)(2K-p_0+q_z)} & C_{\mathrm{F}} &= \frac{4ab}{m^2} \\
A_{\mathrm{F}'} &= \frac{q^2p_0^2B}{m^2ADd} \quad K_{\mathrm{F}'} = \frac{(q_z+\nu)(2K-p_0+q_z)}{(q_z-\nu)(2K-p_0-q_z)} & B_{\mathrm{F}'} &= \frac{4AB}{m^2}
\end{aligned}
$$

The expressions for $I_{\mathrm{F}}\left(1/[t_{\mathrm{F}}(k'-p)^2]\right)$, $I_{\mathrm{F}'}\left(1/[s_{\mathrm{F}'}(k-p)^2]\right)$ and A_{F} in ref. [24, p.386] contain writing errors and are corrected above.

An example of the derivation of the first result in (D.21) is discussed in the subsections of Section 3.5 and its explicit expression is given in eqs. (3.207) and (3.208).

In the following we write down the final expressions for all the three-particle processes including statistical factors and integrations over phase space. We use the symbols

$$
\int M_{\mathrm{i}}^{3\mathrm{W}} S_{3\mathrm{W}} d\mu_{3\mathrm{W}} \qquad \mathrm{W=B,F\ or\ F'}
$$

where

$$
\begin{aligned}
d\mu_{\mathrm{W}} &= \frac{d^3k}{(2\pi)^3 2|k_0|}\frac{d^3k'}{(2\pi)^3 2|k_0'|}(2\pi)^4\delta^4(k'-k-q)\frac{d^4p}{(2\pi)^4}\delta(W^2-M_{\mathrm{W}}^2) \\
W^2-M_{\mathrm{W}}^2 &= \begin{cases} p^2-m^2 & \text{for} \quad \mathrm{W=B} \\ (k-p)^2 & \text{for} \quad \mathrm{W=F} \\ (k'-p)^2 & \text{for} \quad \mathrm{W=F'} \end{cases} \\
S_{3\mathrm{B}} &= S_2\left[1+2n_{\mathrm{B}}(|p_0|)\right]\frac{1}{2} \\
S_{3\mathrm{F}} &= S_2\left[1-2n_{\mathrm{F}}(x_{k-p})\right]\frac{1}{2}
\end{aligned}
$$

$$
\begin{aligned}
S_{3F'} &= S_2\,[1-2n_F(x_{k'-p})]\,\frac{1}{2} \\
S_2 &= \left[\frac{1}{2}-\frac{\epsilon(k_0)}{2}(1-2n_F(x_k))\right]\left[\frac{1}{2}+\frac{\epsilon(k_0+\nu)}{2}(1-2n_F(x_{k+q}))\right] \\
x_k &= |k_0|-\mu\epsilon(k_0).
\end{aligned}
$$

The factor S_2 describes the statistical factors for the *external* either quarks or antiquarks in three-particle processes. The index i on M_i^{3W} takes on only the values $i=\Sigma$ or $i=0$ in order to distinguish between the expressions for the matrix element squared for the sum over all polarizations and for the longitudinal polarization of the virtual photon, respectively.

By inserting the above results from angular integrations into eqs. (3.246) and (3.250) and suppressing only the factors e^2g^2 in the latter equations, one obtains

$$
\begin{aligned}
\int M_\Sigma^{3B} S_{3B}\,d\mu_B &= \frac{1}{4\pi^3 q_z}\int dK\,dp_0\,\theta(1-y)\theta(1+y)S_{3B}\left\{-\left|\frac{q^2}{2p_0}\right|\ln|A_B| \right. \\
&\quad -|q^2|\left[\frac{|p_0|}{4A^2}-\frac{\epsilon(p_0)}{2A}\right]\ln|B_B| - |q^2|\left[\frac{|p_0|}{4a^2}-\frac{\epsilon(p_0)}{2a}\right]\ln|C_B| \\
&\quad \left.-|p_0|\left[1+\frac{a}{A}+\frac{A}{a}+\frac{q^2}{2}\left(\frac{1}{a^2}+\frac{1}{A^2}\right)\right]\right\} \qquad \text{(D.23)} \\
\int M_\Sigma^{3F} S_{3F}\,d\mu_F &= \frac{1}{4\pi^3 q_z}\int dK\,dp_0\,\theta(1-y)(1+y)S_{3F}\left\{-\frac{\epsilon(b)|q^2|}{2p_0}\ln|A_F| \right. \\
&\quad +\frac{\epsilon(b)|q^2|}{q_z}\left[\frac{3}{4}+\frac{a+A}{4q_z^2}(a+A-2p_0)\right]\ln|K_F| \\
&\quad -\epsilon(b)|q^2|\left[\frac{p_0}{4a^2}-\frac{1}{2a}\right]\ln|C_F| \\
&\quad \left.+|b|\left[\frac{1}{2}+\frac{A^2-a^2}{q_z^2}+\frac{q^2}{2a^2}+\frac{A}{a}\right]\right\} \qquad \text{(D.24)} \\
\int M_\Sigma^{3F'} S_{3F'}\,d\mu_{F'} &= \frac{1}{4\pi^3 q_z}\int dK\,dp_0\,\theta(1-y)(1+y)S_{3F'}\left\{-\frac{\epsilon(B)|q^2|}{2p_0}\ln|A_{F'}| \right. \\
&\quad -\frac{\epsilon(b)|q^2|}{q_z}\left[\frac{3}{4}+\frac{a+A}{4q_z^2}(a+A-2p_0)\right]\ln|K_{F'}| - \epsilon(B)|q^2| \\
&\quad \left.\times\left[\frac{p_0}{4A^2}-\frac{1}{2A}\right]\ln|B_{F'}| + |B|\left[\frac{1}{2}-\frac{A^2-a^2}{q_z^2}+\frac{q^2}{2A^2}+\frac{a}{A}\right]\right\} \qquad \text{(D.25)}
\end{aligned}
$$

where the K, p_0 integration region shown in Figure D.2 is determined by the step functions with

$$y=\frac{q^2+2k_0\nu}{2k_0q_z}\,.$$

Corresponding expressions for the longitudinal polarization of the virtual photon ($i=0$) exist but we present them only in the version valid *after* the cancellation of collinear singularities

in eq. (D.28).

After the cancellation of collinear singularities as discussed in Section 3.8, the quantities $A_B, B_B, C_B, A_F, C_F, A_{F'}$ and $B_{F'}$ become:

$$\begin{aligned} \bar{A}_B &= \bar{B}_B = \bar{C}_B = 1 \\ \bar{A}_F &= \frac{b^2}{dD} \quad \bar{C}_F = \frac{b^2}{p_0^2} \\ \bar{A}_{F'} &= \frac{B^2}{dD} \quad \bar{B}_{F'} = \frac{B^2}{p_0^2} \,. \end{aligned} \tag{D.26}$$

The final results for three-particle processes *after* the cancellation of collinear singularities are:

$$\begin{aligned} &\sum_{W=B,F,F'} \int \bar{M}_\Sigma^{3W} S_{3W} d\mu_W \\ &= \frac{1}{4\pi^3 q_z} \int dK dp_0 \theta(1-y)\theta(1+y) \left\{ S_{3B}(-|p_0|) \left[1 + \frac{a}{A} + \frac{A}{a} + \frac{q^2}{2}\left(\frac{1}{a^2} + \frac{1}{A^2}\right)\right] \right. \\ &+ S_{3F} \left[-\frac{\epsilon(b)|q^2|}{2p_0} \ln|\bar{A}_F| - \epsilon(b)|q^2| \left[\frac{p_0}{4a^2} - \frac{1}{2a}\right] \ln|\bar{C}_F| \right. \\ &+ \frac{\epsilon(b)|q^2|}{q_z} \left[\frac{3}{4} + \frac{a+A}{4q_z^2}(a+A-2p_0)\right] \ln|K_F| + |b| \left[\frac{1}{2} + \frac{A^2-a^2}{q_z^2} + \frac{q^2}{2a^2} + \frac{A}{a}\right] \Big] \\ &+ S_{3F'} \left[-\frac{\epsilon(B)|q^2|}{2p_0} \ln|\bar{A}_{F'}| - \epsilon(B)|q^2| \left[\frac{p_0}{4A^2} - \frac{1}{2A}\right] \ln|\bar{B}_{F'}| \right. \\ &- \frac{\epsilon(B)|q^2|}{q_z} \left[\frac{3}{4} + \frac{a+A}{4q_z^2}(a+A-2p_0)\right] \ln|K_{F'}| \\ &\left. \left. + |B| \left[\frac{1}{2} + \frac{A^2-a^2}{q_z^2} + \frac{q^2}{2a^2} + \frac{a}{A}\right] \right] + S_2 \frac{p_0|p_0|(K+p_0/2)}{p_0^2+T^2} \right\}. \end{aligned} \tag{D.27}$$

The expressions for the coefficients of $\ln|\bar{A}_F|$ and $\ln|\bar{A}_{F'}|$ in ref. [24, p.389] contain writing errors and are corrected in eq. (D.27).

The corresponding final result for the longitudinal polarization of the virtual photon is:

$$\begin{aligned} &\sum_{W=B,F,F'} \int \bar{M}_0^{3W} S_{3W} d\mu_W \\ &= \frac{1}{4\pi^3 q_z} \int dK dp_0 \theta(1-y)\theta(1+y) \left\{ -S_{3B} \frac{|p_0|}{q_z^2} \left(-\nu^2 + \frac{q^2}{2}\left[\frac{a}{A} + \frac{A}{a} + \frac{q^2}{2}\left(\frac{1}{a^2} + \frac{1}{A^2}\right)\right]\right) \right. \\ &+ S_{3F} \left\{ -\epsilon(b)\frac{|q^2|}{4p_0 q_z^2} \ln|\bar{A}_F| [q^2 + 4K^2 + p_0^2 - \nu^2] - \epsilon(b)\frac{|q^2|}{2aq_z^2} \left[p_0 \left(\frac{q^2}{4a} + \nu\right) \right. \right. \\ &\left. \left. - \frac{q^2 + 2\nu a}{2} \right] \ln|\bar{C}_F| + \epsilon(b)\frac{|q^2|}{q_z} \left[-\frac{1}{4} - \frac{a+A}{4q_z^2}(a+A-2p_0) \right] \ln|K_F| \right. \end{aligned}$$

$$+\epsilon(b)\frac{b}{q_z^2}\left[-\frac{\nu^2}{2}-A^2+a^2+\frac{q^2}{2}\left(\frac{A}{a}+\frac{q^2}{2a^2}\right)\right]\Bigg\}$$
$$+S_{3F'}\Bigg\{-\epsilon(B)\frac{|q^2|}{4p_0q_z^2}\ln|\bar{A}_{F'}|[q^2+4K^2+p_0^2-\nu^2]-\epsilon(B)\frac{|q^2|}{2Aq_z^2}\left[p_0\left(\frac{q^2}{4A}-\nu\right)$$
$$-\frac{q^2-2\nu A}{2}\right]\ln|\bar{B}_{F'}|-\epsilon(B)\frac{|q^2|}{q_z}\left[-\frac{1}{4}-\frac{a+A}{4q_z^2}(a+A-2p_0)\right]\ln|K_{F'}|$$
$$+\epsilon(B)\frac{B}{q_z^2}\left[-\frac{\nu^2}{2}+A^2-a^2+\frac{q^2}{2}\left(\frac{a}{A}+\frac{q^2}{2A^2}\right)\right]\Bigg\}+S_2\frac{p_0|p_0|(K+p_0/2)}{p_0^2+T^2}\Bigg\}. \qquad \text{(D.28)}$$

The last term in each of eqs. (D.27) and (D.28) has been introduced [24, p.389] to make the integrations over positive and negative p_0 separately convergent for the purpose of numerical calculation. From the definition of K it follows that $K + p_0/2$ is independent of p_0 and therefore that the last term in each of eqs. (D.27) and (D.28) contributes zero when added at a positive and negative value of p_0 but with $|p_0|$ fixed.

From Figure D.2 it can be seen that the K, p_0 integration region for three-particle processes is not subdivided into subregions as in the case of four-particle processes (see Figure D.1). An example of this result for three-particle processes appears in Sections 3.5.3 and 3.5.4 where it is shown that subdivisions of the energy plane (see Figure 3.11) need only to be considered when performing angular integrations in intermediate steps and that these subdivisions disappear after angular integrations.

Appendix E

Derivation of Expressions for Three-Particle Processes

(a) In this section we derive the expression for $Z_2^{-1}(k)$ given in eq. (3.240).

By putting $m_R = 0$ in eq. (3.225) one obtains

$$Z_2^{-1}(k) = 1 - C(k) - \frac{1}{k_0}\frac{\partial}{\partial k_0}[k.D(k)] + \frac{D_0(k)}{k_0} + \mathcal{O}(\alpha_S^2).$$

But

$$k.D = [k.D]_0 - \frac{1}{2}(k^2 - m_R^2 + m^2)C \tag{E.1}$$

where

$$[k.D]_0 \equiv \frac{g^2}{2(2\pi)^3}\int d^4p\{\delta(p^2 - m^2)[1 + 2n_B(|p_0|)] + \delta(p^2 - m_R^2)[1 - 2n_F(x_p)]\}$$

is independent of k_0 and where m is, as always in this work, the gluon mass. From eq. (E.1) it follows that

$$\begin{aligned}\frac{\partial}{\partial k_0}[k.D(k)] &= -k_0C(k) - \frac{1}{2}(k^2 - m_R^2 + m^2)\frac{\partial}{\partial k_0}C(k) \\ &= -k_0C(k) - \frac{1}{2}(k^2 - m_{\text{phys}}^2 + m^2)\frac{\partial}{\partial k_0}C(k) + \mathcal{O}(\alpha_S^2). \end{aligned}\tag{E.2}$$

For k on mass shell ($k^2 = m_{\text{phys}}^2$) and in the limit of zero gluon mass the coefficient of $\frac{\partial}{\partial k_0}C(k)$ in eq. (E.2) vanishes and one obtains the result

$$Z_2^{-1}(k) = 1 + \frac{D_0(k)}{k_0} + \mathcal{O}(\alpha_S^2).$$

(b) In this section we explain how one derives the relations in eqs. (3.247), (3.248) and (3.249). Since these relations are considered to be effective equalities valid under the three-particle phase space integrations, we shall sometimes make use of results already discussed in Section 3.5 for the vertex correction and further useful results not discussed there will be discussed here.

In order to prove the relation in eq. (3.247) we make use of eqs. (3.242)–(3.244) to write

$$(k'-p)^4\Delta = (k'-p)^2\left\{\frac{\delta\,(k-p)^2)}{p^2-m^2}[1-2n_{\rm F}(x_{k-p})]+\frac{\delta(p^2-m^2)}{(k-p)^2}[1+2n_{\rm B}(|p_0|)]\right\}. \tag{E.3}$$

Consider

$$K_2 \equiv (k'-p)^2\frac{\delta(p^2-m^2)}{(k-p)^2} = \frac{k'.p}{k.p}\delta(p^2-m^2). \tag{E.4}$$

As can be seen from eqs. (E.3) and (3.242), K_2 forms part of the socalled bosonic part of three-particle processes. We have already discussed an example phase space integration for the bosonic part of a three-particle process when we discussed the bosonic part of the vertex correction in Section 3.5.2. At present we are not concerned with the actual performance of the phase space integrations but we make use of the ideas encountered when performing them in order to rewrite the results in, e.g., eq. (3.245) in the form given in eq. (3.246). Further on we shall also encounter the socalled fermionic [corresponding to eq. (3.243)] and fermionic primed [corresponding to eq. (3.244)] parts of three-particle processes. The relations derived for the latter two parts in the present considerations are also useful for subsequent fermionic and fermionic primed phase space integrations which we do not discuss explicitly.

By decomposing $\vec{k}'$ into components parallel and perpendicular to $\vec{k}$,

$$\vec{k}' = \vec{k}\frac{\vec{k}.\vec{k}'}{|\vec{k}|^2} + \left(\vec{k}' - \vec{k}\frac{\vec{k}.\vec{k}'}{|\vec{k}|^2}\right),$$

and using the angles as defined in Figure 3.10, we obtain

$$\vec{k}'.\vec{p} = \frac{k_0'}{k_0}\cos\alpha_{\rm B}\vec{k}.\vec{p} + c_1\cos\phi \tag{E.5}$$

where $c_1 = |\vec{k}'||\vec{p}|\sin\alpha_{\rm B}\sin\theta$ is the projection of $\vec{p}$ onto the perpendicular to $\vec{k}$ component of $\vec{k}'$ and where, as usual in this work, we make use of the relation $|\vec{k}| = k_0$ for massless quarks.

From eqs. (E.4), (E.5) and the expression for $\cos\alpha_B$ given in eq. (3.152) there follows that

$$\begin{aligned} K_2 &= \left[\frac{k_0'}{k_0}\left(\frac{q^2}{2k_0k_0'}+1\right) - \frac{p_0q^2}{2k.pk_0} - \frac{c_1\cos\phi}{k.p}\right]\delta(p^2-m^2) \\ &= \left[\frac{k_0'}{k_0}\left(\frac{q^2}{2k_0k_0'}+1\right) - \frac{p_0q^2}{(k-p)^2k_0}\right]\delta(p^2-m^2) \end{aligned} \tag{E.6}$$

where the term proportional to $\cos\phi$ has been dropped since it does not contribute when integrated with respect to ϕ in the phase space integrations.

Next we consider

$$K_1 \equiv (k'-p)^2\frac{\delta\left((k-p)^2\right)}{p^2-m^2} \tag{E.7}$$

which forms part of the socalled fermionic part of three-particle processes and define

$$h \equiv k-p \qquad \Rightarrow \qquad k'-p = h+q.$$

For discussions concerning the fermionic part of three-particle processes, it is convenient to introduce the symbols shown in Figure E.1. By decomposing $\vec{q}$ into components parallel and perpendicular to $\vec{k}$,

$$\vec{q} = \vec{k}\frac{\vec{q}.\vec{k}}{|\vec{k}|^2} + \left(\vec{q} - \vec{k}\frac{\vec{q}.\vec{k}}{|\vec{k}|^2}\right),$$

and using the angles as defined in Figure E.1, we obtain

$$\vec{q}.\vec{h} = \frac{q_z}{k_0}\cos\alpha_F\vec{h}.\vec{k} + c_2\cos(\pi-\phi') \tag{E.8}$$

where $c_2 = \left|\vec{q} - \vec{k}\frac{\vec{q}.\vec{k}}{|\vec{k}|^2}\right||\vec{h}|\cos\alpha_F\sin\theta'$. From $k'^2 = 0$ and $k' = k+q$ there follows that

$$\begin{aligned} (k+q)^2 &= 2k_0\nu - 2k_0q_z\cos\alpha_F + q^2 = 0 \\ \Rightarrow \cos\alpha_F &= \frac{q^2+2k_0\nu}{2k_0q_z} \end{aligned} \tag{E.9}$$

This and eq. (E.8) enable us to write

$$h.q = h.k\frac{q^2+2k_0\nu}{2k_0^2} - \frac{h_0q^2}{2k_0} + c_2\cos\phi'$$

Then K_1 in eq. (E.7) becomes

$$\begin{aligned} K_1 &= \frac{(h+q)^2}{(k-h)^2}\delta(h^2) = \frac{2h.q+q^2}{-2k.h}\delta(h^2) \\ &= \left[-\frac{q^2+2k_0\nu}{2k_0^2} + \frac{p_0q^2}{k_0}\frac{1}{(k-h)^2}\right]\delta(h^2) \end{aligned} \tag{E.10}$$

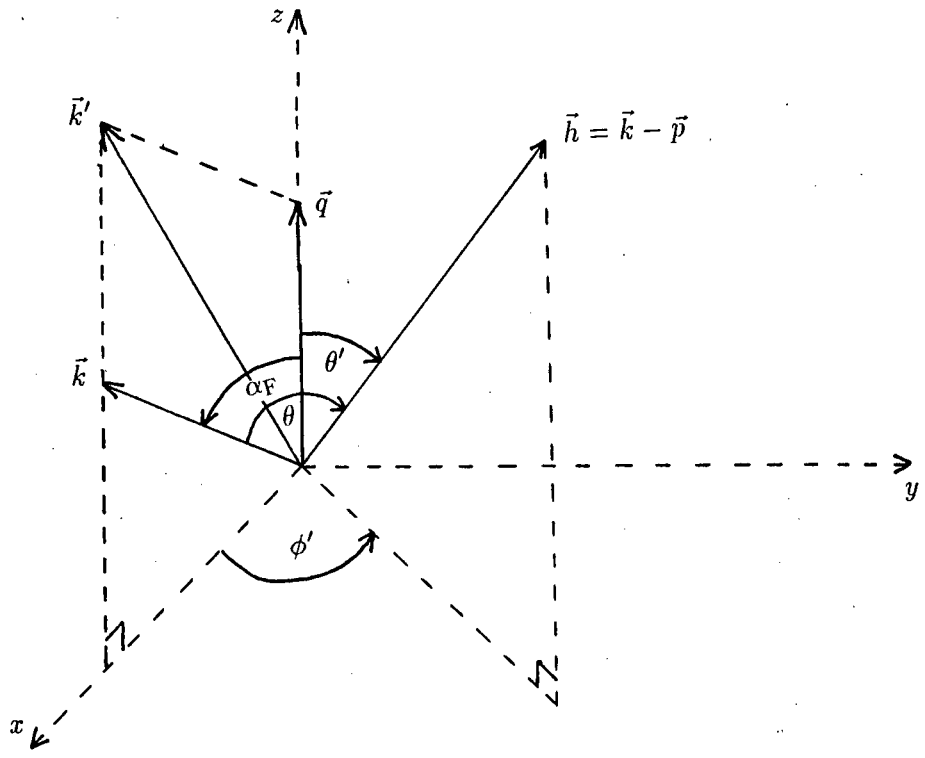

Figure E.1: The reference frame in which we consider the fermionic part of three-particle phase space integrations.

where the term proportional to $\cos\phi'$ has been dropped since it does not contribute when integrated with respect to ϕ' in phase space integrations.

By inserting the expressions for K_1 and K_2 from eqs. (E.4), (E.6),(E.7) and (E.10) into eq. (E.3) we obtain the result of eq. (3.247).

Next we prove eq. (3.248). One can write

$$\begin{aligned} p^4\Delta &= p^2\left\{\frac{\delta\,(k-p)^2)}{(k'-p)^2}[1-2n_{\rm F}(x_{k-p})]+\frac{(k'-p)^2}{(k-p)^2}[1-2n_{\rm F}(x_{k'-p})]\right\} \\ &\equiv K_3[1-2n_{\rm F}(x_{k-p})]+K_4[1-2n_{\rm F}(x_{k'-p})]. \end{aligned} \tag{E.11}$$

Consider K_3 which forms part of the socalled fermionic part of three-particle processes. By decomposing $\vec{k}$ into components parallel and perpendicular to $\vec{q}$,

$$\vec{k} = \vec{q}\frac{\vec{q}.\vec{k}}{q_z^2} + \left(\vec{k} - \vec{q}\frac{\vec{q}.\vec{k}}{q_z^2}\right),$$

and using the angles as defined in Figure E.1, we obtain

$$\vec{k}.\vec{h} = \frac{k_0}{q_z}\cos\alpha_F \vec{q}.\vec{h} + c_3\cos(\phi')$$

where $c_3 = |\vec{k}||\vec{h}|\sin\alpha_F \sin\theta'$. Eq. (E.9) enables us to write

$$k.h = q.h\frac{q^2+2k_0\nu}{2q_z^2} + k_0^2 - k_0p_0 - \frac{\nu(k_0-p_0)(q^2+2k_0\nu)}{2q_z^2} - c_3\cos\phi'.$$

Then K_3 becomes

$$\begin{aligned} K_3 &= \frac{(k-h)^2}{(h+q)^2}\delta(h^2) = \frac{-2k.h}{2h.q+q^2}\delta(h^2) = \left\{-\frac{q^2+2k_0\nu}{2q_z^2}\right. \\ &\quad \left. + \frac{1}{(h+q)^2}\left[-2k_0^2 + 2k_0p_0 + \frac{\nu(k_0-p_0)(q^2+2k_0\nu)}{q_z^2} + q^2\frac{q^2+2k_0\nu}{2q_z^2}\right]\right\}\delta(h^2) \\ &= \frac{\delta\,(k-p)^2)}{(k'-p)^2}\left\{\frac{q^2}{q_z^2}\left[-\frac{q_z^2}{2} + \frac{1}{2}(k_0+k_0')(k_0+k_0'-2p_0)\right] - (k'-p)^2\frac{q^2+2k_0\nu}{2q_z^2}\right. \\ &\quad \left. + (k-p)^2\frac{2k_0'\nu - q^2}{2q_z^2}\right\} \end{aligned} \tag{E.12}$$

where the term proportional to $\cos\phi'$ has been dropped since it does not contribute when integrated with respect to ϕ' in the phase space integrations.

Next we consider K_4 which forms part of the socalled fermionic primed part of three-particle processes. For discussions concerning the fermionic primed part of three-particle processes, it is convenient to introduce the symbols shown in Figure E.2. Let

$$h' \equiv k' - p \qquad \Rightarrow \qquad k - p = h' - q.$$

By decomposing $\vec{k}'$ into components parallel and perpendicular to $\vec{q}$,

$$\vec{k}' = \vec{q}\frac{\vec{q}.\vec{k}'}{q_z^2} + \left(\vec{k}' - \vec{q}\frac{\vec{q}.\vec{k}'}{q_z^2}\right),$$

and using the angles as defined in Figure E.2, we obtain

$$\vec{k}'.\vec{h}' = \frac{k_0'}{q_z}\cos\alpha_{F'}\vec{q}.\vec{h}' + c_4\cos\phi \tag{E.13}$$

where $c_4 = |\vec{k}'||\vec{h}'|\sin\alpha_{F'}\sin\theta$. From $k^2 = 0$ and $k = k' - q$ there follows that

$$(k'-q)^2 = -2k_0'\nu + 2k_0'q_z\cos\alpha_{F'} + q^2 = 0$$

$$\Rightarrow \cos\alpha_{F'} = \frac{-q^2+2k_0'\nu}{2k_0'q_z}.$$

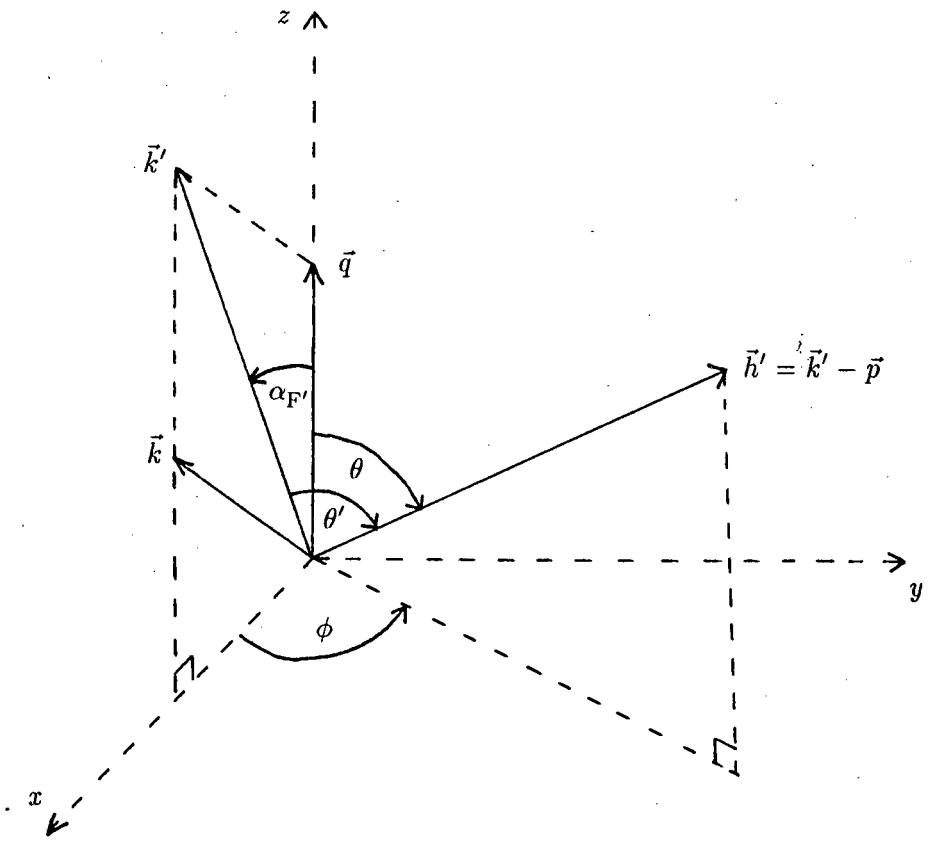

Figure E.2: The reference frame in which we consider the fermionic primed part of three-particle phase space integrations.

This and eq. (E.13) enable us to write

$$k'.h' = q.h' \frac{2k'_0\nu - q^2}{2q_z^2} + k'_0(k'_0 - p_0) - \nu(k'_0 - p_0)\frac{2k'_0\nu - q^2}{2q_z^2} - c_4 \cos\phi$$

Then K_4 becomes

$$\begin{aligned} K_4 &= \frac{(k'-h')^2}{(h'-q)^2}\delta(h'^2) = \frac{-2k'.h'}{-2h'.q+q^2}\delta(h'^2) = \left\{ \frac{2k'_0\nu - q^2}{2q_z^2} \right. \\ &\quad \left. + \frac{1}{(h'-q)^2}\left[-q^2\frac{2k'_0\nu - q^2}{2q_z^2} - 2k'_0(k'_0 - p_0) + \nu(k'_0 - p_0)\frac{2k'_0\nu - q^2}{q_z^2} \right] \right\} \delta(h'^2) \\ &= \frac{\delta\left((k'-p)^2\right)}{(k-p)^2}\left\{ \frac{q^2}{q_z^2}\left[-\frac{q_z^2}{2} + \frac{1}{2}(k_0 + k'_0)(k_0 + k'_0 - 2p_0) \right] - (k'-p)^2\frac{q^2 + 2k_0\nu}{2q_z^2} \right. \\ &\quad \left. + (k-p)^2\frac{2k'_0\nu - q^2}{2q_z^2} \right\} \end{aligned} \tag{E.14}$$

where the term proportional to $\cos\phi$ has been dropped since it does not contribute when integrated with respect to ϕ in phase space integrations.

By inserting the expressions for K_3 and K_4 from eqs. (E.12) and (E.14) into eq. (E.11) we obtain the result in eq. (3.248).

The result in eq. (3.249) can be derived by following steps similar to those followed to prove eqs. (3.247) and (3.248).

Bibliography

[1] W. Keil, Phys. Rev. **D40** (1989) 1176

[2] N.P. Landsman, Ch.G. van Weert, Phys. Rep. **145** (1987) 141

[3] H. Umezawa, H. Matsumoto, M. Tachiki, Thermo Field Dynamics and Condensed States (North-Holland, Amsterdam, 1982)

[4] A.L. Fetter, J.D. Walecka, Quantum Theory of Many-Particle Systems (McGraw-Hill, New York, 1971)

[5] A.A. Abrikosov, L.P. Gorkov, I.E. Dzyaloshinski, Methods of Quantum Field Theory in Statistical Physics (Prentice-Hall, Englewood Cliffs, New Jersey, 1963)

[6] L.P. Kadanoff, G. Baym, Quantum Statistical Mechanics (W.A. Benjamin, New York, 1962)

[7] R.H. Brandenberger, Rev. Mod. Phys. **57** (1985) 1

[8] R. Baier, E. Pilon, B. Pire, D. Schiff, Bielefeld preprint BI-TP 89/10, May 1989

[9] D.A. Dicus, E.W. Kolb, A.M. Gleeson, E.C.G. Sudarshan, V.L. Teplitz, M.S. Turner, Phys. Rev. **D26** (1982) 2694

[10] J.-L. Cambier, J.R. Primack, M. Sher, Nucl. Phys. **B209** (1982) 372

[11] L.D. McLerran, Rev. Mod. Phys. **58** (1986) 1021

[12] R.L. Kobes, G.W. Semenoff, Nucl. Phys. **B272** (1986) 329

[13] L.D. McLerran, T. Toimela, Phys. Rev. **D31** (1985) 545

[14] R. Baier, B. Pire, D. Schiff, Phys. Rev. **D38** (1988) 2814

[15] J. Cleymans, I. Dadić, Z. Phys. **C45** (1989) 57

[16] T. Grandou, M. Le Bellac, J.-L. Meunier, Z. Phys. **C43** (1989) 575

[17] Y. Gabellini, T. Grandou, D. Poizat, Ann. Phys. (NY) **202** (1990) 436

[18] M. Le Bellac, D. Poizat, Z. Phys. **C47** (1990) 125

[19] T. Grandou, M. Le Bellac, D. Poizat, Nice INLN preprint INLN 1991/1, January 1991

[20] T. Altherr, P. Aurenche, T. Becherrawy, Nucl. Phys. **B315** (1989) 436

[21] T. Altherr, P. Aurenche, Z. Phys. **C45** (1989) 99 ; Phys. Rev. **D40** (1989) 4171

[22] T. Altherr, T. Becherrawy, Nucl. Phys. **B330** (1990) 174

[23] Editors: K. L. Kowalski, N. P. Landsman, Ch. G. van Weert, Physica **A158** (1989) 1

[24] (a) Editors: Ezawa et al., Proceedings of the Second Workshop in Thermal Field Theories and Applications (North Holland, Amsterdam, 1991) ; (b) Contribution on p.375 by J. Cleymans and I. Dadić

[25] M. Le Bellac, Nice INLN preprint INLN 1991/6, March 1991

[26] N. P. Landsman, Phys. Rev. Lett. **60** (1988) 1909

[27] N. P. Landsman, Ann. Phys. (NY) **186** (1988) 141

[28] T. Matsubara, Prog. Theor. Phys. **14** (1955) 351

[29] D.J. Gross, R.D. Pisarski, L.G. Yaffe, Rev. Mod. Phys. **53** (1981) 43

[30] P.D. Morley, M.B. Kislinger, Phys. Rep. **51** (1979) 64

[31] J.I. Kapusta, Nucl. Phys. **B148** (1979) 461

[32] B.A. Freedman, L.D. McLerran, Phys. Rev. **D16** (1977) 1130, 1147, 1169

[33] L. Dolan, R. Jackiw, Phys. Rev. **D9** (1974) 3320

[34] K. Takahashi, Phys. Rev. **D29** (1984) 632

[35] L. Leplae, F. Mancini, H. Umezawa, Phys. Rep. **10** (1974) 151

[36] Y. Takahashi, H. Umezawa, Collective Phenomena **2** (1975) 55

[37] A.J. Niemi, G.W. Semenoff, Ann. Phys. (NY) **152** (1984) 105

[38] R. Mills, Propagators for many-particle systems (Gordon and Breach Science Publishers, New York, 1969)

[39] R.L. Kobes, K.L. Kowalski, Phys. Rev. **D34** (1986) 513; K.L. Kowalski, Z. Phys. **C36** (1987) 665

[40] K.L. Kowalski, Phys. Rev. **D35** (1987) 2415

[41] F. Halzen, A.D. Martin, Quarks and Leptons (John Wiley and Sons, New York, 1984)

[42] A.J. Niemi, G.W. Semenoff, Nucl. Phys. **B230**[FS10] (1984) 181

[43] R. Kobes, Phys. Rev. **D43** (1991) 1269

[44] Y. Fujimoto, H. Matsumoto, H. Umezawa, Phys. Rev. **D30** (1984) 1400

[45] R.L. Kobes, G.W. Semenoff, N. Weiss, Z. Phys. **C29** (1985) 371

[46] E.S. Abers, B.W. Lee, Phys. Rep. **9C** (1973) 1

[47] D. Bailin, A. Love, Introduction to Gauge Field Theory (Adam Hilger, Bristol, 1985)

[48] R.J. Rivers, Path Integral Methods in Quantum Field Theory (Cambridge University Press, Cambridge, 1987); First paperback edition with corrections: (1988)

[49] A. Niégawa, Phys. Rev. **D40** (1989) 1199

[50] H. Umezawa, Prog. Theor. Phys. Suppl. **80** (1984) 26

[51] I. Ojima Ann. Phys. (NY) **137** (1981) 1

[52] H. Umezawa, Y. Yamanaka, Advances in Physics **37** (1988) 531

[53] H. Matsumoto, Fortschritte der Physik **25** (1977) 1

[54] R. Kubo, J. Phys. Soc. Japan **12** (1957) 570

[55] P.C. Martin, J. Schwinger, Phys. Rev. **115** (1959) 1342

[56] H. Matsumoto, Y. Nakano, H. Umezawa, Phys. Rev. **D31** (1985) 429

[57] J. Schwinger, J. Math. Phys. **2** (1961) 407

[58] R.A. Craig, J. Math. Phys. **9** (1968) 605

[59] L.V. Keldysh, Sov. Phys. JETP **20** (1965) 1018

[60] M. Marinaro, Phys. Rep. **137** (1986) 81

[61] H. Matsumoto, Y. Nakano, H. Umezawa, F.Mancini, M. Marinaro Prog. Theor. Phys. **70** (1983) 599

[62] H. Matsumoto, Y. Nakano, H. Umezawa, J. Math. Phys. **25** (1984) 3076

[63] M. Horibe, A. Hosoya, N. Yamamoto, Prog. Theor. Phys. **74** (1985) 1299

[64] H. Umezawa, Physica **A158** (1989) 306

[65] H.J. Kreuzer, C.G. Kuper, Collective Phenomena **2** (1976) 131,141

[66] H.J. Kreuzer, C.G. Kuper, J. Phys. G: Nucl. Phys. **2** (1976) 9

[67] W. Israel, Phys. Lett. **57A** (1976) 107

[68] H. Matsumoto, I. Ojima, H. Umezawa, Ann. Phys. (NY) **152** (1984) 348

[69] M. B. Kislinger, P. D. Morley, Phys. Rev. **D13** (1976) 2771

[70] F. Ruiz Ruiz, R. F. Alvarez-Estrada, Z. Phys. **C34** (1987) 131

[71] (a) J. Cleymans, R.L. Thews, Z. Phys. **C37** (1988) 315 ; (b) The corresponding preprint contains some more details: J. Cleymans, R.L. Thews, Bielefeld preprint BI-TP 86/14, March 1986

[72] A. Chodos et al., Phys. Rev. **D9** (1974) 3471

[73] R.P. Feynman, Photon-Hadron Interactions (Benjamin, New York, 1972) ; J.D. Bjorken, E.A. Paschos, Phys. Rev. **185** (1969) 1975

[74] A. Milsztajn et al., CERN preprint CERN-PPE 90-135, September 1990

[75] J.D. Bjorken, S.D. Drell, Relativistic Quantum Mechanics (McGraw–Hill, Inc., New York, 1964)

[76] (a) J.F. Donoghue, B.R. Holstein Phys. Rev. **D28** (1983) 340; (E) **D29** (1984) 3004; (b) J.F. Donoghue, B.R. Holstein, R.W. Robinett, Ann. Phys. (NY) **164** (1985) 233

[77] J. Kwiecinski et al., Phys. Rev. **D42** (1990) 3645

[78] L.W. Whitlow, Ph.D. Thesis, SLAC-Report-357, March 1990

[79] J.J. Aubert et al., Phys. Lett. **105B** (1981) 315